Generic source term determination for tailings storage facilities in the East Rand Basin

A Botha

orcid.org 0000-0001-5870-9272

Dissertation submitted in fulfilment of the requirements for the degree *Master of Science in Environmental Sciences* at the North-West University

Supervisor:	Dr SR Dennis
Co-supervisor:	Mr KN van Zweel

Graduation May 2018

22186077

Acknowledgements

I would like to express my sincere appreciation and gratitude to the following organisations and individuals:

My Lord and Saviour, for His support, guidance and for giving me the privilege and opportunity to study, as well as completing this dissertation;

Dr. Rainier Dennis and Mr. Nicolaus van Zweel who supervised and gave me guidance on my study;

A special thank you to my parents Johan and Susan Botha, who encouraged and supported me with all their love throughout my studies, without which this dissertation would have not been completed; and

To Michelle Janse van Rensburg, Altus Huisamen and Nequita Coetzee for their assistance, support and ongoing encouragement.

Summary

The prolonged leaching of gold tailings is a continuous concern in the East Rand Basin typically resulting in acid generation and the release of elements. The leachable constituents from the tailings influences the water quality of both surface and subsurface water negatively, resulting in degradation of the water sources through Acid Mine Drainage (AMD).

A combination of samples was subjected to XRD, XRF, static tests, leach tests and geochemical modelling; with the aim to develop a generic sulphate source term of tailing impoundments in the East Rand Basin.

A leachable sulphate production was determined for the East Rand Basin tailing dams. Geochemical and moisture profiles were used to produce a generic source term equation through PYROX, based on a generic function of sulphide and developed standardised moisture content within the tailings storage facilities. It was found that the modelling results over estimates the integrated sulphate production rate due to several unknown input parameters. Overall the generic source term equation was in close proximity to the PYROX simulated results, predicting a sulphate load based on the fraction sulphide present as the main variable input. The generic source term can be considered as an approximate estimation of loads expected within the East Rand Basin. The equation makes for a time conserving approach when compared to the PYROX software.

Keywords: East Rand Basin, acid mine drainage, tailings, source term, PYROX, static tests, leach tests.

List of Abbreviations

1-D	One Dimensional
ABA	Acid-Base Accounting
AMD	Acid Mine Drainage
ANC	Acid Neutralization Capacity
AP	Acid Potential
ARD	Acid Rock Drainage
CPT	Cone Penetration Test
FA	Fluvic Acid
GRDM	Groundwater Resource Directed Measures
HA	Humic Acid
HCO_3	Bicarbonate
LIDAR	Light Detection and Ranging
Mg	Magnesium
ML	Monolithic Leaching
MMF	Maximum Mobile Fraction
NAG	Net-Acid Generating
NAPP	Net Acid Producing Potential
NP	Neutralising Potential
pH	Hydrogen Potential
PWT	Pore Water Test
SO_4	Sulphate
SWL	Static Water Level
TDS	Total Dissolved Solids
TSF	Tailings Storage Facility
WRD	Waste Rock Dump
WRC	Water Research Commission
WWF	Wold Wildlife Fund
XRD	X-Ray Diffraction
XRF	X-Ray Fluorescence

Table of Contents

List of Figures

List of Tables

1. Introduction

1.1 Background

South Africa) is the largest producer of gold in the world and respectively the country with the most productive mines (Rosner & Van Schalkwyk, 1999: 137). The main period of production and development was during the 1940's and 1950's where the East Rand Basin was largely mined for gold from the Witwatersrand Supergroup.

The Witwatersrand Supergroups' rock formations contain significant quantities of sulphide minerals, which are liberated during mining and discarded onto Tailing Storage Facilities (TSF). Liberation of the sulphidic minerals increases the potential for tailings to generate Acid Mine Drainage (AMD) when exposed to water and oxygen. Generally the TSFs within the East Rand Basins are underlain by dolomitic aquifers of the Malmani subgroup, which links the mining areas and flow through large compartments and cavities, while some are underlain by Karoo rocks. Although dolomitic aquifers have the potential to buffer, the acidic leachate stemming from the TSFs is unknown, which can infiltrate the dolomite layers and add an additional treat to the groundwater resources.

1.2 Aim

The aim of this study is to develop a generic source contaminant release typically associated with the tailing storage facilities situated within the East Rand Basin. The modelling of complex field processes and consideration of the various interactions present within TSFs is used as a conceptual foundation for the development.

The overall aims of the project can be summarized as follows:

1) Understand the characteristics of gold tailings storage facilities through sampling, instrumental measurement, and laboratory testing of different localities;
2) Identify key parameters and characteristics of TSFs, which can be applied for AMD prediction; and
3) Development of a generic contaminant production in tailings dams associated with the East Rand Basin.

1.3 Objectives

The objectives of this study can be summarised as follows:

- Establish and characterise the mineralogical and geochemical properties of selected East Rand Basin tailings dams;
- To identify the contaminant release;
- To quantify and develop a generic source term for the TSFs located within the East Rand Basin.

2. Literature Survey

2.1 Introduction

According to the World Wildlife Fund (WWF, 2013) South Africa is a chronically water stressed country with huge economic development pressures and social upliftment challenges. As a third world country South Africa is under great pressure concerning its water resources, resulting in inefficient use of these resources and various related pollution problems. “The need for future predictions of impacts on water resources is particularly important at all mines that mine ore bodies or produce mine wastes that contain sulphide minerals. These minerals will oxidise over time, releasing sulphates and other contaminants” (DWAF, 2008: 1).

The subsurface is an open system, where associated interactions are possible, allowing contaminants to be transported, altered and reallocated under a variety of environmental influences, thus an understanding of all the interactions between subsurface components and chemical contaminants is of great importance for the purpose of developing and identifying the generic source term. Figure 1 is a basic representation of the associated interactions and represents a general concept of a tailings dam and it’s affected subsurface.

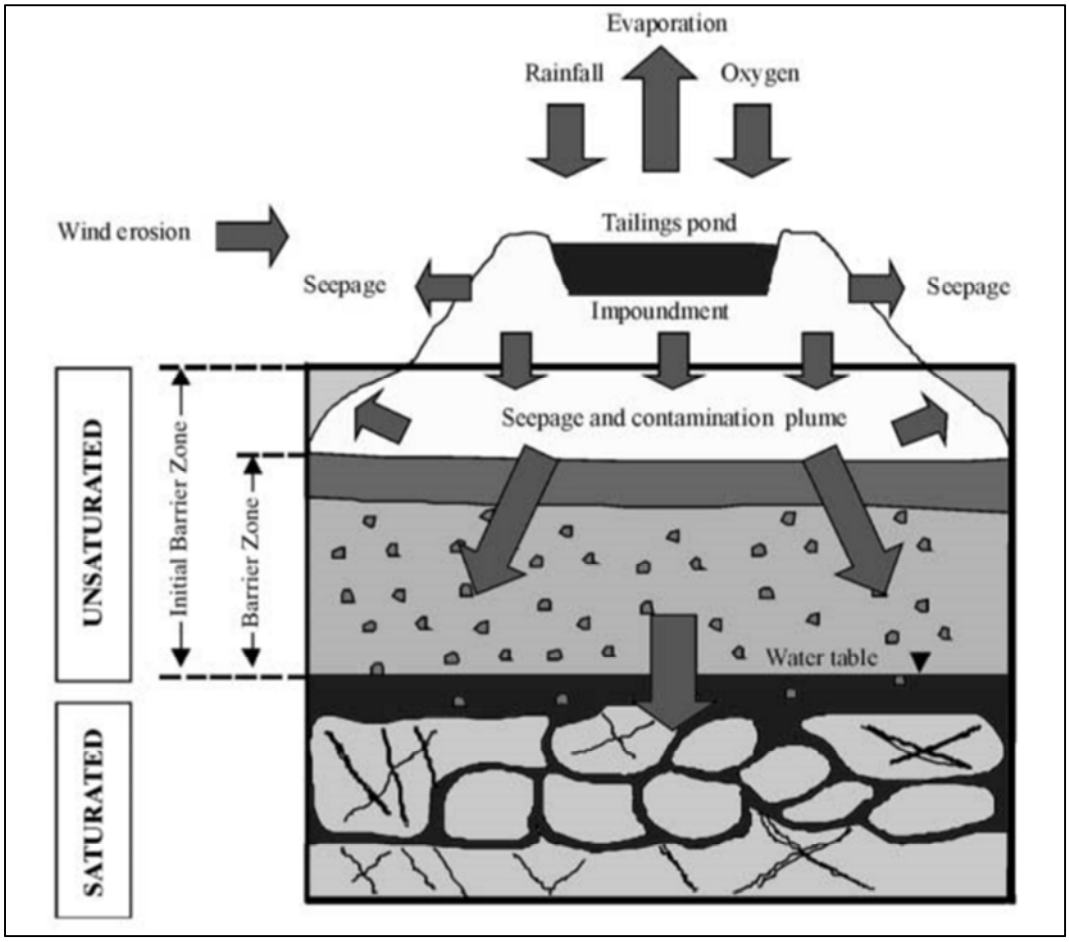

Figure 1: Conceptual model of a tailing dam and subsurface contamination (Rosner & Van Schalkwyk, 1999: 142)

Globally, water is one of the prime environmental resources that are affected by anthropogenic activities. Activities associated with mining can pose a risk for adverse environmental impacts. Mining and mineral beneficiation can affect water quality; alter the hydrological and topographical characteristics on a local scale, and subsequently affect surface runoff, soil moisture, evapo-transpiration and groundwater behaviour as discussed by DWAF (2008: iv). Mining activities can pose a significant risk to South Africa's water resource security. According to DWAF (2008: iv) failure to manage the impacts on water resources in an acceptable manner throughout life-of-mine and post-closure will result in difficulties in terms of community and government support of current and future mining projects. As mining contributes to the economy and releases by-products into the surrounding environment, the degradation of groundwater and associated surface waters is inevitable.

The prolonged leaching of sulphate minerals from gold mining activities is a continuous concern in this area and according to Tutu (2012: 355) this leads to acid generation and the release of certain elements from the tailings. Acid mine Drainage (AMD) from these tailings influences the water quality of surface and subsurface water negatively, resulting in the degradation of the water resources. Nsimba (2009: 16) explains that AMD is responsible for socio-economic impacts and is also the most costly environmental effect to date. This is due to the ongoing surface and groundwater pollution, while degrading soil quality, aquatic sediments and various aquatic fauna.

AMD is an expected concern in the mining industry representative of an oxidation reaction of sulphide minerals. The acid generation process is mainly represented by the oxidation of Pyrite (FeS_2), involving reaction with oxygen and water, in gold tailings and is a global problem contributing to high salt loads and acidification of the environment. There are four sub-reactions involved in producing AMD, while the general oxidation reaction is represented in Equation 2.1 (Kleinman *et al.*, 1981; Ochieng *et al.*, 2009; Singer & Stumm, 1970):

Equation 2.1

$$FeS_2 + \frac{15}{4}O_2 + \frac{7}{2}H_2O \rightarrow Fe(OH)_3 + 2SO_4^{2-} + 4H^+$$

2.2 Pyrite Geochemistry

AMD arises primarily when the sulphate mineral pyrite undergoes oxidation due to contact with oxygenated water. According to McCarthy (2011: 1) pyrite undergoes oxidation in a two-stage process, and is represented by producing sulphuric acid and ferrous sulphate within the first stage, followed by orange-red ferric hydroxide and additional sulphuric acids within the second stage. As mentioned in Section 2.1, four sub-reactions are involved in producing AMD and will be explained in this section by means of the subsequent equations after Ochieng *et al*. (2009), Kleinman *et al* (1981), Nsimba (2009), Singer and Stumm (1970) and Tutu (2012).

Sub-reaction 1 typically occurs at pH levels above 3.5 resulting in Equation 2.1 taking effect, naturally oxidising sulphide to sulphate and ferrous ions. This process occurs abiotically. Ferrous ions are rapidly oxidised at this stage.

Equation 2.1

$$\mathrm{FeS_2} + {}^{7}\!/_{2}\,\mathrm{O_2} + \mathrm{H_2O} \rightarrow \mathrm{Fe^{2+}} + 2\mathrm{SO_4^{2-}} + 2\mathrm{H^+}$$

Sub-reaction 2 follows and is mostly dependant on the presence of bacteria (*Thiobacillus ferrooxidans*) which catalyses the reactions around pH levels below 3.5. The recorded leachate from these reactions characteristically contains acidic conditions:

Equation 2.2

$$\mathrm{Fe^{2+}} + {}^{1}\!/_{4}\,\mathrm{O_2} + \mathrm{H^+} \rightarrow \mathrm{Fe^{3+}} + {}^{1}\!/_{2}\,\mathrm{H_2O}$$

Sub-reaction 3 consists of ferric iron precipitating as ferric hydroxide. The geochemistry undergoes structural re-arrangement to form a common Fe^{3+} oxide (iron hydroxide to FeOOH) known as goethite. Note that the ferric iron activity is increased as the solubility increases:

Equation 2.3

$$Fe^{3+} + 3H_2O \rightarrow Fe(OH)_3 + 3H^+$$

A self-sustaining reaction that produces additional pyrite by ferric ion (Fe^{3+}) is evident at sub-reaction 4. Thus at this stage the tailing dumps are a self-sustaining source of AMD even after mining operations have been ceased for an extended time period

Equation 2.4

$$FeS_2 + 14Fe^{3+} + 8H_2O \rightarrow 15Fe^{2+} + 2SO_4^{2-} + 16H^+$$

2.3 Case studies regarding source term modelling

Several types of leaching tests have been developed over the recent years in order to aid as prediction and indication tools for long term release of pollutants associated with construction materials and wastes. According to Van Der Sloot (1996: 65) these tests focus on two main aspects of leaching and can be identified as: (1) A release as a function of time; (2) and a release as a function of main leaching regulatory parameters, for instance pH, redox and complexation. The literature study discusses the development of different source term identification techniques by analysing previous case studies.

This study focusses on a source term model or release model, to determine the quality of a fluid released into the environment as described by the Oil and Gas Producers (2010: 3). Case studies on different modelling procedures are investigated to ascertain an approach for modelling of the generic contaminant release within the East Rand Basin.

Most of the problems encountered in previous case studies (as discussed in Section 2.3. below) occurs with the proper calibration of models, where monitoring data of field observations were not included, resulting in inaccurate assumptions and model predictions (Govender *et al.*, 2009; Tiruta-Barna *et al.*). Thus the research question associated with this study will aim to develop and determine a generic source term for a cluster of tailings within the East Rand basin.

2.3.1 *Prediction of seepage emanating from a TSF in an arid climate*

A source term characterization study was completed by Govender *et al*. (2009: 873) on a closure design for a Tailing Storage Facility (TSF) containing predominantly magnetite, quartz, pyrite and pyrrhotite. The samples obtained from the TSF were collected from the beach, pool and wall sections (Figure 2) and were subjected to static and kinetic geochemical tests. The laboratory results were used to populate numeric models of the system in terms of a low, average and high case mass load.

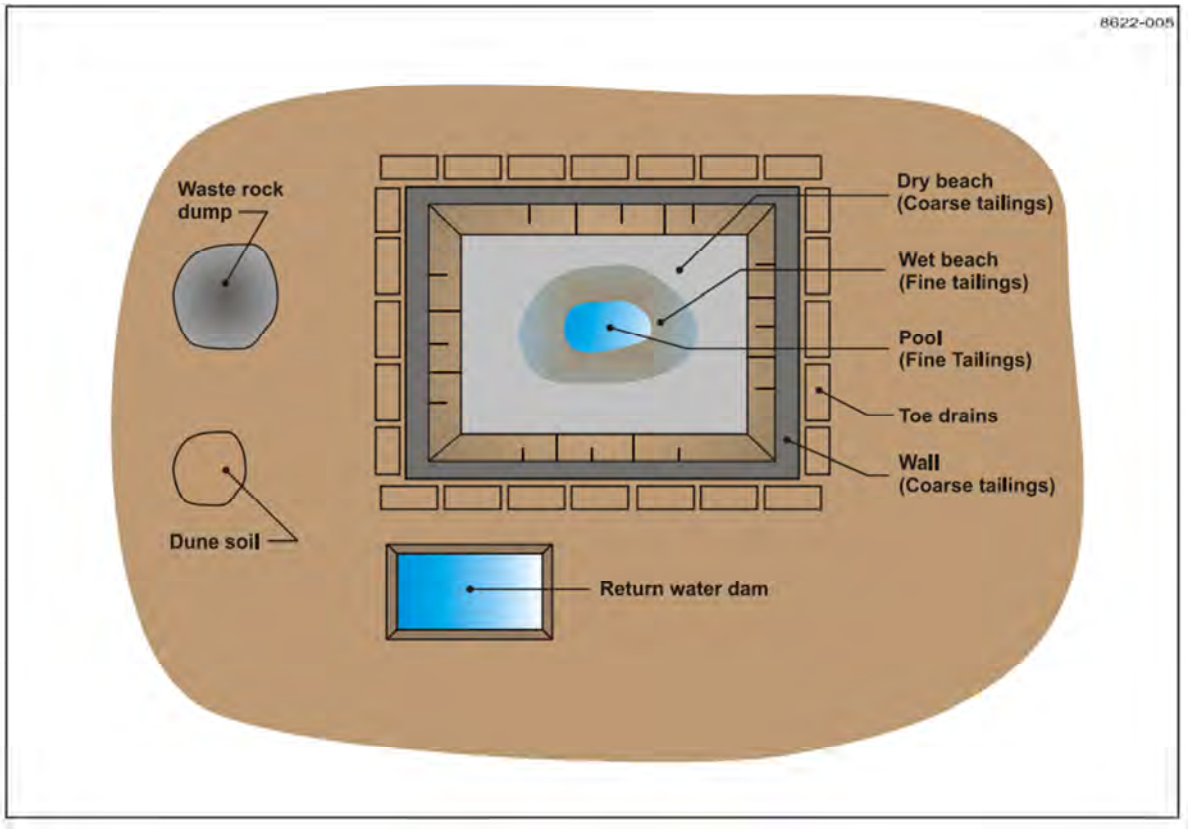

Figure 2: Sampled tailings storage facility including the delineated seepage areas (Govender *et al*., 2009: 874)

The following static tests were performed:

- Acid base accounting (ABA) with sulphur speciation;
- Mineralogical analyses (XRF and XRD);
- Distilled water shake flask test; and
- Quantification of vacuum pore water extracts from saturated samples.

The associated kinetic test used in this study was conducted by two humidity cells; one for coarse tailings and one for fine tailings. The test provided an understanding of the ARD reactions. The geochemical model was used to simulate pore water qualities. Based on the

models findings a post closure preliminary mass balance was developed to assess sulphide oxidation kinetics and the likely rainfall recharge rates.

The final integrated mass load model comprised of two key components:

- A geochemical module; and
- A flow module, each supported by detailed specialist models.

The associated modules considered 1-D profiles for the pool and wet beach area (fine tailings) and dry beach and wall areas (coarse tailings). In this model the quality of seepage is dictated by a dynamic equilibrium between kinetically-controlled sulphide oxidation processes, rainfall recharge rates and mineral solubility constraints. The main processes affecting AMD and contaminant mobilization from the tailings material was considered by Govender *et al*. (2009: 874) and identified as water and gas transport.

The specialist models used for source term determination by Govender *et al*. (2009: 874) included:

- Vadose/W;
- 1D Oxygen diffusion model to model the average oxygen consumption;
- Phreeqc v 2.1; and
- Geochemist's Workbench Ver. 6.0.5 for modelling of equilibrium reactions and identification of geochemical solubility controls on seepage quality.

Govender *et al*. (2009: 875) modelled the unsaturated flow as a function of the project phases, operational rules during the operational phase, the varying climatic conditions, as well as the material properties with the use of the Vadose/W software. Additionally the Darcian equation was applied in order to calculate the seepage from the areas under unsaturated flow conditions, while one dimensional flow profiles were created to simulate saturated flow. Govender *et al*. (2009: 875) also incorporated the profiles to predict seepage rates and moisture conditions for the different TSF sections.

The humidity cell results provided an understanding of the AMD reactions, predicting that acidic leachate will be produced. The moisture conditions were modelled for steady state, which represented a condition where the flows are in equilibrium with the climatic conditions. Additionally the measured humidity cell rates were moderated by applying diffusion rate limitations, based on the material properties and field conditions. The modelled concentrations were based on the assumption that ionic ratios generated through weathering in the field would be similar to those measured in the humidity cells. The O_2 diffusion model

predicted a scaling factor of about a thousand times slower than the O_2 flux calculated from the humidity cell rates. The field scaling up factor was applied (as identified within the O_2 diffusion model) to model the derived theoretical mass load concentrations.

Finally the maximum statistical error in analysis results from the samples was estimated by Govender *et al.* (2009: 880) at 22%, which is one of the many factors contributing to model uncertainty regarding geochemical modelling. Govender *et al.* (2009: 880) advised that the source term model be calibrated against monitoring data during the operational and post-closure phase of the mine. Obtaining improved data on the saturated hydraulic conductivity, identifying the effects of the underlying calcrete and conducting field scale lysimeter test to assess the seepage behaviour would provide an increased confidence of the predicted mass loads.

2.3.2 ***Long-term prediction of the leaching behaviour of pollutants from solidified wastes***

Three experimental tests and a behavioural model was implemented by Tiruta-Barna *et al*. (2004: 697) to assess inorganic contaminant release from cement-based waste materials. The three experimental tests were combined as an experimental “toolbox” and basically consisted of the Pore water test (PWT), the Acid Neutralization Capacity (ANC) test, and the Monolithic Leaching (ML) test, consisting of two equilibrium and one dynamic test as described by Tiruta-Barna *et al*. (2004: 698):

- The Pore Water Test (PWT) evaluates the initial equilibrium composition of the pore solution and the soluble species’ Maximum Mobile Fraction (MMF) regarding leaching;
- The applied acid neutralization capacity (ANC) test is inspired by the European pre-standard ‘Influence of pH on leaching with initial acid-base addition.’ The main objective of this test is to study the influence of pH on the leach ability of inorganic constituents from a waste material by addition of predetermined amounts of acid or base to finally reach desired end pH values in the apparent steady state condition;
- The Monolithic Leaching (ML) test determines the leaching behaviour of monolithic wastes under dynamic conditions. Thus used to determine the dominant release mechanisms of inorganic constituents from regularly shaped specimens of monolithic wastes.

The experimental data supplied by these tests are essential input parameters for the behavioural model that includes: leaching-available quantity, pore water composition, solubility versus pH and the released mass at the end of each leach sequence. This leach model incorporates the transport phenomena coupled with main physicochemical reactions in the saturated pore system of the material, as well as to eluate and supply the suitable input values for parameters of the leach model.

The behavioural model is a combined mass transfer-chemical reaction model comprising of two linked compartments as explained by Tiruta-Barna *et al*. (2004: 699) namely:

- The pollution source term (stabilized waste): a reactive material involving dissolution or precipitation, acido-basic and complexation reactions in the pore water and diffusional transport of the solubilized species through the porous system; and
- The chemical equilibria (dissolution or precipitation, acido-basic and complexation) and mass transfer in the eluate (continuous stirred reservoir with convection) in contact with the source term.

The behavioural model is extremely complex and it is essential to improve the release description of the target pollutants (in this case lead and amphoteric metal) from the leached waste material in the renewal conditions fixed by the scenario.

This method of determining a source term consists of a leaching “toolbox” to determine the parameters controlling the release of pollutants from the waste materials and a leaching model intended to predict the long-term leaching behaviour of the pollutants. Three associated materials were analysed and subjected to this method of source term determination. Tiruta-Barna *et al*. (2004:710) concluded that the in situ validation step of the long-term leaching behavioural model is lacking in the long-term leaching phase and that constitutes is an essential next step of the methodology.

2.3.3 *A geochemical modelling approach for the leaching and reactive transport of elements in municipal solid waste incineration bottom ash*

Dijkstra *et al*. (2008: 1546) made use of a predictive “multi-surface” modelling approach that simultaneously predicts the leaching and reactive transport of a broad range of major and trace elements. Dijkstra *et al*. (2008: 1546) collected bottom ash samples which were introduced to pH-static leaching experiments and percolation tests with different flow velocities and flow interruption (for verification of the equilibrium assumption) to be

incorporated in the geochemical and transport modelling for the long-term prediction of leaching.

After the leach tests were conducted the results, comprising of the major and trace elements (i.e., pH, Na, Al, Fe, Ca, SO_4, CO_3, Cl, Ni, Cu, Zn, Cd, Pb, Mo) and fulvic acids, were geochemically modelled with respect to surface complexation or precipitation on Fe/Al hydroxides with humic and fulvic acids (HA and FA) and mineral dissolution. Thus Dijkstra *et al*. (2008: 1544) combined the geochemical part of the model with advective/dispersive transport of water and first-order mass transfer between mobile and stagnant zones to enable the reactive transport calculations.

This approach included solubility-controlled elements representing a finite amount of minerals that are constrained by availability estimates and sorption-controlled elements as solution concentrations of all major and trace elements, whether they are based on solubility and/or sorption reaction. These controlled elements were estimated simultaneously in a single model run. According to Dijkstra *et al*. (2008: 1547) the mineral solubility, inorganic speciation and geochemical modelling approach was calculated by thermodynamic data using MINTEQA2 version 4.0. Specific and non-specific sorption of protons and ions to HA and FA was modelled with the NICA-Donnan model using the set of ‘‘generic” binding parameters, except for the binding of Fe-III to FA, for which the more recent NICA-Donnan parameters were used.

Dijkstra *et al*. (2008: 1549) predicted the bottom ash leaching and transport in a percolation regime by extending the geochemical part of the model with a one-dimensional transport of water to represent a transport model. Dijkstra *et al*. (2008: 1549) used the “dual porosity” approach to account for physical non-equilibrium, thus assuming that the liquid phase is partitioned in a mobile and immobile zone.

Dijkstra *et al*. (2008: 1560) explains that the combination of standardized leaching test methods, selective chemical extractions and mechanistic modelling, creates a promising generic approach to assess the long-term environmental impact. The “multi-surface” reactive transport modelling approach yields accurate results as a strongly improved model prediction compared to previous reactive transport modelling.

2.3.4 *Probabilistic Modelling of Long-Term Mass Loads from a Covered Dry-Stack Tailings Facility*

Schafer (2006: 1189) conducted a source term analyses on the Greens Creek Mine situated on the northern Admiralty Island, Alaska. The tailing associated with the mining events of this area contains approximate 10% to 18% pyritic sulphur, with abundant calcite from 15 to 30%. These tailings samples were then introduced to kinetic testing, that predicted an alkaline pH for tens to hundreds of years through oxidizing conditions, but could become acidic after long-term exposure. With the use of SoilCover, a 1-D water and gas flux model, Schafer (2006: 1190) was able to determine the net percolation through the cover with a decreasing oxygen flux per year.

By developing a predictive source term model, Schafer (2006: 1192) was able to stimulate the geochemical characteristics of the oxidized and reduced portions of the pile and predict how water and oxygen will migrate in the long-term and influence the mass loads. The probabilistic model created by Schafer (2006: 1192) was implemented as a spreadsheet and designed using a statistical distribution of input data or parameters (Table 1) to stimulate water quality at three distinct locations in the tailings by receiving water from:

- The interstitial water within the tailings;
- Water within the underdrain, which consists of interstitial water, groundwater and runoff; and
- Groundwater at the compliance point down-gradient of the tailings where the underdrain water would mix with receiving localized groundwater recharge.

The long-term water quality was derived from the model predicting the concentration of each constituent by assuming that the rate of oxygen flux controls the release of the soluble form of the constituent, and that the reaction products dissolve in the available water. This quality as described by Schafer (2006: 1195) represents the chemical equilibrium with the lower oxygen flux and is only achieved after the mass of stored oxidation products are removed. The quantity of metal release based on sulphide oxidation was collected from the kinetic tests.

Schafer (2006: 1195) considers upwelling groundwater interception by the drain layer, runoff from the TSF, and seepage through the tailings with respect to the source term model of the respective hydrology. This model was calibrated via daily monitoring within the tailings' water management system through means of hydrograph separation techniques to isolate groundwater inflow from runoff and simulated the range of distribution to measured

hydrology by means of duration curves, which depicts the distribution of instantaneous flow from the TSF from all sources. The model designed by Schafer (2006: 1198) provided relatively close agreement with the observed wet borehole chemistry, with only a few exceptions regarding SO_4, HCO_3 and hardness (which were higher in wet boreholes), but overall the source term model provided a good indication relative to the measured wet borehole chemistry.

Table 1: *Parameters used for the simulation of a long-term source model (Schafer, 2006)*

Alternative Description	Proposed Action - place additional 6 million tons of tailings in expanded facility	Continuous carbonate addition	Use of organic carbon amendment as a continuous addition or as a veneer to promote sulphate reduction
Tailings Placement Area	24.8 ha	33.0 ha	25.2 ha
Chemistry of Tailings Pore Water			
Initial tailings pore water (0 to 1 pore volume)	Interstitial water represented by water samples obtained from deep piezometers and in which sulphate reduction is occurring.		
Intermediate tailings pore water (1 to tens of pore volumes)	Water from the upper oxidized portion of the pile will replace the reduced water as carbon supplies are exhausted. Water chemistry is best represented by the shallow lysimeters in tailings.	Water from the upper oxidized portion of the pile will replace the reduced water as carbon supplies are exhausted. Water chemistry is best represented by the shallow lysimeters in tailings.	Water will become reduced as the added carbon initiates sulphate reduction. Water chemistry is best represented by deep tailings piezometer samples in which sulphate reduction has occurred.
Long-term tailings pore water (>tens of pore volumes)	Water retains higher sulphate and trace element concentrations associated with the oxidized zone until the accumulated secondary minerals are rinsed. Concentrations will decline to lower concentrations determined by the rate of long-term oxygen flux pile.	Similar to proposed action.	Water will remain reducing so that concentrations will change little. Some elements may decrease in concentration in response to decreased oxygen flux.
Hydrology Assumptions			
Infiltration coefficient (operational)	10 to 15 %, median 12 % of rainfall		
Infiltration coefficient (post-closure)	8 to 12 %, median 10 % of rainfall		
Residual Water Content	30 to 33.6%, median 31% volumetric		

Alternative Description	Proposed Action - place additional 6 million tons of tailings in expanded facility	Continuous carbonate addition	Use of organic carbon amendment as a continuous addition or as a veneer to promote sulphate reduction
Oxygen flux (operational)	Variable dependent on (and inverse to) water content ranging from 3 to 30 $M/m^2/yr$		
Oxygen flux (closure)	0.127 to 0.131 $M/m^2/yr$, median $M/m^2/yr$		
Operating Period	20 yrs		
Oxygenated depth	1 m		
Dispersion coefficient	0.02 unit less		
Upwelling Groundwater	0.72 to 5.0 L/s, median of 2.11 L/s with Pearson distribution		
Mixing Zone Assumptions			
Area	=500 m *1000 m		
Recharge Rate	10 % of rainfall		
Groundwater Recharge (m^3/day)	Area + Recharge Rate * Rain		
Runoff	Dependent on rainfall (45.4 % of days) and following a Pearson distribution		

2.3.5 *Modelling of Contaminant release from a Uranium Mine Tailings Site*

Kahnt & Metschies (2007: 1) studied four tailing sites from uranium mining sites with the purpose of setting up a management model for remediation and associated surroundings as well as relevant sources of contaminant loads from different waste rock piles. Tailing samples were subjected to analyses for the relative sulphur concentrations, in the range of 2% – 5% in mass, with a limited neutralization potential. A simplified approach was applied to model the source term in the impoundments for this site.

Kahnt & Metschies (2007: 3) developed a compartment model of the tailing impoundments and the surrounding aquifers. Contaminant release and transport was calculated using the GOLDSIM software. This model defined the time dependant hydraulic conditions within the tailings and surrounding aquifers taking into consideration the relative hydraulic and geotechnical processes involved as well as the processes that influence the hydraulic properties of the tailings material. These processes included sorption and retardation, resulting in a simple geochemical approach with the use of Darcy's law to define the contaminant release. These compartments representing the tailings material are divided into 3 sub-compartments according to the different materials as described by Kahnt & Metschies (2007: 3). The grain size distribution and Cone Penetration Test (CPT) measurements resulted in the geometric characterization of the 3 different material zones (fine-slime, sandy and transition material) of the relevant tailings. The difference of the tailings materials varies in hydraulic geotechnical and geochemical behaviour with regards to predicting contaminant release.

Darcy's law was implemented as a simple hydraulic model, where Kahnt & Metschies (2007: 4) used it to determine the water balance within the modelled system, as well as to include the quantity of water flow between the compartments. This model was calibrated by historic measurement data of the fluctuating water tables as well as seepage and discharge rates, where the contaminant release was based on a simple approach of solubility controlled release or adsorption controlled release.

The geochemical part of the model was based on sorption processes and retardation by applying the distribution coefficient or kd-approach, to describe the release and transport within the hydraulic system. Thus Kahnt & Metschies (2007: 1) used this model to include results of detailed geochemical modelling on individual tailing zones and related them to the source term model of the contaminant transport in the aquifer and receiving environment.

Kahnt & Metschies (2007: 5) described the general purpose of this model as the evaluation of different technical measurements with regards to the reduction of the environmental impacts. The system was modelled over a time period of 100 years. The robustness of the model was also assessed by equating the historical observations through changes of the hydraulic and geochemical system from the 1960's to 2007, where the concentrations of the high number of groundwater observation wells were averaged.

This model predicts the effect of various remediation scenarios in a fast and transparent manner, and the conducted work demonstrated that the applied system modelling approach using a compartment model with an internal substructure of the compartments is extremely flexible and powerful.

2.3.6 *Mathematical geophysical model for prediction of pyrite oxidation and pollutant leaching in coal waste dumps*

A combined mathematical geophysical model was developed and used by Doulati *et al*. (2008: 517) for the prediction of pyrite oxidation and pollutant leaching associated with a coal washing waste dump. A few samples were taken from different depths at three points on the waste dump to assess the pyrite oxidation and the pollution generated. These samples were then analysed by using an AA-670 Shimadzu atomic absorption to determine the fraction of pyrite remained within the waste.

A numerical finite volume model using the PHOENICS package was used to develop and simulate pyrite oxidation and pollution generation from the Alborz Shargi coal washing waste dump. The pyrite oxidation reaction was described by die shrinking-core model, where the concentration of oxygen within the pore spaces was converted to the liquid phase from Henry's law and the gas law. Doulati *et al*. (2008: 520) determined the reaction skin depth from the pyritic surface area, surface reaction rate constant and the oxygen diffusion coefficient in the solution phase. In this study Doulati *et al*. (2008: 520) calculated pyritic surface area (α) to 100/m, taking into account particles containing reactive pyrite as spheres.

The incorporated equations used in the study were recalculated to include the reduction in surface area of pyrite as time progresses. The PHOENICS package was used repeatedly in this study to solve partial differential equations as it is a general-purpose Computational Fluid Dynamic (CFD) package which can be used for simulation of fluid flow, heat transfer, mass transfer and associated chemical reactions as well as stress analysis in solids. The oxidation of pyrite within the waste dump sites was described by this shrinking-core model,

which is a one-dimensional simulation performed in PHOENICS software. The model's parameters or input data used to assess this source term of pyrite in coal waste dumps are presented in Table 2.

Table 2: *Parameters used for the simulation (Doulati et al., 2008: 520)*

Parameter	Value	Reference
Effective diffusion coefficient (m^2/s)	variable ($1x10^{-8}$ - $1x10^{-6}$)	Elberling *et al.* 1994
Pyrite fraction (%)	(1.6 - 1.8)	
Bulk density of spoil (kg/m^3)	2300	
Molar density of pyrite within particle (mol/m^3)	23 (5900 kg/m^3)	Jaynes *et al.* 1984b
Surface area of pyrite per unit volume of spoil (m)	100	
Diameter of particles (m)	$2x10^{-6}$	
First-order rate constant for oxygen (m/s)	$8.3x10^{-10}$	Jaynes *et al.* 1984b
Diffusion coefficient of oxygen in water (m^2/s)	$1.0x10^{-11}$	Jaynes *et al.* 1984b
Recharge value (m/y)	0.25	
Water column depth (m)	5	
Simulation time (year)	2 - 5	
Number of iterations	24	
Cell numbers	30	
Size of each control volume (m)	0.17	

The results of the numerical model were compared with field observations, as well as a simple mathematical model. The incorporation of advection and hydrodynamic dispersion processes was introduced to verify the results of a geophysical study, which included a potable ABEM 2000 for very low frequency data as well as geo-electrical data measured by an ABEM SAS 100 C instrument. The survey comprised of very low frequency data on six (6) profiles downstream of the waste dumps showing transportation of the pollutants through the downstream of the waste dumps. The results of the numerical model, mathematical model and geophysical survey was in close agreement with the associated identification of pollutant transport from the waste dump, thus this method of modelling achieved close agreement with field observation and can be used for designing an effective environmental management program.

3. Study Area

3.1 East Rand Basin background

The East Rand Basin located within the Gauteng Province includes the towns of Nigel, Springs and Germiston. Gold mining covers an area of 56 091 ha, although currently production is only a fraction of what was historically mined (Hansen, 2014:25). The East Rand Basin's main land use is regarded as urban and suburban development, with areas of agricultural land within the southern part, compromising of maize and stock farming practises. The mining in this area grew throughout the 1940's and 1950's and according to Scott (1995: 19) most of the mines were closed during the 1960's. Presently most of the mines are inactive and mining has ceased, with the exception of reworking of the current TSFs present. The three main reefs mined included the Black Reef, Kimberly Reef and the Main Reef. Mining and the associated surface rock piles, sand and TSFs has resulted in an increased salt load to streams, rivers and the groundwater environment.

The study area is located within the East Rand Basin, which is primarily mined for gold (Figure 3). The East Rand Basin has an Aerial extent of 561 km^2 and consists of many geochemical environments (Côte, 2010; Barthel, 2008). According to Scott (1995: 5) the reefs have a shallow basin-like structure, that covers 768 km^3 including municipal districts from Springs, Nigel, Heidelberg, Boksburg, Benoni and Brakpan. This basin is distinctive from other mined basins in the Witwatersrand, because it differs geographically and geohydrologically. Scott, 1995: 20) defined the East Rand Basin as a relatively shallow, lagoon-like extension of the main Witwatersrand Supergroup Basin.

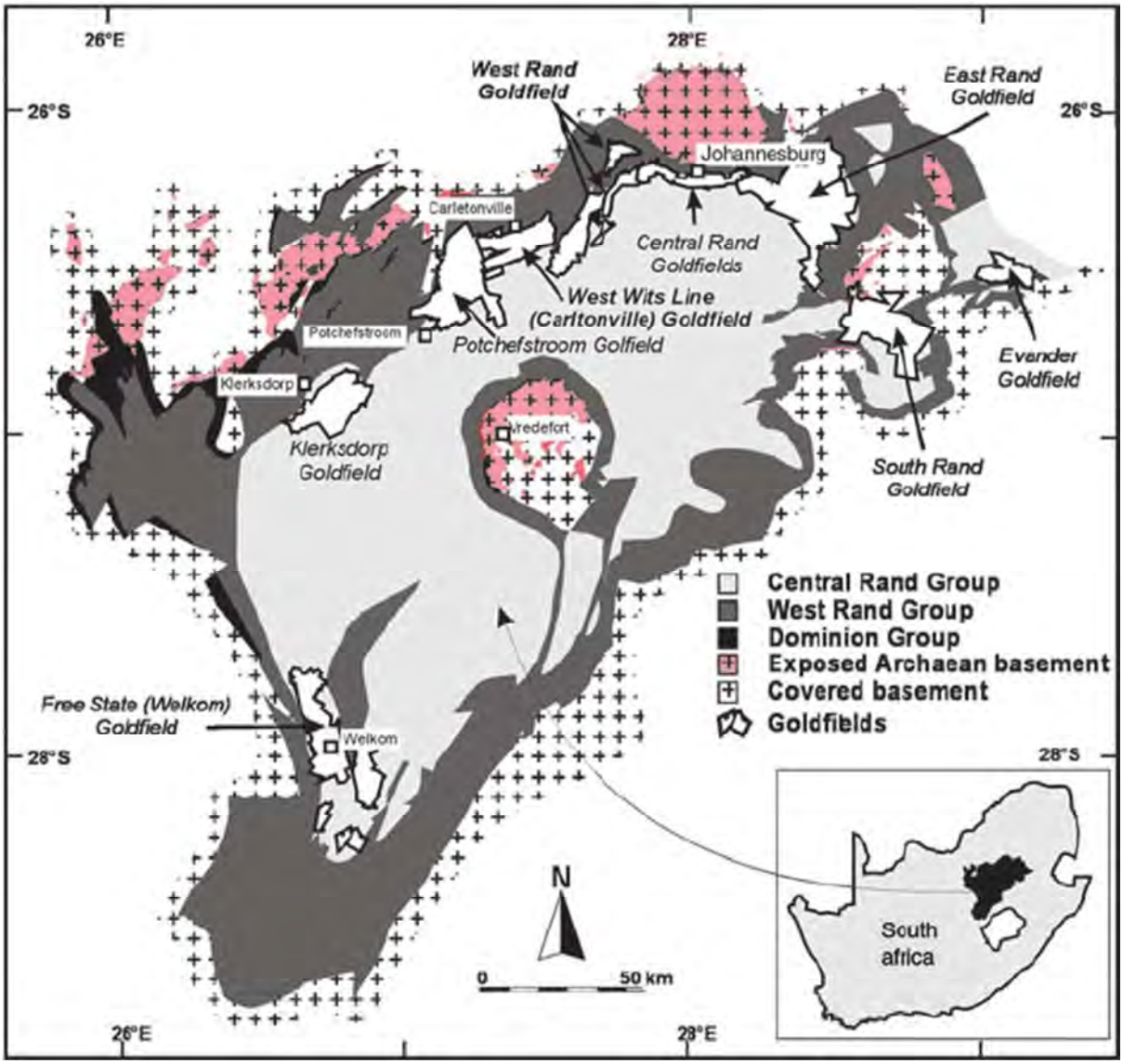

Figure 3: Distribution of Witwatersrand Supergroup goldfields located in the East Rand basin (Manzi *et al*., 2012, Dunkert & Hein, 2010).

3.2 Disposal of wastes within the East Rand Basin

Frostner and Wittmann (1976: 43) explained that the total waste disposal cumulatively mined by the end of 1972 from the ores was approximately 3.15 billion metric tons. The waste included waste rock, cyanided sand and slimes, surplus water and sulphuric acid. The waste rock has commercial value and is frequently used as concrete aggregate or rail-ballast. However, several of the slimes dams are currently remined. The tailings not only consist of slimes residue, but various other effluents from the mine as identified by Frostner and Wittmann (1976: 43). These residues can include excess pollutants in solution from the treatment plants or surplus groundwater. According to AngloGold Ashanti (cited by Oelofse *et al.* 2008:1), the majority of tailings within the Witwatersrand basin are unlined and not vegetated. This results in atmospheric pollution by dust and eroded tailings that contaminate the nearby rural areas. The continuous leaching of heavy metals and constituents from these tailings causes acidic conditions that are aggravated by discharge of effluents to storm-water drains and furrows effecting or reaching the surface and groundwater.

3.3 Investigated sites within the study area

3.3.1 *Tailing Storage Facilities and Waste Rock Dumps*

In general the tailing storage facilities in the East Rand basin are relatively old, contributing to hard outer surfaces with vegetation growth from rehabilitation practices. The TSFs have often undergone extreme weathering, resulting in weathering gullies, visible on the side's slopes of the tailings. A map of the relevant features is present in Figure 4.

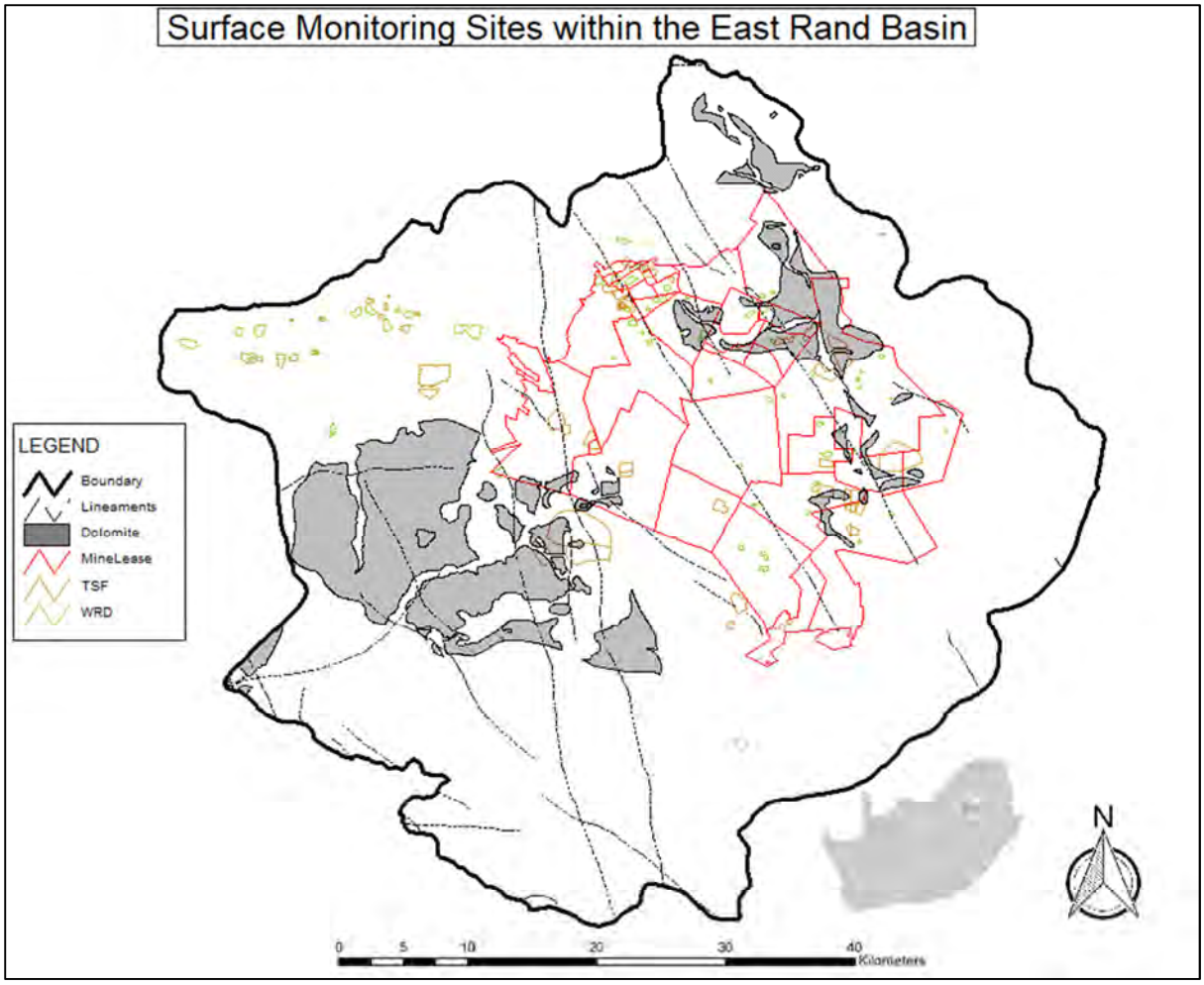

Figure 4: TSF and WRD locations within the East Rand Basin

3.4 Topography and Drainage

According to Rademeyer (2007: 172) the regional topography is relatively flat and some areas are gently sloped with isolated higher areas. The low gradients of the related streams in this area are also an indication of the flat topography, resulting in swampy rivers as stated by Scott (1995: 17). The most conspicuous topographic features in this area are anthropogenic, consisting of Tailings Storage Facilities (TSFs) that are currently being reworked into two mega tailing dams. The topography of the East Rand Basin as determined by light detection and ranging (LIDAR) survey, is relatively flat lying with an average elevation of 1602 m (maximum height of 1710 m – minimum height of 1492 m) (Hansen, 2014: 25; Rademeyer, 2007: 172).

The difference from the highest point (Duduza) to the lowest (Blesbokspruit exit point) is 120 m. The low gradients of the related streams in this area are also an indication of the flat topography. According to Scott (1995: 16) two stream systems drain the study area and includes the Blesbokspruit system, draining the northern and eastern portions, while the Riet Spruit drains the central and western parts of the this area. The Blesbokspruit catchment covers 1427 km^2 while the Riet Spruit occupies 820 km^2 (WRC, 2005: 55). The digital elevation model of the East Rand Basin, including the gold field area, drainage and quaternaries are presented in Figure 5.

The East Rand Basin consists of four quaternary catchments, with the mean annual recharge, precipitation and evaporation for the study area is summarised in Table 3 (WR; 2005).

Table 3: *East Rand Basin summary per quaternary catchment* (*WR, 2005*)

Name	Quaternary Catchment	Area (km^2)	Mean Annual Precipitation (mm)	Mean Annual Evaporation (mm)
East Rand Basin	C21D	445.8	698	1625
	C21E	628.2	690.7	1625
	C21F	426.6	703.7	1625
	C22B	391.5	691.4	1630
	C22C	465.2	683.8	1625

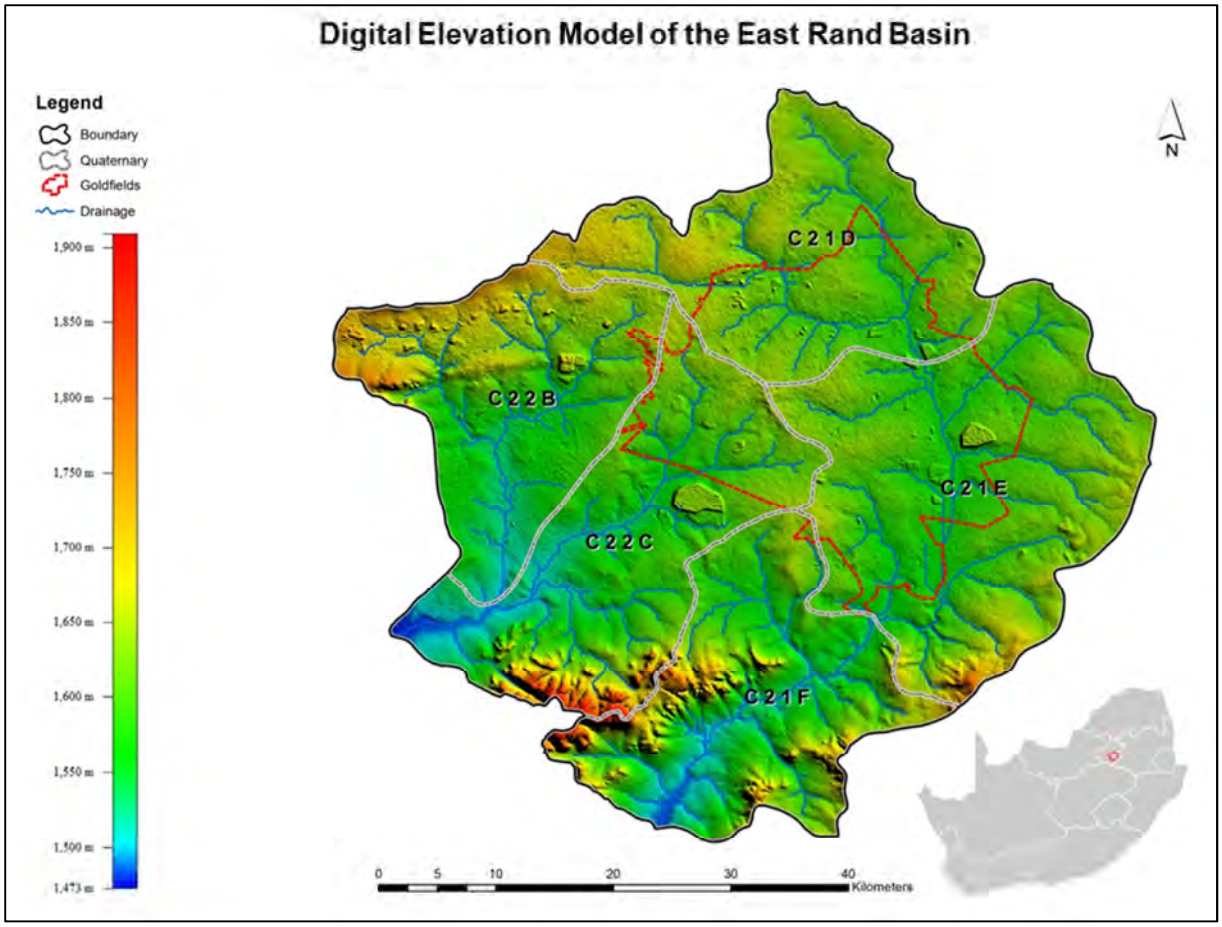

Figure 5*:* Digital elevation model of the East Rand Basin, including the gold field area, Drainage and quaternaries.

3.5 Climate

3.5.1 *Rainfall*

Rademeyer (2007: 167) describes the rainfall of the East Rand Basin as highly seasonal, where precipitation over the eastern Gauteng follows an annual cycle. It is within a summer rainfall area with an average annual precipitation of 684.1 mm as recorded by the Department of Water Affairs (DWS) from 1959 to 2017. Figure 6 represents the average rainfall figures. Rainfall occurs primarily during summer and is related to October to April, where winter months are generally dry. Table 3 reflects the average rainfall per month.

Table 4: *Average rainfall data from station C2E007 between 1959 to 2017 (DWS, 2017)*

	Jan	Feb	Mar	Apr	May	Jun	Jul	Aug	Sep	Oct	Nov	Dec	Total
Ave rainfall (mm)	126.9	88.5	78.8	50.3	16.1	7.1	3.0	7.0	22.5	71.6	99.5	111.9	684.1

3.5.2 *Evaporation*

Evaporation rates within the East Rand Basin exceeds precipitation, resulting in a net loss throughout the year and according to Scott (1995: 18) it fluctuates between 1416 mm/year to 1765 mm/year from the Symons pan. The mean annual evaporation as retrieved from DWA (2017) is calculated at 1528.4 mm/a, while the monthly averages is presented in Figure 6.

Table 5: *Average evaporation from station C2E007 between 1959 to 2017 (DWS, 2017)*

	Jan	Feb	Mar	Apr	May	Jun	Jul	Aug	Sep	Oct	Nov	Dec	Total
Average evaporation (mm)	166.9	137.5	128.4	101.1	85.6	68.2	76.4	107.1	144.3	163.0	161.3	170.1	1528.4

3.5.3 ***Temperature***

The long-term average maximum, mean and minimum temperatures were retrieved from the South African Weather Services for data from 1951 to 2005 (Rademeyer, 2007: 168). The typical weather can be described as temperate, Highveld, including a short cold winter and hot summer as interpreted from Scott (1995: 18). The temperature in the East Rand Basin varies greatly from summer to winter, with a daily maximum of 25.6°C in January and as reported by Rademeyer (2007: 168) and a daily maximum of 16.0°C in June. Thus a great variance between summer and winter temperatures can be confirmed, with minimum temperatures that range between 14.7°C (January) and 4.1°C (June). The annual temperature variation, with respect to the average, minimum and maximum temperatures are presented in Figure 6 and Table 6.

Table 6: *The average maximum, mean and minimum temperature (Rademeyer, 2007: 168)*

	Jan	**Feb**	**Mar**	**Apr**	**May**	**Jun**	**Jul**	**Aug**	**Sep**	**Oct**	**Nov**	**Dec**
Maximum	25.3	24.9	23.9	21.2	18.6	16.0	16.5	19.2	22.7	23.9	24.1	25.0
Minimum	14.3	14.1	12.9	10.2	7.0	4.0	4.2	6.0	9.2	11.3	12.7	13.8
Mean	19.8	19.5	18.4	15.7	12.8	10.0	10.4	12.6	15.9	17.6	18.4	19.4

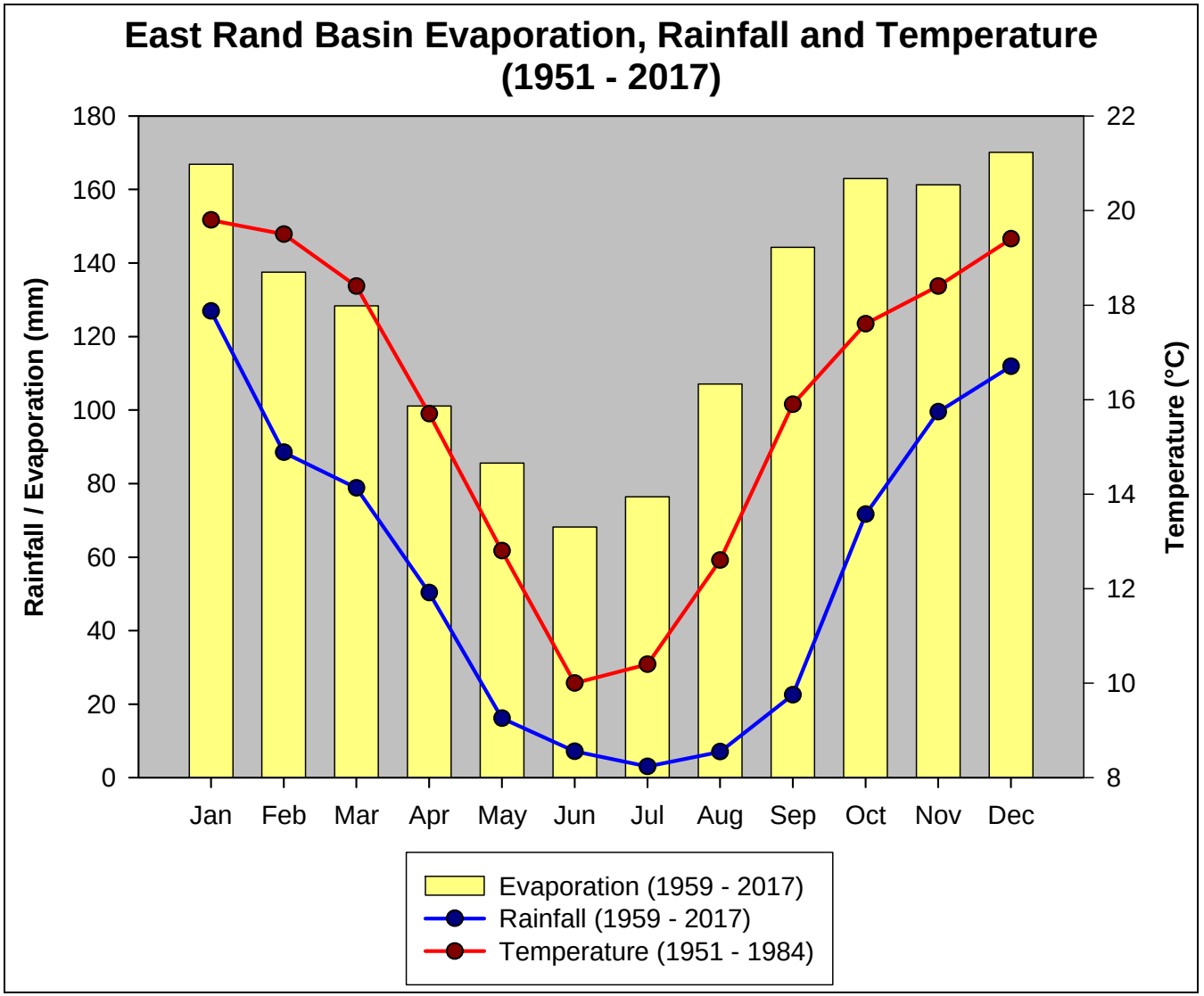

Figure 6: Average rainfall, evaporation and temperature of the East Rand Basin.

3.6 Geology

The East Rand Basin, represented by the Witwatersrand Supergroup, consists of the Turfontein and Johannesburg subgroups, belonging to the Central rand Group. The Witwatersrand Supergroup consists of repetitive layers of quartzite, conglomeratic quartzite, diamictite, shale and volcanic rocks (Figure 7 and Figure 8). Overlying the Witwatersrand Supergroup are shale, sandstone and dolomitic rocks of the Transvaal Supergroup. Scott (1995: 20) describes the sediments on the Witwatersrand Supergroup as unconformably, south-west plunging syncline, which dips at 45 degrees on the northern limb and at 25 degrees in the southern limb. The surface area is dominated by Karoo Supergroup rocks (East Rand Basin 1:250 000 Geological map).

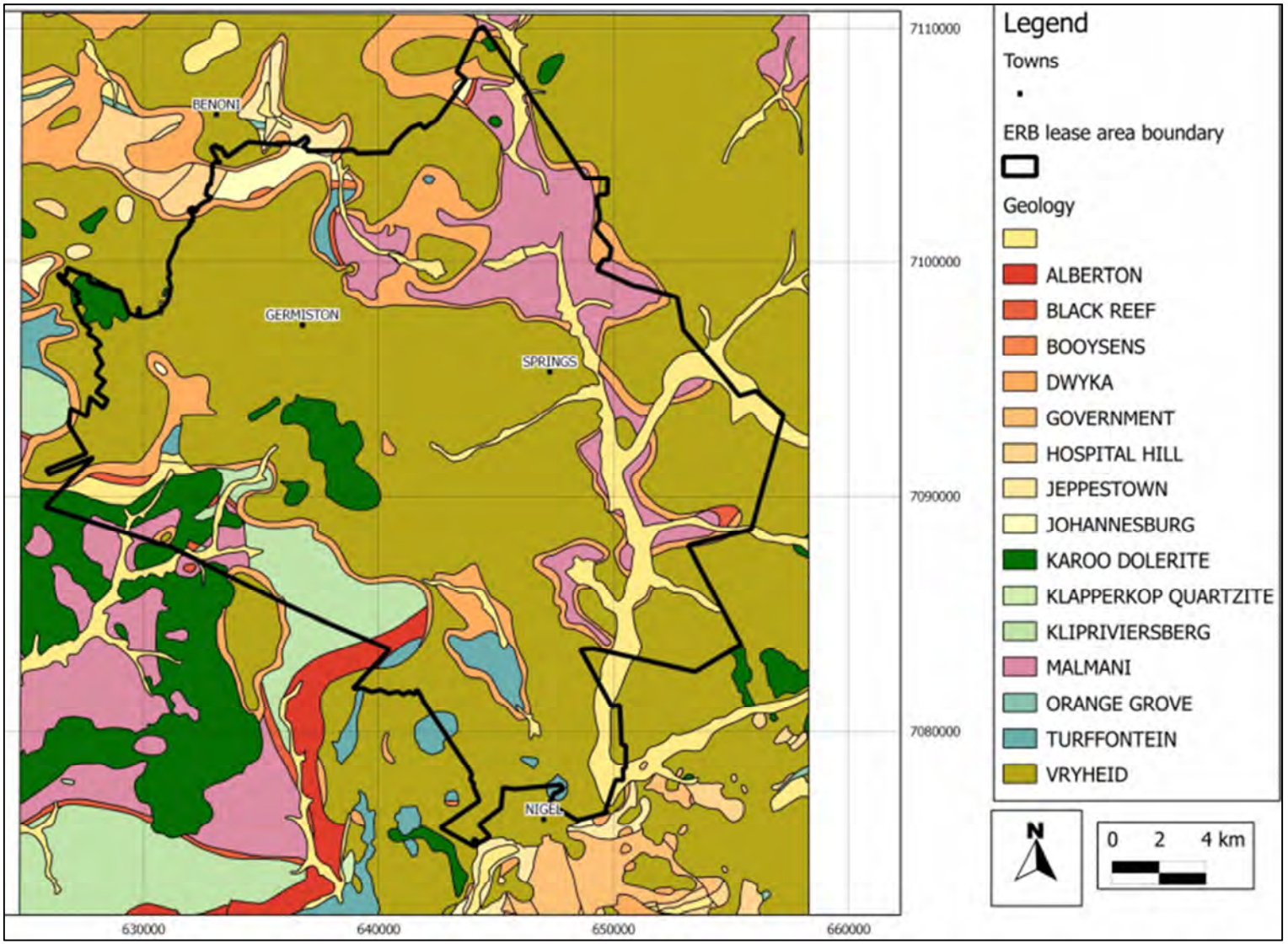

Figure 7: East Rand Basin geological map with simplified formations (Hansen; 2014: 28).

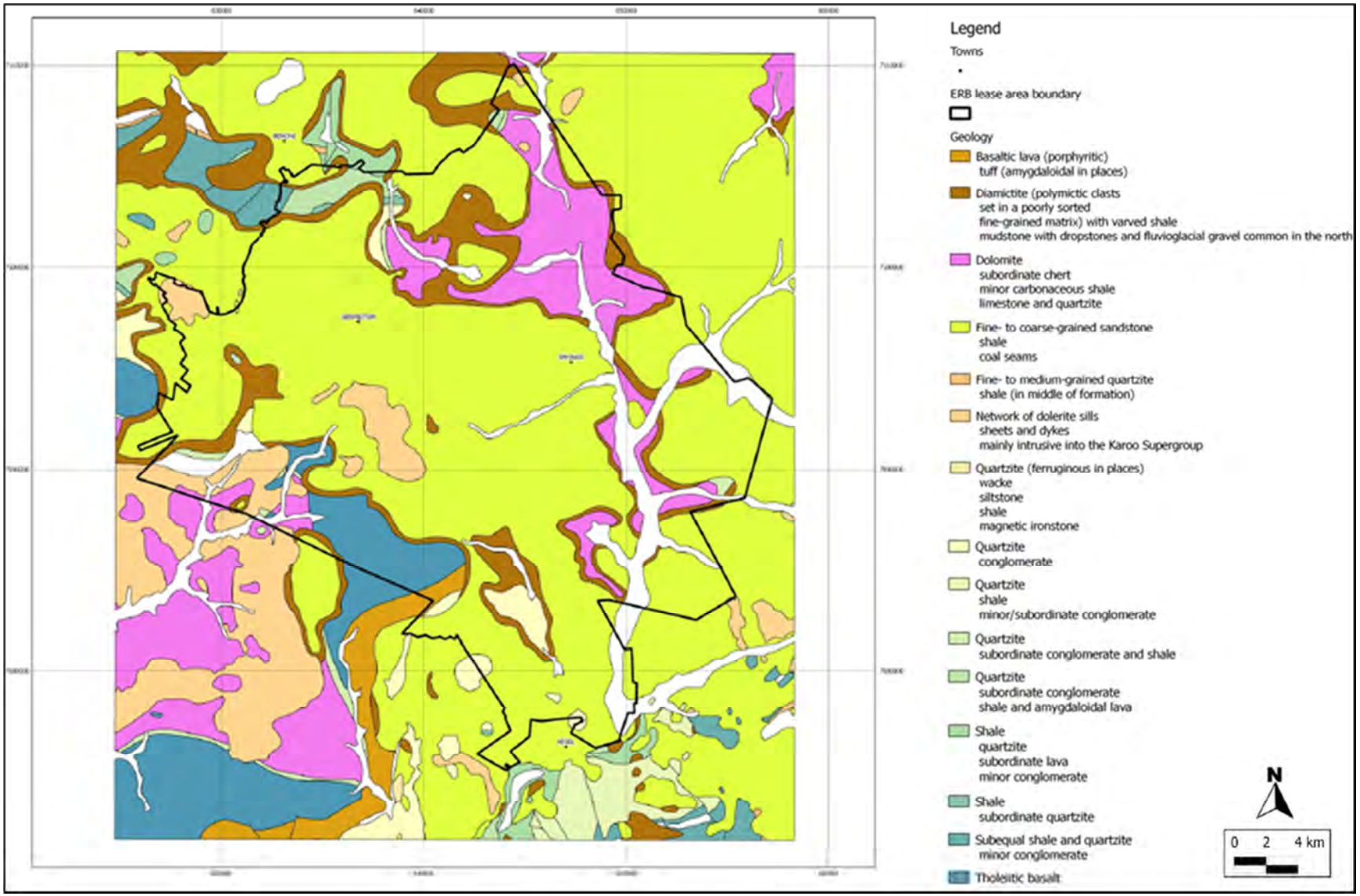

Figure 8: East Rand Basin geology descriptions (Hansen; 2014: 29).

The sediments on the Witwatersrand Supergroup lie unconformably and have been gently folded to form a syncline that is asymmetrical and plunging south-west.

The two active reefs mined within the East Rand basin is presented in Table 7, while the reef cross section is illustrated within Figure 9. Note that a third reef (Main reef) has already been mined out. Additionally, the generalised geology showing the lithostratigraphic section of the East Rand Basin, as well as the Witwatersrand Basin gold deposits is presented within Figure 10.

Table 7: *Mined reefs within the East Rand Basin (Scott, 2001: 21)*

Reef	**Status**
Black Reef	Sporadically mined
Kimberley Reef	Incipiently mined (Future mining)
Main Reef	Extensively mined (Mined out)

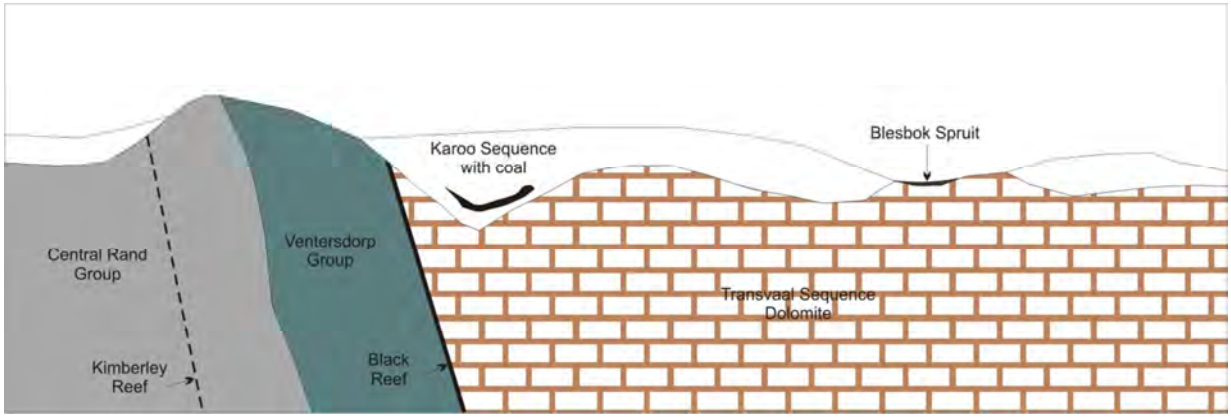

Figure 9: Cross section of the mined reefs within the East Rand Basin (modified after Scott, 2001: 23)

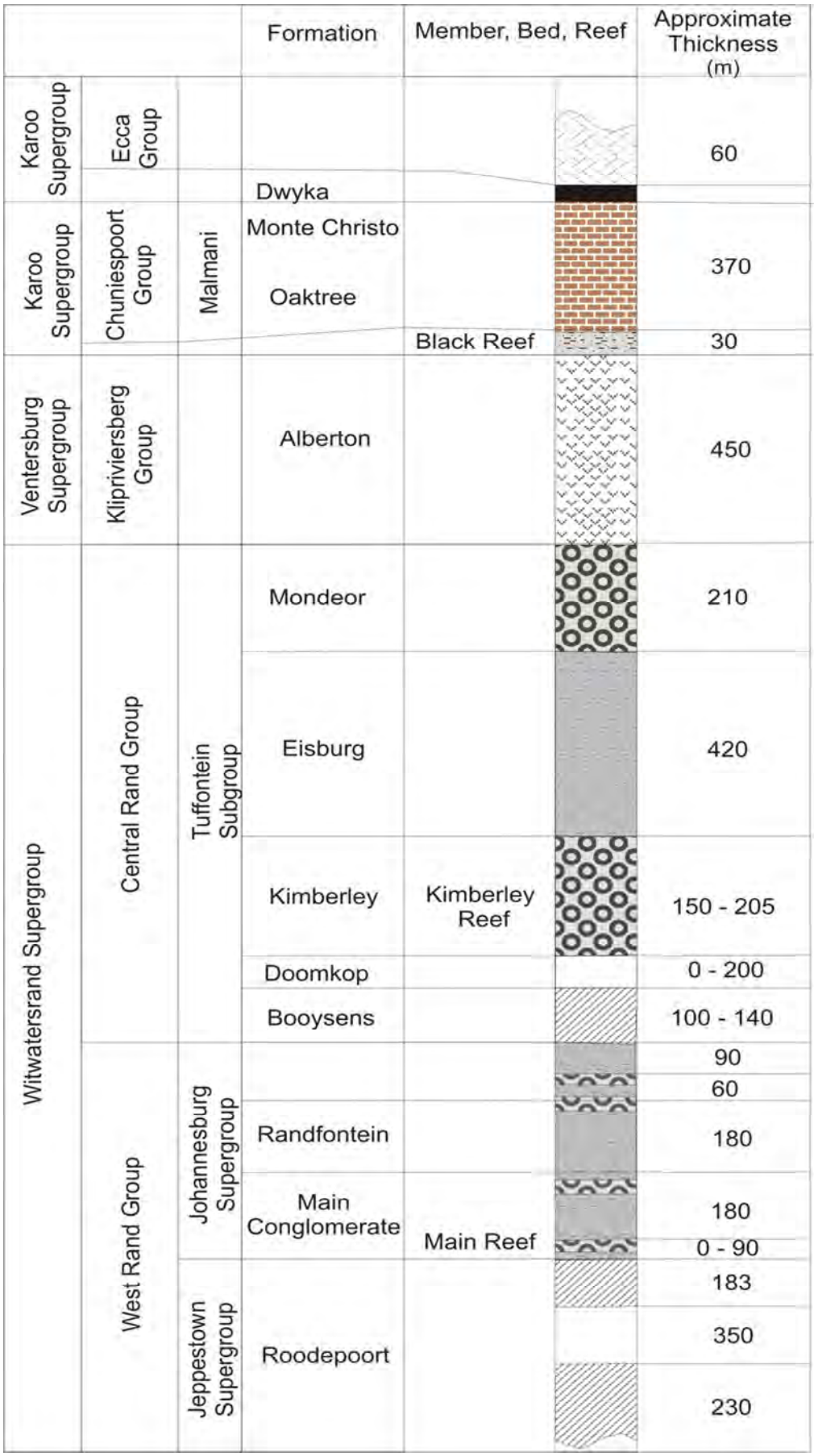

Figure 10: Lithostratigraphic Section of the East Rand Geology (after Scott, 2001: 21)

Rademeyer (2007: 171) describes that the pronounced ridges in the Germiston area consist of the Witwatersrand Supergroup sediments, which outcrop within the region.

Scott (1995: 23) and Rademeyer (2007: 171) also explains that the western portion of the study area is overlain by rocks from the Ventersdorp Supergroep, which are in turn overlain by the Black Reef Formation (Quartzite) and dolomites of the Malmani Subgroup (Dolomite) of the Transvaal Sequence. Surface outcrops are present where a post Karoo Sequence is exposed by erosion in the East Rand Basin (refer to Figure 3), which cover the older strata with unconformable Dwyka and Vryheid Formations, consisting of several coal seams.

The closure of the plunging syncline occurs in the central and eastern part of the study area, where Ecca Group sediments of the Karoo Sequence overlay Ventersdorp rocks. According to Scott (1995: 23) further east the Witwatersrand sediments are covered with the Transvaal basin compromising of the Black Reef Formation and the Malmani Subgroup.

The geology of the East Rand Basin is complex and contributes to base flow and movement within the dolomite distributions, which represent an important aquifer in the area and supplies water, seeping into the underground workings. These dolomites have a neutralising or buffering effect on the surface and subsurface water as it comprises of calcium and maintains a high pH.

3.7 Geohydrology

The geohydrology of the investigated area consists of two distinctive dolomite aquifers as illustrated in Figure 11, occurring in the northern and south-western portion of the East Rand basin. Firstly the northern dolomite of the area overlies the respective Witwatersrand sediments and as stated by Scott (1995: 24) this aquifer is up to 200m thick. A perched water table is distinctive with shallow water levels within the Green Sill, which consists of a conspicuous set of sills below 60 meters within the dolomite portion. Scott (1995: 23) describes the second aquifer as a hydraulic barrier between the Witwatersrand sediments, consisting of dolomite that overlay the Ventersdorp Supergroup sediments or rocks within the south-western portion of the area.

The Witwatersrand Supergroup is classified as a fractured aquifer system, thus the groundwater is associated with secondary fracture systems (Lourens, 2013: 272) (Figure 11), where fissures occur throughout the layer, containing great amounts of water that disappears into the cracks in the lower portions of the formation. The aquifer system is considered a low to moderate yielding aquifer system where Lourens (2013: 300) reports maximum yields of 30 l/s. Large volumes of groundwater flow into the mines as a result of fault zones within the deep gold mines (± 2000 mbgl)

The Black Reef Formation is classified as a fractured aquifer system. Low transmissivities were recorded for quartzites in the Black Reef Formation. This formation generally acts as a barrier for groundwater flow from adjacent lithologies. Groundwater movement is generally from the Black Reef Formation towards the dolomite, where the gradient is steeper through the quartzitic rocks when compared to the dolomitic formations (Van Dyk & Kisten, 2006). Dolomites in the vicinity are extremely cavernous in certain portions with respective sinkhole development.

The rocks weather to sandy soil that may locally promote recharge, while groundwater generally discharges through springs or seeps along the floors and slopes of the principle valleys. Three distinctive springs are identified by Scott (1995: 24) within these dolomites northeast of Springs (Figure 11), while several other springs are present along the streams, with a swampy description due to the flat topography and low gradients.

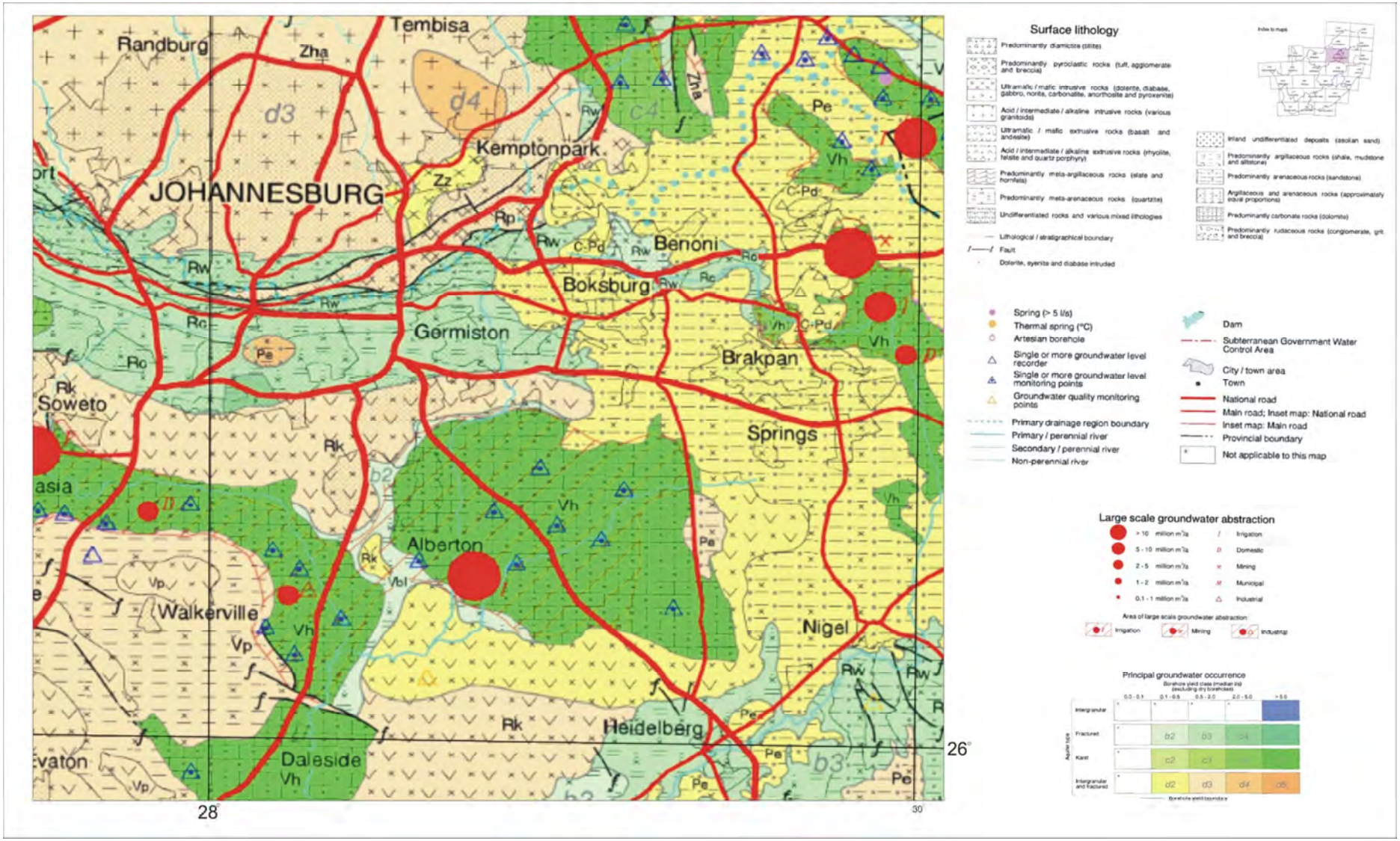

Figure 11: Geohydrology and aquifer types within the East Rand Basin (1:250 000 Hydrogeological map series)

Shallow water level depths ranging between 10 and 25 mbgl are reported for the Witwatersrand Supergroup. Generally deeper water levels are associated with hills (Lourens, 2013; 272). A groundwater flow map with associated water levels is presented within Figure 12, while static water levels and elevations are presented within a conceptualised diagram (Figure 13). A cross section within the East Rand Basin study area (East – West and North – South) was generated to infer water levels based on the monitored boreholes.

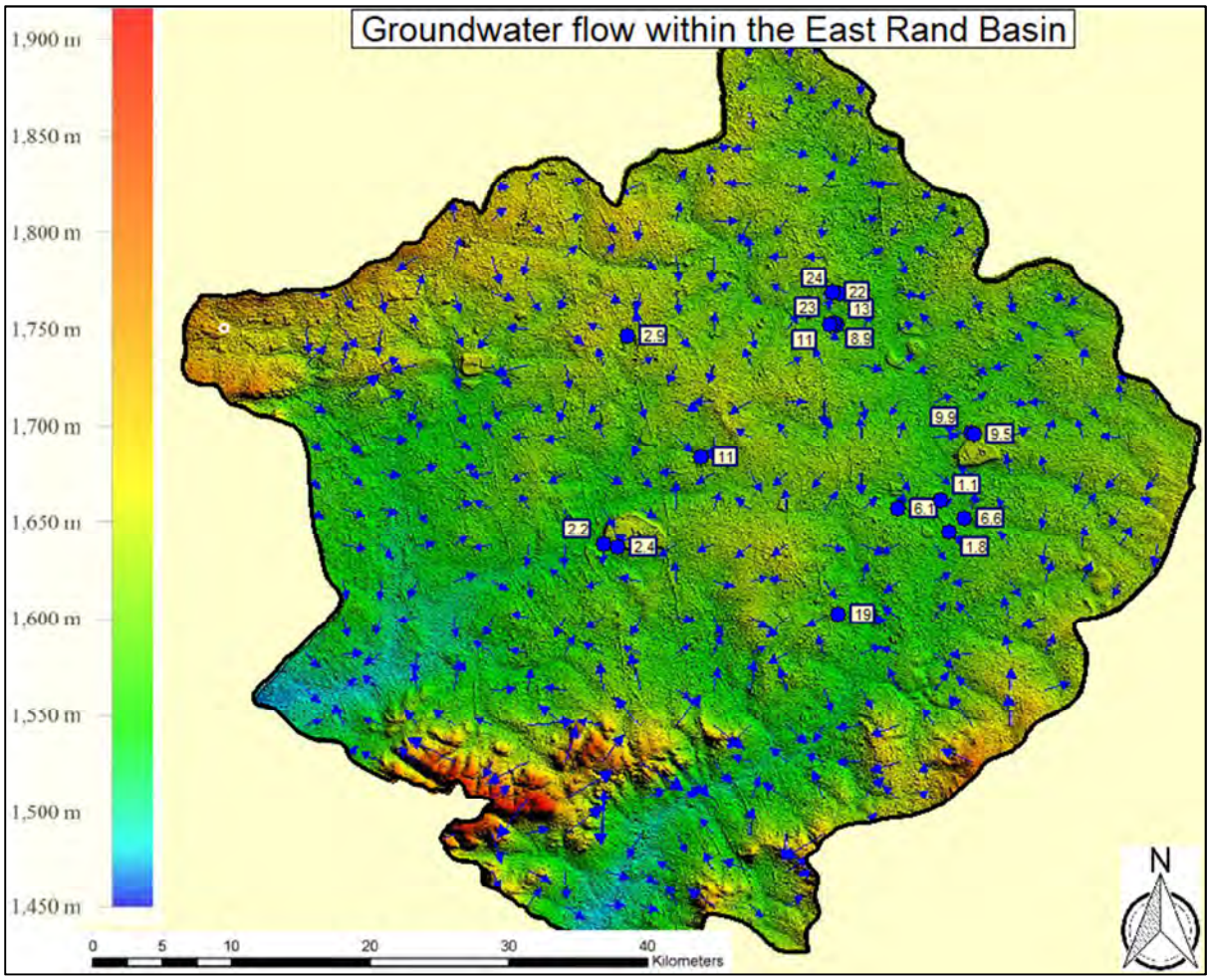

Figure 12: Groundwater level and flow within the East Rand Basin

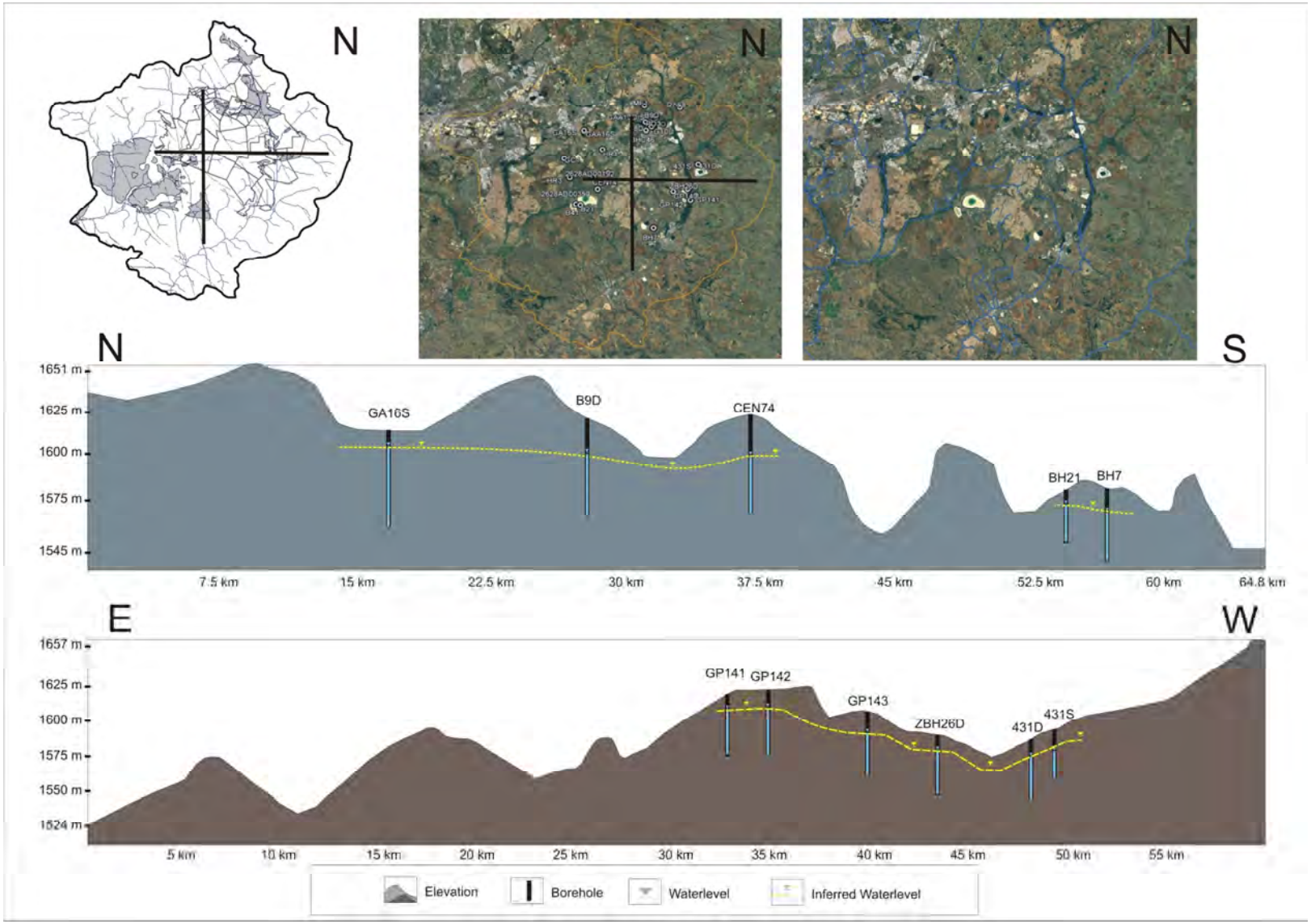

Figure 13: Conceptual groundwater level and elevation of monitored borehole

3.8 Monitoring Data

3.8.1 *Regional Water Quality*

The regional water quality of the East Rand basin is presented in the section below and includes the surface and groundwater quality. Surface water quality sites include streams and surface water bodies spread across the study area, while the groundwater quality is represented by monitoring boreholes sampled within the vicinity.

Physical and chemical water analysis (including metals) was performed on all water samples obtained. The physical water quality included the recorded electrical conductivity and pH values. These properties typically affect the aesthetic, as well as chemical quality of the water. Moreover the chemical quality of the water refers to the nature and concentrations of dissolved substances such as organic or inorganic compounds (including metals) in the water body.

Please note that due to field conditions, no pH, EC, or temperature readings were taken in situ in terms of the chemistry data. As sampling takes place over different time periods in the field, temperature will vary from samples taken at 08h00 in the morning to samples taken at midday, and late afternoon. These temperature variations will induce pH and EC fluctuations, and will ultimately make the data incomparable. Thus pH and EC readings are taken under controlled laboratory conditions to make data sets more comparable.

3.8.2 *Groundwater Quality*

The groundwater composition as described by Berkowitz *et al*. (2007: 25) is mainly controlled by chemical and biochemical interactions with the associated geology materials and incoming water. The inorganic components dissolved in groundwater are primarily in an ionic form, and thus groundwater is considered as an electrolyte solution with a varying conductance. Groundwater also contains dissolved gases and as stated by Berkowitz *et al*. (2007: 25) this is due to exposure to the surface environment, contact with the subsurface gaseous phase, and gas produced biologically below the water table. AMD contains high concentrations of inorganic pollutant and is not limited in solubility within aqueous solutions, contributing to high concentration within natural groundwater as seen in the East Rand Basin. The results of pyrite within these tailings contribute SO_4^{2-} to the groundwater as these minerals are soluble. The groundwater quality rest on the substances dissolved and the chemical behaviour of these compounds, thus the water quality or composition can

transform as it moves through the aquifer or in this case the tailings, contributing to an acidic water quality. The migration of contaminants (in this case sulphur) within the aquifers depends upon various properties of the contaminant itself and includes the aquifer geology and groundwater seepage velocity as indicated by Palmer (1992: 119).

The prominent groundwater pollution present in the East Rand Basin is mainly due to AMD Historically contaminated groundwater is a result of close situating TSFs, enabling leachate through the surrounding tailings and subsurface geology, buffering the sulphuric acid to a neutral pH, but high TDS and sulphate concentrations are observed. Scott's (1995: 25) analyses of the water quality is representative of dolomitic waters where the majority of the samples are high in HCO_3, Mg^{2+} and Ca^{2+}, expressive of simple mixing or dissolution. This was also verified by Rosner and Van Schalkwyk (1999:139). The prominent pollution compound, as previously mentioned, is SO_4^{2-} that varies throughout the area. Scott (1995: 25) explains that a natural scheme for groundwater evolution is present; however the groundwater followed a sulphate enrichment history due to contamination. The contamination of these waters can be traced to geographical locations thus being point source contamination from adjacent located TSFs. Currently the groundwater quality has already deteriorated to a degree where the viability of aquifers is threatened. Several water pollution studies from the Rand Water Board, Water Research Commission and Crown Gold Recovery indicate that the drainage systems of the East Rand Basin as well as Central Rand Basin have been polluted by AMD, resulting in high salt loads and acidic waters (Davison, 2003; Forstner & Wittmann, 1976; Jones *et al*., 1988; Marsden, 1986; Rosner *et al*., 2001; Rosner & van Schalkwyk, 2000; Scott, 1995; Tutu, 2012).

For current groundwater composition within the East Rand Basin, a hydrocensus (Appendix A) was performed and water samples were collected from different areas within East Rand Basin. The sampling protocol consisted of groundwater samples collected during three occasions during the 2013 to 2014 period. The first sampling round was done during November 2013, the second in March 2014 and the third in June/July 2014.

A total of ninety-nine (99) water samples were retrieved from boreholes on a quarterly basis, with bailers from specified depths (Figure 14).

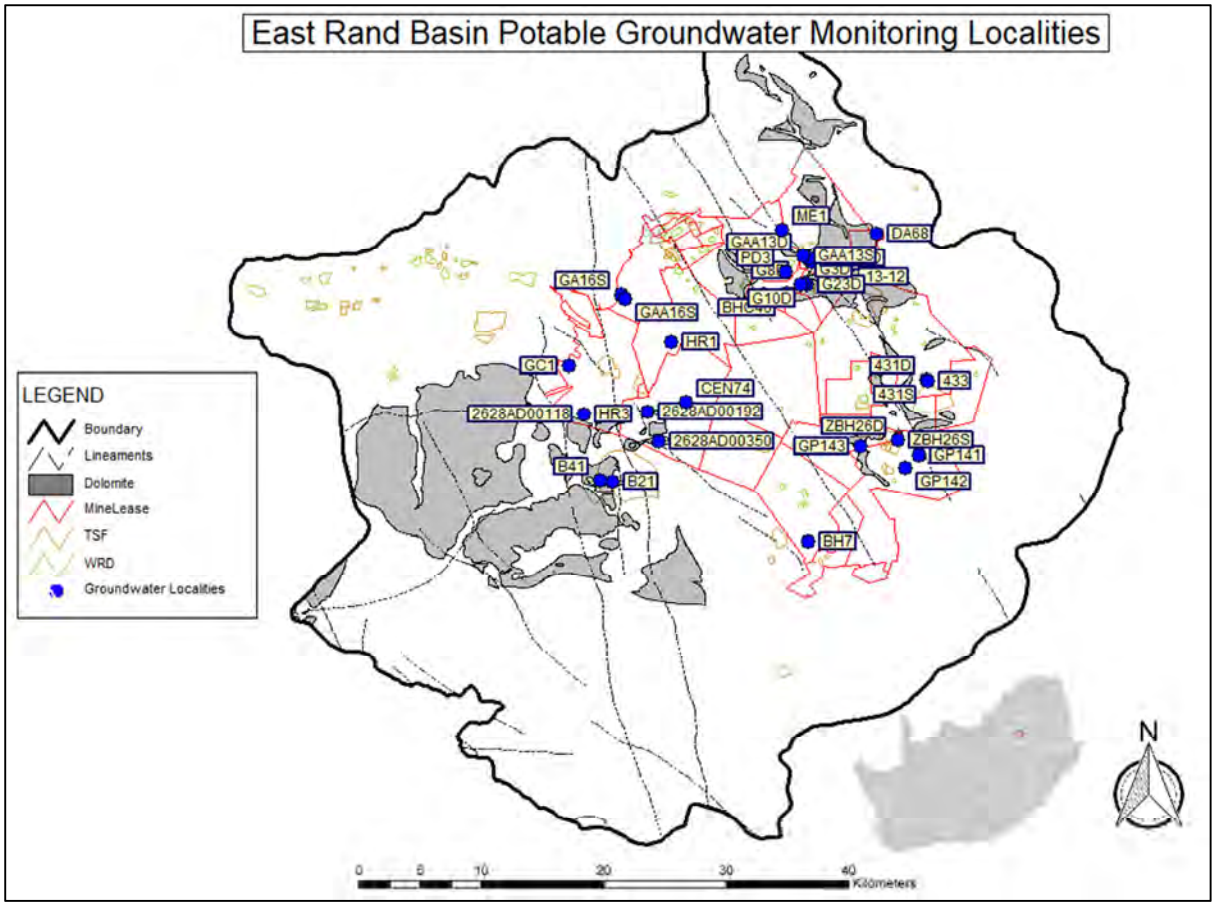

Figure 14: Monitoring borehole locations within the East Rand Basin to relevant TSFs and WRDs

The sampling depth for each related borehole was identified with an EC-meter; regarding the perforated casing for preferential flow measurements and analysis. The groundwater samples were filtered, preserved by adding HNO_3 and stored on ice, and transported to the laboratory as per Weaver *et al*. (2007: 112) groundwater sampling guide. The borehole locations based on NGA data vary throughout the East Rand Basin, although most of them have been destroyed; the current active monitoring boreholes were obtained through a hydrocensus. Boreholes in the East Rand Basin area are not purged before sampling. The International Organisation for Standardisation (ISO) 5667-11 guideline recommends that purging only be applied to boreholes being pumped, such as abstraction boreholes or water supply boreholes, while Weaver *et al*. (2007: 126) suggest boreholes that are not pumped, has to be purged before a representative sample from the aquifer can be drawn. Due to the fact that the majority of the monitoring boreholes sampled in this study are for observation purposes, specific depth sampling was implemented based on electrical conductivity profiles of the boreholes.

Each monitoring borehole was analysed via a conductivty profile to asses the optimal sampling depth. The conductivity profiles reveal an in situ evaluation or assesment of the borehole within the field, taking into account the associated salinity measurement. Electrical conductivity (EC) is a measurement of the ease with which water conducts electricity, and indicates the amount of total dissolved salts (TDS) present within the water. This in-situ field analysis method indicates the exact position of the perforated casing, identifying the received water from the aquifer to the associated borehole. These profiles are presented in Appendix B. Note that the borehole profiles that recorded a maximum electrical conductivity throughout the depth or boreholes that are equipped with a pump is not presented within the figures. All monitored groundwater site names were kept the same as used in historic reports and datasets.

Nine (9) of the monitored groundwater localities are used for domestic purposes (including potable water). With this in mind the groundwater quality is compared against the SANS 241-1:2015 Drinking Water Standard to evaluate and establish the suitability of the samples for domestic purposes (Note that a locality map is presented in Figure 15). The nine (9) representative potable water localities (collected from taps) included the following:

- 2628AD00192
- 2628AD00350
- 433
- BHC46
- DA68
- GC1
- HR1
- HR3
- ME1

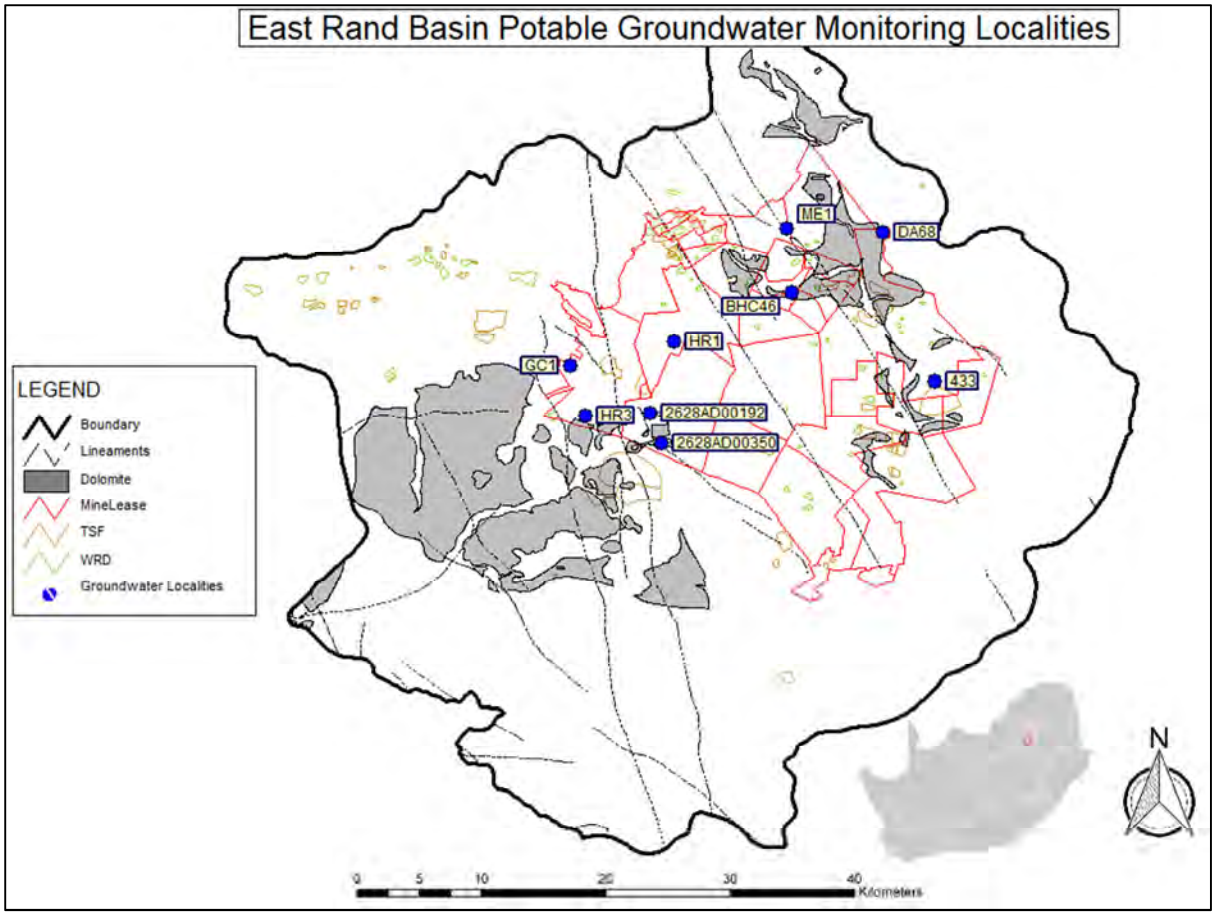

Figure 15: Potable monitoring borehole locations within the East Rand Basin

The variable concentrations obtained throughout the monitoring program (November 2013, April 2014 and July 2014) are presented in Appendix C. Note that the assesment will particularly focus on sulphate.

The pH and EC parameters are used as macro indicators of associated changes in water quality between wet and dry season. The pH and EC concentrations are presented on value maps (Figure 16 and Figure 17) with relation to the spatial distribution of the TSFs and WRDs. Additionally the groundwater quality trends can be seen in Appendix D.

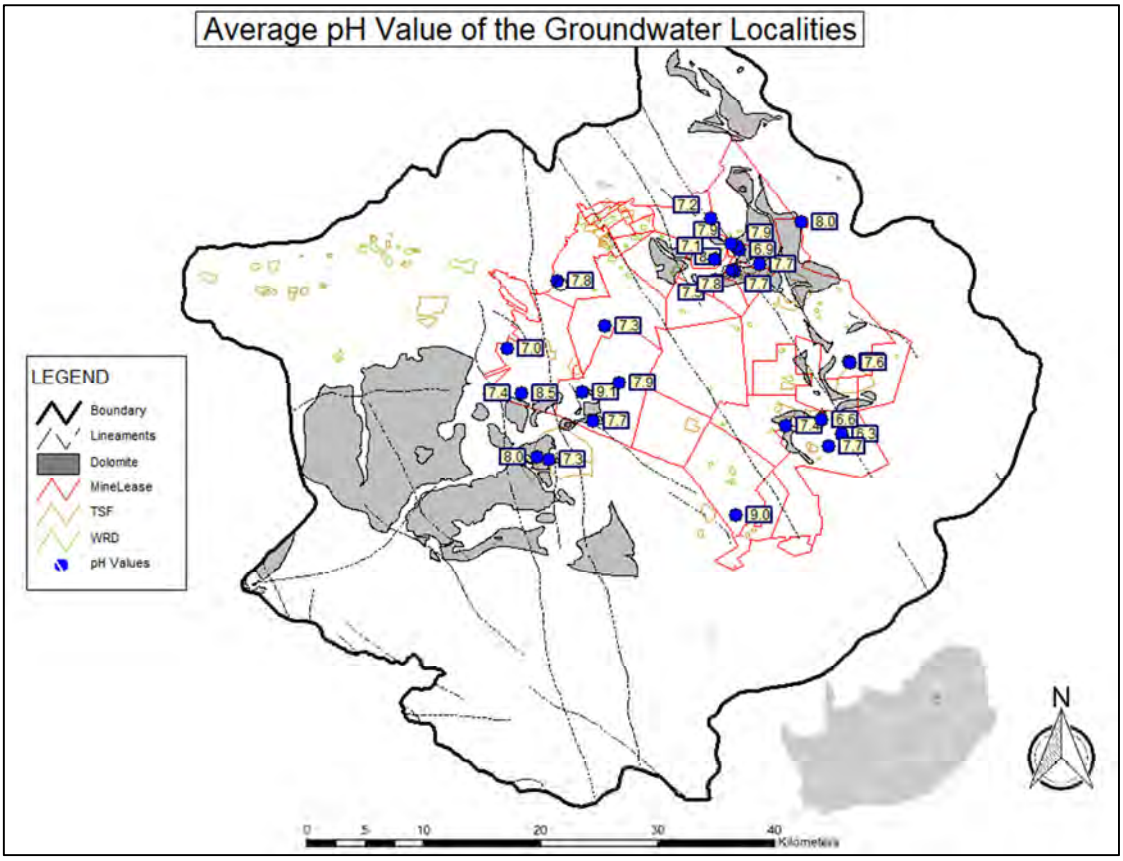

Figure 16: Average pH values regarding the monitored groundwater localities

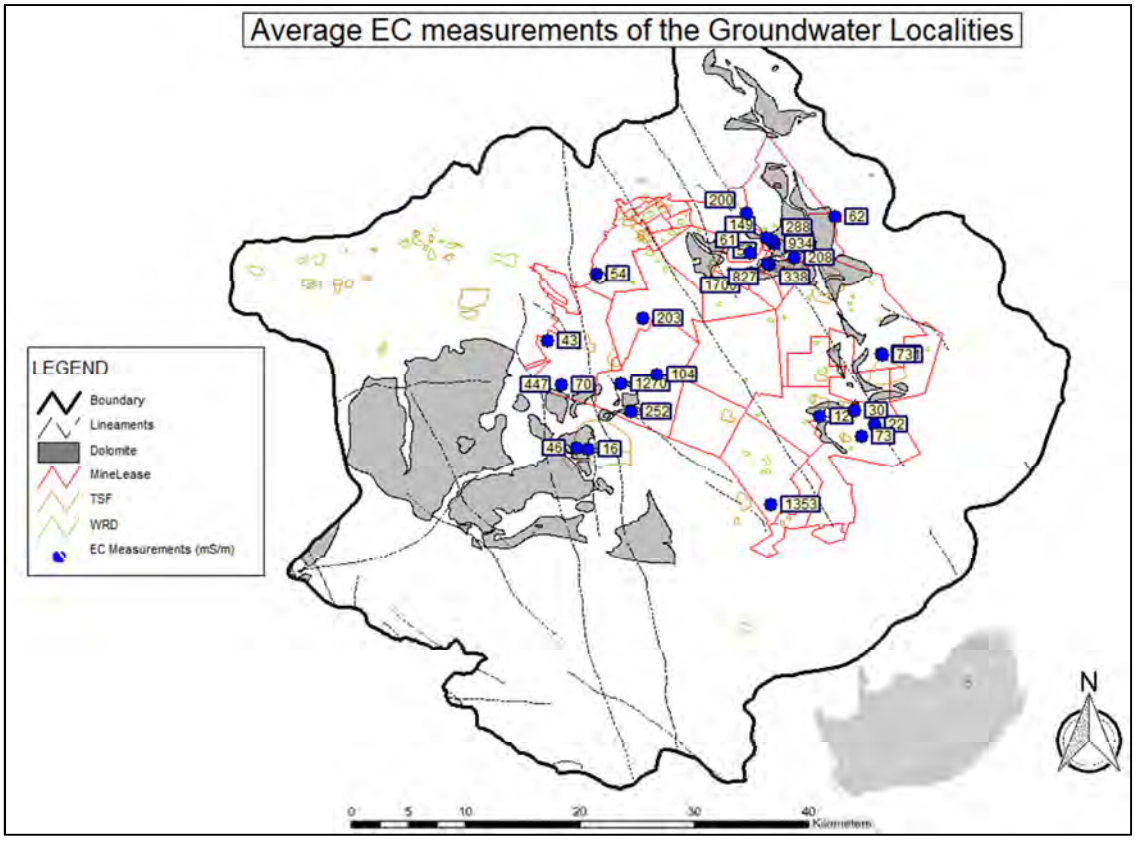

Figure 17: Average EC readings regarding the monitored groundwater localities

The stable EC concentrations from the groundwater trends (Appendix D) are to be expected when compared to the surface water salinity fluctuations; as the movement rate is particularly confined. With an increase in surface water flow, the reactivity of constituents also increases, generating additional acid or neutralising the existing acid, thus the total dissolved solids (TDS) of the water content rises.

Sulphate concentrations were extremely high during the monitoring period (Figure 18), revealing that 39,4% of all the boreholes sampled, exceeded the permissable sulphate concentration as set out by the SANS 241-1:2015 Drinking Water Standards. Due to the majority of the TSFs being unlined, the high sulphate concentrations recorded within the monitored boreholes are mainly a result of seepage from the TSFs.

The EC and Total Dissolved Solids (TDS) content of groundwater is a good indicator of the overall water quality conditions as it provides a measurement of the total inorganic salinity/salt content of the water. The elevated TDS and SO_4 content recorded is a clear indication of high salt loads and leaching within the area, emanating from the various TSF'S.

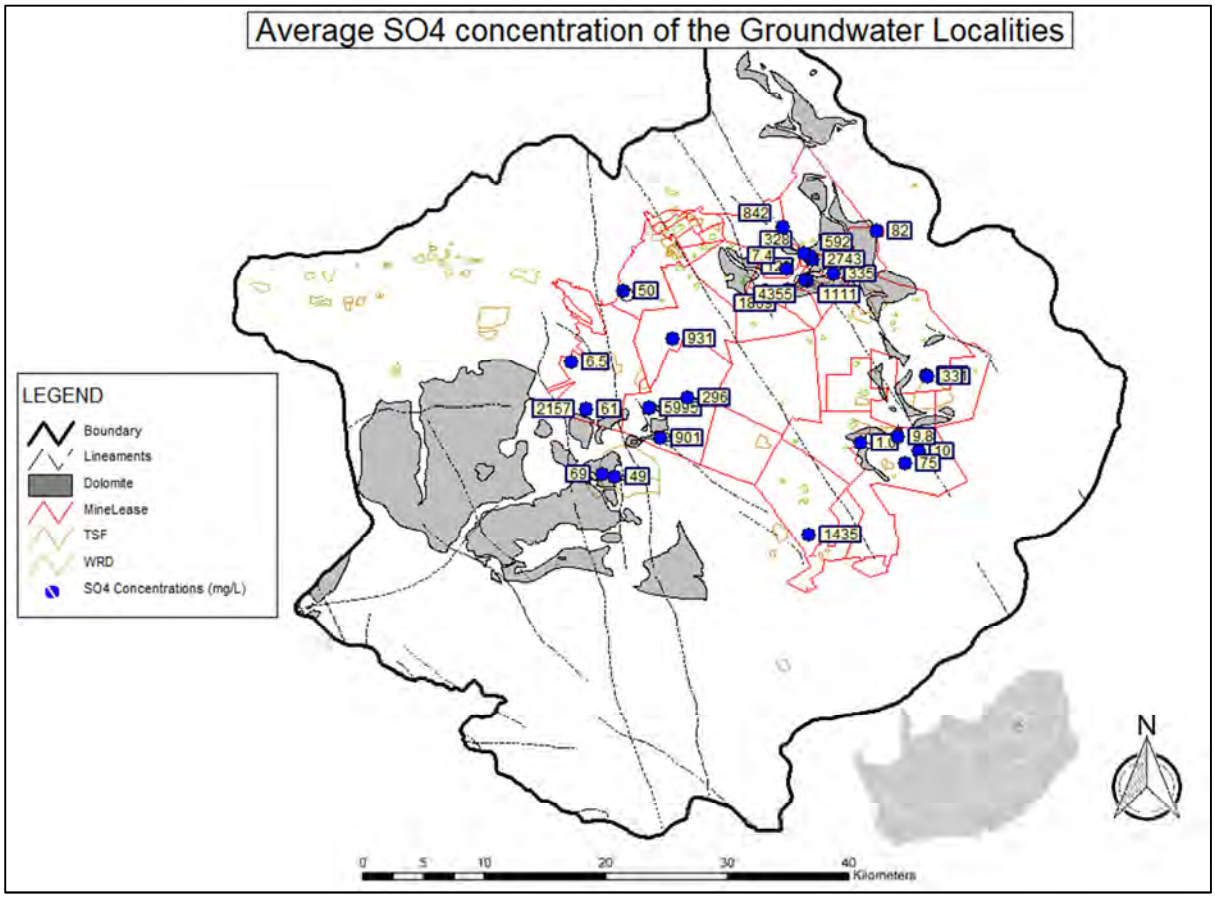

Figure 18: Average sulphate (SO_4) concentrations regarding the monitored groundwater localities

3.8.3 *Surface Water Quality*

The current surface water composition within the East Rand Basin was determined by identifying several streams and surface water bodies across the study area. The sampling consisted of thirty six (36) localities presented in Appendix E and Figure 19.

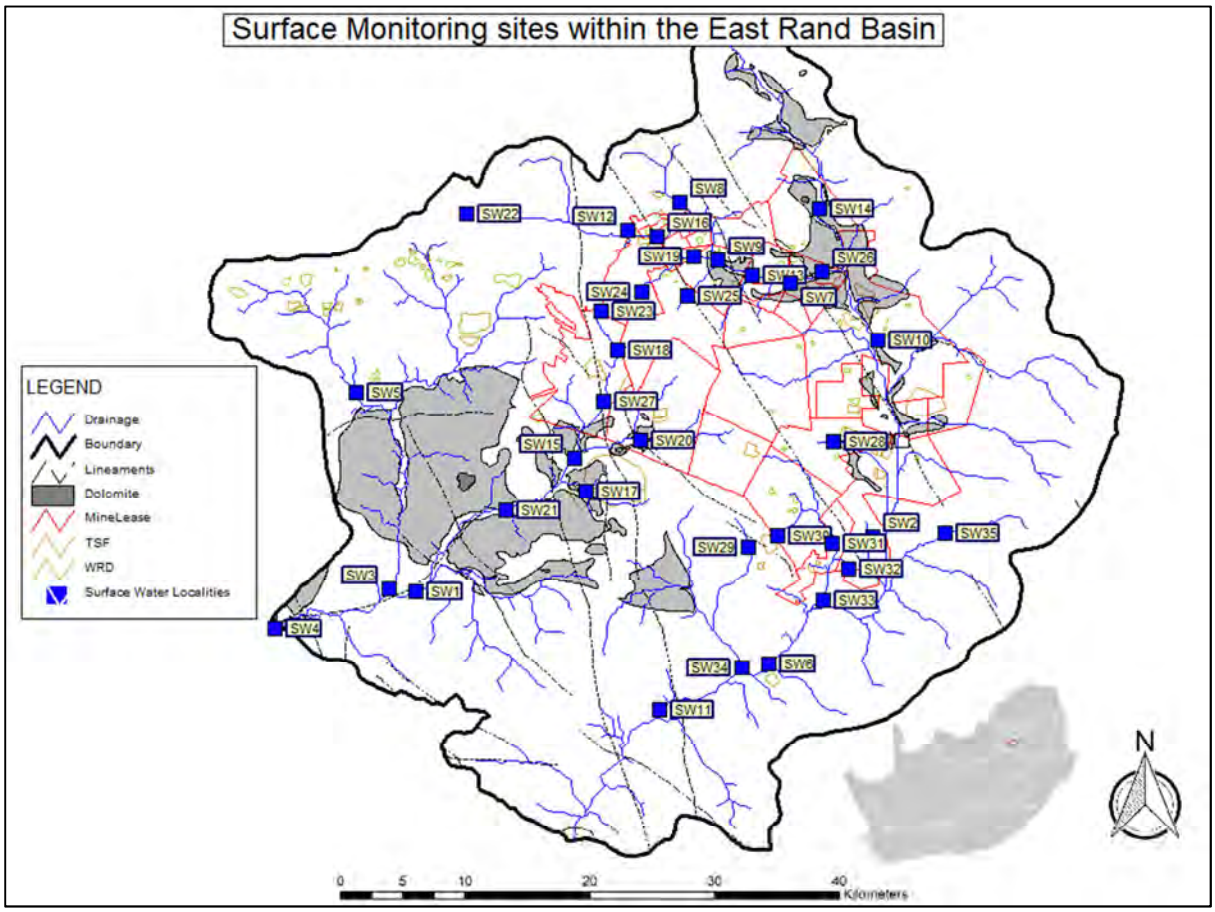

Figure 19: Spatial distribution of surface water quality monitoring sites

The variable concentrations obtained throughout the monitroring program is presented in Appendix F. The related pH, EC and SO_4 values regarding the surface water sites are illustrated in Figure 20, Figure 21 and Figure 22 respectively, while the trends can be located within Appendix G. The pH and EC values remained fairly constant seasonally, while locality SW13 presented a significant increase in water alkalinity, resulting in an improvement in physical water quality (decrease in acidity). Additionally the associated sulphate concentrations also revealed relative low and stable concentrations, while a drastic decrease was recorded from SW13, resulting in the neutral pH change observed. SW30 revealed the highest recorded EC and SO_4 value when compared to the remainder of the surface water qualities, thus it is also evident that SO_4 is directly correlated to the salinity present and may be seen as a major constituent.

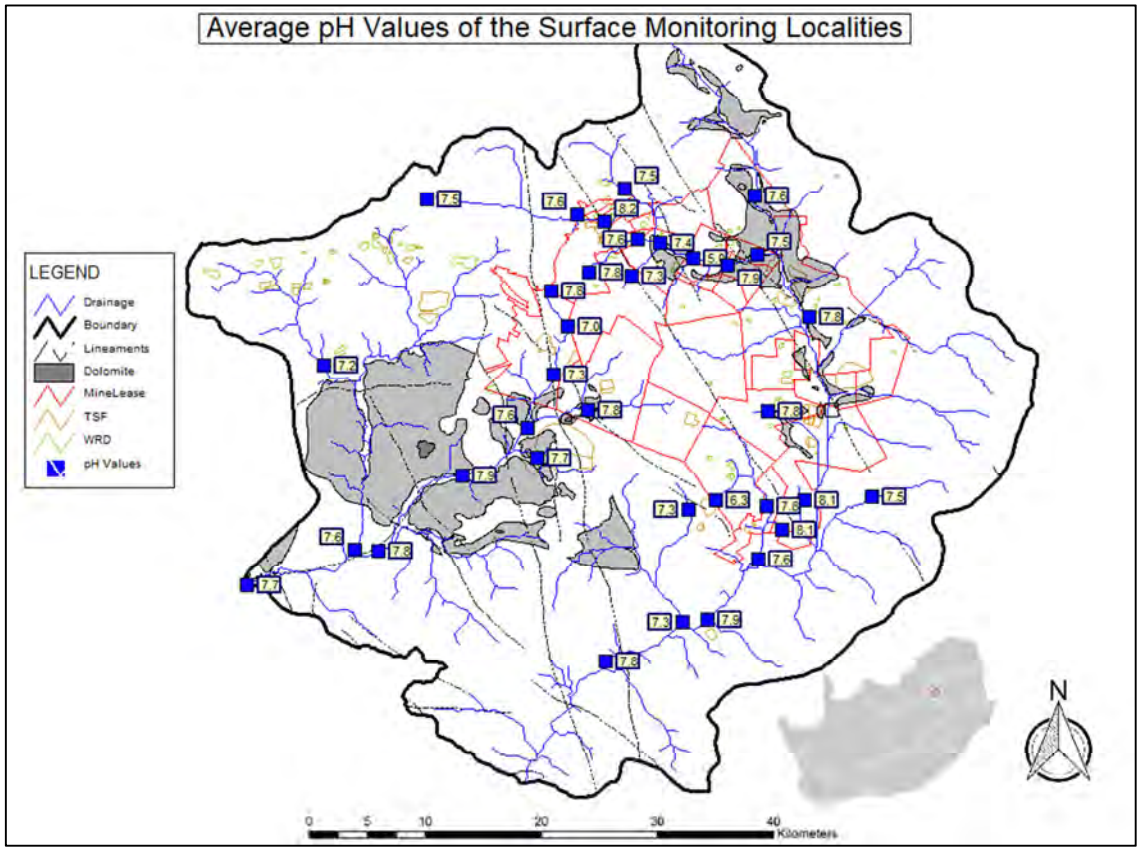

Figure 20: Average pH values for surface water quality sites

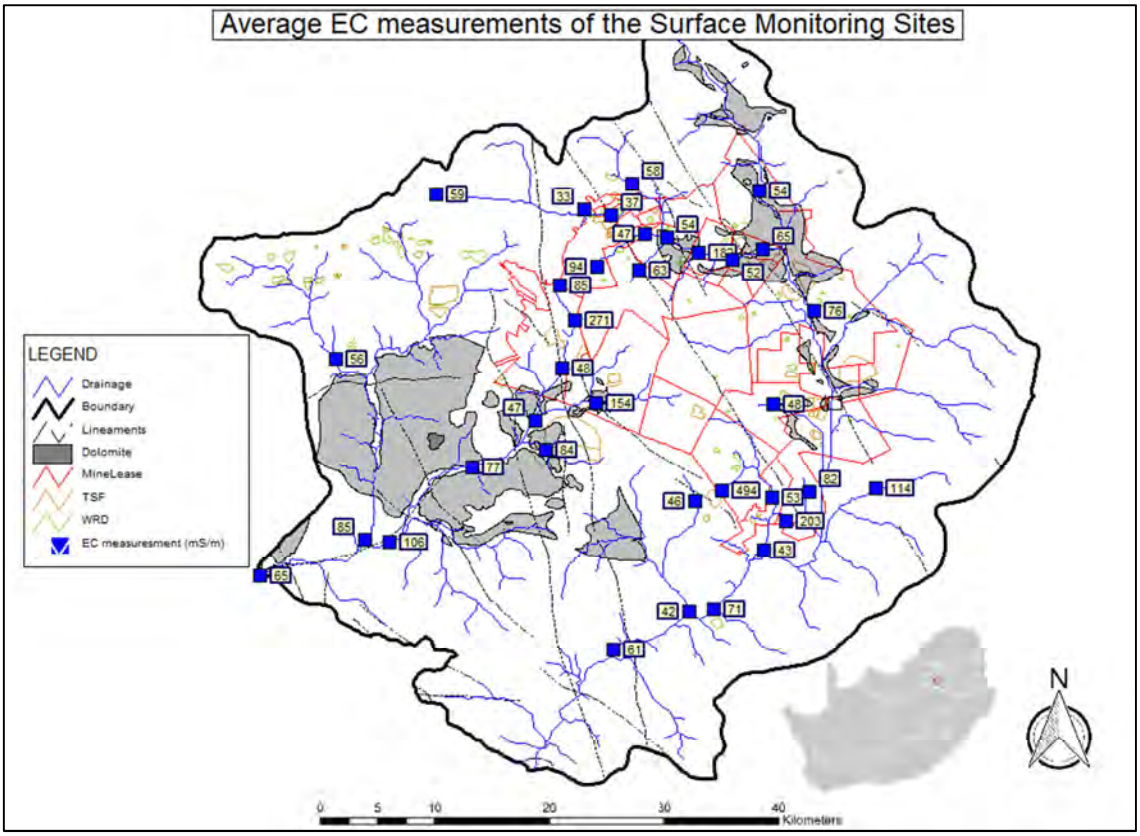

Figure 21 : Average EC measurements for surface water quality sites

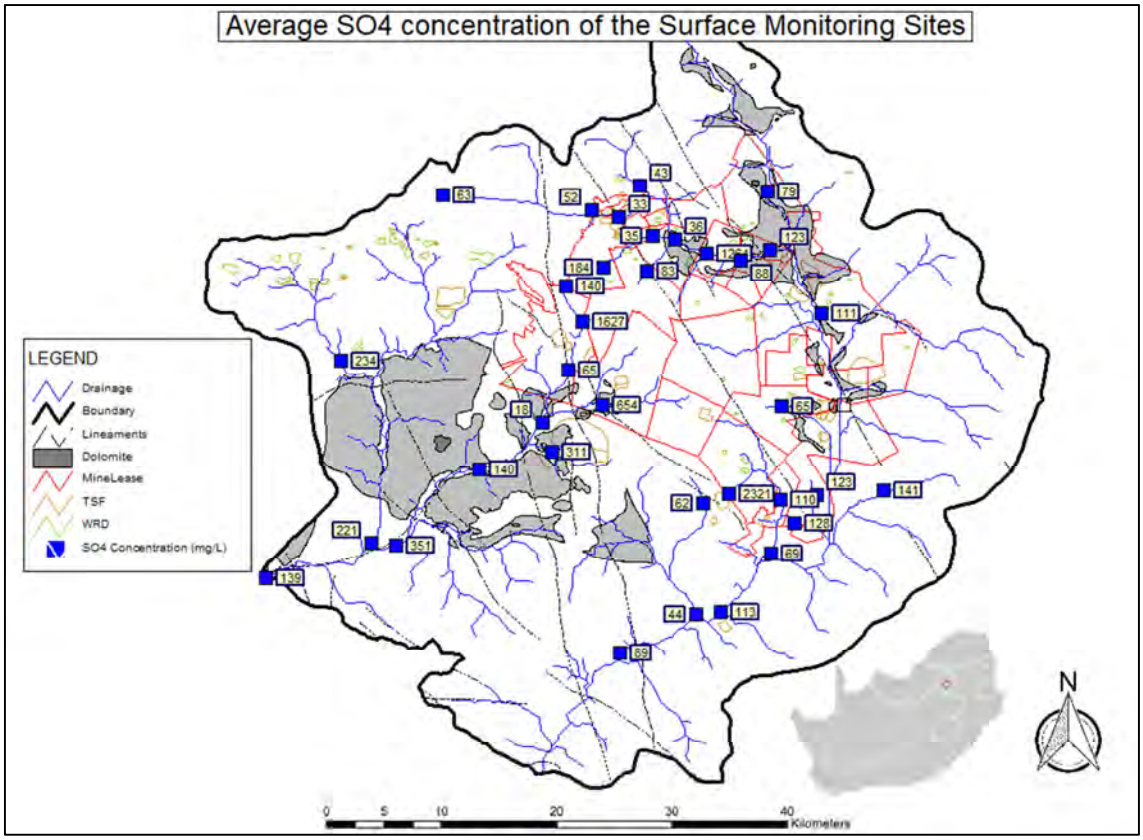

Figure 22 : Average sulphate (SO_4) concentrations for surface water quality sites

4. Methodology

4.1 Introduction

Identifying the source term will be done by using geochemical modelling through PYROX version 1.1. This software will be used with input obtained from the geochemical testing to conduct forward modelling.

The methodology that will be used in this thesis makes use of kinetic column testing or cells, which simulates the weathering of TSFs material and acid production of the unaltered environment, providing a more accurate description of acid potentials produced instead of theoretical maximums. Thus the use of kinetic column leach testing provides the evolution trends of AMD with regards to the oxidation of pyrite and the weathering rate.

According to Barnard (quoted by Nsimba, 2009: 49) the methodology process involves the following steps, regarding sampling plans and protocol:

1. Development of sampling and analysis plans
   Sampling patterns (simple, random, grid, or nested sampling).
2. Sampling and data collection
   Sample amounts, preservation procedures, field measurements and observations.
3. Data analysis
   Interpretation of the data after collection (graphs, mapping, statistics and modelling).

The general methodology steps followed within this study is presented in Figure 23 (operating flow diagram) and is based on Morin and Hutt (cited by Usher *et al.* 2001: 4).

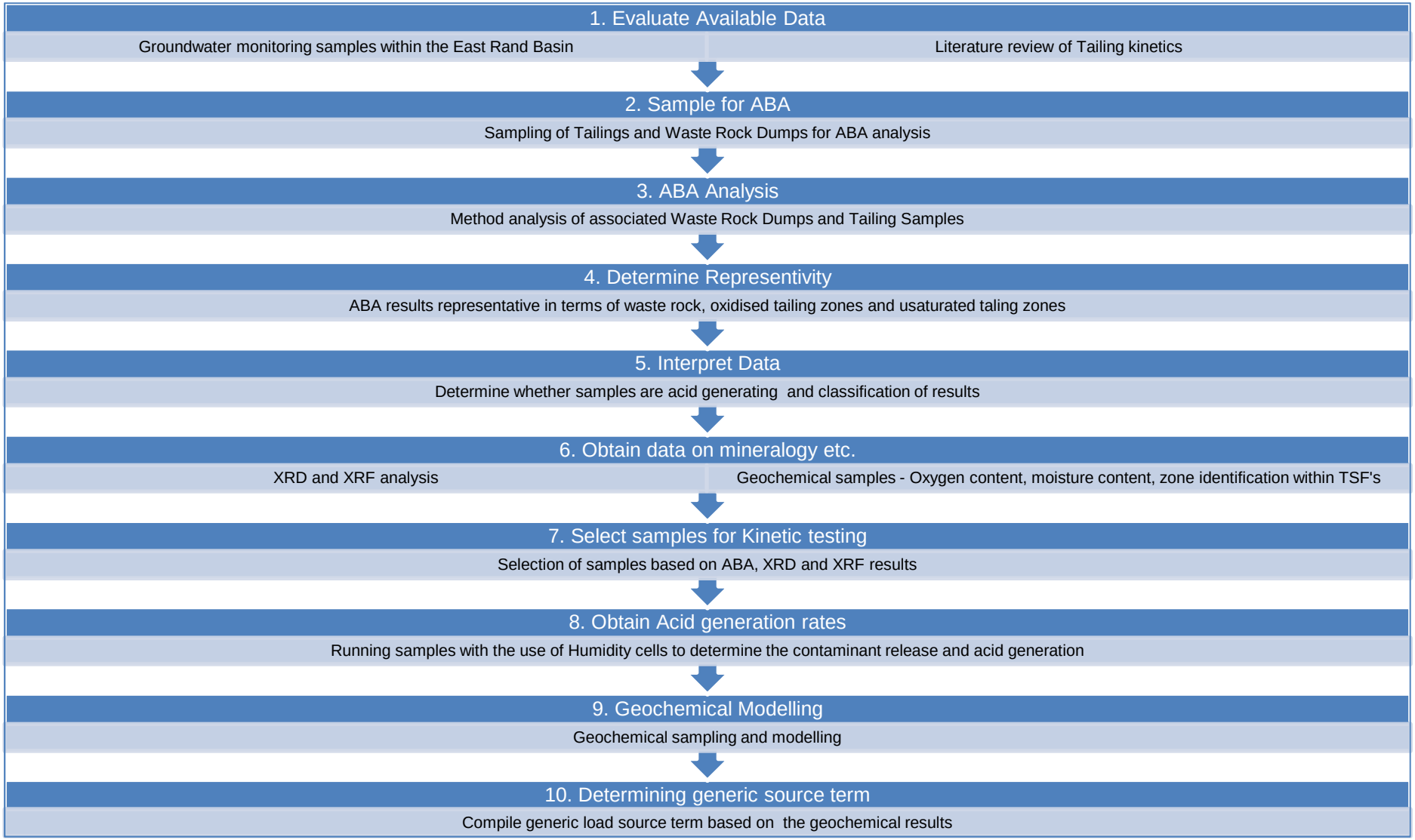

Figure 23: General method or flow path of the study (after Morin and Hutt, 1999: 5)

4.2 Tailing Storage Facility sampling

In the study area eighteen (18) TSFs were identified from different sites with twelve (12) waste rock dumps (WRDs) relative to the TSFs.

Tailing samples were collected from eighteen (18) different sites in June 2014 (refer to Figure 24). The samples were attained with an electrical operated auger and shovel. Sampling of these sites produced only four (4) samples from the anoxic zone, while a sample from each tailings dam within the oxic zone was obtained. The samples from the oxic zone were partially oxidised and weathered. The tailing sample name and co-ordinates are presented in Appendix H.

The samples were subjected to ABA, XRF and XRD to determine the chemical characteristics, after which selective tailings were subjected to kinetic leach testing.

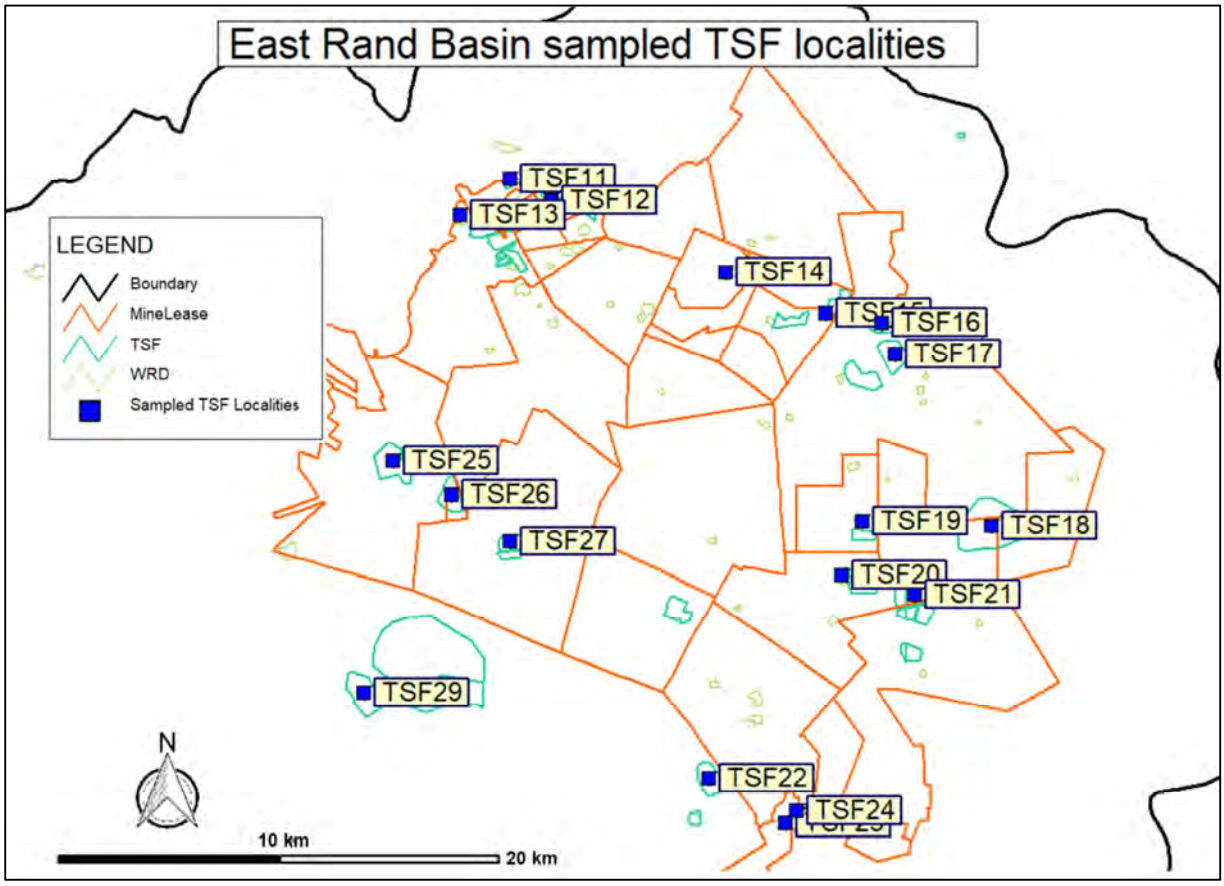

Figure 24: TSFs localities sampled within the East Rand Basin

4.3 Rock Waste Dump sampling

The waste rock dumps (WRDs) were sampled in June 2014. The location of the dumps are given in Appendix H. The waste rock dumps were grouped for sampling as they are located within the same regions, and representative of each other. Four (4) different groups were sampled and comprised of several different dumps within each group identified (Figure 25). Finally a total of twelve (12) dumps were sampled for analysis and leach testing.

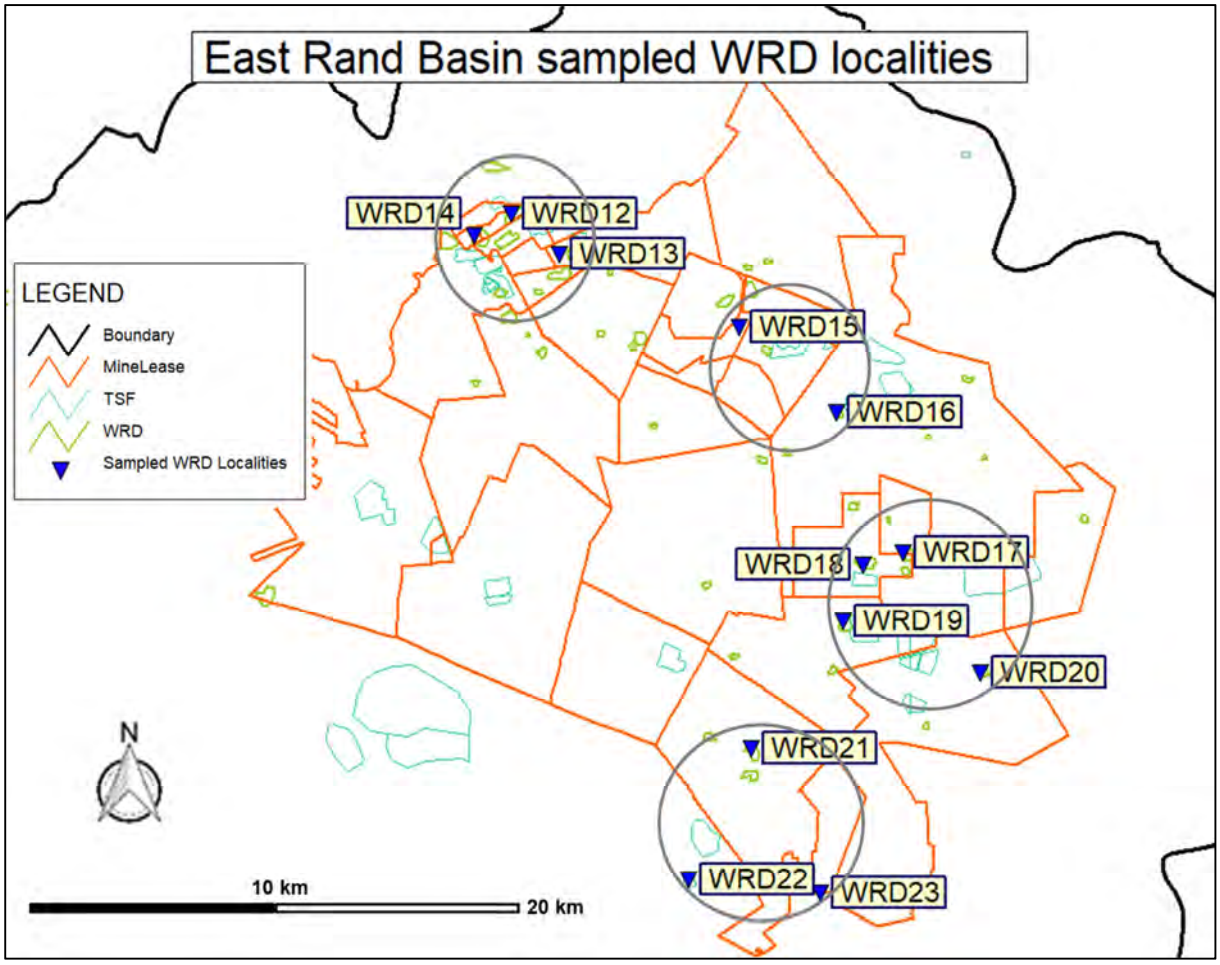

Figure 25: WRDs sampled within the East Rand basin according to grouping parameters

4.4 **Acid base Accounting (Static Test)**

According to Usher *et al.* (2001: 27) and Sherlock (1995:26) Acid Base Accounting is considered a screening procedure which determines the acid neutralising -and acid generating potential of relevant samples. Different methods of ABA test work will generate different sets of samples for evaluation (Usher *et al.,* 2001: 27). This screening procedure provides long-term prediction but no kinetic information (speed of generation), thus ABA is referred to as a static procedure. ABA tests were one of the methods of analysis used to determine the acid-base potential of the rock and tailings samples. This study makes use of the basic H_2O_2 method as explained by Usher *et al.* (2001: 10). These static tests are basically used to assess the acid producing potential by two methodologies, which are theoretical maximums of acid potential and acid neutralisation through Net Acid Producing Potential (NAPP) analysis and Net-Acid Generating (NAG) pH testing.

The use of a modified ABA procedure by Lawrence and Wang (1996) will result in more accurate data for analysis as a screening procedure for the TSFs and WRDs. This modified ABA will reduce the potential for overestimation of the neutralisation potential and according to Benzaazoua *et al.* (2004: 2) is represented by the difference between the Neutralising Potential (NP) and Acid Potential (AP) values. The method is given by Usher *et al.* (2001: 10) and broadly entails the use of H_2O_2, described in Appendix I.

4.5 XRD and XRF analyses

The tailings and rock samples were subjected to X-Ray Diffraction (XRD) and X-Ray Fluorescence (XRF) analysis to determine the different minerals present and the exact concentration of the components within these samples. The waste rock samples were finely grounded and homogenised (crushed to powder form) before analysis were performed.

The mineralogical analysis (XRD) determines the crystallographic structure and physical/structural properties of crystalline materials. In summary XRD determines the mineralogical analysis of the tailing and rock samples analysed, returning an average bulk composition identifying primary and secondary minerals present. It should be noted that all trace minerals cannot always be determined as the detection limit remains around 2% (weight percentage) of the sample.

XRF is used to determine the chemical analysis of rocks and minerals. This method comprises of the overall mineral composition of the samples, identifying oxides present from major and trace components, focusing particularly on bulk chemical analysis.

These procedures were used to group the waste rock samples according to the physical and chemical characteristics, as they are mined from the same reef with various dump localities. The tests are implemented to determine the mineralogical and total chemical analysis of the associated rock and tailings samples, which in return provides information to formulate a generic source term.

4.6 Geochemical Sampling

To model the representative source term additional geochemical fieldwork of the TSFs were conducted in the study area (NWU, 2016), and consisted of additional monitoring holes to be drilled and sampled with respect to the heaps. The sampling as per (NWU, 2016) included oxygen concentration-and moisture profiles of identified TSFs to the determining the amount and form in which sulphur is present.

Problems associated with the sampling were mainly due to inaccessibility or the TSFs were still operational, while some of the optional TSFs were too small or not yet fully developed to be classified as a tailing. A total of five accessible TSFs were sampled and equipped with oxygen chambers. The sites visited during the additional field work are shown in Figure 26 and Table 8 below.

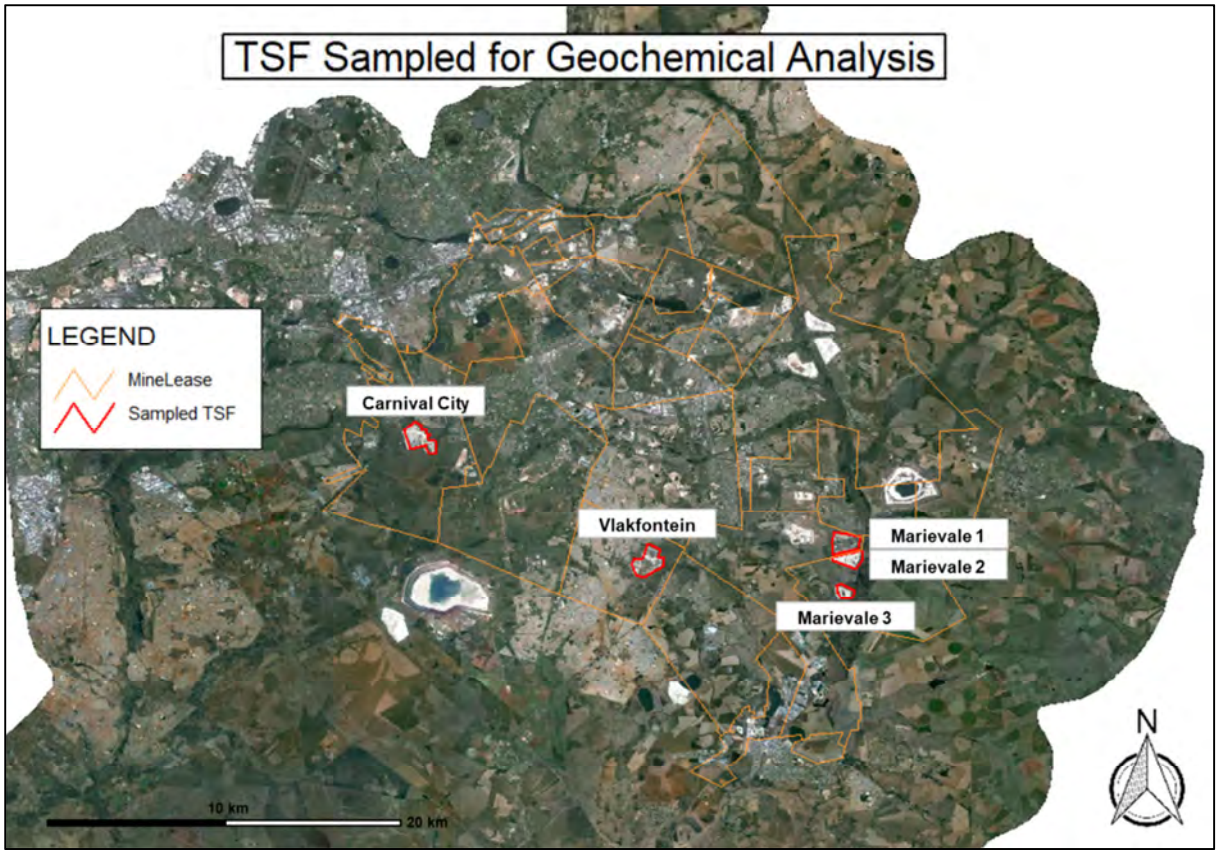

Figure 26: TSF locations of additional geochemical samples

Table 8: *Summary of TSFs visited during the additional field work (from NWU, 2016)*

Name	Status	Comment
Marievale 1	Sampled	N/A
Marievale 2		
Marievale 3		
Vlakfontein		
Carnival City		
TSF18	Not Sampled	Operational and inaccessible
TSF20		Inaccessible
TSF19*		Very small rehabilitated heap roughly 1 meter high
TSF23		Very small rehabilitated heap roughly 1 meter high
TSF24		Inaccessible, as the heap is being reworked
TSF26		Only the berms were developed

Four (4) monitoring holes were drilled by NWU (2016) to a depth of six meters, which included the Marievale 1, Marievale 2, Marievale 3 and Carnival City tailings, while another to a depth of ten meters (Vlakfontein) and equipped with oxygen chambers at specific depths. The placement depths of the holes were selected in order to measure an oxygen concentration profile. Figure 27 illustrates a schematic diagram of a borehole equipped with oxygen chambers.

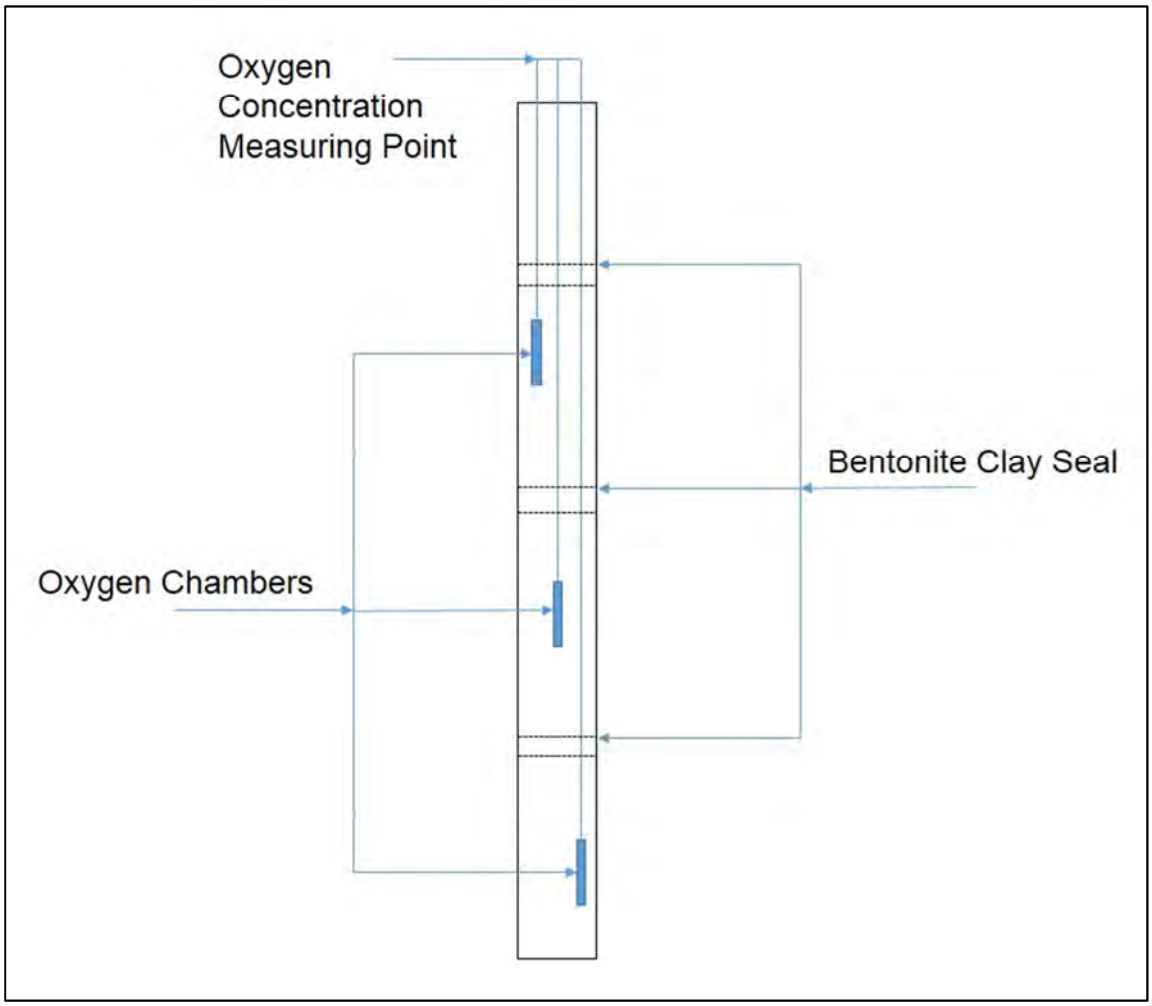

Figure 27: Diagram of oxygen chambers for measuring the oxygen concentration profile (from NWU, 2016)

Eight oxygen chambers were equipped within the six (6) meter drilled holes, while the deepest hole (10 meters) was equipped with ten chambers. All chambers were placed at 0.5 meter increments.

A total of 217 samples were taken from the representative holes and submitted to Metron Laboratory for moisture content and %S analysis (NWU, 2016).

4.7 Humidity Cells (Kinetic tests)

A variety of leaching test have been developed over the recent years to be used as prediction and indication tools regarding construction materials and wastes for long term release of pollutants, rather than a subjective pass or fail test. These tests can be classified as characterization tests, compliance tests or on-site verification tests to confirm release prediction capabilities in the field and are regarded as an important aspect of the new development of leaching tests.

Kinetic testing is described by Mills (quoted by Aphane, 2014: 34) as a group of test work procedures defining acid generation characteristics of a sample, with respect to time (in this project 9 weeks). Thus the rate of acid generation, sulphide oxidation and neutralisation are assessed, and the weathering process is accelerated to provide the effluent chemistry data. This test is a weekly leach cycle, continuing for a period of 9 weeks.

The conventional humidity cell of Sobek (1978) was used as a guideline and the cells were constructed with a height of 20 cm and diameter of 10 cm. This procedure is especially designed for mining wastes and uses a modified column as the humidity cell.

- A kilogram tailings- and rock sample was weighed and placed in the sealed plastic column;
- Dry air is passed from the bottom of the cell upwards for 3 days, followed by moist air for another 3 days;
- Every seventh day the column is flushed with 500ml of deionized water; the leachate is then collected and submitted to chemical analysis.

The air is passed through a nozzle at the bottom of the humidity cell, where the 500 ml of water is also retrieved, although added from the top region of the column, allowing percolation throughout the samples.

The leachate results are analysed and the data is used to identify the contaminant release of the TSFs, which will be geochemically modelled and incorporated to quantify a generic source term.

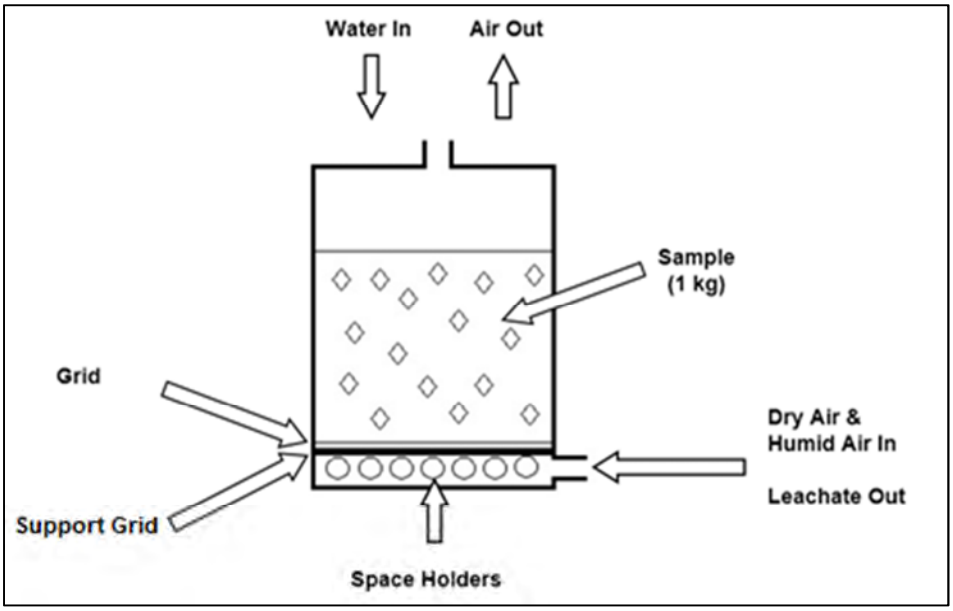

Figure 28*:* Basic schematic kinetic test cell (modified after Mills, 1998; Lawrence, 1995 and Usher *et al*., 2001)

5. Results and Discussion

5.1 Acid Base Accounting (Static tests)

Tailing and rock samples comprise of various minerals that leach into the surrounding environment. These minerals can either have a neutralising or acid producing effect which have to be identified using ABA as a screening or qualitative tool to determine specified potential.

ABA was performed on all samples obtained to provide results for Acid Potential (AP) and the Neutralising Potential (NP) of the various samples. The results produced a summary of the NNP, NPR and the total %S (percentage sulphide), calculating the NP:AP ratio of the tailing and rock samples as followed by cited by Usher *et al.* 2001. As mentioned by Aphane (2014: 55) and Usher *et al.* (2001:91) a sample will produce acid if the sulphide present is 0.3% or more, these samples will turn acidic until the sulphide minerals are depleted.

The ABA results of the tailings samples were plotted in graphs representing the Initial and Final pH versus the NNP (Figure 29) as well as the NPR versus the percentage sulphate present (Figure 30).

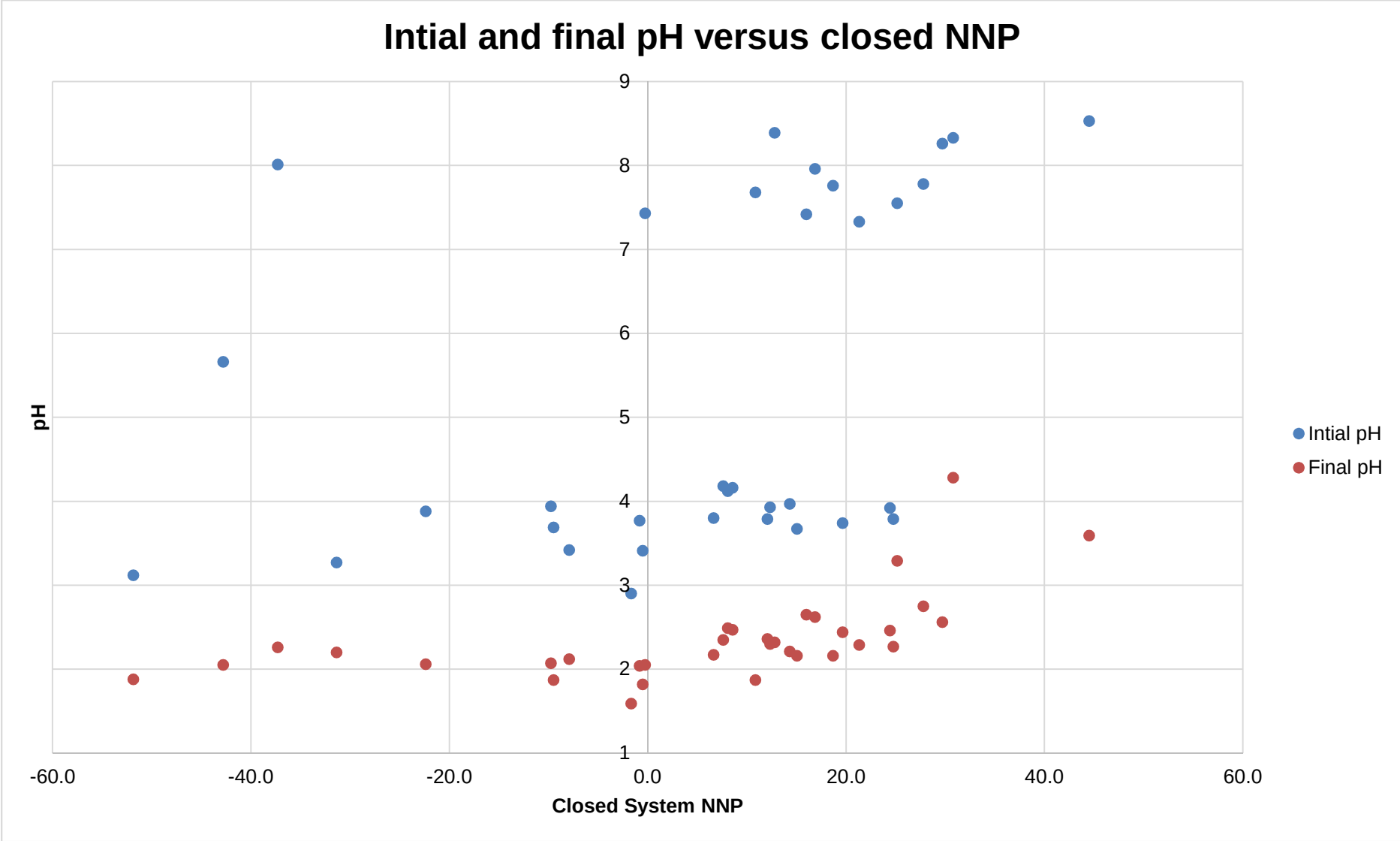

Figure 29: Initial and Final pH versus the closed system NNP

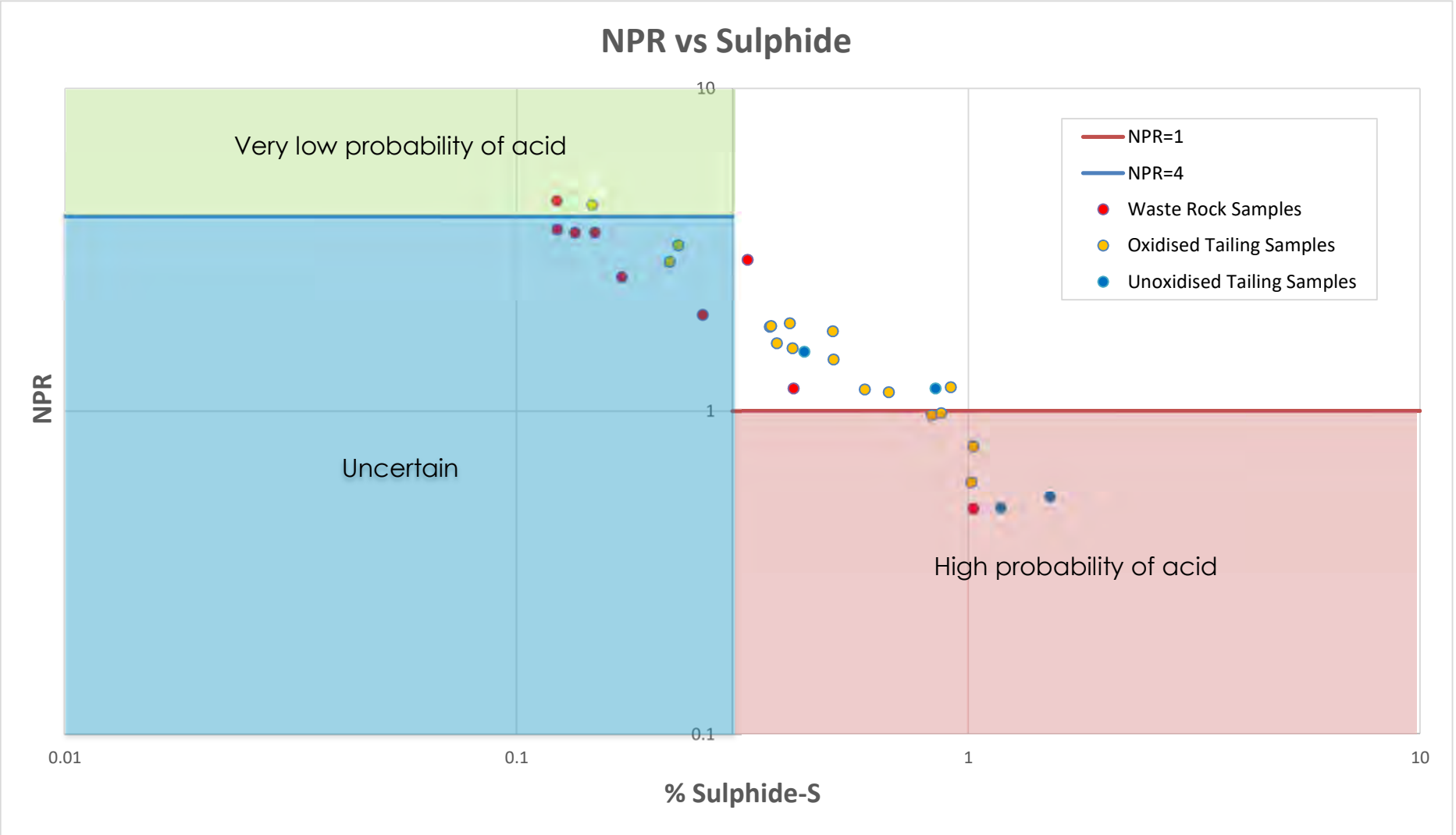

Figure 30: The NPR versus the percentage Sulphide present in the samples for evaluating the probability of acid generation

Please note that Figure 30 provides a summary of the NPR (all associated tailing and rock samples) that were analysed. According to Figure 29 and Figure 30 very high neutralising capabilities at the majority of the samples that were collected from the oxic zone were present (plotting within the white region. The majority of the remaining oxic zone samples displayed a likelihood or high probability of producing acid. The very low acid producing potential at TSF14 (oxic zone) is a likely observation; due to the fact that the sampled tailing is moderately old and acid production has already occurred over several years; resulting in limited available sulphide minerals to produce acid within the future. Overall only two (2) of the anoxic zone samples (TSF15SZ and TSF17SZ) presented a high probability of producing acid.

In summary, some of the samples are inconclusive which can be correlated to the secondary sulphate minerals resulting in an overestimation of the % sulphide, thus the methodology includes the assumption that all % sulphide is pyrite. A low 6.8% acid generating risk subsists, while a high risk potential for generating acid consists only for 24% of the total samples (mostly sampled from the overburden or oxidized zone).

5.2 XRD and XRF analysis

A total of thirty four (34) samples (Table 9) were analysed from various locations within the area (refer to Figure 4) including both waste rock and tailings samples. The samples were mostly sampled from the oxidized zone and three (3) samples from the saturation zone within the tailings. Mineralogical analysis was performed to determine or identify the different constituents present in terms of dominant (>40%), major (10-40%), minor (2-10%), accessory (1-2%) and rare/trace (<1%) and is presented in Appendix J.

Mineral components in the tailings samples consisted of dominant quartz and muscovite, while TSF24 presented an exception - dominance in terms of hematite and quartz as the major constituent. Sulphur and iron is presented in the form of jarosite within the samples and varied from minor to rare, while the jarosite percentage recorded at TSF14 is an accessory to the rare fraction.

The mineral composition of the associated waste rock samples also comprised of dominant quartz with muscovite as a major component, while WRD20 illustrated a dominance of both quartz and pyrophyllite with muscovite still as a major component. WRD15 recorded muscovite as a minor component.

Overall the most dominant minerals recorded within the samples are quartz (71.84 wt. %) as well as muscovite with an average of 18.78 wt. %. Pyrophyllite is present from dominant to trace amounts, while chlorite and jarosite are present in both minor to trace proportions. From the data presented in Table 9, sepiolite, illite, gupeiite, pyrolusite, gypsum, kaolinite, magnesioriebeckite, phlogopite, feldspar and oxides are minerals that have been identified in a few of the samples, mostly representing one of the above minerals per sample.

X-ray fluorescence (XRF) analysis was also done on all thirty four (34) samples and can be located within Appendix J. The samples displayed a representation of a variety of different oxides present, consisting mainly of SiO_2 and Al_2O_3, while additional oxides (Fe_2O_3, SO_3, K_2O and MgO) were present in reduced concentrations compared to the two major oxides. The presence of Fe_2O_3 varies from 0.373% to 7.7%, with an exception at TSF27 revealing Fe_2O_3 as the main oxide present (71.3%).

SiO_2 and Al_2O_3 recorded higher concentrations when compared, excluding the previously mentioned exception. On average SiO_2 recorded as the highest average weight percentage (68.56%) and a median of 69.9%, in addition to Al_2O_3 as the second highest chemical constituent (average of 10.78 wt. % and median of 10.75 wt. %).

Table 9: *X-Ray Diffraction results of the associated Tailings and Waste Rock Dumps*

Mineral Identification	Sample ID																	
	TSF11	TSF12	TSF13OZ	TSF13SZ	TSF14	TSF15OZ	TSF15SZ	TSF16OZ	TSF16SZ	TSF17OZ	TSF17SZ	TSF18	TSF19	TSF20	TSF21	TSF22	TSF23	TSF24
Quartz	59.8	53	71.4	67.1	88.5	74.1	71.2	81.6	77.3	71	79.3	83.9	91.8	76.3	83.4	76.5	86.3	71.3
Muscovite	12.1	10.4	19	18.4	11.1	23.5	21	11.8	15.1	23.2	19.9	8.1		23	14	20.8	12.2	21.9
Chlorite		0.8						1.6	2.5	1	0.7	7.7	4.2	0.7	2.5	2.6		0.6
Pyrophyllite	28.1	35.8	5.3	14.5				5	5.1	3		0.3	0.1					
Jarosite			4.2		0.4	2.4	7.7			1.7							1.4	6.3
Sepiolite							0.1											
Illite													3.9					
Mineral Identification	Sample ID																	
	TSF25	TSF26	TSF27	TSF29	WRD11	WRD13	WRD14	WRD15	WRD16	WRD17	WRD18	WRD19	WRD20	WRD21	WRD22	WRD23		
Quartz	77.8	88.6	21	92.8	82	75.3	53.6	90.9	70.6	42.6	75.2	62	40.5	62.5	72.8	70.5		
Muscovite	15.3	10.2		5.3		10.4		7.9	23.4	51.6	22.5	33	16.3	31.2	24.7	26.2		
Chlorite	0.9			1	2.3			0.5	6	5.8	2.2	5	1	6.3	2.5	2.6		
Pyrophyllite		0.4			10		41						42.2			0.6		
Jarosite	6																	
Gupeiite								0.7										
Magnesium Iron Oxide		0.8							0.8									
Hematite			72							72.9								
Pyrolusite			6.1							6.1								
Gypsum				0.9														
Kaolinite						7.9	0.8											
Magnesiorie-beckite						6.4												
Phlogopite					5.8													
Illite							4.1											
Feldspar group							0.6											

5.3 Cluster identification of waste materials

Figure 31 illustrates the grouping of all the samples collected from tailings and waste rock sites according to their chemical characteristics. The horizontal axis on the dendrogram represents the dissimilarity or distance between the clusters.

The dendrogram was used to identify three (3) clusters of waste rock samples, to be introduced to kinetic leach testing, ensuring the three different chemical compositions are included in the leach test analysis. Note that the horizontal axis on the dendrogram is representative of the dissimilarity or distance between the clusters or in this case the sample chemistry, while the vertical axis presents the clusters and objects being studied. With the use of the dendrogram, samples with similarity (chemical composition) can be identified taking into account some variance.

When referring to Figure 31, a four branch cluster was identified which occur around the same horizontal distance (grey line). Note that this cluster range was used to identify three waste rock samples with different chemical compositions. One of the four clusters only included a tailing sample (TSF27) and can be located at the top of the dendrogram, thus the remaining three clusters was used to select the waste rock samples for kinetic testing.

Three samples were selected and included the following rock waste samples: WRD15 (selected from cluster number 2), WRD14 (identified in cluster number 3) and WRD21 (cluster number 4). The samples were obtained through random selection within the three different clusters. The three individual samples identified will be introduced to humidity cell testing as an overall conclusion of the waste rock dumps' rate of sulphate production.

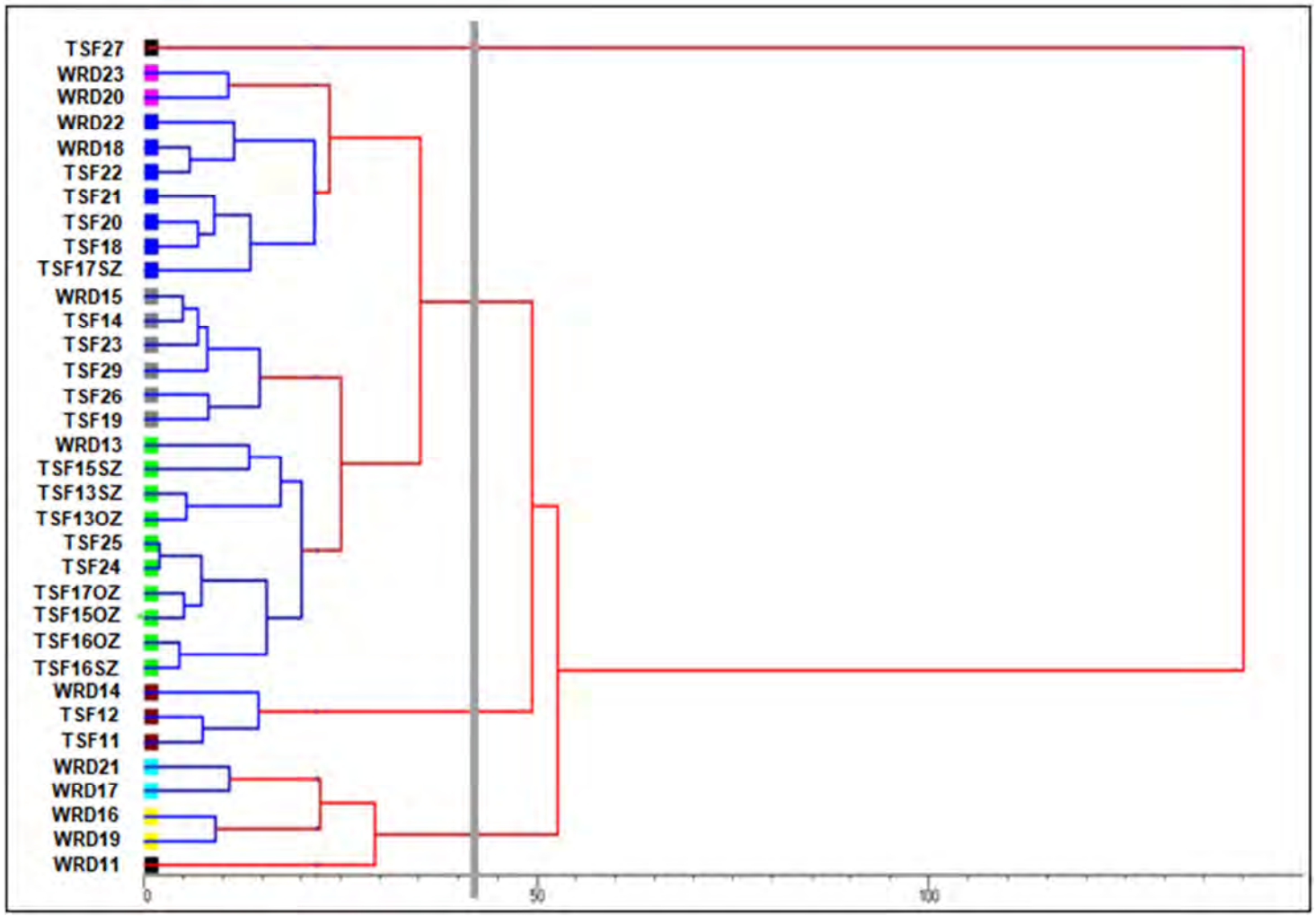

Figure 31: Grouping regarding the sampled materials (TSFs and WRDs)

5.4 Humidity Cells (Kinetic tests)

5.4.1 *TSF and WRD selection*

Table 10 lists the samples subjected to kinetic leach testing as well as the associated ABA results. A total of nine (9) samples were used for the analysis based on the chemistry character, as well as inconclusive and high acid potential (refer to Table 11).

Table 10: *Kinetic leach tests samples with associated ABA analysis*

Sample	%S	AP ($H2SO_4$/t)	NP ($CaCO_3$/t)	NNP (open)	NNP (closed)	NPR	Initial pH	Final pH
TSF13OZ	0.22	6.82	-19.80	-26.62	-33.43	2.91	3.74	2.44
TSF13SZ	0.85	26.46	-31.08	-57.54	-83.99	1.17	3.77	2.04
TSF15OZ	0.87	27.25	-26.82	-54.07	-81.32	0.98	3.69	1.87
TSF15SZ	1.52	47.43	-25.62	-73.05	-120.49	0.54	3.12	1.88
TSF17OZ	0.59	18.44	-21.48	-39.92	-58.36	1.17	3.42	2.12
TSF17SZ	1.18	36.94	-18.48	-55.42	-92.37	0.50	5.66	2.05
WRD14	0.02	0.70	-17.34	-18.04	-18.73	24.95	7.78	2.75
WRD15	0.12	3.83	-17.22	-21.05	-24.88	4.50	7.33	2.29
WRD21	0.17	5.34	-13.92	-19.26	-24.61	2.60	8.39	2.32

Five of the tailing samples indicated inconclusive results within the ABA screening procedure; these samples included oxidised zone and saturated zone samples. The remaining tailings samples recorded a high likelihood of producing acid, while one waste rock sample was indicative of a low probability for acid production (presented in Table 11.

Table 11: *Samples subjected to Kinetic leach tests with associated ABA analysis conclusion*

Sample Names	ABA conclusion
TSF13OZ	Inconclusive
TSF13SZ	Inconclusive
TSF15OZ	High acid generating potential
TSF15SZ	High acid generating potential
TSF17OZ	Inconclusive
TSF17SZ	High acid generating potential
WRD14	Inconclusive
WRD15	Low acid generating potential
WRD21	Inconclusive

The expanded Durov diagram below is based on the 1:2 extract results of the TSFs, where two distinct groups were identified (Figure 32). Additionally it was also evident that the tailings extract revealed similar chemical character based on the stiff diagrams illustrated in Figure 33. The identified TSF samples included two (2) samples from Group 1, as well as four samples from Group 2.

All of the oxidised samples that were inconclusive or indicated a high acid-neutralising potential within the ABA analysis, was accompanied with a sample from the saturation zone. This included the oxidation zone sample and the accompanied saturation zone sample that was introduced to the kinetic leach tests. The criteria also included the grouping of the waste rock samples as previously described, with a random selection within the associated clusters.

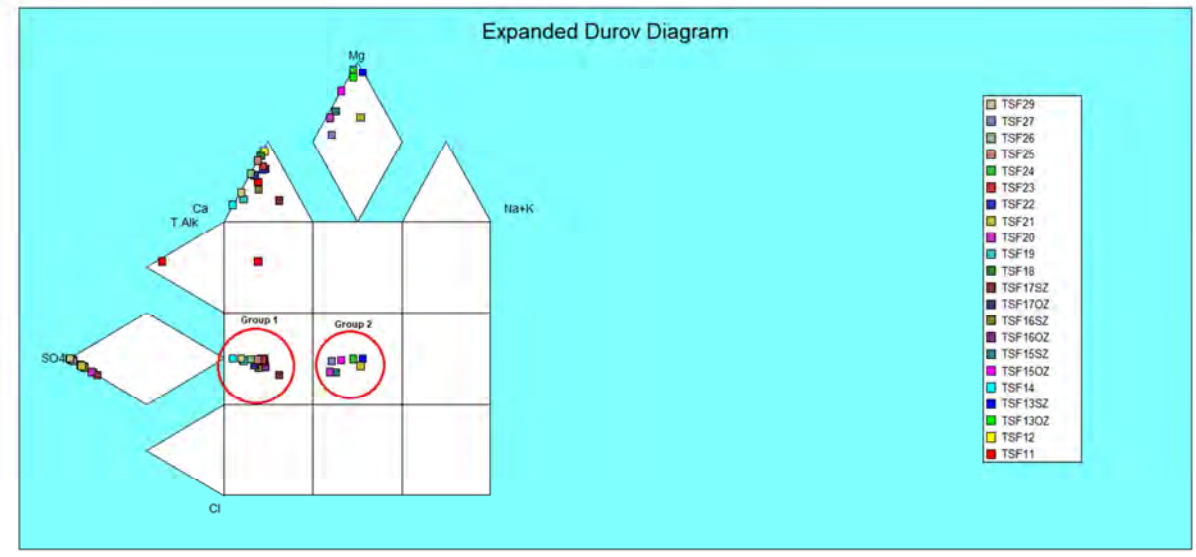

Figure 32: Expanded Durov diagram on 1:2 tailings extract

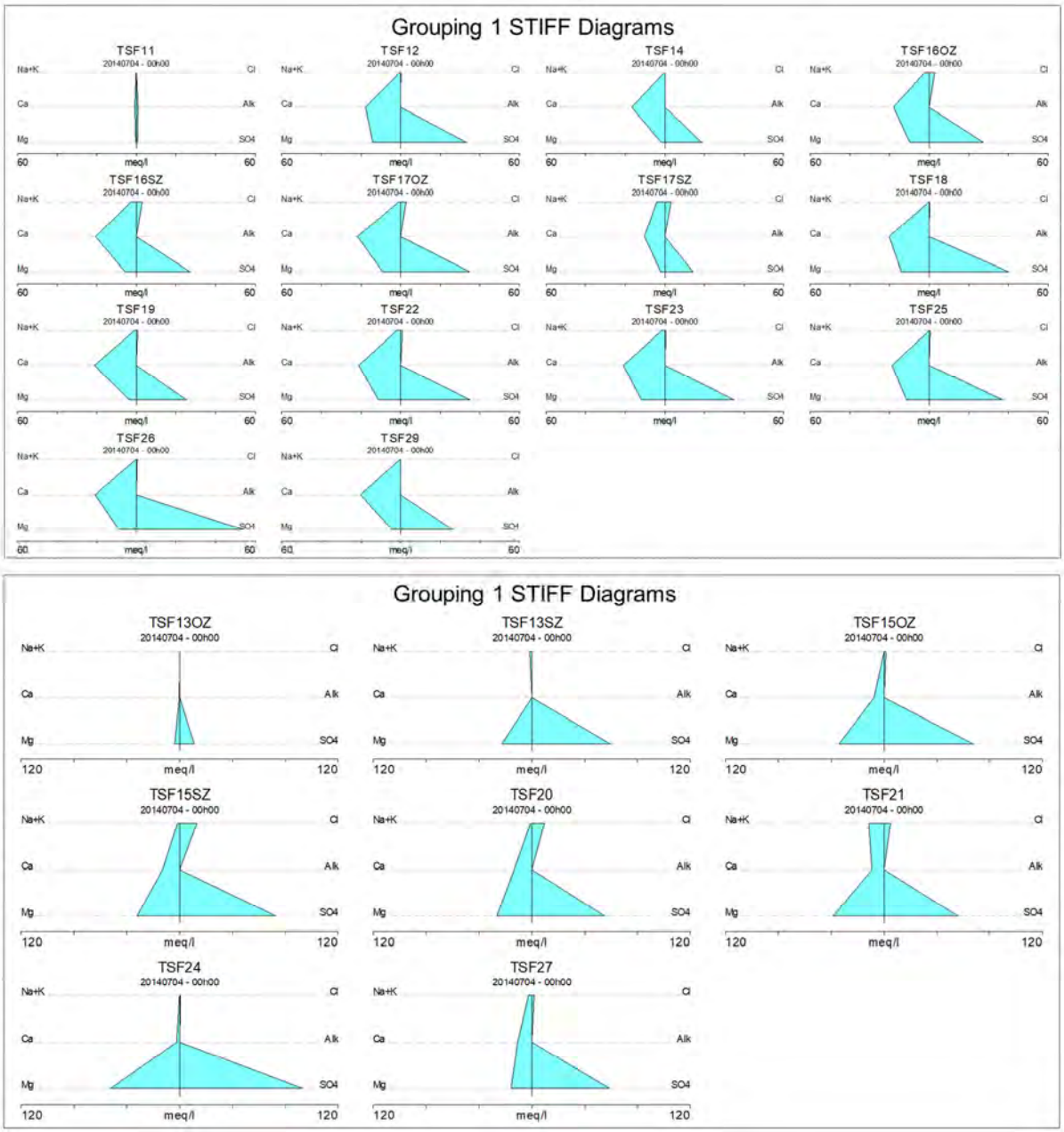

Figure 33: Stiff diagram of 1:2 tailings extract

5.4.2 *Humidity Cell Results*

The selected TSFs and WRDs were subjected to humidity cell leaching and the results of the nine (9) week leaching test are presented within Appendix K.

Several leachable elements were recorded form the humidity results, including Calcium (Ca,) Magnesium (Mg), Potassium (K), Sodium (Na), Chloride (Cl), Nitrate (NO_3), Iron (Fe), Manganese (Mn), Copper (Cu), Zinc (Zn), Boron (B) and Sulphate (SO_4). The overall chemical results of the kinetic cell tests recorded Mg, Ca, Fe and SO_4 as the major leachable elements. The observed pH, Fe and SO_4 release of the associated TSFs and WRDs are discussed below.

The recorded pH values of the sampled TSFs (Figure 34) were very low and are typically associated with a low buffering capacity of the samples. Overall the unoxidized samples revealed a general lower pH when compared to the oxidized samples, this correlates with the assumption that more pyrite particles are available in the saturated samples for oxidation. When referring to the observed WRD pH values (Figure 35), a significantly higher trend relative to the TSF samples was present, correlating to the ABA results indicating a low probability to generate acid.

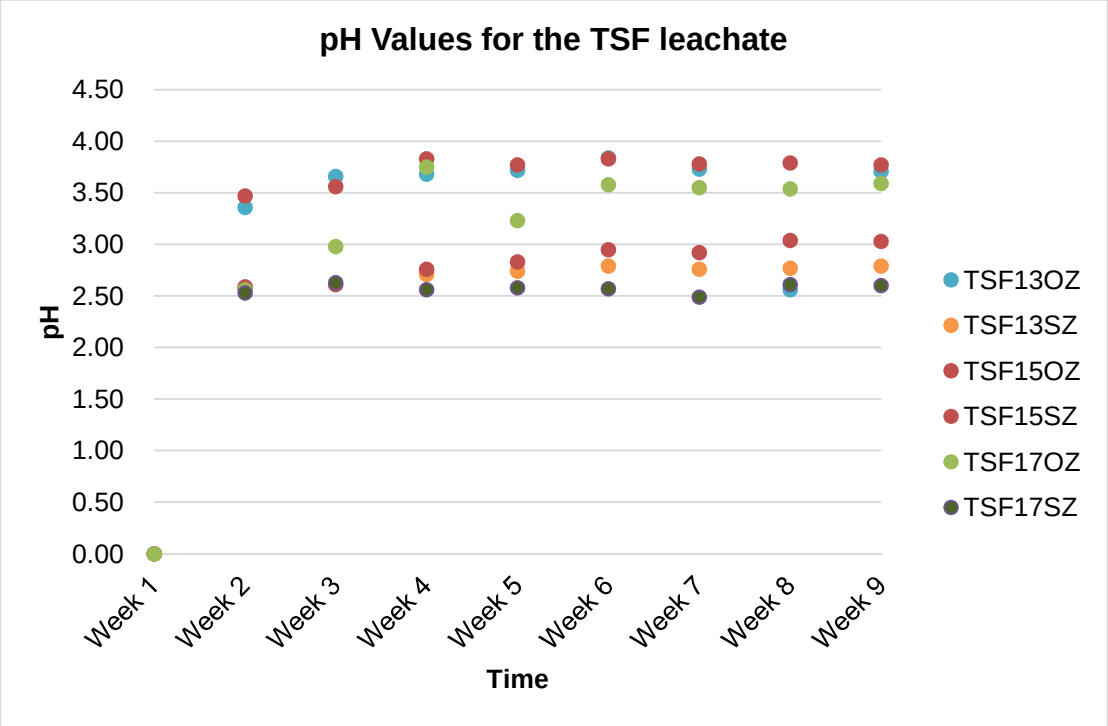

Figure 34: Weekly pH values observed from the TSF leachate

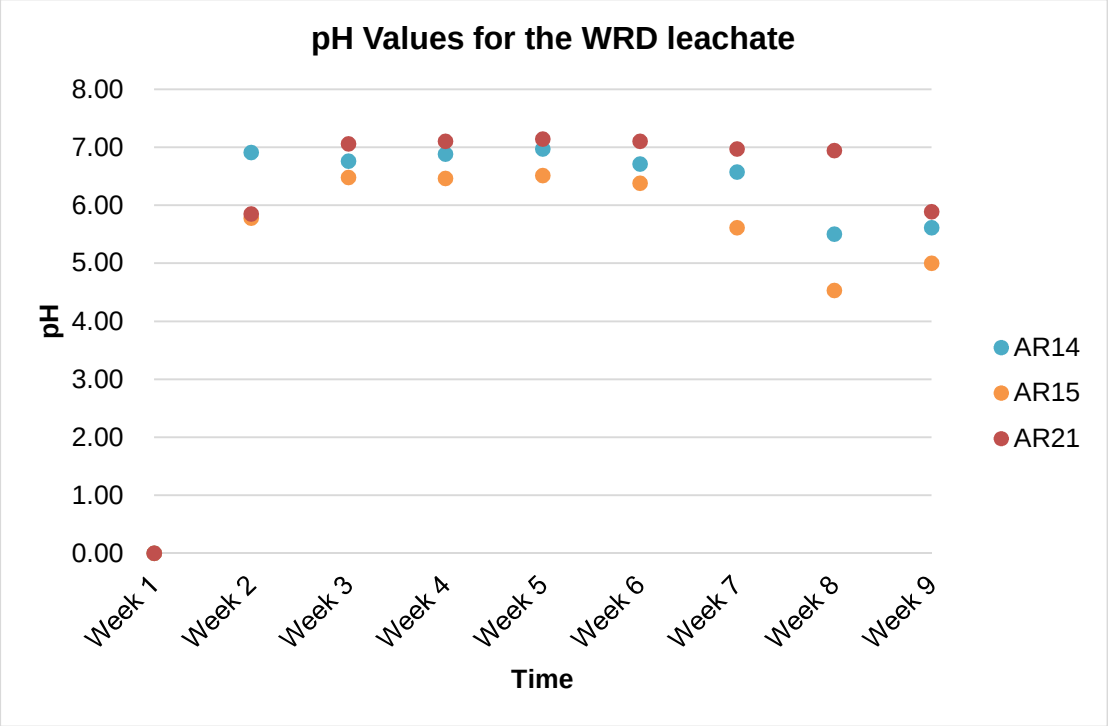

Figure 35: Weekly pH values observed from the WRD leachate

When referring to Figure 36 and Figure 37 below, the release of metals shows a strong correlation with the very low pH recorded. This observation is expected, where it is evident that the unoxidized samples presented an increase in iron release, while the oxidized samples revealed an inverse or decline. When referring to the mineralogy, the majority of the iron bearing minerals in the oxidized zones is jarosite. As jarosite has a low solubility, a lower release of iron and sulphates is expected from the oxidized zones.

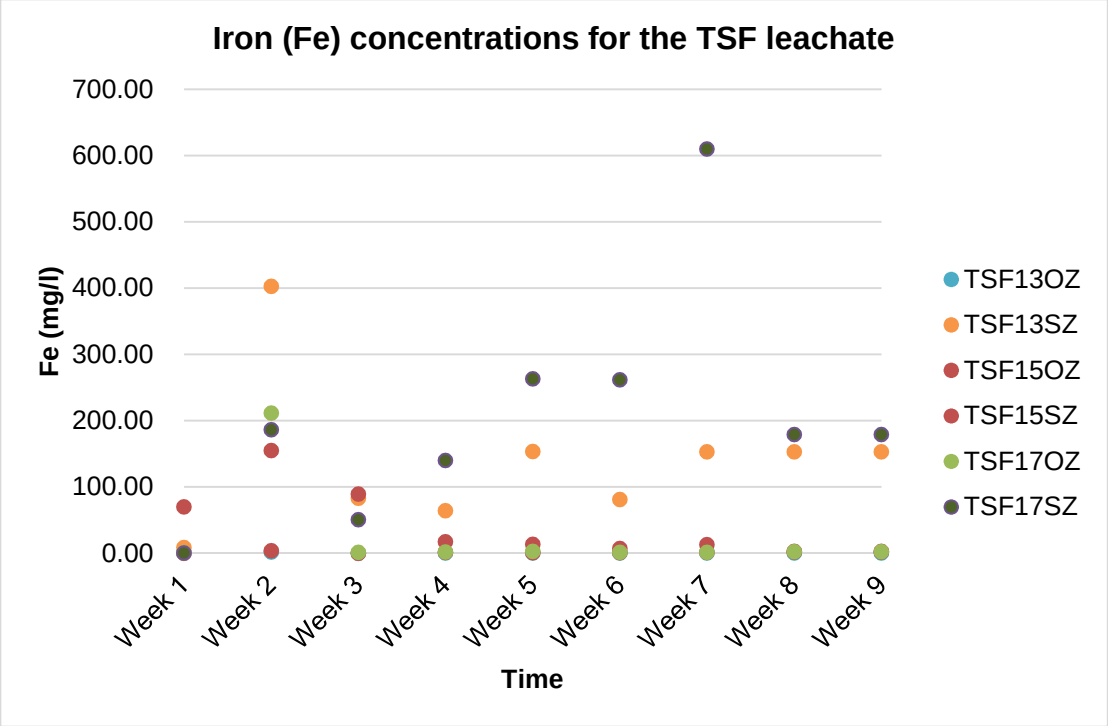

Figure 36: Weekly Iron (Fe) concentrations observed from the TSF leachate

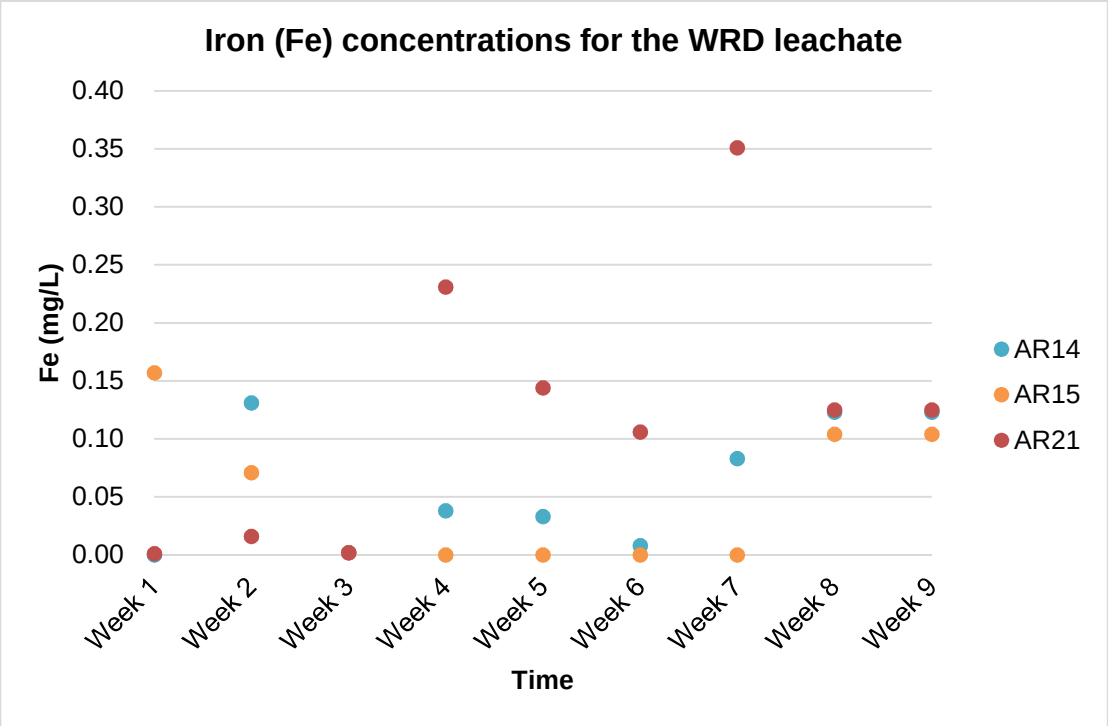

Figure 37: Weekly Iron (Fe) concentrations observed from the WRD leachate

As the main constituent of this study is regarded as sulphate, the humidity cell sulphate release of the associated tailing and waste rock samples is presented in Figure 38 to Figure 42.

When referring to the below figures, the production rate of acid is lower for all of the samples in the beginning of the analysis, followed by a spike within the second week of leaching. The initial increase in sulphate concentrations may be attributed to the dissolution of secondary sulphate minerals that generally precipitate in pyrite baring TSFs, which is then flushed out.

The highest recorded sulphate concentration at the end of week 9 can be seen at TSF13SZ with a production rate of 1848.74 mg/kg/week. Generally the unoxidised samples revealed a higher sulphate release, with the exclusion of TSF15. Overall from the elevated sulphate release it can be concluded that a high buffering capacity within the samples is not present. It is can also be concluded that the acid potential of the respective TSFs would decrease over several years as oxygen becomes limited within the facilities, in addition to slow diffusion processes within the site conditions.

The lowest recorded sulphate release of the waste rock samples was from WRD14, revealing a production rate that ranged from 2.51 mg/kg/week to 45.240 mg/kg/week. The minor sulphate release within the waste rock samples is expected as the sulphide particles are not exposed to oxygen and water to the extent of the tailings samples; as particle size is directly correlated to the reaction process. This can also be concluded with regards to the ABA results, where the waste rock dumps recorded either inconclusive or a low probability of acid generation.

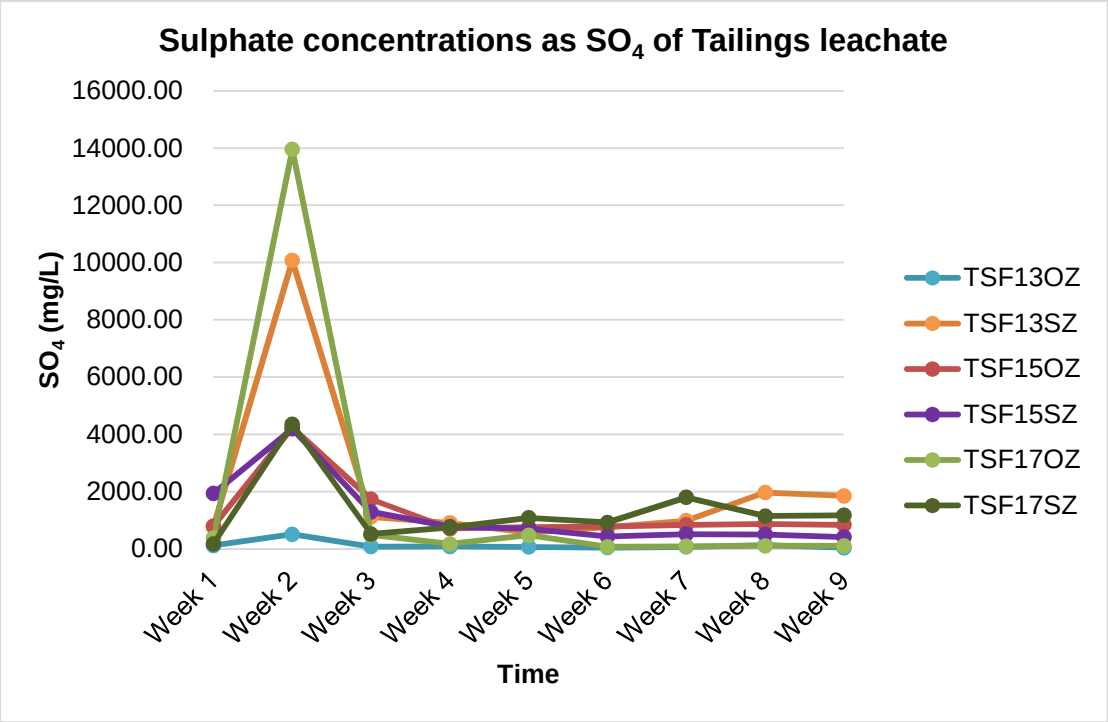

Figure 38: Weekly sulphate concentrations observed from the associated TSFs leachate

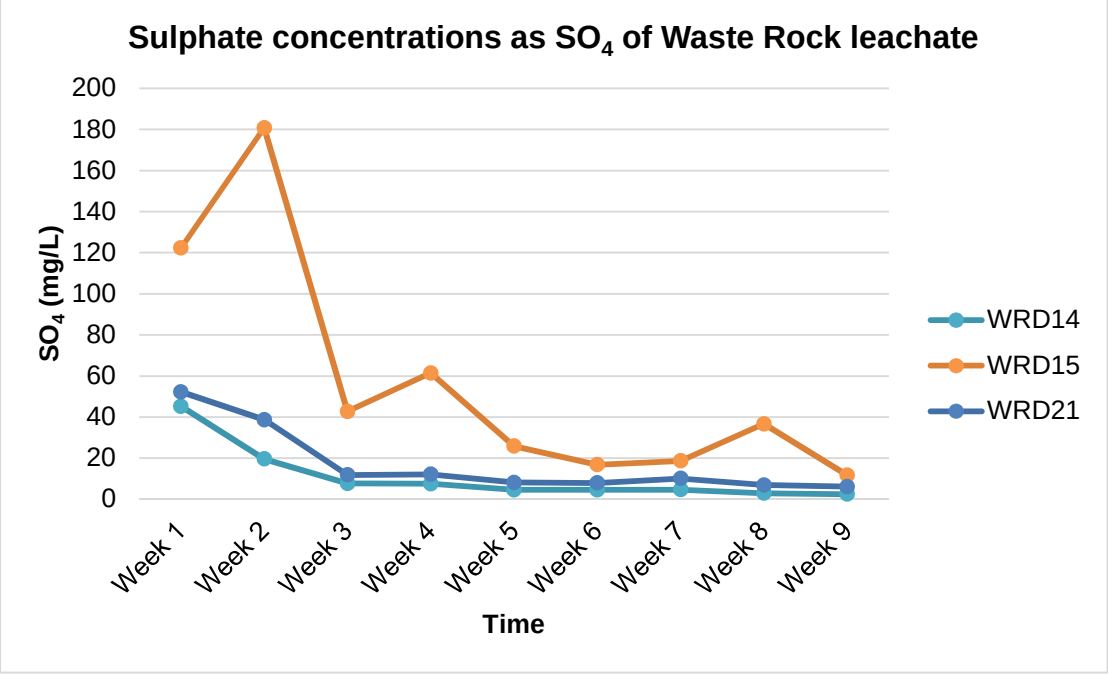

Figure 39: Weekly sulphate concentrations observed from the associated WRD leachate

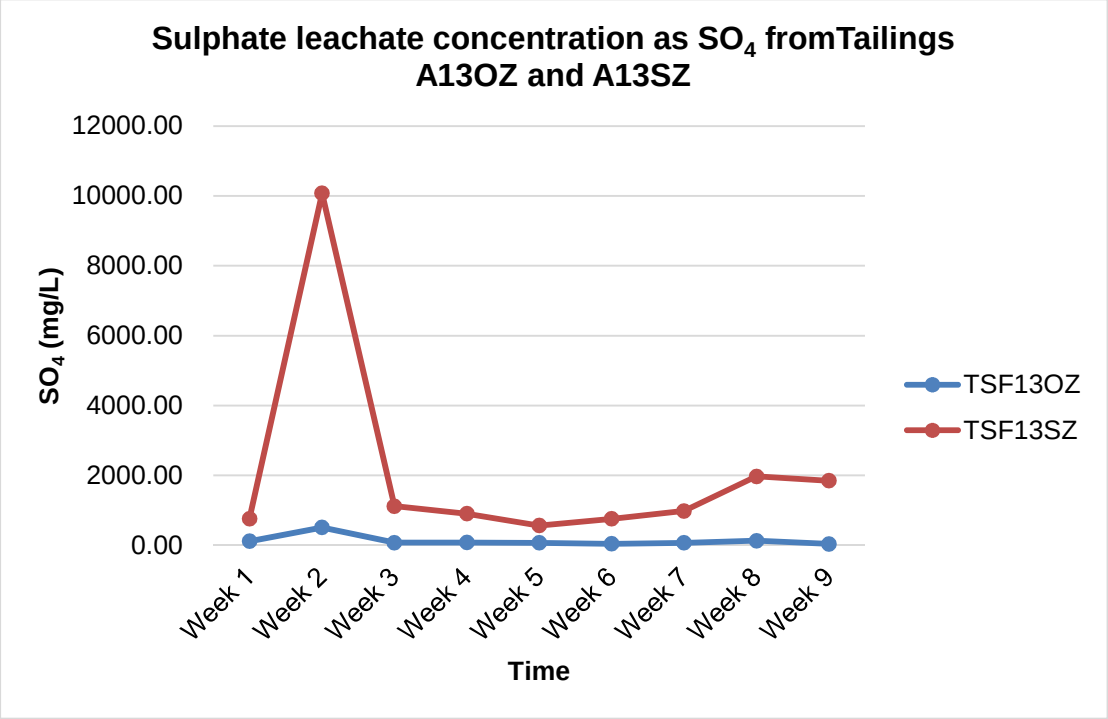

Figure 40: Sulphate leachate concentrations from the saturated and unsaturated zones of TSF13

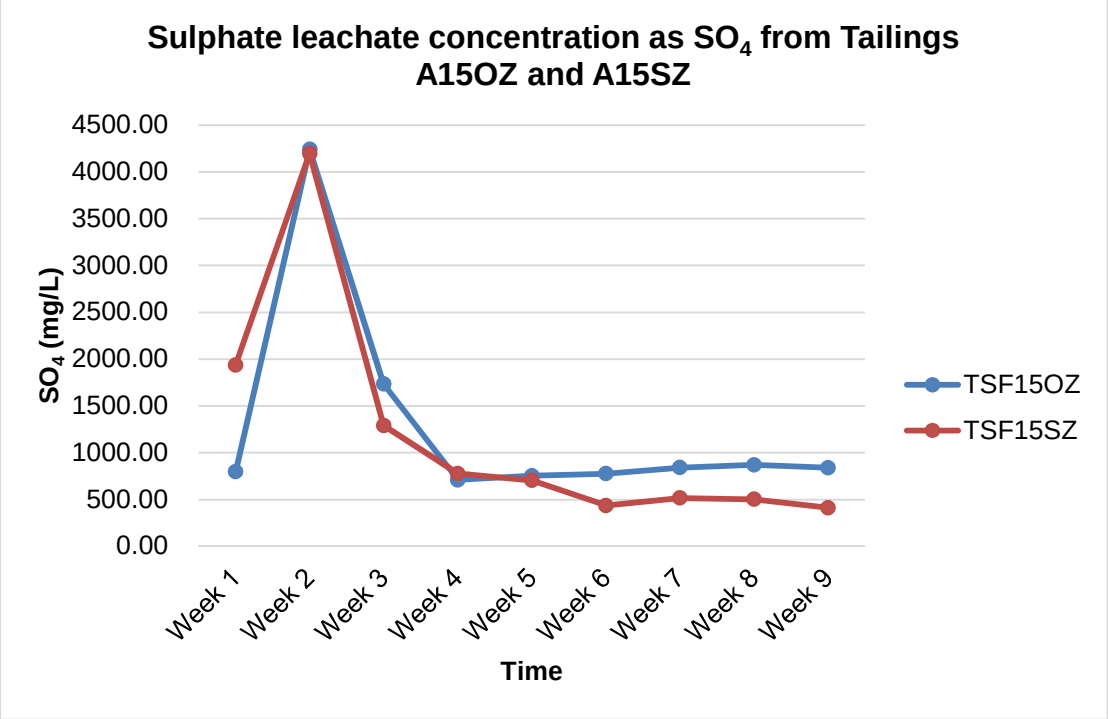

Figure 41: Sulphate leachate concentrations from the saturated and unsaturated zones of TSF15

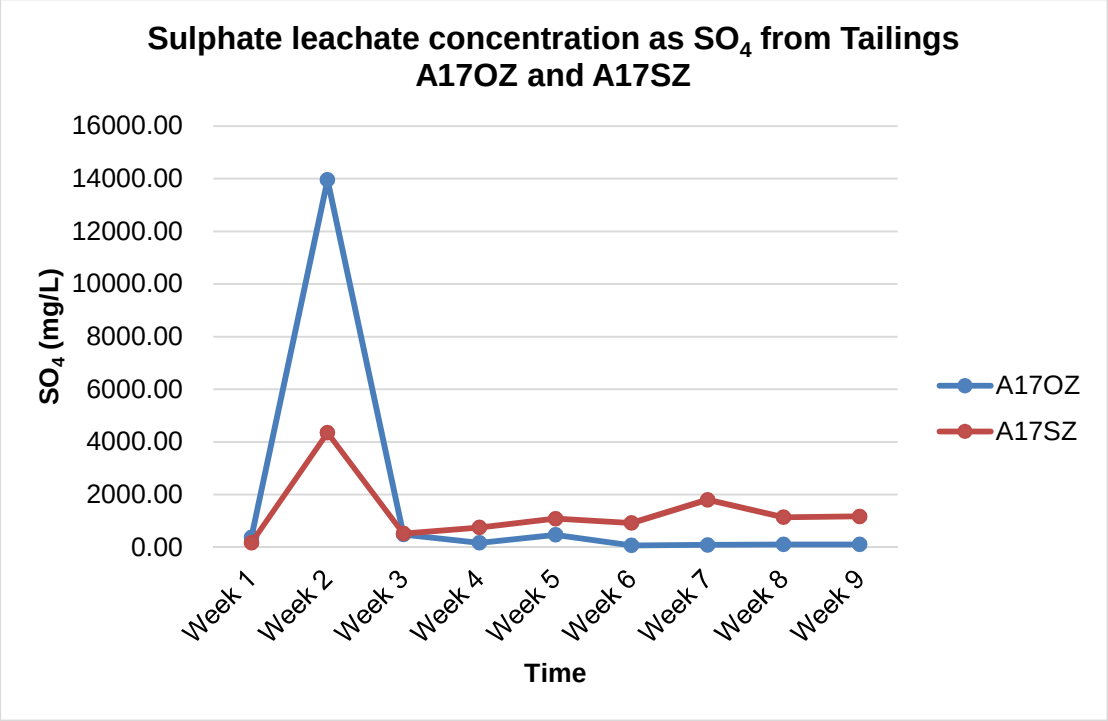

Figure 42: Sulphate leachate concentrations from the saturated and unsaturated zones of TSF17

5.5 Geochemical Sampling

The geochemical results obtained from the oxygen chambers as well as the %S are discussed below according to each of the five individual tailing heaps. Note that in-situ identification of the saturated zone is also compared to the geochemical result (oxygen levels).

5.5.1 ***Marievale 1***

Based on Figure 43 (illustrating the oxygen concentration- and moisture profile drilled in Marievale 1), the unoxidized zone was identified at five (5) meters. The oxygen concentration profile recorded an exponential decrease within the first 5 meters, where the oxygen is nearly entirely consumed. The %S results presented within Appendix L; revealed a minor percentage of S which comprises out of SO_4. This observation correlates to the exponential decrease of oxygen concentration with depth.

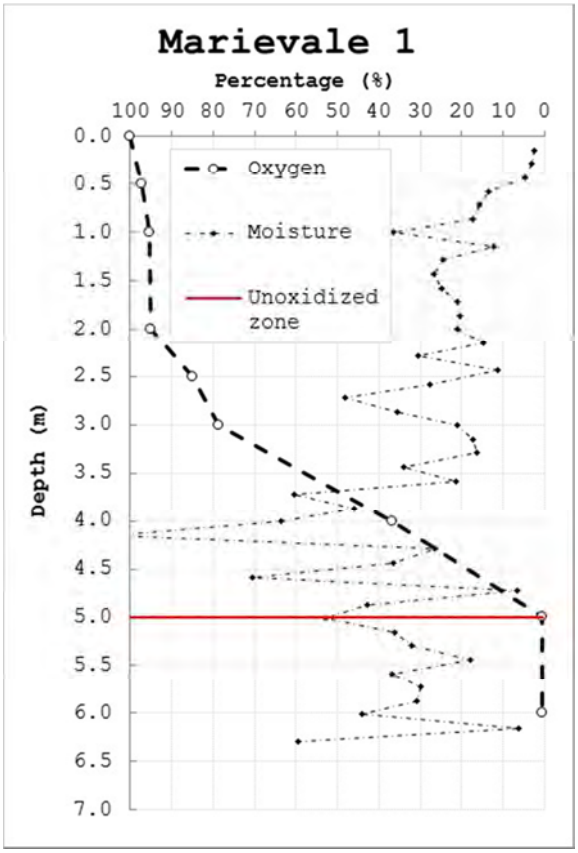

Figure 43: Oxygen and moisture concentration profile of Marievale 1 (from NWU, 2016)

5.5.2 ***Marievale 2***

The six (6) meter section drilled at Marievale 2 is shown in Figure 44. Field observations included a distinctive colour change (yellow to grey) at 0.4 meters, where it was assumed to be the transition to the unoxidized zone. Based on the oxygen- concentration profile from (NWU, 2016) the unoxidized zone may be considerable deeper at around 4.5 to 5 meters, indicating a low oxygen profile. The sulphur analysis also revealed a very low %S throughout the profile, while a decline in SO_4 was present with depth (below 20% after 5.5 meters). A large transition zone is observed, where the unoxidized zone is not clearly identified within the oxygen profile. The decline in SO_4 also confirms that the actual unoxidized zone may be deeper.

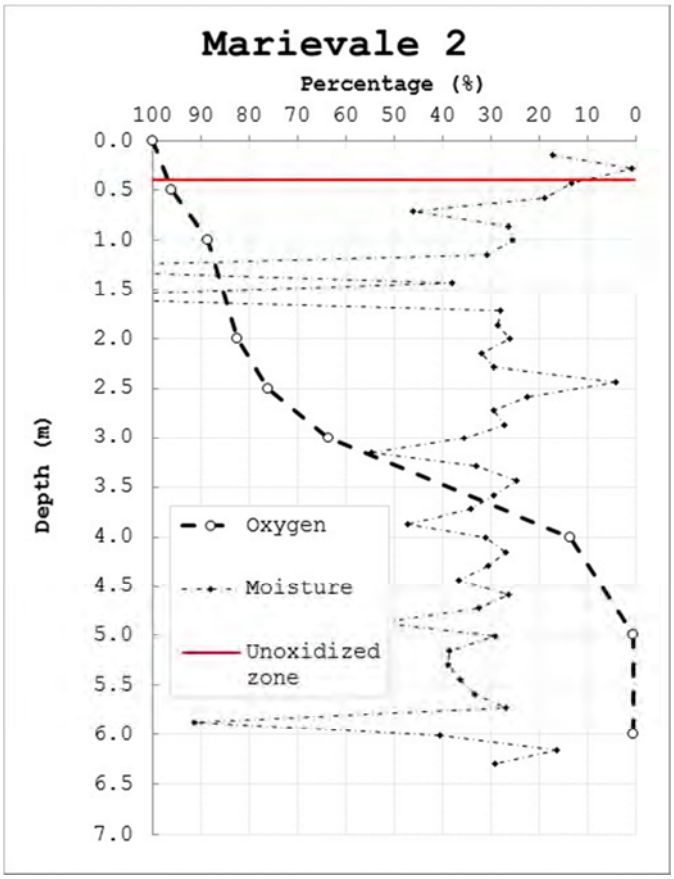

Figure 44: Oxygen and moisture concentration profile of Marievale 2 (from NWU, 2016)

5.5.3 ***Marievale 3***

Similar observations to Marievale 2 were apparent from the data collected at Marievale 3 (Figure 45). From the field observations it was assumed that the unoxidized zone was 1 meter below the surface of the heap, while the oxygen concentration profile, in addition to the sulphur analysis indicated the zone to be located approximately 4 meters below the surface of the heap.

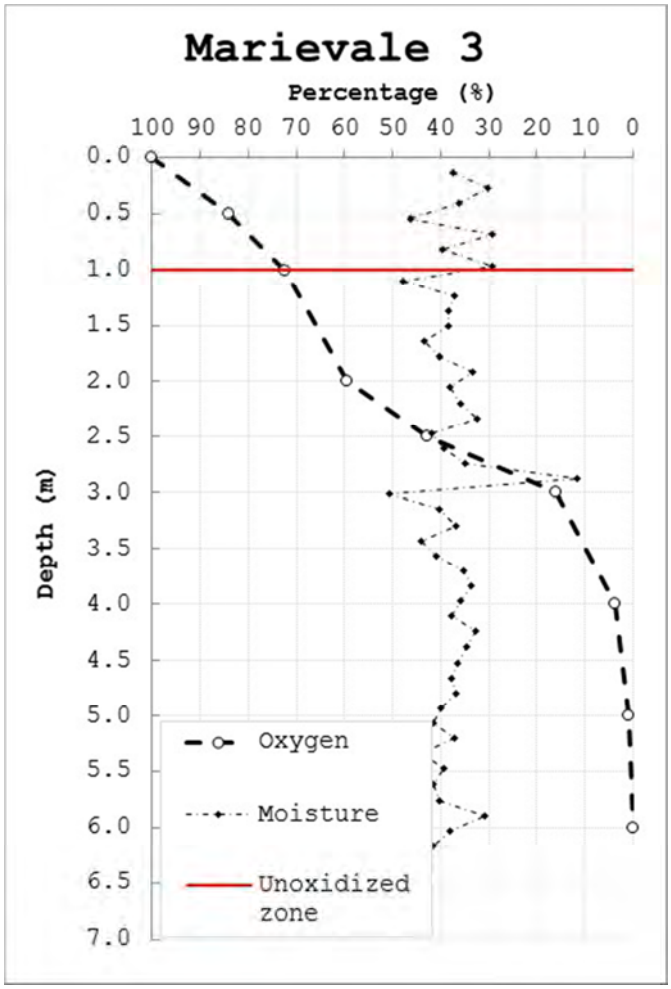

Figure 45: Oxygen and moisture concentration profile of Marievale 3 (from NWU, 2016)

5.5.4 *Vlakfontein*

Note that two holes were drilled within the Vlakfontein TSF heap. The ten (10) meter hole was used to install the oxygen chambers, while the second was drilled for more accurate sample collection regarding a hand auger. The unoxidized zone was estimated by the oxygen concentration profile and correlation with regards to the sulphur analysis.

From %S analysis and oxygen concentration profile the sulphide minerals in the first six (6) meters are close to fully oxidized as identified through NWU (2016). Due to the oxidizing conditions, a more linear decrease is observed within the oxygen concentration profile.

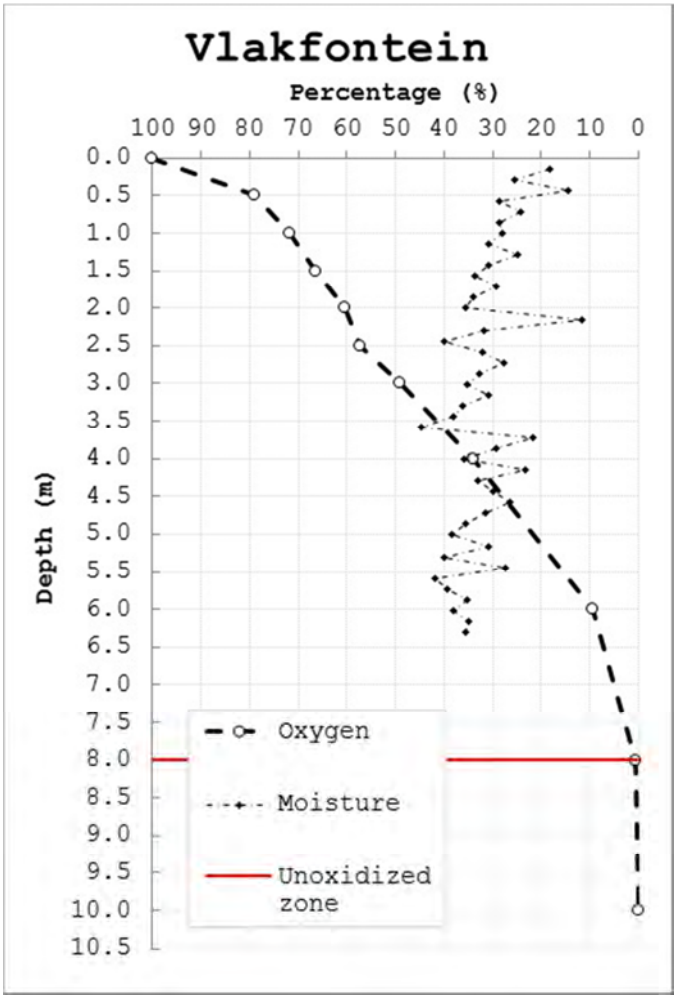

Figure 46: Oxygen and moisture concentration profile of Vlakfontein (from NWU, 2016)

5.5.5 ***Carnival City***

The six (6) meter Carnival City TSF heap recorded high moisture content, revealing the unoxidized zone to be located at two (2) meters below the surface. This observation was also correlated with the oxygen concentration profile. The shallow oxidized zone revealed fairly saturated conditions, which correlates to the heap becoming very saturated with depth.

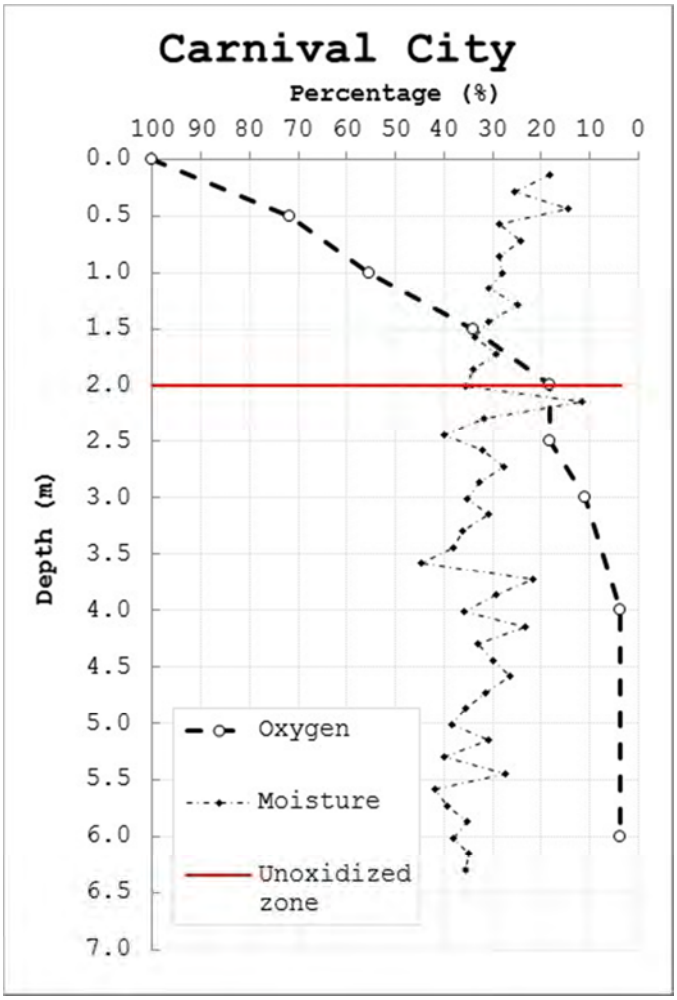

Figure 47: Oxygen and moisture concentration profile of Carnival City (from NWU, 2016)

5.6 Geochemical Modelling

Based on NWU (2016) to approximate the possible pollution impacts, the study area had to be simplified. Data obtained from the previous field work and lab results was used as input parameters, in addition to PYROX version 1.1. modelling of the heaps.

5.6.1 *Model setup and assumptions*

The parameters required to setup a PYROX model run can be located within Table 12. Even though input parameters was present using the in-field readings and laboratory data, various parameters still needed to be estimated and calibration of the PYROX models were complicated. NWU (2016) calibrated the model by using the oxidized zone depth and estimating the age of the heap. The analytical model developed by Davis & Ritchie (1986) was incorporated to determine an initial estimation. Several assumptions relating to the input parameters and model set up were included and can be described by NWU (2016) as follows:

- Values for grain size were obtained from Yibas *et al*., 2010, which results in an over estimation as TSFs are generally heavily stratified and particle size differs - the particle size distribution was assumed to be homogeneous for all the heaps;
- Fresh unoxidised particles were assumed in terms of the starting radius, as the ash layers was presumed to be at time zero (before oxidation started),
- The height of the heap is equal to the unsaturated depth, as the unsaturated depth was unknown, which is also an overestimation. This assumption does not compensate for the phreatic head, which in return allows all material to be oxidised;
- From the geochemical samples the sulphur mineral content was obtained, and assumed that the only sulphide mineral present is pyrite;
- Porosity values were determined regarding unconsolidated sediment as per Yibas *et al*., 2010 and assumed to be the same for all the heaps;
- Moisture content was determined experimentally from the geochemical samples presented in Section 5.5;

Table 12: *Parameters required to setup a PYROX model*

Parameter	Description
Grain size	The grain size of the particles in the heap
Starting Radius	The radius of the unoxidised particle at the start of the simulation
D_2	The diffusion coefficient of oxygen through the ash layer
Unsaturated depth	Section of the TSF that is unsaturated
Sulphur mineral content	Mass fraction of sulphur minerals present that can be oxidized
Porosity	-
Moisture content	-
Bulk Density	-

5.6.2 ***Results***

Calibration of the model consisted of calculating the age of the heap from the reaction front depth, while varying the pyrite percentage and moister content in order to fit the model within the observed oxygen profile. The NWU (2016) PYROX oxygen concentration results did not reveal satisfactory correlation to the field measurements, where it was evident that the high variation in moisture content from the heaps influenced the model. More over the limited data availability presented several assumptions regarding the PYROX model, and was essentially calibrated to the moisture- and oxygen concentration profiles.

Figure 48 to Figure 52 below illustrates the measured data compared to the values modelled by PYROX.

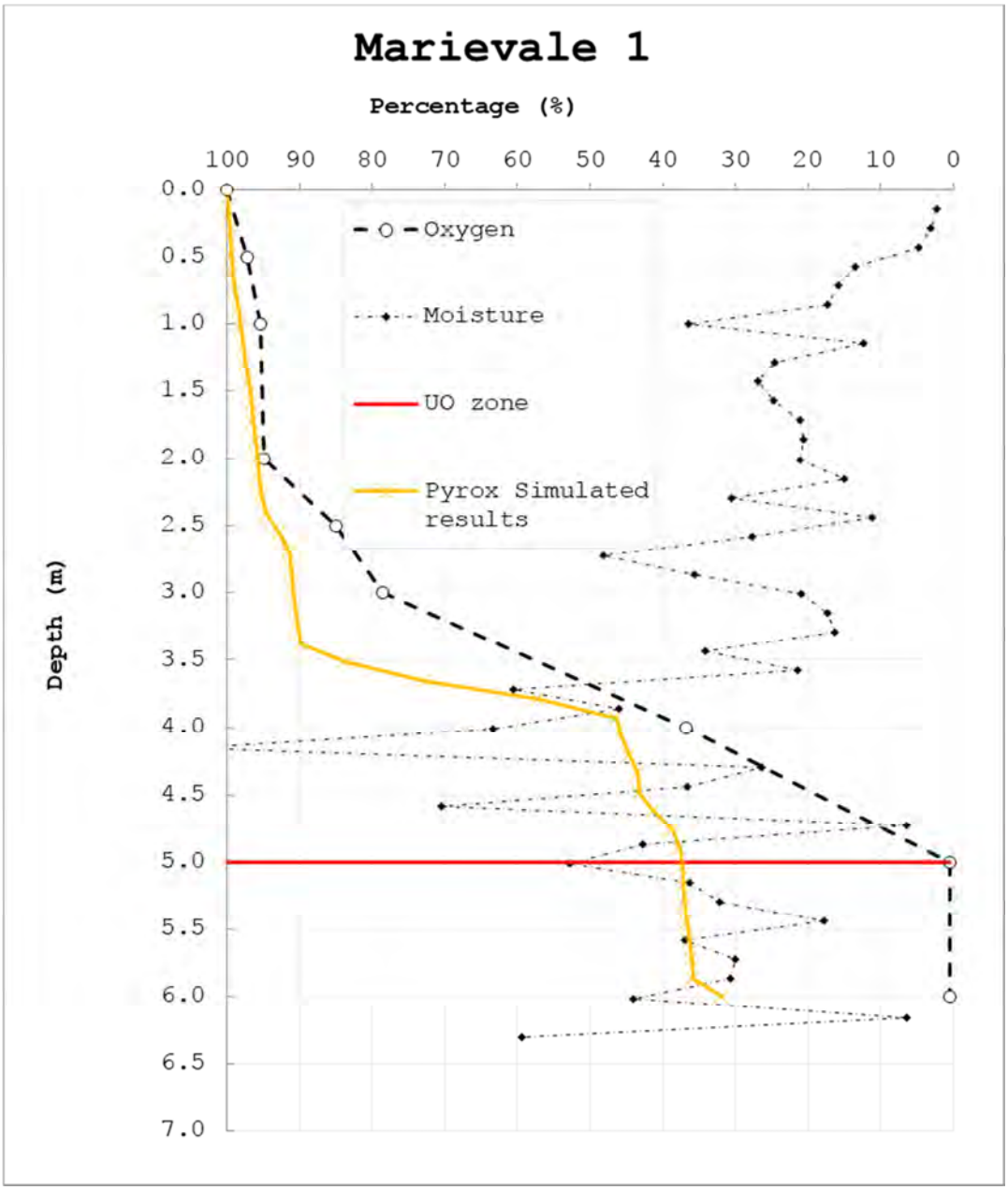

Figure 48: Marievale 1 PYROX model results (from NWU, 2016)

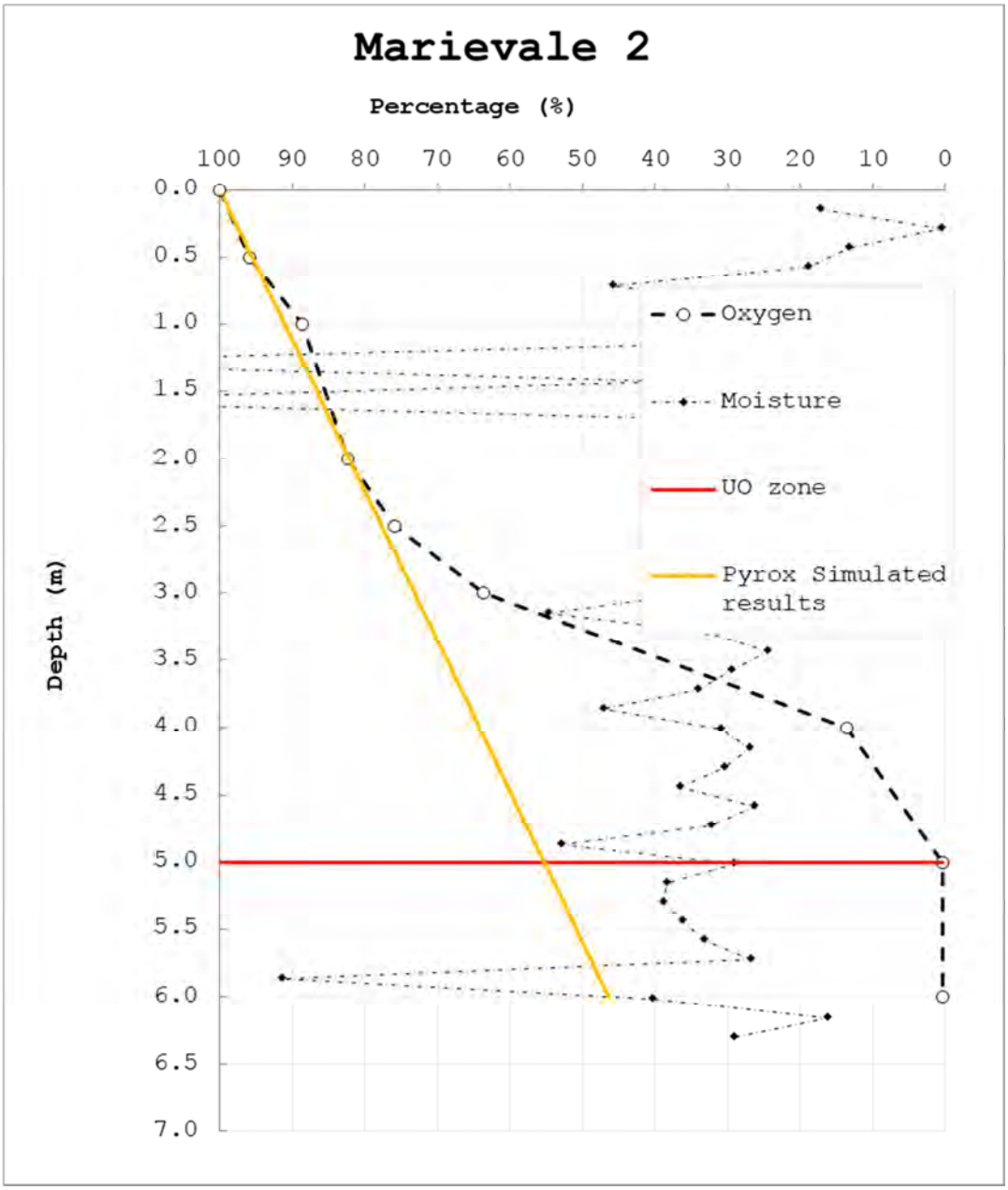

Figure 49: Marievale 2 PYROX model results (from NWU, 2016)

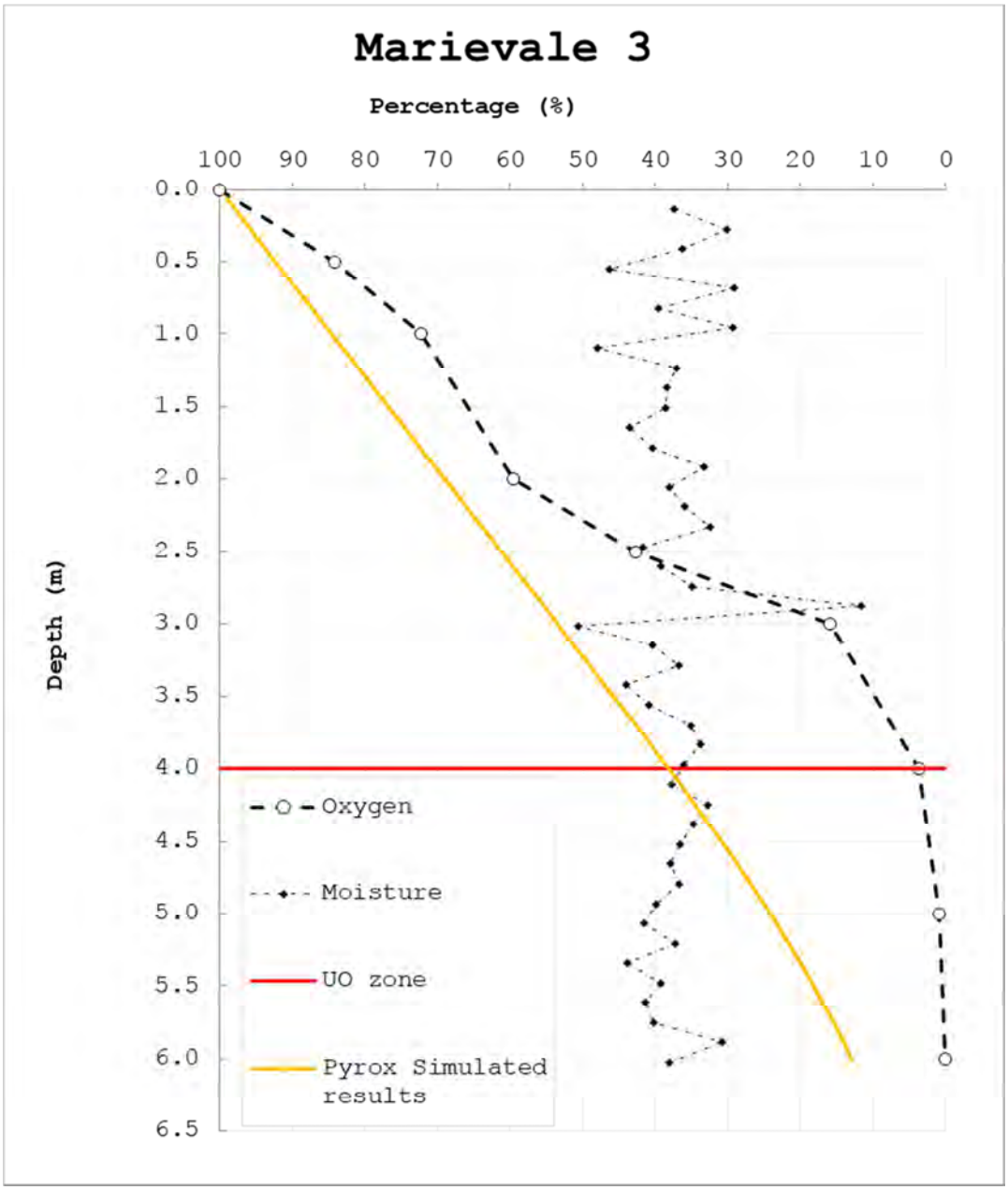

Figure 50: Marievale 3 PYROX model results (from NWU, 2016)

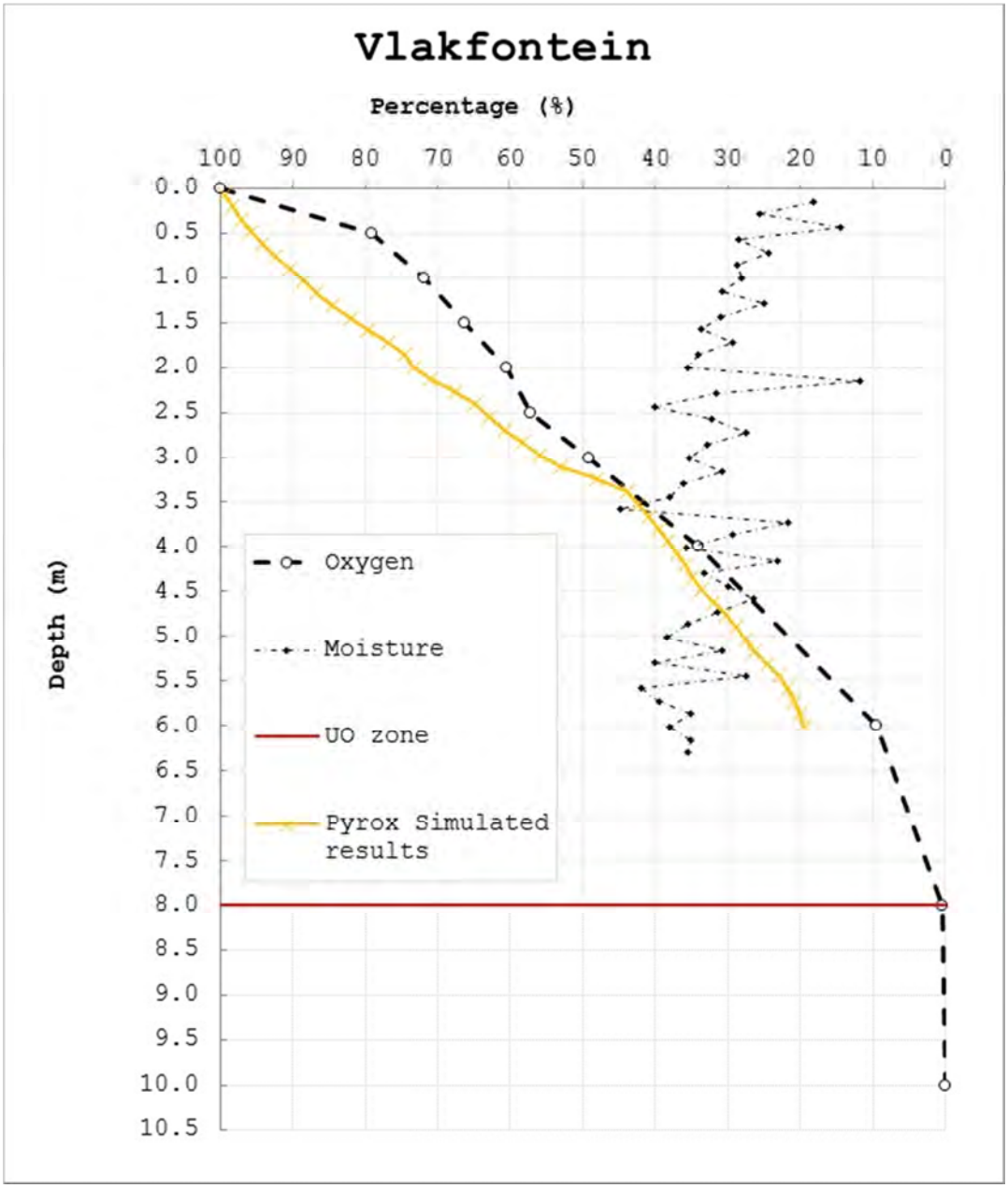

Figure 51: Vlakfontein PYROX model results (from NWU, 2016)

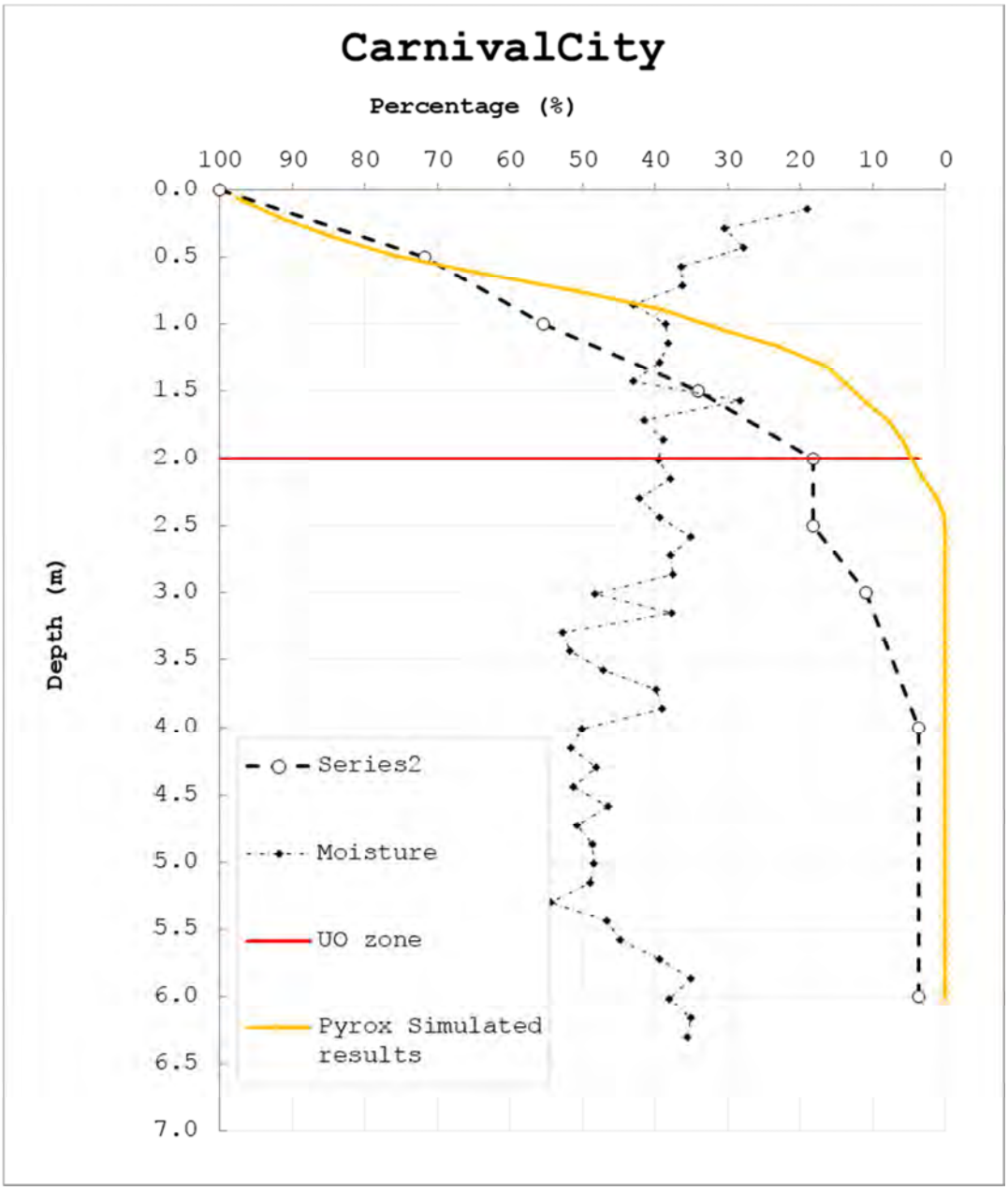

Figure 52: Carnival City PYROX model results (from NWU, 2016)

Figure 53 illustrates the sulphate load over a time span as modelled using PYROX. The modelled sulphate load is also presented in Table 13 regarding a fifty (50) year span. An initial spike is still evident as confirmed with the leach test data, while the Carnival City TSF recorded the highest expected sulphate load.

Table 13: *Modelled Sulphate Production Rate over a 50 year span*

Time (yr)	Integrated Sulphate Production Rate (kg/m^3)				
	Marievale 1	**Marievale 2**	**Marievale 3**	**Vlakfontein**	**Carnival City**
5	20.944	20.228	18.655	36.595	134.485
10	9.61	10.709	8.423	19.449	99.674
15	6.841	9.281	6.956	13.249	86.336
20	5.251	8.247	6.09	8.626	78.353
25	4.238	7.505	5.516	4.676	72.792
30	3.548	6.933	5.099	2.471	68.59
35	3.019	6.476	4.789	1.685	65.246
40	2.595	6.098	4.456	1.397	62.488
45	2.263	5.779	4.152	1.185	60.154
50	1.984	5.513	3.878	1.083	58.137

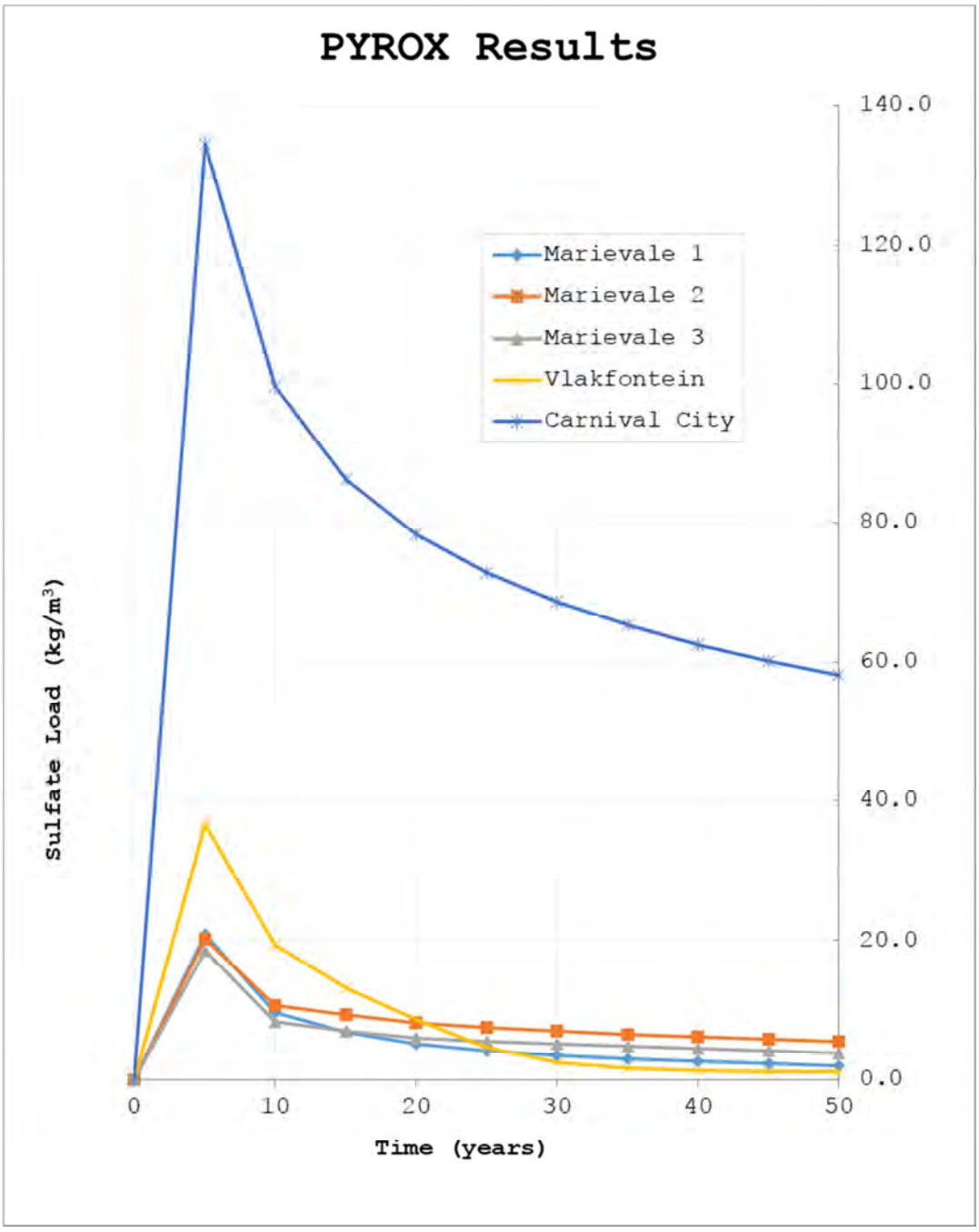

Figure 53: PYROX model results (from NWU, 2016)

5.7 Standardised Source Term

As previously described a generic source term will be produced based on the recorded static, kinetic and geochemically modelled results. The standardised source term will serve as an indication of the current salt load mass expected within the TSFs situated within the East Rand Basin. The end result is a simplified method rather than individual models and salt load determination.

5.7.1 *Weighting Scale*

For an initial rough estimation a weighting scale can be assigned to the TSFs. The scale is determined and dependent on the surface area of the heap, as well as the sulphide content. Overall the percentage sulphide is multiplied by the heap area for a rough estimation with regards to the TSF sulphide production rate. Thus the scale is based on the amount of sulphide which will be oxidised. The weightings calculated for the various TSFs are presented in Table 14. TSF18 was used as the maximum on the weighting scale (highest sulphide mass to be oxidised). The remainder of the TSFs are adequately distributed on the weighting scale.

Table 14: *Weighting calculated from surface area and sulphur content*

Sample ID	%S	Area (m^2)	Weighting
TSF18	0.5031	4 443 000	10
TSF27	1.0268	831 100	3.8
TSF20	0.8312	834 000	3.1
TSF17	0.70408	958 000	3
TSF26	0.6667	881 000	2.6
TSF15	0.87194	641 000	2.5
TSF22	0.3657	1 030 000	1.7
TSF16	0.40855	745 000	1.4
TSF19	0.3635	390 800	0.6
TSF12	0.2278	387 000	0.4
TSF23	0.5015	131 500	0.3
TSF24	0.915	71 700	0.3
TSF11	0.0001	192 590	0

Based on the weighting scale, it is evident that TSF18 will produce the highest expected sulphate load when compared to all of the sampled tailing, while TSF27 is likely to produce the second highest sulphate load. Even though TSF27 recorded a higher %S fraction, it is apparent that the sulphate release is directly correlated to the surface area, thus it is expected that a greater area would produce a higher sulphate load.

5.7.2 *Generic Load Model*

As the mineralogy and humidity cells of the TSFs presented similar chemical characteristics and leachate constitutes, the concept of the generic source term was developed based on the geochemical modelled results.

With the use of Hydrus and PYROX, a variance in sulphide and a standardised moisture percentage can be incorporated to produce different outputs. A generic function can be obtained with the relevant sulphide content as the main variable input, where a generic equation can be determined.

A. Generic moisture profile determination

To develop the generic source term, the current moisture profiles within the East Rand Basin TSFs was determined. Instead of assuming constant moisture content throughout the heap, Hydrus-1D was used to set up a standardised varying moisture profile based on the moisture content derived from the geochemical samples.

The hydraulic model was based on a single porosity (van Genuchten) as it was assumed that the TSFs are open for air entry, while the bottom boundary is set at free drainage.

The moisture contents were extrapolated from the field samples and the model was calibrated based on a 10 m heap. As several variable parameters were unknown, assumptions and parameter values had to be obtained. The incorporated input parameters and assumptions to set up the Hydrus model are listed in Table 15 below.

Table 15: *Input parameters and associated assumptions*

Parameter	**Value**	**Assumption**	**Reference**
Number of Soil Materials	1	It was assumed that the heap was homogeneous	
Depth of Soil Profile	10 m	The heap was assumed to be 10 meters in height	
Residual soil water content (Qr)	0.1115		Singh & Verma (2011)
Saturated soil water content (Qs)	0.4		Retrieved from the geochemical samples
Alpha (α)	1.36		Huisamen (2013), Jorgensen *et al.* (1998) and Malmstrom *et al.* (2006)
Soil water retention function (n)	1.41		
Saturated hydraulic conductivity (Ks)	3.4×10^{-4}		
Tortuosity parameter (l)	0.5		
Precipitation	0.0001	Average rainfall and infiltration within the East Rand Basin	DWS (2017) and as Xu & Beekman (2003)

As the TSFs within the East Rand Basin are no longer operational; a loss in water content is present. Thus as the geochemical investigation was performed within 2016 by NWU, a decline in moisture content is already present to date. The model was run for a 5 year period, where the current generalised moisture profile of the TSFs was obtained from the modelled 1 year profile (T1). The modelled moisture content results are presented within Figure 54 and tabulated within Appendix M.

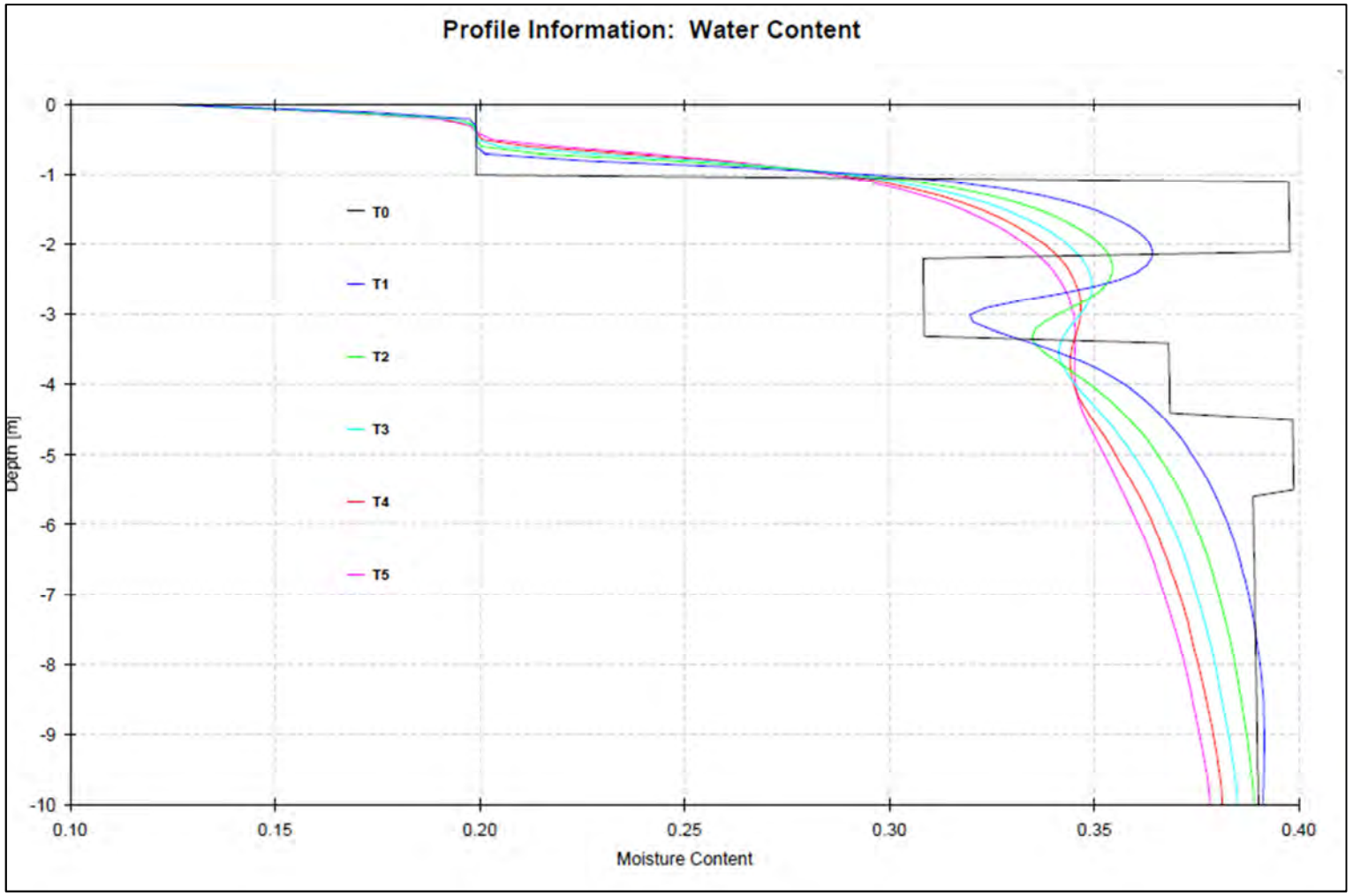

Figure 54: Hydrus modelled moisture profiles over 5 years

From Figure 54 a definitive decline in moisture content is presented between 3 to 4 meters. The decrease in moisture content is directly correlated to the moisture profiles of the geochemical samples, where the Hydrus modelled results presented accurate conditions when compared and based on the geochemical data. From the results it is also evident that a slight recharge effect is present with each year at the 3 to 4 meters mark, which is attributed to the rainfall incorporated into the model.

B. Generic PYROX model

A similar approach to NWU (2016) was used to determine the PYROX generic source term equations, while the current determined moisture content was implemented instead of a constant content throughout the heap. The model was set up in terms of a general TSF, specifying the moisture content determined with Hydrus, and implementing a change in fraction sulphur mineral content. The input parameters are specified within Table 16, while the same assumptions apply as described in Section 5.6.1.

Table 16: *Set parameters of the Generic PYROX model*

Parameter	**Description**
Mineral	Pyrite
Grain size	0.0008 m (retrieved from Yibas *et al*., 2010)
Starting Radius	0.99 (Fresh unoxidised particles)
D_2	0.08d-11 (Davis & Richie, 1986)
Time step in year	1.0d-2
Unsaturated depth	10 m (Assumed to be the same as the heap height)
Porosity	0.55 (retrieved from Yibas *et al*., 2010)
Temperature	18ºC
Bulk Density	1250 kg/m^3
Fraction Sulphide	Varied from 0.2, 0.4, 0.6, 0.8 and 1.0
Moisture content	Specified according to the determined moisture profile from Hydrus

To accurately develop a generic equation producing the source term with the use of PYROX; several function equations were determined (based on NWU, 2016) which is then incorporated into a final generic equation:

- Standardised sulphate production equation;
- Initial sulphate concentration equation;
- Sulphide fraction ratio equation;
- Sulphide to sulphate production ratio equation;

Initially the PYROX model was run in terms of the specified sulphide fractions and moisture content over a fifty (50) year span. The sulphate production results modelled is presented within Table 17, which in return was also used to determine the standardised sulphate production equation over the change in sulphide content (Figure 55). The equations were based on a trend line which included a power regression as the best fit. Overall the PYROX modelled results presented an overestimation in sulphate production, as several assumptions were incorporated.

Table 17: *Generic PYROX result based on a change in sulphide fraction*

Integrated Sulphate Production Rate (kg/m^3)					
% Sulphide	0.2	0.4	0.6	0.8	1
Years					
5	142.15	167.61	182.52	192.84	200.60
10	93.82	116.88	131.65	142.60	151.32
15	78.31	99.12	112.67	122.88	131.11
20	69.22	88.51	101.22	110.85	118.66
25	62.95	81.11	93.17	102.35	109.83
30	58.26	75.51	87.05	95.87	103.07
35	54.56	71.05	82.15	90.67	97.63
40	51.53	67.38	78.10	86.35	93.12
45	48.99	64.28	74.67	82.69	89.28
50	46.83	61.61	71.71	79.52	85.95

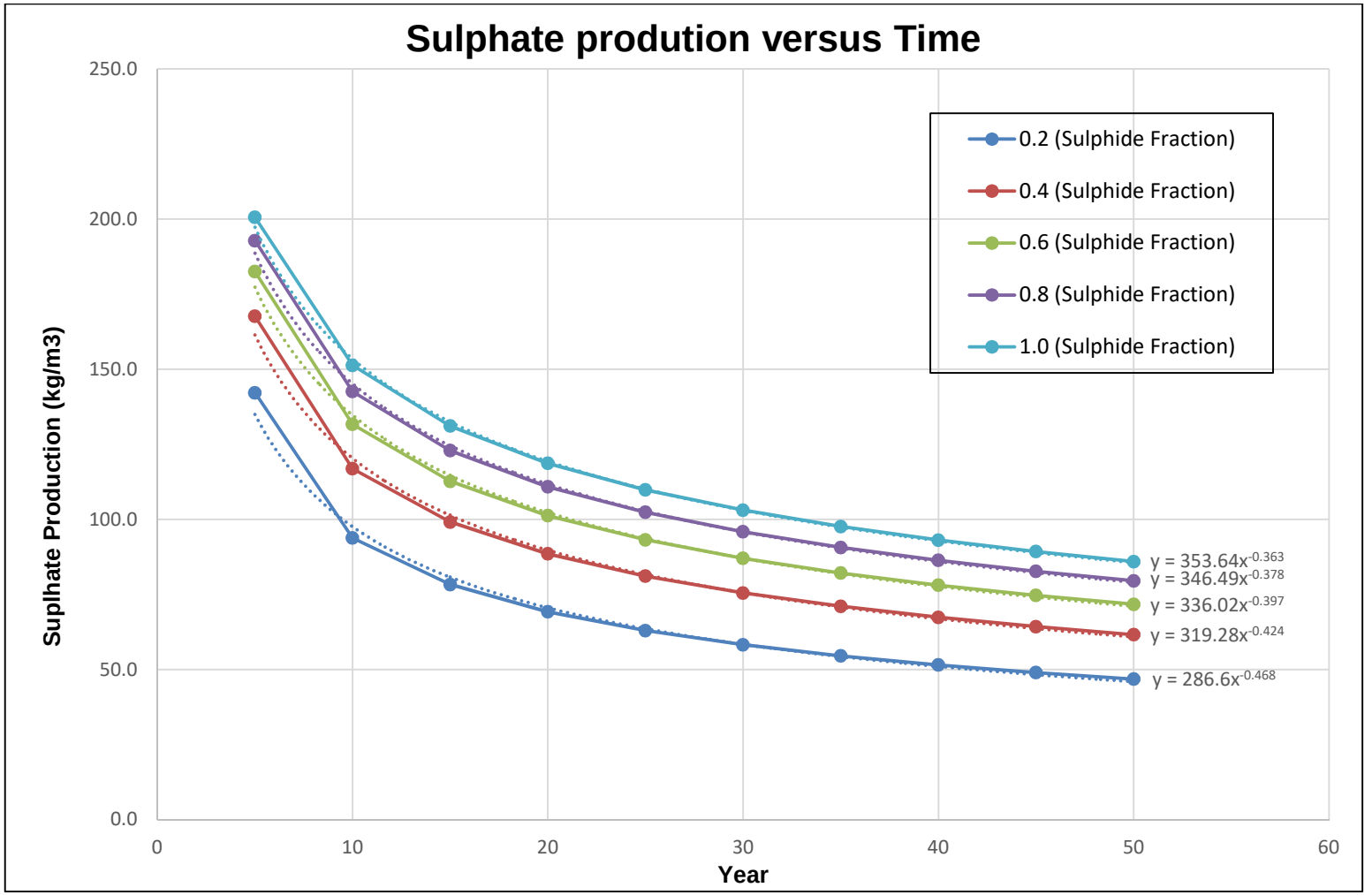

Figure 55: Standardised sulphate production equations

The initial sulphate production equation was determined in terms of the variation in sulphide fraction relative to the sulphate production (refer to Table 18 and Figure 56) and can be stipulated as:

Equation 5.1

$$y = 36.404 \ln(x) + 200.88$$

Table 18: Sulphide Fraction relative to the initial sulphate production

% Sulphide	Initial Sulphate Production (kg/m^3)
0.200	142.148
0.400	167.614
0.600	182.517
0.800	192.841
1.000	200.603

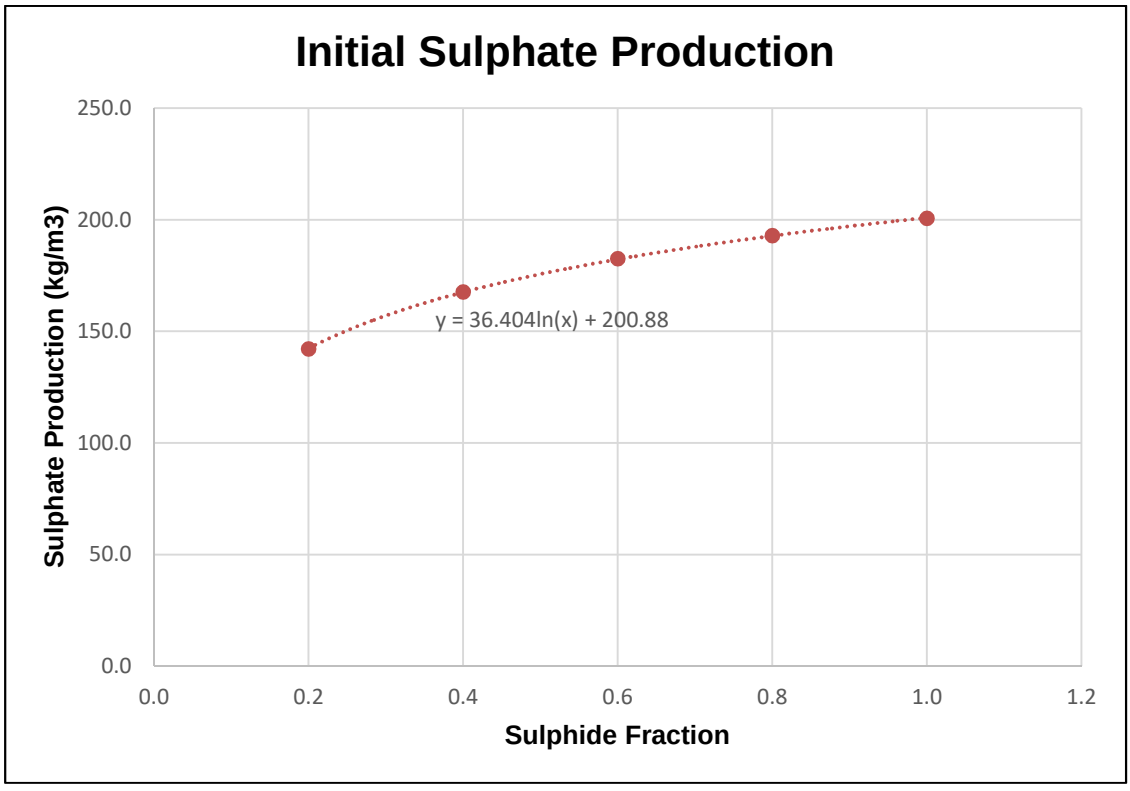

Figure 56: Initial sulphate production equation

From the equations presented within Figure 55; the sulphide fraction ratio equation can be derived by plotting the percentage sulphide concentration relative to the power of the standardised sulphate production equation. The values are presented in
Table 19, while the derived equation is illustrated in Figure 57.

Equation 5.2

$$y = 0.0653 \ln(x) - 0.3635$$

Table 19: *Modelled sulphide content relative to the sulphate production equation*

% Sulphide	Equation Power
0.2	-0.468
0.4	-0.424
0.6	-0.397
0.8	-0.378
1	-0.363

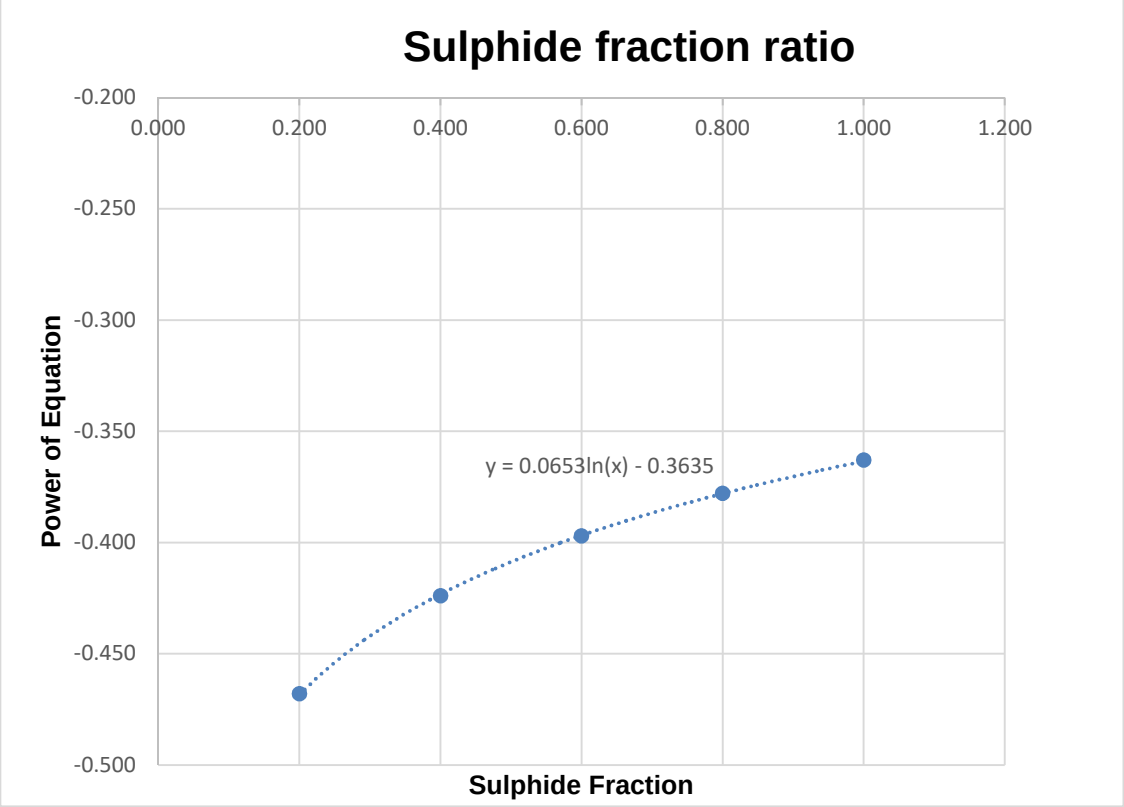

Figure 57: Sulphide fraction ratio equation

A similar approach was used to determine the representative sulphate production per five (5) year span, plotting the sulphate production rate relative to the standardised sulphate production equation. The determined equation (Equation 5.3) and data plotted is presented within Figure 58 and Table 20.

Equation 5.3

$$y = 1.1521x + 124.32$$

Table 20: *Modelled sulphate production relative to the sulphate production equation*

Sulphate Production	Equation Value
142.1	286.6
167.6	319.28
182.5	336.02
192.8	346.49
200.6	353.64

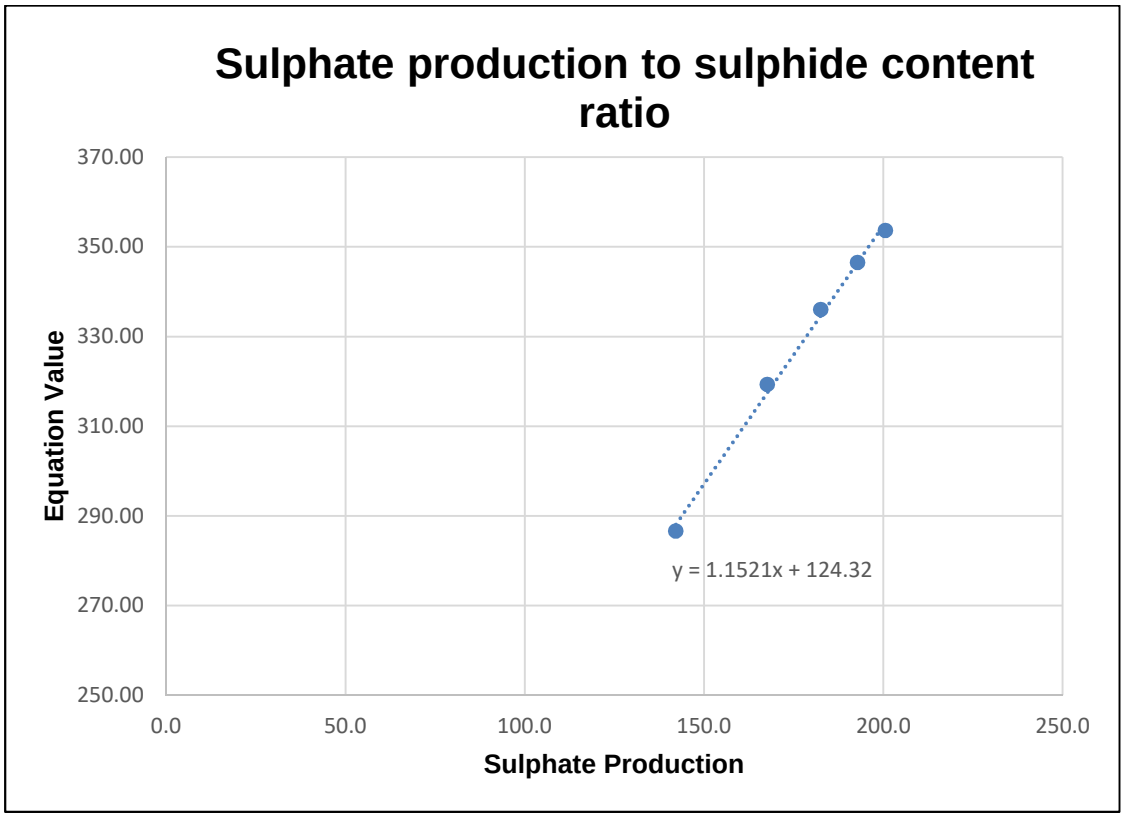

Figure 58: Sulphate production relative to the sulphide content

5.7.3 *Generic Equation*

From the modelled results several equations were derived based on regression lines. From the regression trends it is evident that PYROX presents a generic approach to modelling a sulphate release.

Based on the derived equations as followed by NWU (2016), an overall generic equation can be determined regarding die mass load of the tailings. One (1) set of the modelled results was used to correlate and determine the sulphate production based on the generic input parameters. The data set used was based on the sulphide concentration as recorded within the Carnival City TSF, where the sulphide content was considered at 0.8. The set sulphide concentration is also considered as a worst case scenario within the TSFs.

The initial sulphate production equation as determined in the previous section was used for an initial sulphate estimation, while the generic equation developed is presented below:

Equation 5.4

$$y = [(1.1521x + 124.32)\,(\mathrm{T})^{0.0653\ln(x)-0.3635}]]$$

x = %S (set at 0.8)

T = Time in years

Table 21 and Figure 59 present the generic results compared to the PYROX modelled results.

Table 21: *Generic source term results compared to the PYROX modelled values*

Sulphate Production (kg/m^3)		
Time	**PYROX Results**	**Generic Equation**
Initial Sulphate Estimation		192.757
5	192.84	188.50
10	142.60	145.04
15	122.88	124.43
20	110.85	111.61
25	102.35	102.58
30	95.87	95.74
35	90.67	90.32
40	86.35	85.88
45	82.69	82.14
50	79.52	78.93

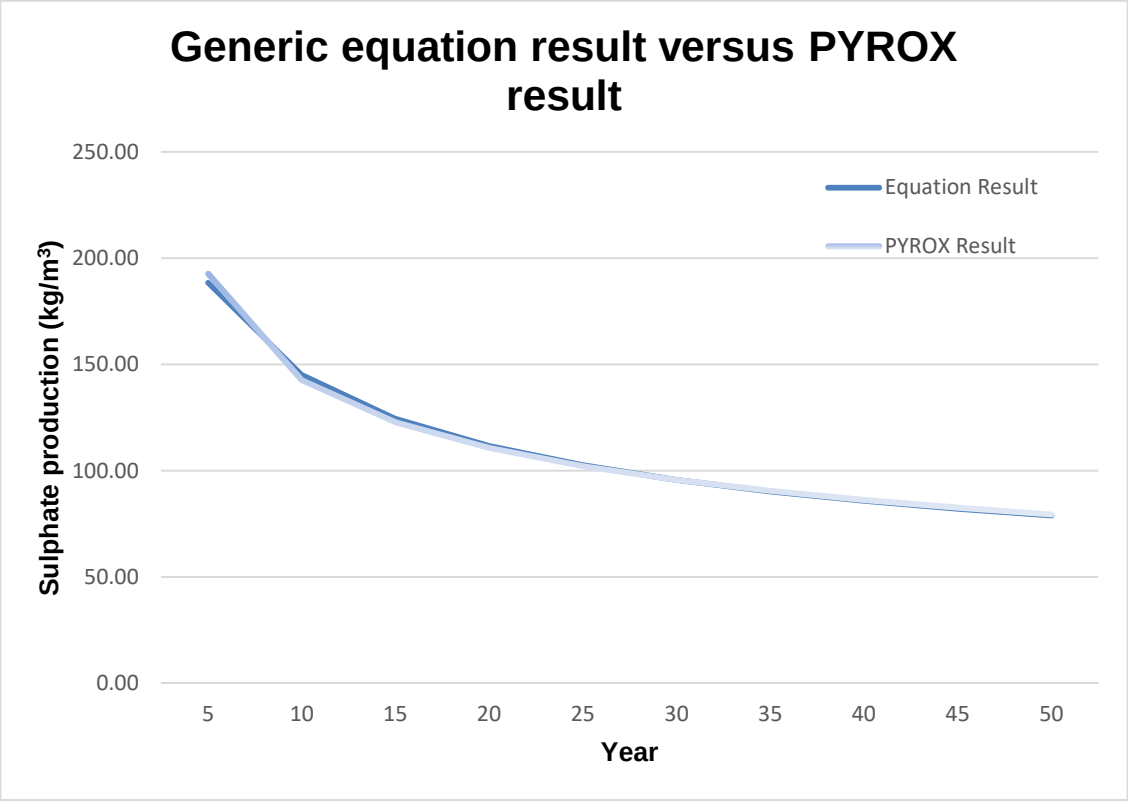

Figure 59: Generic source term versus PYROX results

When referring to the generic source term (Figure 59), the standardised source term is in close proximity to the modelled results. From the initial sulphate production with regards to the 5 year marker, a noticeable deviation (under estimation of 2.25%) compared to the modelled results is apparent, after which the final 50 year release also slightly under predicts (0.74%). The spatial variation of the source term trend is representative of a normalised sulphate release as well as the trends identified within the humidity cells. Overall there appears to be an accurate relation between the generic source term and the modelled results, taking into account that the sulphide percentage and moisture content is considered a generic function. An overall overestimation is present as data availability remained limited presenting several assumptions.

The generic source term is not an exact interpretation of the sulphate release but an approximate estimation of loads expected within the current East Rand Basin TSFs. The generic equation provides a function where in order to produce an expected sulphate load the %S can be substituted accordingly. The generic equation developed makes for a quicker and time conserving approach when compared to the PYROX software and can be Microsoft Excel based, resulting in a quick estimation of the expected load.

5.7.4 *Generic sulphate mass of the investigated TSFs*

Overall the generic source term is expressed in kg/m^3, where it was assumed that the modelled unsaturated zone was equal to the height of the heap. As the modelled results were based on a uniform 10 meter heap, the final result is obtained by multiplying the generic release with the volume (area and height) of the associated TSF. Based on the generic equation derived, the worst case scenario prediction sulphate mass was calculated regarding the investigated TSFs and presented within Table 22. As estimated with the weighting scale; TSF18 revealed the highest expected load, which might be stating the obvious as the overall area of a TSF is directly proportional to an expected release.

Table 22: *Estimated sulphate mass in terms of the sampled TSFs*

Time (yr)	Generic Source Term (kg/m^3)	Integrated Sulphate Production (kg)							
		TSF11	TSF12	TSF15	TSF16	TSF17	TSF18	TSF19	TSF20
Area (m^2)		192 590 m^2	387 000 m^2	641 000 m^2	745 000 m^2	958 000 m^2	4 443 000 m^2	390 800 m^2	834 000 m^2
Height (m)		10 m							
5	188.5	363 031 938	729 494 575	1 208 284 296	1 404 324 182	1 805 828 948	8 375 050 119	736 657 571	1 572 089 084
10	145.04	279 340 587	561 320 977	929 733 195	1 080 579 142	1 389 523 246	6 444 312 923	566 832 656	1 209 668 462
15	124.43	239 639 825	481 544 277	797 596 593	927 003 841	1 192 039 838	5 528 426 934	486 272 619	1 037 746 582
20	111.61	214 942 971	431 917 180	715 397 706	831 468 472	1 069 190 331	4 958 677 078	436 158 227	930 798 263
25	102.58	197 553 330	396 973 564	657 519 521	764 199 755	982 689 081	4 557 502 701	400 871 496	855 493 417
30	95.74	184 394 601	370 531 754	613 723 137	713 297 562	917 233 644	4 253 934 320	374 170 050	798 510 291
35	90.32	173 955 251	349 554 401	578 977 702	672 914 802	865 305 209	4 013 101 297	352 986 718	753 303 282
40	85.88	165 391 221	332 345 410	550 473 921	639 786 383	822 705 174	3 815 531 408	335 608 750	716 217 239
45	82.14	158 187 861	317 870 617	526 498 878	611 921 473	786 873 518	3 649 351 816	320 991 828	685 023 501
50	78.93	152 010 491	305 457 500	505 938 649	588 025 419	756 145 439	3 506 841 528	308 456 824	658 272 751
Total		2 128 448 074	4 277 010 254	7 084 143 599	8 233 521 031	10 587 534 427	49 102 730 123	4 319 006 737	9 217 122 873
Time (yr)	Generic Source Term (kg/m^2)	Integrated Sulphate Production (kg)							
		TSF22	TSF23	TSF24	TSF26	TSF27			
Area (m^2)		1 030 000 m^2	131 500 m^2	71 700 m^2	88 1000 m^2	831 100 m^2			
Height (m)		10 m							
5	188.5	1 941 548 869	247 877 356	135 154 421	1 660 684 032	1 566 622 587			
10	145.04	1 493 955 055	190 733 097	103 996 677	1 277 839 227	1 205 462 181			
15	124.43	1 281 629 471	163 625 510	89 216 343	1 096 228 703	1 034 138 110			
20	111.61	1 149 547 016	146 762 556	80 021 865	983 253 321	927 561 674			
25	102.58	1 056 544 628	134 888 950	73 547 815	903 704 677	852 518 680			
30	95.74	986 169 784	125 904 201	68 648 906	843 510 271	795 733 696			
35	90.32	930 338 586	118 776 237	64 762 404	795 755 625	750 683 882			
40	85.88	884 536 878	112 928 737	61 574 072	756 579 602	713 726 796			
45	82.14	846 012 237	108 010 300	58 892 308	723 627 943	682 641 525			
50	78.93	812 974 741	103 792 406	56 592 514	695 369 657	655 983 793			
Total		11 383 257 265	1 453 299 350	792 407 326	9 736 553 058	9 185 072 925			

From Figure 60, it is evident that a lack of monitoring boreholes downstream of the tailings facilities is present. With this in mind a direct correlation to the modelling results and associated borehole salt loads cannot be accurately described.

Monitoring boreholes 431S and 431D was identified close to tailing TSF18 and is representative of the uncontaminated upstream water profile, recording sulphate concentrations well below the SANS 241:2015 permissible limit. Additionally locality 2628AD00192 is representative of the downstream groundwater quality from tailing TSF25 and TSF26, even though the recorded sulphate concentrations were elevated, the monitoring borehole is not in an approximate downstream distance to determine accurate salt load contribution results. Thus several tailings contribute to the surrounding groundwater sulphate concentrations, and with the lack of downstream monitoring boreholes in terms of the studied tailings, a direct correlation of individual tailing sulphate contribution in association with the monitored boreholes cannot be accurately interpreted. Due to budget constraints, monitoring boreholes directly downstream of the TSFs could not be drilled.

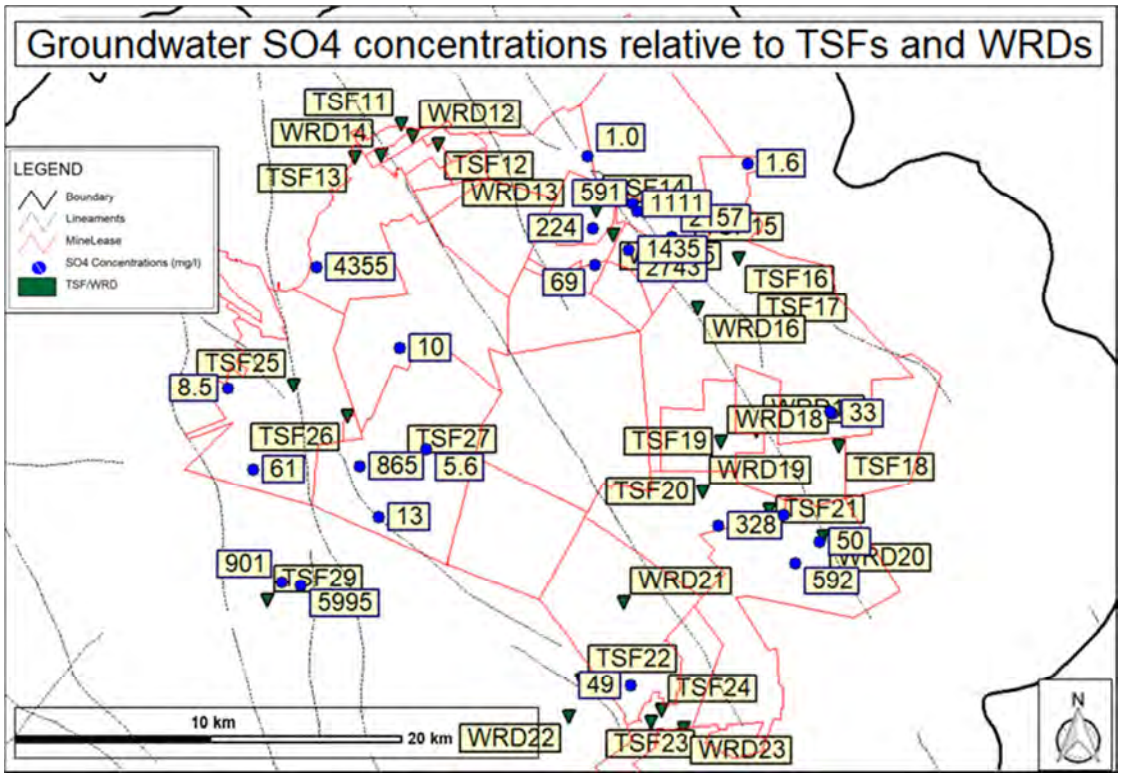

Figure 60: Graphical illustration regarding the monitored boreholes and associated TSFs

The monitored surface points are located closer to the associated TSFs (Figure 61) when compared to the groundwater localities. The recorded SO_4 concentrations downstream of the tailings are representative of sulphate pollution within the area. Although a dilution effect is present, extremely elevated sulphate loads were recorded from SW13, SW18 and SW30.

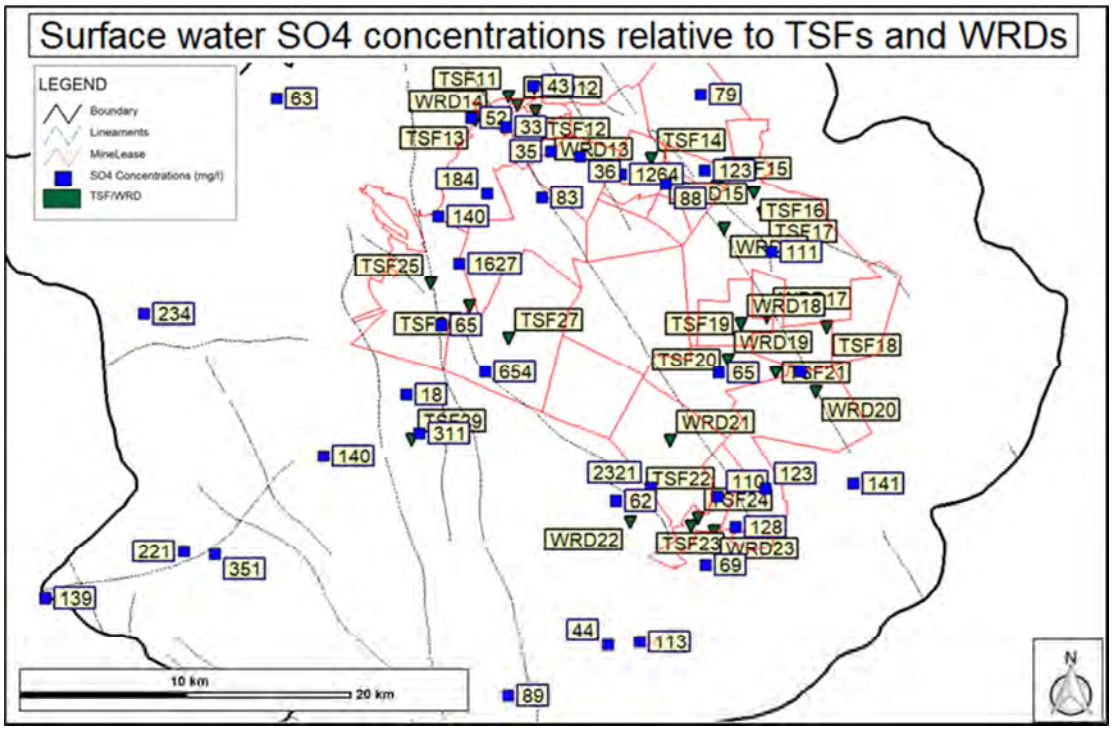

Figure 61: Graphical illustration of the monitored surface localities and associated TSFs

6. Conclusions and Recommendations

The prominent water pollution present in the East Rand Basin is mainly due to oxidation and reaction of sulphide minerals producing sulphuric acid. Contaminated groundwater is considered a result of close situating TSF's, enabling leachate through the surrounding tailings and subsurface geology, buffering the sulphuric acid to a neutral pH. Elevated TDS and SO_4 content was detected and is a clear indication of high salt loads and leachate emanating from the various TSFs within the East Rand Basin. With the use of sampling, static tests, kinetic tests and conceptual modelling the aim to develop a generic source term was implemented. Typical obstacles with regards to determining a generic source term instead of an individual model per TSF commonly included the proper calibration of models, where a lack of monitoring data, field observations is present, resulting in several assumptions and overestimated model predictions. Even though a monitoring program with respect to groundwater, tailing dams and waste rock dumps were incorporated, assumptions with respect to the model were still present.

In order to establish is the mineralogical and chemical characteristics of the TSFs and WRDs, samples were collected from different sites and introduced to ABA, XRF and XRD analysis. Mineral components in the tailings and rock samples consisted of dominant quartz and muscovite, while sulphur content was accessible in the form of jarosite which varied from minor to rare. The XRF analysis confirmed the mineralogical conclusions, consisting mainly of SiO_2 and Al_2O_3 which is typically associated with the Witwatersrand goldfields. On average SiO_2 recorded as the dominant average weight percentage (68.56%), in addition to Al_2O_3 presenting as the second highest chemical constituent (average of 10.78 wt. %). Supplementary oxides were also present in reduced concentrations and included Fe_2O_3, SO_3, K_2O and MgO. The ABA screening procedure displayed an inconclusive or very low probability of producing acid regarding the majority of the analysed samples. A 6.8% acid generating risk was observed within the sampled TSFs and WRDs, while a total of 24% recorded a high risk potential for generating acid. The low acid producing potential is also a likely observation when taken into account the sampled TSFs are moderately old and acid production has already occurred over several years; resulting in limited available sulphide minerals to produce acid.

Based on similar mineralogical and chemical characteristics; in addition to the screening procedure which identified acid potential; a total of nine (9) samples were subjected to selective kinetic leach testing (humidity cell), identifying the contaminant release process. A

lower pH was recorded from the unoxidised zones, and was directly correlated to the release of metals, especially iron (Fe), as well as the fact that more pyrite particles are available in the saturated samples for oxidation. An initial increase in sulphate concentration was apparent, after which the production decreases or produces a more constant release. This may be attributed to the removal of the already oxidised products that flush out, as well as the dissolution of secondary sulphate minerals that generally precipitate in pyrite baring TSFs. The minor sulphate release was expected from the waste rock samples as particle size is directly correlated to the reaction process, in addition to the low probability of acid generation detected from the ABA screening. The acid potential of the representative tailing samples concluded that a decrease over several years will be expected as slow diffusion processes are present and oxygen becomes limited over time.

To accompany the generic source term, geochemical fieldwork was obtained to identify the oxygen concentration profiles. Five (5) boreholes were drilled and equipped with oxygen chambers at specific depths, while numerous samples were taken for moisture content and %S. The unoxidised zones were identified at each tailing with respect to the moisture and %S. The study area was simplified to approximate possible pollution impacts emanating from the various sites and modelling with respect to PYROX version 1.1. was implemented. Based on the field and laboratory data, calibration of the PYROX model remained challenging as numerous input parameters were unknown. Due to the fact that the model is generic and was based on the moisture – and oxygen concentration profiles an acceptable correlation between the modelled -and measured profiles could not be obtained. This is mainly due to the variation of the moisture content within the associated heaps. The model revealed several difficulties with respect to unknown input parameters and recorded a great sensitivity in terms of the pyrite concentration.

The concept of the generic source term was developed based on the geochemical modelled results from NUW (2016). With the use of Hydrus and PYROX, a variance in sulphide and determined current standardised moisture content was used to produce different outputs and a generic equation was determined where % S is considered as a main variable input. The PYROX model was set up in terms of a general TSF, incorporating standardised moisture content for current TSF conditions. A change in fraction sulphur mineral content was implemented and the model was run to determine sulphate production. The sulphate production results were used to determine a generic sulphate production equation, where it was concluded that the standardised source term is in close proximity to the modelled results. An initial under estimation of 2.25% compared to the modelled results was apparent, after which the final 50 year release also presented a slight underestimation (0.74%). Overall an accurate relation between the generic source term and the modelled results was present, while the generic source term is an approximate estimation of loads expected within the East Rand Basin based on a worst case scenario. It was evident that an overestimation of sulphate production is present as data availability remained limited presenting several unknown parameters, in addition to the model revealing extremely sensitive to the pyrite concentration. Due to the model being generic, changing moisture content within the heaps over a relevant time frame could not be incorporated; which is considered one of the main limitations of the developed generic source term. Recommendations regarding the generic source term is addressed below:

- It is recommended that further field observation and analysis is conducted to identify the following unknown parameters:
    - Particle size distribution;
    - Porosity of the heaps;
    - Determine a more accurate height function of the tailings;
    - Identify the generic depth of the unsaturated zone.
- Additional parameters have to be implemented to account for different sulphur minerals as the model assumes only pyrite is available for oxidation.

A direct correlation in terms of the modelled salt loads and recorded groundwater sulphate concentrations could not be made, as a lack of downstream monitoring boreholes is present. It is advised that downstream monitoring boreholes be identified or drilled within the direct vicinity of the tailings, which will aid in the interpretation and evaluation of the modelled generic source term results.

7. References

Apane, V.V. 2014. Evaluation of acid rock drainage potential in the Waterberg Coalfield. Bloemfontein: University of the Free State. (Thesis – MSc).

Barthel, R., Janisch, J., Schwartz, N., Trifkovic, A., Nickel, D., Schultz, C. and Mauser, W. 2008. An integrated modelling framework for simulating regional-scale actor responses to global change in the water domain. *Environmental Modelling & Software* 23, 1095-1121.

Berkowitz. B., Dror, I. & Yaron, B. 2007. Contaminant Geochemistry: Interactions and Transport in the Subsurface Environment. Heideberg: Springer

Benzaazoua, M., Bussiere, B. & Dagenais, A.M. 2004. Comparison of kinetic tests for sulphide mine tailings. www.envirogeremi.polymtl.ca/pdf/articles/Benzaazoua_et_al-paper.pdf Date of Access: 25 March 2015

Côte, C.M., Moran, C.J., Hedemann, C.J. and Koch, C. 2010. Systems modelling for effective mine water management. *Environmental Modelling & Software* 25, 1664-1671

Dankert, B. T. and Hein, K. A. A. 2010. Evaluating the structural character and tectonic history of the Witwatersrand Basin: Precambrian Research, 177, 1–22, doi: 10.1016/j.precamres.2009.10.007.

Davis, G.B. & Ritchie, A.I.M. 1986(a). A model of oxidation in pyritic mine waste: part 1: equations and approximate solution, Applied Mathematical. Modelling, vol. 10, pp. 314–322.

Davis, G.B. & Ritchie, A.I.M. 1986(b). A model of oxidation in pyritic mine waste: part 2: comparison of numerical and approximate solution, Applied Mathematical. Modelling, vol. 10, pp. 314–322.

Davis, G.B. & Ritchie, A.I.M. 1986(c). A model of oxidation in pyritic mine waste: part 3: import of particle size distribution, Applied Mathematical. Modelling, vol. 10, pp. 314–322.

Davison, C. 2003. Catchment diagnostic framework for the Klip River catchment, Vaal barrage. Johannesburg: University of the Witwatersrand. (Thesis – MSc).

Department Of Water Affairs. Hydrology. http://www.dwa.gov.za/Hydrology/Verified/hymain.aspx Date of Access: 01 August 2017

Department Of Water Affairs and Forestry. 2008. Best Practice Guidelines G4: Impact prediction. ISBN: 978-0-9802679-9-0. South Africa: Pretoria.

Department of Water Affairs and Forestry (DWAF). 2008. Best Practice Guidelines Series A: Activity guidelines: Best Practice Guidelines Series A4. Water Management for Surface Mines

Dijkstra, J.J., Meeussen, J.C.L., Van Der Sloot, H.A. & Comans, R.N.J. 2008. A consistent geochemical modelling approach for the leaching and reactive transport of major and trace elements in MSWI bottom ash (*In* Applied Geochemistry, 23:1544–1562).

Doulati Ardejani, F., Jodieri Shokri, B., Moradzadeh, A., Soleimani, E., Ansari Jafari, M. 2008. A combined mathematical geophysical model for prediction of pyrite oxidation and pollutant leaching associated with a coal washing Waste dump. Int. J. Environ. Sci. Tech., 5 (4), 517-526.

Elberling, B.; Nicholson, R. V.; Scharer, J. M. 1994. A combined kinetic and diffusion model for pyrite oxidation in tailings: a change in controls with time. J. Hydrol., 157 (1), 47-60.

Forstner, U. & Wittmann, G.T.W. 1976. Metal Accumulations in Acidic Waters from Gold Mines in South Africa. Geoforum, Vol.7, 41-49.

Govender, K., Bezuidenhout, N., Van Zyl, A. & Rousseau, P. 2009. Prediction of seepage emanating from a TSF in an arid climate. ISBN: 978-0-9802623-5-3. South Africa: Pretoria

Hansen, R.N. 2014. Numeric geochemical reaction modelling, incorporating systems theory and implications for sustainable development – Study on East Rand Basin acid mine drainage, Witwatersrand, South Africa. Stellenbosch: SU. (Dissertation – PhD) 196 p.

Hodgson, F.D.I., Usher, B.H., Scott, R., Zeelie, S., Cruywagen, L.M. and De Necker, E. 2001. Prediction techniques and preventative measure relating to the post-operational impact of underground mines on the quality and quantity of groundwater resources, Report to the Water Research Commission, WRC Report No. 669/1/01, 286p.

International Association of Oil & Gas Producers. 2010. Consequence modelling. http://www.ogp.org.uk/pubs/434-07.pdf. Date of access: 15 Jan. 2015

International Organisation for Standardisation (ISO) 5667-1. 2006 Part 1: Guidance on the design of sampling programs and sampling techniques.

Jaynes, D. B.; Rogowski, A. S. and Pionke, H. B., 1984b. Acid mine drainage from reclaimed coal strip mines, 2: Simulation results of model. Water Resour. Res., 20 (2), 243-250.

Jones, G. A., Brierley, S. E. & Howard, J. R. 1988. Research on the contribution of mine dumps to the mineral pollution load in the Vaal Barrage, *Report to the Water Research Commission*, WRC Report No. 136/1/89, Pretoria, South Africa

Jorgensen, P.R., McKay, L.D., Spliid, N.H. 1998. Evaluation of chloride and pesticide transport in a fractured clayey till using large undisturbed columns and numerical modelling, Water Resources Research, Vol. 34, no. 4, pp.539-553

Kahnt, R. & Metschies, T. 2007. Modelling of contaminant release from a uranium mine tailings site: Germany, Belgium. *In: 11th International Conference on Environmental Remediation and Radioactive Waste Management (ICEM), 2-6 September, Bruges.* Belgium: ASME, p. 1-6.

Kleinman, R. L. P., Crerar, D. A. and Pacelli, R. R. 1981. Biogeochemistry of acid mine drainage and a method to control acid formation, Mining Engineering: 300–305.

Lawrence, R.W. 1995. Prediction of Acid Rock Drainage - Fundamentals and Tools, notes from MEND Workshop, Montreal, PQ, December. pp. 7-8.

Lawrence, R.W. & Wang, Y. 1996. *Determination of Neutralization Potential for Acid Rock Drainage Prediction*, MEND Report 1.16.3, Ottawa, ON, 149p.

Lourens, P.J.H., 2013. The relationship between South African Geology and Geohydrology, MSc. Thesis (Unpublished), pp. 246 -250.

Lloyed, J.A. & Heathcote, J.A. 1985. Natural inorganic hydrochemistry in relation to groundwater: An introduction. Oxford Uni. Press, New York. 296p.

Malmstrom, M.E., Gleisner, M., Herbert, R.B. 2006. Element discharge from pyritic mine tailings at limited oxygen availability in column experiments, Applied Geochemistry, Vol. 21, pp. 184-202

Manzi, M.S.D., Durrheim, R.J., Hein, K.A.A. and King, N. 2012. 3D edge detection seismic attributes used to map potential conduits for water and methane in deep gold mines in the Witwatersrand basin, South Africa.

Marsden, D. D. 1986. The current limited impact of Witwatersrand gold-mine residues on water pollution in the Vaal River system*. Journal of the South African Institute of Mining and Metallurgy*, 86, 481-504

McCarthy, T. S. 2006. The Witwatersrand Supergroup. In: M. R. Johnson, C. R. Anhaeusser & R. J. Thomas, eds. The Geology of South Africa. Pretoria: Geological Society of South Africa & Council for Geoscience, pp. 155-186.

McCarthy, T.S. 2011. The impact of acid mine drainage in South Africa. S Afr J Sci. 107(5/6), Art #712, 7 pages.

Mills, C. 1998. Kinetic Test work procedure. http://technology.infomine.com/enviromine/ard/Kinetic%20Tests/kinetic%20procedures. Date of access: 29 November 2014

Molson, J., Aubertin, M. & Martin, V. 2006. Conceptual and numerical models of oxygen diffusion, sulphide oxidation and acid mine drainage within discretely fractured porous media. http://www.enviro-geremi.polymtl.ca/pdf/articles/iah2006.pdf Date of Access: 25 July 2014

Morin, K.A & Hutt, N.M. 1999. Humidity Cells: How Long? How Many? Proceedings of Sudbury '99, Mining and the Environment II, Volume 1, p.109-117, Sudbury, Canada.

North West University (NWU). 2016 East Rand Basin Source Apportionment Study, Council for Geoscience, Pretoria.

Nsimba, E.B. 2009. Cyanide and cyanide in the goldmine polluted land in the East and Central Rand Goldfields. Johannesburg: UW. (Dissertation – M.Sc.) 195 p.

Ochieng, L., Harck, T., & Peters, M. 2009. Net Neutralisation Potential (NNP) in Kimberley Diamond Tailings and Slimes Waste Materials. ISBN: 978-0-9802623-5-3. South Africa: Pretoria

Oelofse, S.H.H., Hobbs, P.J., Rascher, J & Cobbing, J.E. 2007. *The pollution and destruction threat of gold mining waste on the Witwatersrand – A West Rand case study.* Symposium on

Environmental Issues and Waste Management in Energy and Mineral Production (SWEMP 2007). 11 – 13 December 2007. Bangkok.

Palmer, C M. 1992. Principles of Contaminant Hydrogeology Lewis Publishers, Chelsea, MI, 211 pp

Rademeyer, B. 2007. The Influence of Environmental Impacts on Tailings Impoundment Design: Integrating environmental impacts with engineering costs for the design of tailings impoundments. Pretoria: University of Pretoria (Thesis - PhD) 378 p.

Ravikumar, R., Somashekar, R.K. & Prakash, K.L. 2016. A comparative study usage of Durov and Piper diagrams to interpret hydrochemical processes in groundwater from SRLIS river basin, Karnataka, India. *Elixir International Journal*, 80(2015):31073-31077.

Rosner, T. 1999. The environmental impact of seepage from gold mine tailings dams near Johannesburg, South Africa. Pretoria: University of Pretoria (Thesis – PhD) 184 p.

Rosner, T. & Van Skalkwyk, A. 1999. The environmental impact of gold mine tailings footprints in the Johannesburg region, South Africa. Bull ENG Geol ENV (2000) 59: 137-148.

Rosner, T., Boer, R., Reyneke, R., Aucamp, P. & Vermaak, J. 2001. A preliminary assessment of pollution contained in the unsaturated and saturated zone beneath reclaimed gold-mine residue deposits, *Water Research Commission Report* No. 797/01/01, Pretoria, 210

South African National Standard (SANS) 241-1:2015: *Drinking Water, Part 1: Microbiological, Physical, Aesthetic and Chemical Determinants*, Edition 1, 2015.

Schafer, W.M. 2006. Probabilistic Modelling of Long-Term Mass Loads from a Covered Dry-Stack Tailings Facility (*In* Barnhisel, R.I., eds, The American Society of Mining and Reclamation: 7th International Conference on Acid Rock Drainage, St. Louis, Missouri. Lexington, KY: ASMR. p. 1189-1902)

Scott, R. 1995. Flooding of Central and East Rand Gold Mines: An investigation into controls over the inflow rate, water quality and the predicted impacts of flooded mines (Paper delivered by the Water Research Commission by the Institute of Groundwater studies at the University of the Orange Free State.) Bloemfontein. 275p.

Sherlock, E.J. 1995. *Evaluation of Static and Kinetic prediction test data and comparison with field monitoring data* (Dissertation – M.Sc.). University of British Columbia, Vancouver.

Singer, P. C. & Stumm W. 1970. Acid mine drainage: rate determining step, *Science* 167, 1121-1123.

Singh, S.R. & Verma, C.L. 2011. Water retention characteristic form particle size distribution and bulk density data of soils. India. *Proc Indian Natn Sci Acad* (2011) 77: 249-262.

Sobek, A.A., Schuller, W.A., Freeman, J.R & Smith, R.M. 1978. Field and laboratory methods applicable to overburden and mine soils. EPA 600/2-78-054, 203pp.

The World Wildlife Fund (WWF). 2013. Water Balance Program: Freshwater in South Africa. http://www.wwf.org.za/what_we_do/freshwater/water_balance/
Date of access: 17 November 2013

Tiruta-Barna, L, Imyim, A. & Barna, R. 2004. Long-term prediction of the leaching behaviour of pollutants from solidified wastes (*In* Advances in Environmental Research, 8:697-711).

Tutu, H. 2012. Mining and Water Pollution, Water Quality Monitoring and Assessment, Dr. Voudouris (Ed.), ISBN: 978-953-51-0486-5, InTech, Available from: http://www.intechopen.com/books/water-qualitymonitoring-and-assessment/mining-and-water-pollution. Date of use: 08 Apr. 2013

Usher, B.H., Cruywagen, L.M., Necker, E. & Hodgon, F.D.I. 2001. On-site and Laboratory Investigations of Spoil in Opencast Collieries and the Development of Acid-Base Accounting Procedures (Paper delivered as part of the course in Groundwater Studies at the University of the Free State.) Bloemfontein. 313p.

Van Der Sloot, H.A. 1996. Developments in evaluating environmental impact from utilization of bulk wastes using laboratory leaching tests and field verification. *Waste Management*, 16(1):65-81.

Van Dyk, G. & Kisten, S. 2006. An explanation of the 1:500 000 general hydrogeological map. Pretoria: Department of Water Affairs.

Water Reasearch Commission (WRC). 2005. Water Resources of South Africa 2005. Water Research Commission Report K5/1491

Water Resources of South Africa, Study (WR). 2005. User's guide Version1: December 2008. WRC Report Number TT 381/08

Weaver, J.M.C, Cave, L. & Talma, A.S. 2007. Groundwater Sampling: A comprehensive guide for sampling methods. ISBN: 978-1-77005-545-2. South Africa.

Wunderly, M.D. & Blowes, D.W. 1997. PYROX version 1.1 user's manual. Institute for Groundwater Research. University of Waterloo, Canada, 8 p.

Xu, Y & Beekman, H.E., 2003. Groundwater recharge estimation in Southern Africa. UNESCO IHP Series No. 64, UNESCO Paris. ISBN 92-9220-000-3.

Yibas, B., Pulles, W. & Nengovhela, C. 2010. Kinetic development of oxidation zones in tailings dams with specific reference to the Witwatersrand gold mine tailing dams, Report to the Water Research Commission, WRC Report No. 1554/1/10, 105p.

Appendix A: Groundwater Hydro-census

Basic Groundwater Hydrocensus						
ID	X-coordinate	Y-coordinate	Static Water level (mbgl)	Borehole Depth (mbgl)	Use	Comments
102	-26.057780	28.400000	-	-	Monitoring borehole	
433	-26.285400	28.529590	-	-	Domestic	
2628AD00118	-26.308330	28.288890	-	-	Monitoring borehole	
2628AD00192	-26.306940	28.333330	-	-	Domestic	
2628AD00350	-26.328260	28.341110	-	-	Domestic	
431D	-26.284753	28.528619	10.1	40	Monitoring borehole	
431S	-26.285420	28.529620	9.81	-	Monitoring borehole	
6L13-12	-26.212907	28.463114	3.13	-	Monitoring borehole	
B21	-26.356166	28.309000	2.35	-	Monitoring borehole	
B9D	-26.202250	28.448669	21.19	99	Monitoring borehole	
BH7	-26.397403	28.445706	31.13	37	Monitoring borehole	
BHC46	-26.224125	28.431031	-	-	Domestic	
CEN74	-26.300041	28.360796	11.45	25	Monitoring borehole	
G14D	-26.217986	28.444989	8.59	17	Monitoring borehole	
G23D	-26.217986	28.444989	13.03	41	Monitoring borehole	
G8D	-26.217819	28.441025	12.51	51	Monitoring borehole	
GAA12D	-26.199411	28.446918	23.9	100	Monitoring borehole	
GAA13D	-26.197923	28.442553	22.56	70	Monitoring borehole	
GAA13S	-26.197923	28.442553	21.85	35	Monitoring borehole	Blow yield of 2.5 l/s
GAA16S	-26.227880	28.317670	-	-	Monitoring borehole	
GC1	-26.274985	28.278551	-	-	Domestic	
GP141	-26.338000	28.524110	8.12	47	Monitoring borehole	
GP142	-26.346726	28.514374	6.78	33	Monitoring borehole	
GP143	-26.331709	28.482316	2.1	-	Monitoring borehole	
GV1D	-26.255150	28.500940	-	-	Monitoring borehole	
GV1S	-26.255150	28.501150	-	-	Monitoring borehole	
HR1	-26.258330	28.350000	-	-	Domestic	
ME1	-26.179520	28.428130	-	-	Domestic	
PD3	-26.209526	28.430171	22.15	-	Monitoring borehole	
UNK	-26.217978	28.445000	-	-	Monitoring borehole	
ZBH26D	-26.327216	28.509185	-	-	Monitoring borehole	
HR3	-26.308334	28.288888	-	-	Monitoring borehole	
G3D	-26.216850	28.443597	9.28	-	Monitoring borehole	
431D	-26.284753	28.528619	-	-	Monitoring borehole	
431S	-26.285420	28.529620	9.81	22	Monitoring borehole	
G10D	-26.217977	28.445000	13.03	74.1	Monitoring borehole	
B41	-26.354672	28.300719	2.5	14	Monitoring borehole	
DA68	-26.182477	28.494377	-		Domestic	

GA16S	-26.225055	28.315486	26.41	28	Monitoring borehole	
003	26.215841	28.441486	9.78	11	Monitoring borehole	
006	26.209570	28.430143	22.15	80	Monitoring borehole	
ZBH26D	26.327216	28.509185	1.15		Monitoring borehole	
ZBH26S	26.327216	28.509185	0.97	11	Monitoring borehole	
SRK			1.09	4.7	Monitoring borehole	

Appendix B: Borehole Conductivity Profiles

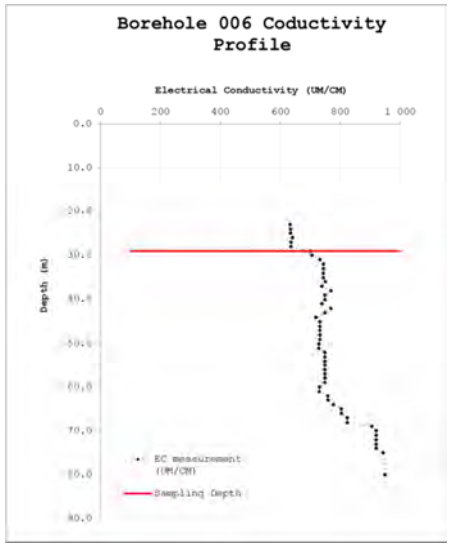
Borehole 006 Coductivity Profile
Electrical Conductivity (UM/CM)
Depth (m)
EC measurement (UM/CM)
Sampling Depth

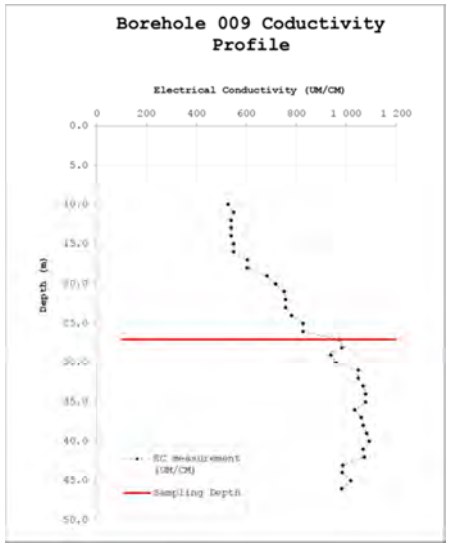
Borehole 009 Coductivity Profile
Electrical Conductivity (UM/CM)
Depth (m)
EC measurement (UM/CM)
Sampling Depth

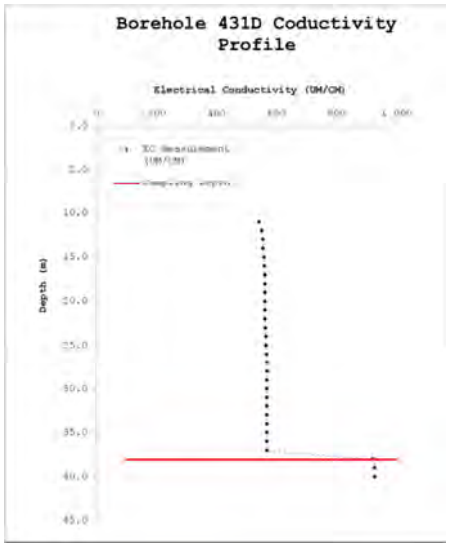
Borehole 431D Coductivity Profile
Electrical Conductivity (UM/CM)
Depth (m)

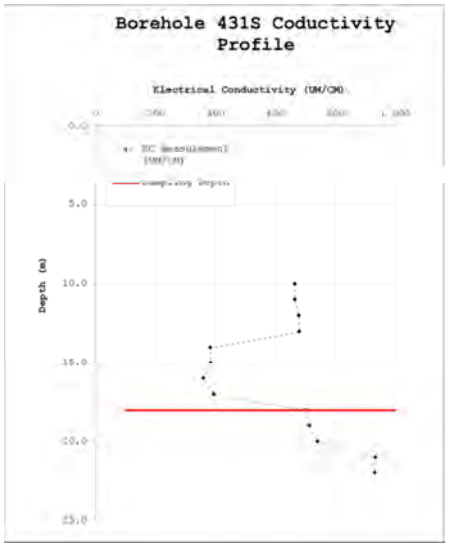
Borehole 431S Coductivity Profile
Electrical Conductivity (UM/CM)
Depth (m)

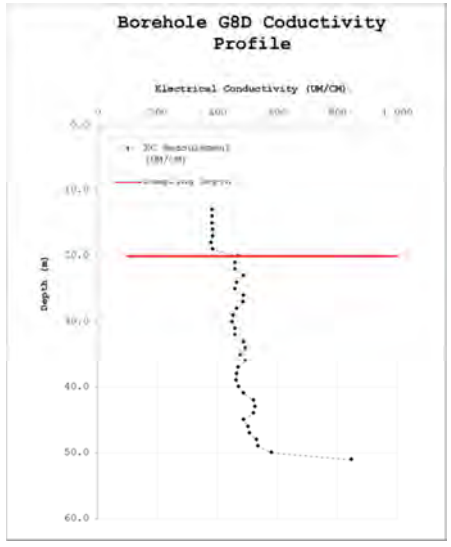
Borehole G8D Coductivity Profile
Electrical Conductivity (UM/CM)
Depth (m)

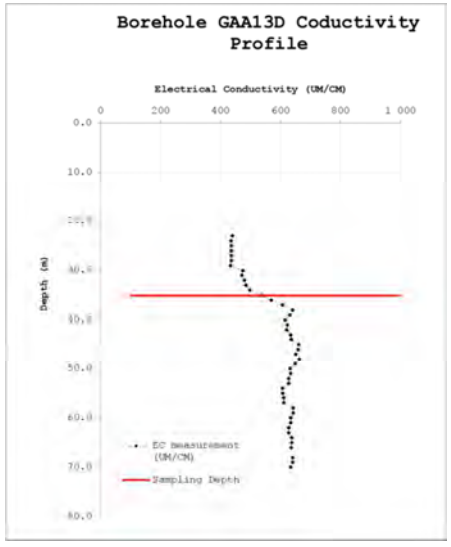
Borehole GAA13D Coductivity Profile
Electrical Conductivity (UM/CM)
Depth (m)
EC measurement (UM/CM)
Sampling Depth

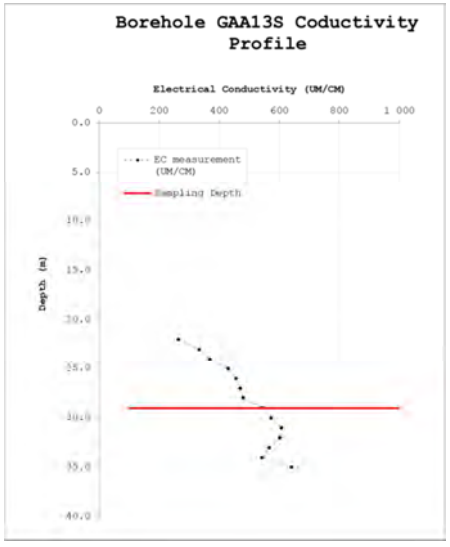
Borehole GAA13S Coductivity Profile
Electrical Conductivity (UM/CM)
Depth (m)
EC measurement (UM/CM)
Sampling Depth

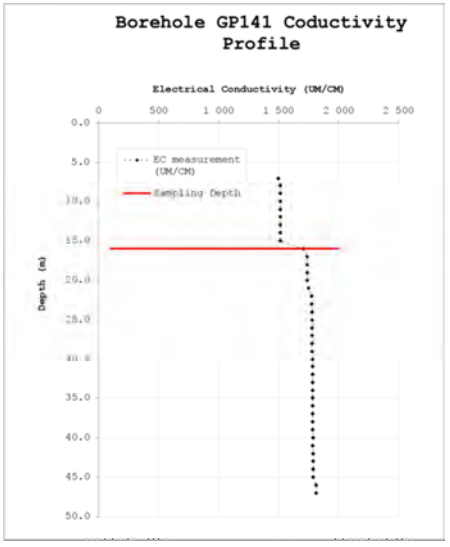
Borehole GP141 Coductivity Profile
Electrical Conductivity (UM/CM)
Depth (m)
EC measurement (UM/CM)
Sampling Depth

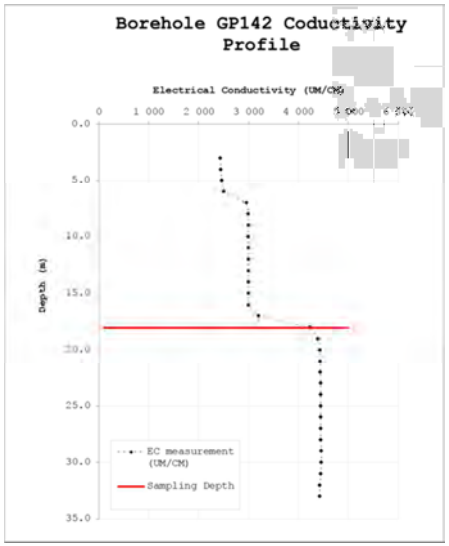
Borehole GP142 Coductivity Profile
Electrical Conductivity (UM/CM)
Depth (m)
EC measurement (UM/CM)
Sampling Depth

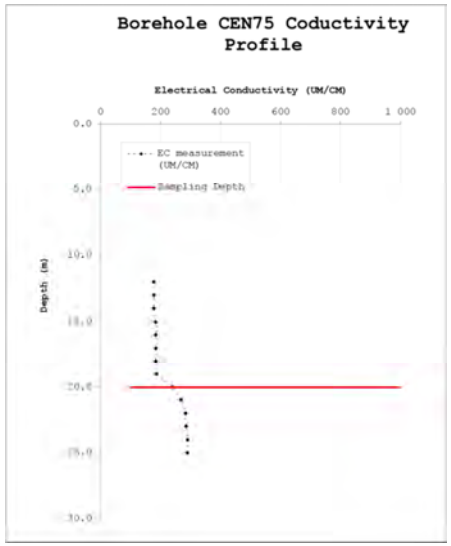
Borehole CEN75 Coductivity Profile
Electrical Conductivity (UM/CM)
Depth (m)
EC measurement (UM/CM)
Sampling Depth

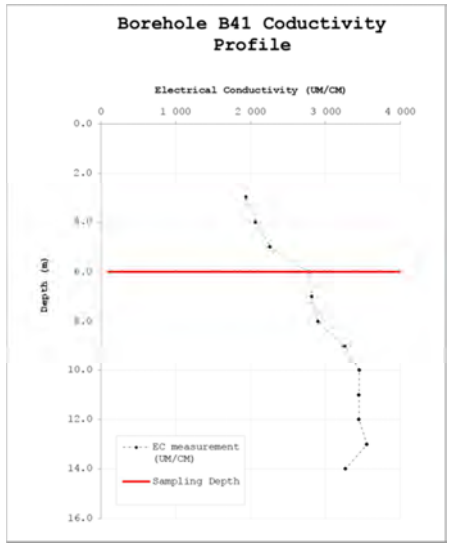
Borehole B41 Coductivity Profile
Electrical Conductivity (UM/CM)
Depth (m)
EC measurement (UM/CM)
Sampling Depth

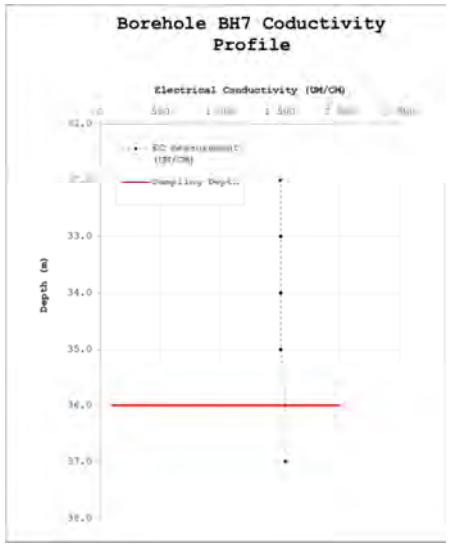
Borehole BH7 Coductivity Profile
Electrical Conductivity (UM/CM)
Depth (m)

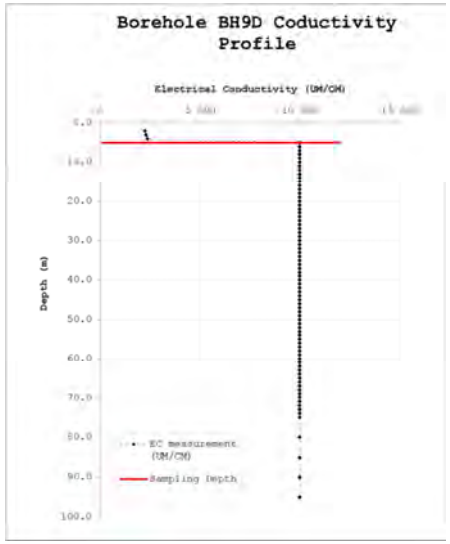
Borehole BH9D Coductivity Profile
Electrical Conductivity (UM/CM)
Depth (m)
EC measurement (UM/CM)
Sampling Depth

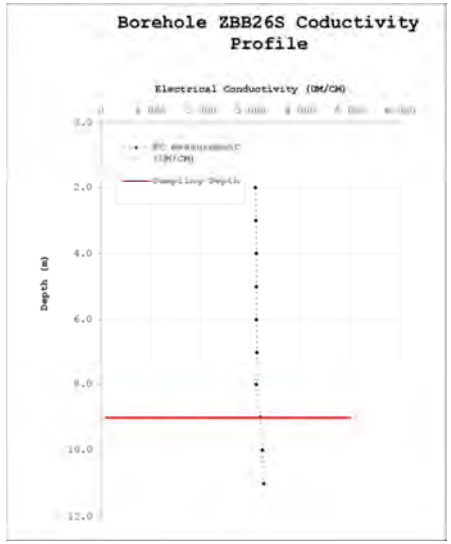
Borehole ZBB26S Coductivity Profile
Electrical Conductivity (UM/CM)
Depth (m)

Appendix C: Groundwater Chemistry Results

SANS241-1:2015	Nov-2013	mS/m	mg/l	mg/l	mg/l	mg/l	mg/l	mg/l	mg/l	mg/l	mg/l	mg/l	mg/l	mg/l	mg/l	mg/l	mg/l	mg/l	mg/l	mg/l	mg/l	mg/l	mg/l	mg/l
Acceptable	5<pH<9.7	0	0	0	0	0	0	0	0	0	0	0	0	0	0	0	0	0	0	0	0	0	0	0
Allowable		170	1200	200	70	0.3	300	50	150	0.2	0.05	0.5	2	0.5	0.07	2	5	0.01	0.01	0.003	0.006	0.01	0.015	500
Unacceptable	pH<4;pH>10	370	2400	400	100	0.5	600	100	300	0.5	0.5	1	2	1	0.35	2	10	0.05	0.05	0.01	0.006	0.05	0.015	600
Sample	**pH**	**EC** Electrical Conductivity	**TDS** Total Dissolved Solids	**Na** Sodium 23.0	**Mg** Magnesium 24.3	**Al** Aluminium 27.0	**Cl** Chloride 35.5	**K** Potassium 39.1	**Ca** Calcium 40.1	**V** Vanadium 50.9	**Cr** Chromium 52.0	**Mn** Manganese 54.9	**Fe** Iron 55.8	**Co** Cobalt 58.9	**Ni** Nickel 58.7	**Cu** Copper 63.5	**Zn** Zinc 65.4	**As** Arsenic 74.9	**Se** Selenium 79.0	**Cd** Cadmium 112.4	**Hg** Mercury 200.6	**Pb** Lead 207.2	**U** Uranium 238.0	**SO4** Sulphate 96.1
BH7	7.33	15.00	97.50	10.19	3.56	0.0638	4.60	6.90	5.92	0.000136	0.000026	0.11	0.16	0.0008	0.0045	0.0001	0.00046	0.000071	0.000367	0.0000277	0.00000343	0.000132	0.000006	14.74
B9D	8.07	195.00	1267.50	124.60	126.10	0.0002	258.60	5.28	88.22	0.000135	0.000021	0.33	0.42	0.0042	0.0000	0.0000	0.00051	0.000077	0.000365	0.0000281	0.00000294	0.000129	0.000008	397.30
B41	6.87	302.00	1963.00	100.70	199.70	0.0001	474.20	3.69	250.90	0.000132	0.000009	0.82	1.12	0.0026	0.0000	0.0001	0.00052	0.000062	0.000331	0.0000279	0.00000336	0.000129	0.000008	1277.24
BHC46	8.20	47.00	305.50	8.69	24.86	0.0001	11.50	1.86	46.67	0.000131	0.000030	0.00	0.18	0.0000	0.0000	0.0001	0.00043	0.000076	0.000373	0.0000283	0.00000381	0.000135	0.000007	73.33
CEN74	8.38	30.00	195.00	19.08	12.21	0.0031	7.88	3.11	20.04	0.000131	0.000032	0.00	0.07	0.0000	0.0000	0.0001	0.00045	0.000077	0.000372	0.0000279	0.00000416	0.000131	0.000007	8.44
GAA12D	8.14	340.00	2210.00	223.80	182.50	0.0001	569.11	6.04	264.60	0.000129	0.000003	0.39	1.14	0.0092	0.0000	0.0000	0.00051	0.000074	0.000346	0.0000276	0.00000470	0.000134	0.000002	1038.48
GAA13D	8.30	63.00	409.50	9.82	36.22	0.0001	33.35	3.56	59.99	0.000133	0.000031	0.05	0.25	0.0000	0.0000	0.0001	0.00049	0.000077	0.000366	0.0000285	0.00000462	0.000133	0.000006	123.21
GAA13S	8.38	57.00	370.50	8.51	30.60	0.0002	26.24	3.19	44.75	0.000136	0.000036	0.08	0.22	0.0000	0.0000	0.0001	0.00053	0.000078	0.000374	0.0000280	0.00000462	0.000132	0.000007	128.83
GA16S	8.17	850.00	5525.00	1264.00	297.40	0.0000	1012.68	13.38	328.20	0.000119	0.001393	0.05	1.39	0.0000	0.0147	0.0295	0.00048	0.000068	0.000299	0.0000284	0.00000484	0.000133	0.005337	4238.10
G3D	8.31	105.00	682.50	59.72	39.27	0.0000	64.53	5.00	71.07	0.000133	0.000019	0.03	0.32	0.0000	0.0000	0.0000	0.00054	0.000066	0.000302	0.0000277	0.00000475	0.000133	0.000007	259.99
G8D	8.45	63.00	409.50	42.62	18.46	0.0002	75.58	9.68	49.49	0.000136	0.000028	0.00	0.22	0.0000	0.0000	0.0001	0.00053	0.000077	0.000365	0.0000278	0.00000486	0.000126	0.000402	71.88
G14D	9.00	1353.00	8794.50	994.10	1.65	0.0001	5119.11	31.67	1783.00	0.000104	0.016850	0.00	7.75	0.0420	0.0143	0.0117	0.00053	0.000048	0.319500	0.0000272	0.00000479	0.000124	0.000008	1434.86
G23D	7.52	1706.00	11089.00	1150.00	576.20	0.0002	7437.07	16.25	875.50	0.000107	0.018120	3.44	4.90	0.0075	0.0035	0.0124	0.00045	0.000064	0.311600	0.0000277	0.00000474	0.000123	0.000005	1869.17
GP141	8.50	50.00	325.00	13.65	15.56	0.0002	26.06	4.75	52.73	0.000132	0.000004	0.10	0.44	0.0000	0.0000	0.0001	0.00048	0.000077	0.000367	0.0000270	0.00000486	0.000096	0.000006	31.44
GP142	8.20	376.00	2444.00	306.10	160.60	0.0002	731.55	10.55	278.10	0.000131	0.000978	0.14	1.16	0.0000	0.0016	0.0000	0.00053	0.000075	0.000319	0.0000279	0.00000476	0.000129	0.001413	824.31
GP143	8.17	172.00	1118.00	42.52	88.66	0.0023	308.90	8.24	186.40	0.000133	0.000017	0.68	0.79	0.0138	0.0000	0.0001	0.00052	0.000076	0.000333	0.0000282	0.00000482	0.000135	0.000003	375.10
ME1	7.44	10.00	65.00	5.57	2.30	0.0002	7.90	5.61	3.35	0.000138	0.000041	0.06	0.00	0.0000	0.0064	0.0000	2.74700	0.000078	0.000373	0.0000242	0.00000495	0.000138	0.000008	1.50
2628AD00350	8.26	52.00	338.00	16.01	25.22	0.0002	40.62	3.30	43.95	0.000131	0.000038	0.00	0.15	0.0000	0.0000	0.0001	0.00051	0.000077	0.000370	0.0000281	0.00000481	0.000119	0.000007	12.65
431D	8.45	62.00	403.00	27.78	28.06	0.0002	79.26	11.09	49.91	0.000137	0.000043	0.24	0.19	0.0000	0.0000	0.0001	0.00051	0.000072	0.000366	0.0000282	0.00000497	0.000136	0.000006	10.70
431S	8.57	76.00	494.00	82.46	16.01	0.0001	141.34	10.85	25.61	0.000133	0.000037	0.15	0.12	0.0000	0.0000	0.0000	0.00050	0.000060	0.000357	0.0000277	0.00000505	0.000134	0.000007	6.21
433	8.50	72.00	468.00	32.49	33.00	0.5706	73.95	5.95	73.19	0.000058	0.000013	0.39	0.59	0.0012	0.0138	0.2368	0.50380	0.000069	0.000365	0.0000229	0.00000437	0.000068	0.000017	58.78
6L13-12	8.33	471.00	3061.50	398.60	220.10	0.0060	744.30	13.13	393.60	0.000133	0.000013	2.33	1.55	0.0478	0.0094	0.0016	0.00043	0.000074	0.000315	0.0000274	0.00000492	0.000125	0.000006	2235.81
PD3	8.55	89.00	578.50	53.40	38.41	0.0041	107.64	2.97	73.30	0.000118	0.000036	0.00	0.28	0.0023	0.0000	0.0000	0.00048	0.000076	0.000371	0.0000275	0.00000511	0.000126	0.000006	215.53
HR1	6.09	23.00	149.50	17.03	9.40	0.039570	17.15	8.49	13.83	0.000071	0.000009	0.002532	0.004191	0.000019	0.000060	0.000021	0.007326	0.000054	0.000268	0.000021	0.000003	0.000101	0.000002	6.32
GC1	6.65	27.00	175.50	13.70	16.24	0.000264	17.51	2.13	18.54	0.000090	0.000015	0.017000	0.002170	0.000019	0.000059	0.000008	0.000359	0.000053	0.000261	0.000021	0.000003	0.000112	0.000002	7.38
2628AD00118	8.51	70.00	455.00	13.01	42.82	0.017970	40.49	3.34	76.53	0.000068	0.000013	0.000021	0.176700	0.015830	0.000041	0.000039	0.000370	0.000051	0.000255	0.000021	0.000003	0.000103	0.000221	60.61
2628AD00192	7.23	200.00	1300.00	57.98	138.80	0.000346	156.02	4.71	259.10	0.000079	0.000002	0.025240	0.688000	0.016200	0.000023	0.000018	0.000416	0.000052	0.000250	0.000021	0.000002	0.000113	0.000184	842.11
431D	7.13	61.00	396.50	31.21	32.05	0.006136	78.37	11.41	55.54	0.000095	0.000015	0.129500	0.145000	0.000016	0.015150	0.001243	0.000325	0.000048	0.000263	0.000022	0.000003	0.000100	0.000080	7.39
102	0.75	30000.00	195000.00	0.54	0.03	0.000206	48.17	0.17	0.10	0.000097	0.036550	0.002126	0.123700	0.000008	0.017190	0.006337	0.000004	0.000053	0.000266	0.000022	0.000002	0.000097	0.000001	67.20

SANS241-1:2015	Apr-2014	mS/m	mg/l	mg/l	mg/l	mg/l	mg/l	mg/l	mg/l	mg/l	mg/l	mg/l	mg/l	mg/l	mg/l	mg/l	mg/l	mg/l
Acceptable	5<pH<9.7	0	0	0	0	0	0	0	0	0	0	0	0	0	0	0	0	0
Allowable		170	1200	200	70	0.3	300	50	150	0.2	0.05	0.5	2	0.5	0.07	2	5	0.01
Unacceptable	pH<4;pH>10	370	2400	400	100	0.5	600	100	300	0.5	0.5	1	2	1	0.35	2	10	0.05
Sample	**pH**	**EC** Electrical Conductivity	**TDS** Total Dissolved Solids	**Na** Sodium 23.0	**Mg** Magnesium 24.3	**Al** Aluminium 27.0	**Cl** Chloride 35.5	**K** Potassium 39.1	**Ca** Calcium 40.1	**V** Vanadium 50.9	**Cr** Chromium 52.0	**Mn** Manganese 54.9	**Fe** Iron 55.8	**Co** Cobalt 58.9	**Ni** Nickel 58.7	**Cu** Copper 63.5	**Zn** Zinc 65.4	**As** Arsenic 74.9
6L13-12	7.25	451.00	2931.50	340.10	183.10	0.000350	718.20	10.95	316.70	0.000078	0.002663	1.375000	2.064000	0.035850	0.000125	0.004506	0.000270	0.000040
G8D	7.99	62.00	403.00	40.41	17.96	0.000360	53.15	8.19	42.04	0.000087	0.000037	0.053460	0.261600	0.000012	0.000064	0.000012	0.000307	0.000043
G3D	7.96	111.00	721.50	68.45	39.51	0.000381	78.64	4.74	62.32	0.000085	0.000040	0.283300	0.390000	0.000029	0.036220	0.000024	0.000297	0.000041
G10D	6.84	957.00	6220.50	878.70	294.40	0.000444	2431.88	22.34	423.60	0.000053	0.022610	0.565100	4.737000	0.005719	0.000096	0.009220	0.043390	0.000036
B9D	7.79	211.00	1371.50	130.70	148.30	0.000434	333.32	5.26	87.18	0.000079	0.001963	0.458800	0.538300	0.003130	0.000152	0.000037	0.000342	0.000042
GAA12D	7.48	337.00	2190.50	209.60	178.00	0.000475	587.35	5.35	226.20	0.000073	0.003564	0.185200	1.408000	0.006706	0.000143	0.000030	0.000340	0.000039
DA68	8.18	39.00	253.50	6.58	14.80	0.000456	24.74	2.28	22.14	0.000085	0.000034	0.000059	0.098580	0.000024	0.000170	0.000060	0.116800	0.000044
ME1	7.27	13.00	84.50	4.87	4.95	0.000528	3.76	5.09	0.90	0.000089	0.000050	0.605300	0.000475	0.000016	0.010090	0.000057	0.016340	0.000044
BH7	7.16	25.00	162.50	14.28	6.91	0.000449	6.84	2.80	6.52	0.000088	0.000055	0.206000	0.000062	0.003133	0.005238	0.000062	0.000324	0.000043
B41	7.83	226.00	1469.00	97.72	152.50	0.000450	460.74	4.14	126.10	0.000079	0.001021	0.081750	0.762400	0.000007	0.000161	0.000043	0.000329	0.000032
GC1	7.73	29.00	188.50	11.83	14.40	0.000362	19.12	1.92	9.75	0.000082	0.000046	0.000037	0.004784	0.000024	0.000164	0.000012	0.024800	0.000043
GA16S	7.72	811.00	5271.50	1281.00	304.70	0.000436	1007.18	13.73	328.70	0.000066	0.007908	0.661500	2.091000	0.009499	0.006670	0.018810	0.000307	0.000033
431S	7.03	78.00	507.00	82.49	17.22	0.000382	150.70	8.94	21.07	0.000080	0.000022	0.007389	0.083330	0.000016	0.000161	0.000053	0.000336	0.000030
431D	7.42	75.00	487.50	38.42	29.03	0.000401	115.49	14.76	41.77	0.000085	0.000039	0.113400	0.223800	0.000019	0.000153	0.000023	0.000282	0.000041
433	7.94	73.00	474.50	31.33	32.67	0.000359	78.99	4.48	56.40	0.000077	0.000041	0.000017	0.309600	0.000020	0.000154	0.000043	0.192000	0.000043
2628AD00350	8.28	53.00	344.50	14.78	25.43	0.000392	44.00	3.03	36.97	0.000083	0.000044	0.000065	0.195700	0.000002	0.000176	0.000061	0.000310	0.000043
2628AD00192	7.72	212.00	1378.00	50.55	124.00	0.000499	171.13	3.85	230.30	0.000071	0.000023	0.004547	1.396000	0.012120	0.000151	0.000064	0.000341	0.000041
GP143	8.11	123.00	799.50	29.63	64.10	0.000395	230.83	6.50	96.52	0.000085	0.000027	0.374000	0.555100	0.002052	0.000156	0.000061	0.000338	0.000042
GP142	8.27	124.00	806.00	130.00	64.20	0.000481	279.98	7.34	5.23	0.000084	0.000021	0.071470	0.000312	0.000024	0.000177	0.000048	0.000364	0.000043
GP141	7.48	58.00	377.00	16.23	20.07	0.000405	31.42	5.34	48.86	0.000071	0.000051	0.000044	0.265600	0.000021	0.000161	0.000061	0.000342	0.000041
CEN74	7.34	35.00	227.50	21.14	15.36	0.000534	7.32	3.34	17.71	0.000081	0.000062	0.223900	0.264100	0.000009	0.000161	0.000061	0.000253	0.000042
HR1	6.44	21.00	136.50	13.53	6.93	0.000317	18.09	6.89	4.14	0.000049	0.000063	0.000057	0.000275	0.000024	0.000168	0.000061	0.000270	0.000043
HR3	7.75	74.00	481.00	11.24	38.18	0.000450	44.09	2.86	55.97	0.000066	0.000048	0.000062	0.301100	0.014420	0.000171	0.000056	0.000326	0.000043

SANS241-1:2015	Jul-2014	mS/m	mg/l	mg/l	mg/l	mg/l	mg/l	mg/l	mg/l	mg/l	mg/l	mg/l	mg/l	mg/l	mg/l	mg/l	mg/l
Acceptable	5<pH<9.7	0	0	0.00	0.00	0	0	0	0	0	0	0	0	0	0	0	0
Allowable		170	1200	200.00	70.00	0.3	300	50	150	0.2	0.05	0.5	2	0.5	0.07	2	5
Unacceptable	pH<4;pH>10	370	2400	400.00	100.00	0.5	600	100	300	0.5	0.5	1	2	1	0.35	2	10
Sample	**pH**	**EC** Electrical Conductivity	**TDS** Total Dissolved Solids	**Na** Sodium 22.99	**Mg** Magnesium 24.31	**Al** Aluminium 27.0	**Cl** Chloride 35.5	**K** Potassium 39.1	**Ca** Calcium 40.1	**V** Vanadium 50.9	**Cr** Chromium 52.0	**Mn** Manganese 54.9	**Fe** Iron 55.8	**Co** Cobalt 58.9	**Ni** Nickel 58.7	**Cu** Copper 63.5	**Zn** Zinc 65.4
HR3	7.62	72.00	468.00	11.41	38.58	0.000045	42.47	3.26	73.62	0.0005	0.0010	0.0009	0.0501	0.0203	0.0000	0.0000	0.0001
CEN74	7.13	33.00	214.50	23.40	15.75	0.000058	6.32	4.02	25.12	0.0000	0.0000	0.0340	0.0219	0.0003	0.0000	0.0000	0.0000
2628AD00192	7.34	206.00	1339.00	51.91	127.00	0.000068	165.12	4.85	249.20	0.0000	0.0026	0.0125	0.1481	0.0163	0.0000	0.0008	0.0002
HR1	6.29	21.00	136.50	13.45	7.14	0.035330	13.63	8.02	11.01	0.0018	0.0000	0.0052	0.0214	0.0002	0.0000	0.0000	0.0000
GC1	7.10	29.00	188.50	13.33	16.04	0.000031	20.77	2.27	17.63	0.0000	0.0000	0.0026	0.0138	0.0000	0.0000	0.0018	0.0294
G10D	7.03	911.00	5921.50	943.30	331.00	0.007916	2360.94	24.51	404.00	0.0000	0.0132	1.0070	0.5726	0.0046	0.0012	0.0093	0.0000
GP141	7.35	55.00	357.50	17.44	20.90	0.000059	25.73	6.10	70.32	0.0009	0.0016	0.0116	0.0500	0.0002	0.0000	0.0000	0.0002
GA16S	7.36	819.00	5323.50	-1.00	323.50	0.026810	958.48	15.31	355.20	0.0000	0.0068	0.0158	0.2502	0.0016	0.0145	0.0208	0.0001
GP142	7.20	363.00	2359.50	326.00	172.40	0.000061	749.89	11.57	271.90	0.0000	0.0050	0.1715	0.1813	0.0011	0.0010	0.0252	0.0002
G3D	7.46	97.00	630.50	64.49	38.83	0.001244	79.13	6.27	66.07	0.0000	0.0016	0.0527	0.0547	0.0010	0.0040	0.0012	0.0002
GP143	7.54	151.00	981.50	34.25	91.15	0.007076	239.51	8.96	159.10	0.0000	0.0038	0.4388	0.1357	0.0051	0.0004	0.0000	0.0001
GAA12D	7.33	338.00	2197.00	233.00	200.60	0.000059	573.51	6.73	287.00	0.0000	0.0046	0.3188	0.1695	0.0114	0.0000	0.0000	0.0002
B41	8.42	227.00	1475.50	111.00	169.30	0.000023	495.54	12.75	130.30	0.0000	0.0037	0.0997	0.0923	0.0015	0.0000	0.0097	0.0002
ZBH26D	7.31	203.00	1319.50	43.66	145.20	0.000056	167.22	9.10	232.90	0.0000	0.0019	0.0523	0.1869	0.0106	0.0001	0.0000	0.0002
G8D	7.57	62.00	403.00	45.95	19.81	0.000034	52.04	8.94	51.33	0.0000	0.0009	0.0538	0.0438	0.0007	0.0086	0.0000	0.0002
431S	7.31	64.00	416.00	33.21	29.57	0.000036	81.91	12.39	49.81	0.0000	0.0013	0.1210	0.0339	0.0003	0.0001	0.0050	0.0002
431D	7.08	78.00	507.00	92.69	19.62	0.000086	142.78	10.50	30.75	0.0000	0.0000	0.1490	0.0402	0.0010	0.0000	0.0000	0.0002
BH7	7.31	9.00	58.50	11.60	1.64	0.043750	4.39	1.94	2.57	0.0000	0.0004	0.0056	0.0411	0.0004	0.0000	0.0053	0.0002
PD3	7.54	104.00	676.00	61.08	49.80	0.013120	95.82	3.37	87.92	0.0002	0.0019	0.0103	0.0736	0.0040	0.0008	0.0000	0.0002
6L13-12	7.32	436.00	2834.00	408.80	218.20	0.000039	735.02	14.14	325.50	0.0000	0.0043	1.0770	0.3147	0.0238	0.0009	0.0000	0.0002
2628AD00350	8.03	51.00	331.50	17.66	26.80	0.000067	39.25	3.45	44.45	0.0000	0.0009	0.0006	0.0338	0.0018	0.0000	0.0000	0.0002
B9D	7.70	208.00	1352.00	129.70	138.50	0.000030	261.58	5.89	66.73	0.0000	0.0019	0.4589	0.0489	0.0018	0.0000	0.0000	0.0002
433	7.79	75.00	487.50	33.25	35.81	0.000026	75.70	5.31	68.10	0.0026	0.0037	0.0009	0.0402	0.0004	0.0000	0.0000	0.0002
BHC46	7.88	45.00	292.50	9.72	26.24	0.020900	11.02	2.11	46.53	0.0000	0.0000	0.0003	0.0401	0.0007	0.0000	0.0000	0.0002
DA68	7.94	40.00	260.00	9.10	20.67	0.000018	23.10	3.15	37.12	0.0000	0.0000	0.0031	0.0216	0.0004	0.0000	0.0451	0.1323
B21	9.07	1270.00	8255.00	-1.00	1214.00	0.005407	2528.26	4.35	66.80	0.0000	0.0139	1.3190	0.1292	1.1660	0.0000	0.0106	0.0002

Appendix D: Groundwater Chemistry Trends

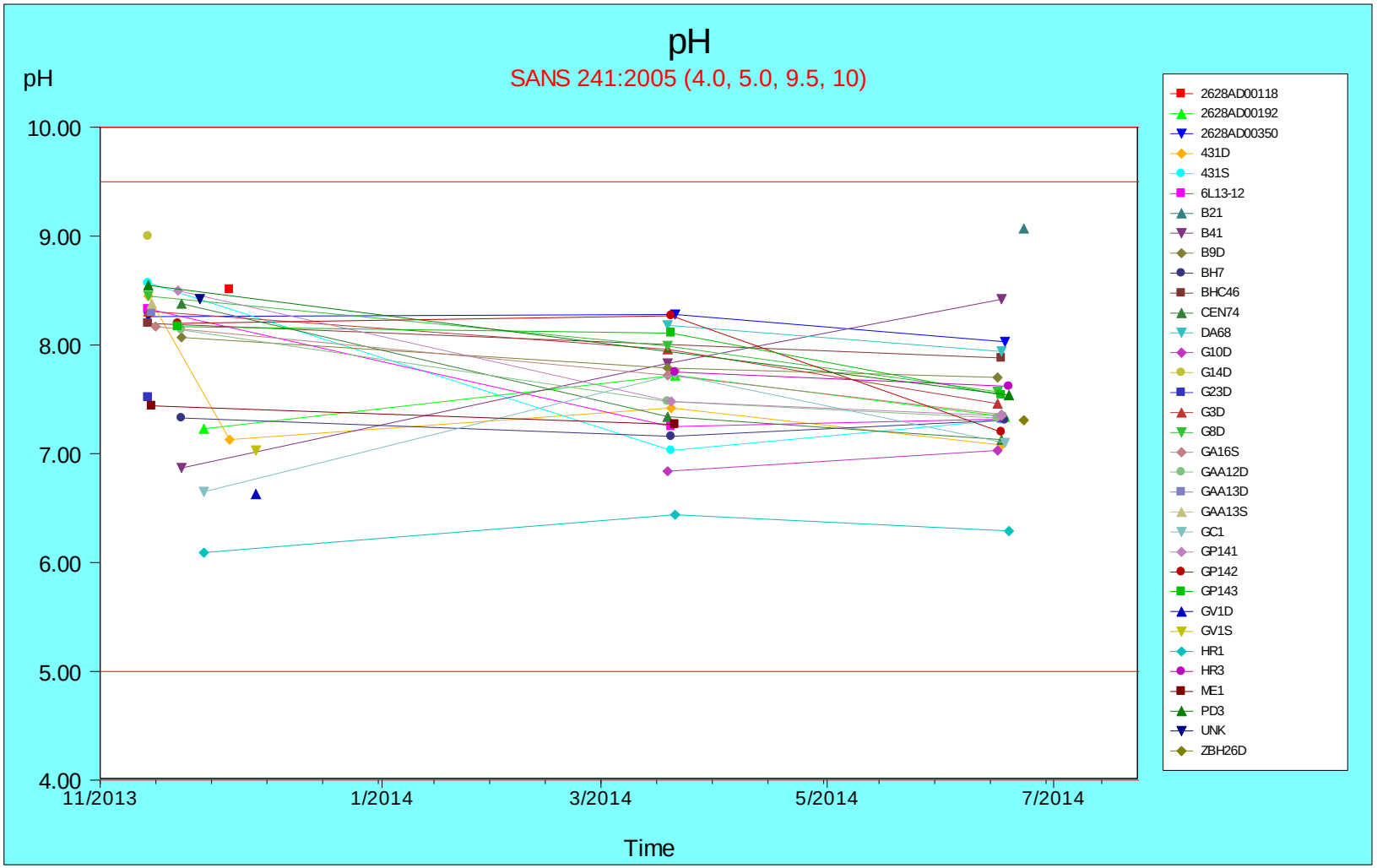
pH
SANS 241:2005 (4.0, 5.0, 9.5, 10)
pH
10.00
9.00
8.00
7.00
6.00
5.00
4.00
11/2013
1/2014
3/2014
5/2014
7/2014
Time
2628AD00118
2628AD00192
2628AD00350
431D
431S
6L13-12
B21
B41
B9D
BH7
BHC46
CEN74
DA68
G10D
G14D
G23D
G3D
G8D
GA16S
GAA12D
GAA13D
GAA13S
GC1
GP141
GP142
GP143
GV1D
GV1S
HR1
HR3
ME1
PD3
UNK
ZBH26D

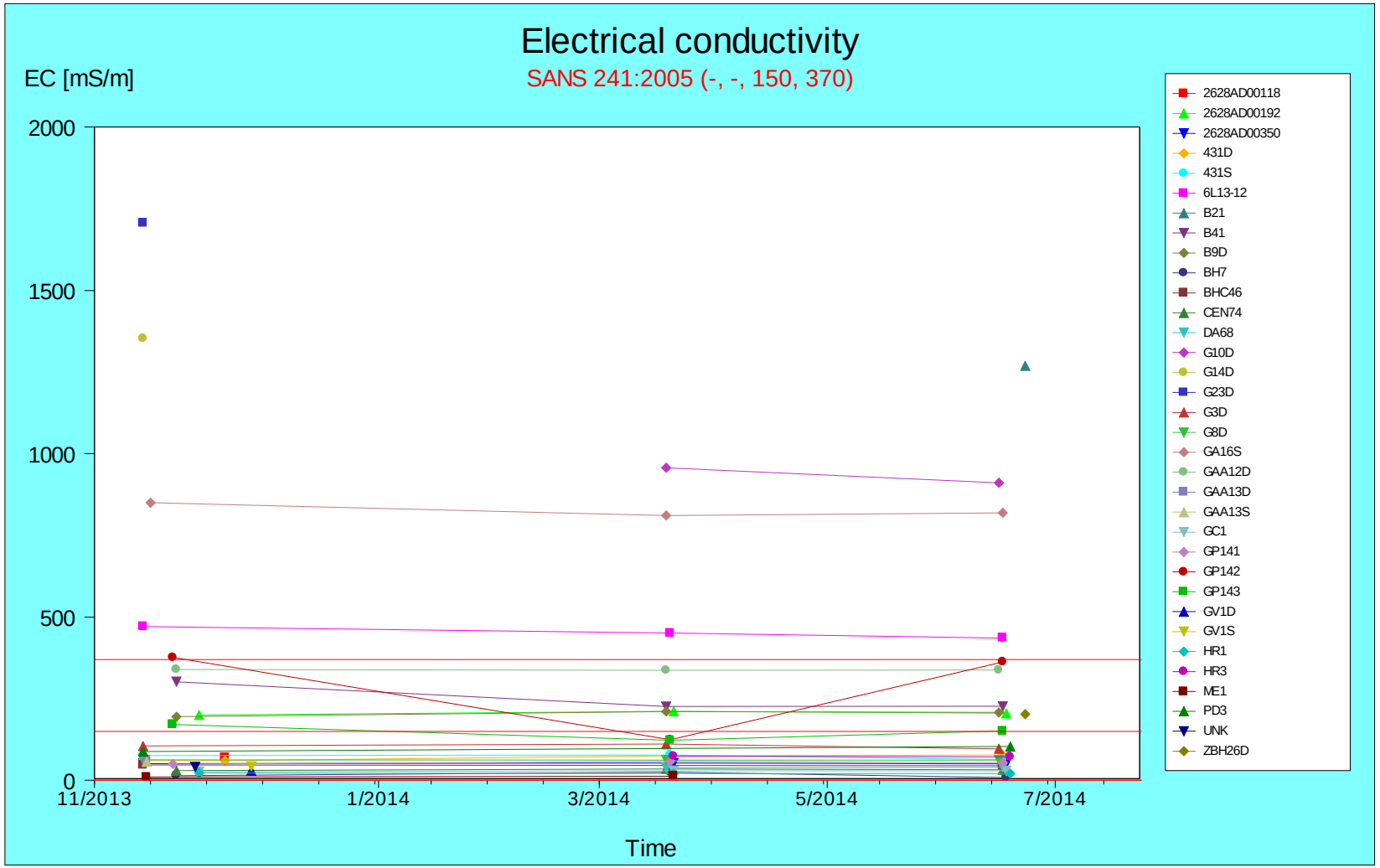
Electrical conductivity
SANS 241:2005 (-, -, 150, 370)
EC [mS/m]
2000
1500
1000
500
0
11/2013
1/2014
3/2014
5/2014
7/2014
Time
2628AD00118
2628AD00192
2628AD00350
431D
431S
6L13-12
B21
B41
B9D
BH7
BHC46
CEN74
DA68
G10D
G14D
G23D
G3D
G8D
GA16S
GAA12D
GAA13D
GAA13S
GC1
GP141
GP142
GP143
GV1D
GV1S
HR1
HR3
ME1
PD3
UNK
ZBH26D

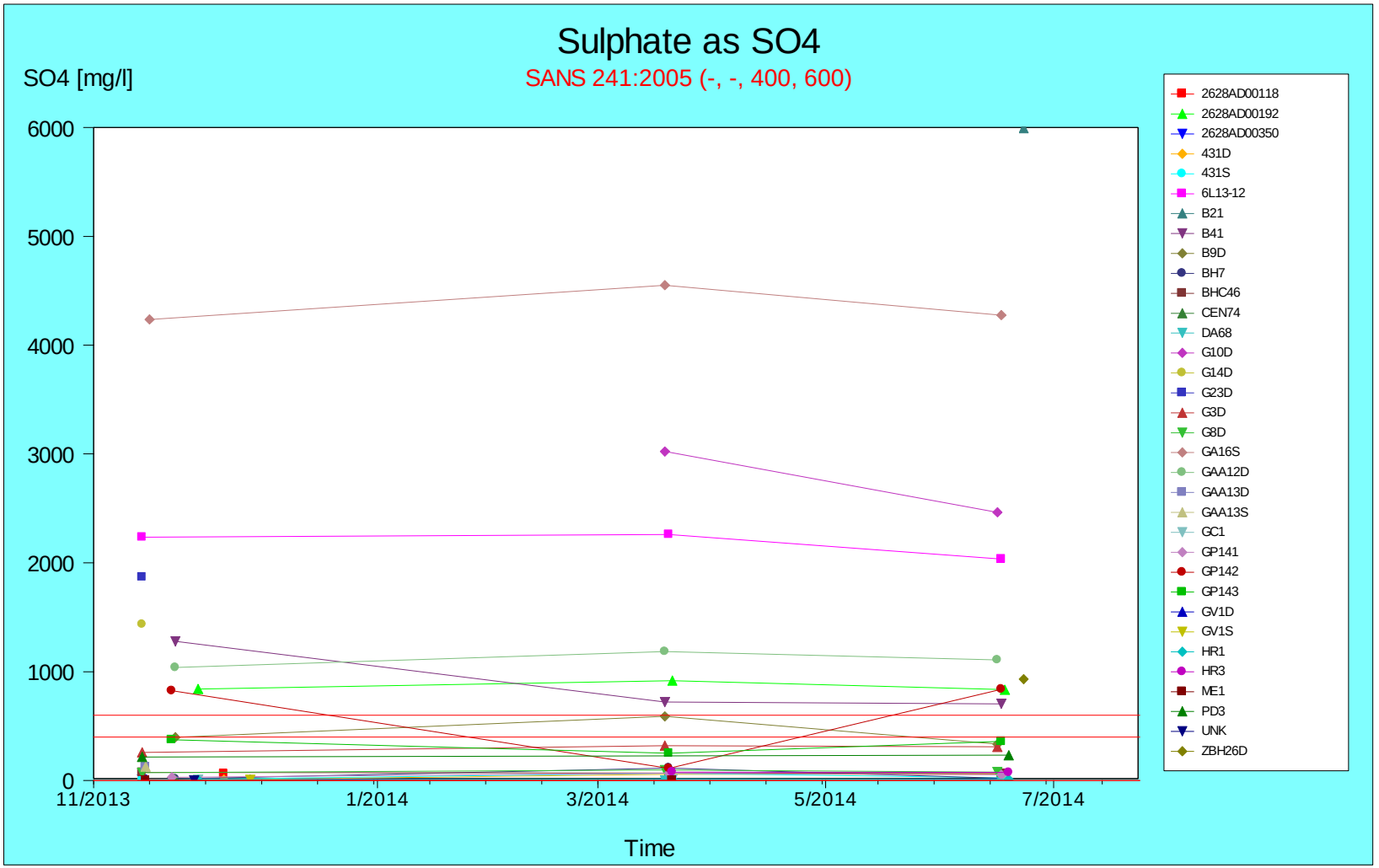
Sulphate as SO4
SANS 241:2005 (-, -, 400, 600)
SO4 [mg/l]
6000
5000
4000
3000
2000
1000
0
11/2013
1/2014
3/2014
5/2014
7/2014
Time
2628AD00118
2628AD00192
2628AD00350
431D
431S
6L13-12
B21
B41
B9D
BH7
BHC46
CEN74
DA68
G10D
G14D
G23D
G3D
G8D
GA16S
GAA12D
GAA13D
GAA13S
GC1
GP141
GP142
GP143
GV1D
GV1S
HR1
HR3
ME1
PD3
UNK
ZBH26D

Appendix E: Surface Water Localities

Site	Latitude	Longitude
SW1	-26.4286	28.182647
SW2	-26.3911	28.497423
SW3	-26.427	28.164682
SW4	-26.4536	28.085614
SW5	-26.2911	28.142113
SW6	-26.4786	28.425473
SW7	-26.2165	28.440178
SW8	-26.16	28.364746
SW9	-26.2003	28.391046
SW10	-26.2553	28.500869
SW11	-26.5094	28.35027
SW12	-26.1791	28.329043
SW13	-26.211	28.414757
SW14	-26.1649	28.460372
SW15	-26.3371	28.292263
SW16	-26.1839	28.349168
SW17	-26.3593	28.299524
SW18	-26.2621	28.322046
SW19	-26.1977	28.374464
SW20	-26.3242	28.337204
SW21	-26.3721	28.244781
SW22	-26.3241	28.517132
SW22	-26.1676	28.217913
SW23	-26.2355	28.31005
SW24	-26.222	28.33798
SW25	-26.2247	28.369747
SW26	-26.2086	28.462272
SW27	-26.2976	28.311891
SW28	-26.325	28.470691
SW29	-26.3975	28.411922
SW30	-26.3902	28.431716
SW31	-26.3953	28.469811
SW32	-26.4126	28.480397
SW33	-26.4348	28.463155

SW34	-26.4805	28.407075
SW35	-26.388	28.547202

Appendix F: Surface Water Chemistry Results

Site Name	DateTimeMeas	pH	EC mS/m	TDS mg/l	MALK mg/l	PO4 mg/l	SO4 mg/l	NO3-N mg/L	NH4 mg/l	Cl mg/l	NO2-N mg/L	Be mg/L	B mg/L	Na mg/l	Mg mg/l	Al mg/l	P mg/L	K mg/l	Ca mg/l	Ti mg/L	V mg/l	Cr mg/l	Mn mg/l	Fe mg/l	Co mg/l	Ni mg/l	Cu mg/l	Zn mg/l
SW12	2013-12-05	7.39	30.00	195.0	75.0	-0.01	37.24	2.95	1.50	29.26	0.09	0.00002	0.062	25.07	9.40	0.0002	0.1729	5.44	25.01	0.00157	0.00007	0.00878	0.00895	0.058	0.00002	0.00003	0.00004	0.00033
SW13	2013-12-05	3.76	280.00	1820.0	0.0	0.55	2203.33	7.41	8.66	94.21	0.70	0.01654	0.333	108.40	150.10	65.0900	0.0441	22.77	276.00	0.00270	0.00008	0.09081	58.56000	2.650	2.92600	5.74600	0.71050	8.47300
SW14	2013-12-05	7.33	50.00	325.0	109.5	1.50	74.09	3.17	1.39	58.04	0.44	0.00002	0.100	51.10	12.70	0.0001	0.9786	9.37	32.15	0.00200	0.00007	0.00439	0.02623	0.072	0.00001	0.02618	0.00536	0.00037
SW15	2013-12-05	7.43	51.00	331.5	215.0	1.09	17.80	0.22	0.94	29.00	0.05	0.00002	0.029	68.07	17.83	0.0002	0.5357	2.33	39.26	0.00157	0.00009	0.00210	0.30630	0.106	0.00002	0.00001	0.00960	0.00037
SW16	2013-12-05	9.42	26.00	169.0	62.5	0.06	44.67	1.34	0.94	15.63	0.12	0.00002	0.041	19.82	7.84	0.2647	0.1096	5.15	24.94	0.01511	0.00002	0.00171	0.01023	0.186	0.00001	0.01091	0.00042	0.00035
SW17	2013-12-05	7.42	96.00	624.0	75.0	0.05	534.61	1.08	0.99	49.54	0.09	0.00002	0.072	75.11	35.98	0.0003	0.0764	7.75	100.60	0.00083	0.00009	0.00088	0.00533	0.265	0.02107	0.02987	0.00098	0.00040
SW18	2013-12-05	7.24	316.00	2054.0	135.0	-0.01	2038.44	4.59	8.98	168.63	0.78	0.00002	0.024	244.50	125.80	0.0002	0.0425	16.52	353.50	0.00088	0.00009	0.00076	14.26000	1.008	0.49110	0.06249	0.00193	0.00039
SW19	2013-12-05	7.37	40.00	260.0	120.0	-0.01	45.47	1.89	0.85	26.95	0.38	0.00002	0.043	30.11	14.26	0.0002	0.1728	12.09	37.07	0.00179	0.00007	0.00018	0.01613	0.119	0.00000	0.00599	0.00001	0.00035
SW20	2013-12-05	7.74	135.00	877.5	185.0	-0.01	512.39	3.20	0.92	84.09	0.19	0.00002	0.034	83.22	70.24	0.0002	0.2531	7.38	159.10	0.00242	0.00006	0.00000	0.70700	0.416	0.00810	0.06894	0.00077	0.00037
SW21	2013-12-05	8.06	98.00	637.0	210.0	4.36	201.23	0.70	0.97	141.52	0.01	0.00002	0.178	108.50	24.97	0.0001	1.6270	12.89	77.67	0.00221	0.00008	0.00025	0.00267	0.194	0.00001	0.01135	0.00003	0.00040
SW22	2013-12-05	7.43	66.00	429.0	137.5	0.83	101.96	1.73	1.19	93.18	0.76	0.00002	0.143	76.47	13.36	0.0001	0.3973	13.58	49.95	0.00090	0.00008	0.00006	0.00594	0.144	0.00001	0.03715	0.01022	0.00036
SW22	2013-12-12	7.53	52.00	338.0	125.0	0.13	31.45	0.77	0.25	68.59	1.02	0.00002	0.015	54.51	15.51	0.0093	0.0757	5.44	25.75	0.00000	0.00006	0.01067	0.00979	0.073	0.00002	0.00207	0.08229	0.00027
SW23	2013-12-12	7.92	89.00	578.5	172.5	-0.01	109.75	0.18	0.13	89.07	0.29	0.00002	0.151	83.74	33.72	0.0001	0.1119	21.60	49.28	0.00051	0.00004	0.00173	0.00001	0.086	0.00002	0.00000	0.03868	0.00030
SW24	2013-12-12	7.77	101.00	656.5	200.0	-0.01	146.71	10.81	0.20	100.10	-0.01	0.00002	0.123	105.10	38.28	0.0002	0.0772	24.51	50.19	0.00001	0.00008	0.00092	0.20460	0.086	0.00001	0.01110	0.04527	0.00037
SW25	2013-12-12	7.13	58.00	377.0	85.0	-0.01	40.99	10.65	0.81	92.61	-0.01	0.00002	0.088	66.32	10.31	0.0807	0.2170	10.53	29.05	0.00330	0.00003	0.00079	0.06538	0.103	0.00001	0.00204	0.07573	0.00026
SW26	2013-12-12	7.83	55.00	357.5	110.0	-0.01	46.19	2.54	0.16	66.22	0.35	0.00002	0.059	57.08	12.45	0.0680	0.2315	10.32	36.94	0.00082	0.00007	0.00091	0.00106	0.090	0.00001	0.03217	0.03603	0.00032
SW27	2013-12-12	7.39	33.00	214.5	50.0	-0.01	47.29	0.24	0.07	16.03	0.13	0.00002	0.008	18.63	11.25	0.0002	0.0000	4.22	26.48	0.00000	0.00009	0.00000	0.03468	0.070	0.00001	0.00860	0.03727	0.00030
SW28	2013-12-12	7.54	54.00	351.0	119.0	-0.01	47.41	0.31	0.65	53.23	0.44	0.00002	0.010	42.76	17.43	0.2356	0.0395	12.63	39.18	0.01215	0.00008	0.00015	0.05415	0.198	0.00002	0.01925	0.05053	0.00017
SW29	2013-12-12	7.59	46.00	299.0	102.5	-0.01	39.48	4.33	0.38	41.70	1.13	0.00002	0.000	38.85	11.53	0.1557	0.0504	8.06	35.77	0.00437	0.00007	0.00000	0.00122	0.124	0.00002	0.00456	0.03675	0.00035
SW30	2013-12-12	6.43	491.00	3191.5	5.0	-0.01	1972.00	1.80	0.23	712.00	-0.01	0.00002	0.298	486.90	146.10	0.1963	0.1990	66.88	427.80	0.00140	0.00008	0.00338	0.81100	1.399	0.03506	0.28720	0.05705	0.55170
SW31	2013-12-12	7.48	51.00	331.5	120.0	-0.01	44.07	0.15	0.23	46.60	0.22	0.00002	0.005	55.02	12.45	0.1424	0.0598	7.29	36.75	0.00885	0.00007	0.00000	0.47460	0.143	0.00234	0.04173	0.10480	0.00020
SW32	2013-12-12	7.97	213.00	1384.5	220.0	-0.01	177.30	3.50	0.38	522.80	-0.01	0.00002	0.269	288.80	54.06	0.0450	0.0813	30.08	39.86	0.00255	0.00001	0.00131	0.00895	0.072	0.00001	0.02780	0.04538	0.00029
SW33	2013-12-12	6.43	7.00	45.5	7.5	-0.01	10.95	2.77	0.56	2.46	-0.01	0.00002	0.000	2.70	1.23	0.5432	0.1195	1.51	5.06	0.02123	0.00008	0.00119	0.01073	0.272	0.00002	0.00047	0.12390	0.02072
SW34	2013-12-12	6.79	33.00	214.5	60.0	1.73	28.15	12.94	2.63	23.07	5.34	0.00002	0.000	23.03	8.13	0.5977	0.6033	5.27	17.01	0.05637	0.00406	0.00075	0.07382	0.356	0.00002	0.00001	0.07223	0.00035
SW35	2013-12-12	7.51	124.00	806.0	217.5	-0.01	201.89	2.27	1.73	140.41	-0.01	0.00002	0.155	126.90	33.76	0.0287	0.5790	41.49	84.86	0.00304	0.01023	0.00000	0.23850	0.204	0.00057	0.01540	0.03257	0.00029

Site Name	DateTimeMeas	pH	EC mS/m	TDS mg/l	MALK mg/l	PO4 mg/l	SO4 mg/l	NO3-N mg/L	NH4 mg/l	Cl mg/l	NO2-N mg/L	Be mg/L	B mg/L	Na mg/l	Mg mg/l	Al mg/l	P mg/L	K mg/l	Ca mg/l	Ti mg/l
SW1	2014-04-09	7.96	122.00	793.0	193.0	0.19	417.73	4.60	0.18	70.23	0.07	0.00001	0.004	65.16	46.94	0.0004	0.0167	7.57	111.50	0.0000
SW2	2014-04-09	7.87	58.00	377.0	145.0	4.11	89.05	0.11	0.07	63.80	0.11	0.00001	0.003	39.02	13.34	0.0003	0.6541	8.68	38.77	0.0000
SW3	2014-04-09	7.52	71.00	461.5	112.5	0.83	184.29	14.73	0.13	79.32	2.79	0.00001	0.003	45.84	18.23	0.0004	0.1457	8.55	51.47	0.0000
SW4	2014-04-09	7.58	65.00	422.5	105.0	0.52	145.74	18.43	0.05	75.54	1.12	0.00001	0.004	50.89	16.94	0.0004	0.1983	8.83	45.19	0.0000
SW5	2014-04-09	7.07	46.00	299.0	27.5	-0.01	199.62	5.19	0.78	30.35	0.34	0.00001	0.005	16.40	13.96	0.0001	0.0001	4.35	37.09	0.0000
SW6	2014-04-09	7.82	54.00	351.0	127.5	2.31	83.53	2.68	0.13	57.15	0.44	0.00001	0.005	42.06	13.94	0.0003	0.5449	7.98	37.46	0.0000
SW7	2014-04-09	7.55	40.00	260.0	67.5	0.02	85.95	3.55	0.13	37.92	0.43	0.00001	0.005	27.93	9.69	0.0003	0.0872	6.05	21.65	0.0000
SW8	2014-04-09	7.39	57.00	370.5	60.0	3.31	45.86	0.56	7.04	77.76	0.84	0.00001	0.006	47.23	10.08	0.0004	0.7777	9.81	24.08	0.0000
SW9	2014-04-09	7.08	45.00	292.5	90.0	6.52	39.12	2.50	1.91	53.53	2.14	0.00001	0.006	38.30	9.37	0.0004	0.9963	6.70	20.43	0.0000
SW10	2014-04-09	7.47	57.00	370.5	118.0	3.03	106.93	0.21	0.92	60.41	0.10	0.00001	0.006	40.00	12.81	0.0004	0.4068	7.15	31.07	0.0000
SW11	2014-04-09	7.73	52.00	338.0	117.5	2.53	77.29	5.59	0.18	52.84	0.61	0.00001	0.006	35.13	12.24	0.0004	0.4122	6.93	30.25	0.0000
SW12	2014-04-09	7.67	35.00	227.5	67.5	0.21	59.48	6.56	0.14	35.28	0.10	0.00001	0.007	22.67	10.40	0.0000	0.0198	4.57	20.86	0.0000
SW13	2014-04-09	4.04	104.00	676.0	0.0	0.46	598.00	1.92	0.27	21.70	0.18	0.00000	0.007	31.44	34.69	1.8060	0.0003	7.50	109.00	0.0000
SW14	2014-04-09	7.54	44.00	286.0	85.0	0.72	76.72	2.93	0.34	50.12	0.13	0.00001	0.007	35.03	10.97	0.0004	0.1993	6.43	22.40	0.0000
SW15	2014-04-09	7.68	43.00	279.5	152.5	2.92	4.08	0.49	0.20	46.70	0.05	0.00001	0.008	30.76	13.29	0.0004	0.5080	8.38	24.25	0.0000
SW16	2014-04-09	7.92	57.00	370.5	162.5	0.09	17.41	0.29	0.16	66.54	0.08	0.00001	0.008	32.07	13.68	0.0002	0.0002	5.49	32.78	0.0000
SW17	2014-04-09	7.88	72.00	468.0	172.5	0.02	152.07	2.29	0.14	66.67	0.15	0.00001	0.008	49.85	21.46	0.0004	0.0225	9.64	52.60	0.0000
SW18	2014-04-09	6.87	236.00	1534.0	102.5	-0.01	1365.08	13.09	1.75	131.60	1.40	0.00001	0.008	129.00	101.30	0.0005	0.0003	11.92	262.30	0.0000
SW19	2014-04-09	7.38	55.00	357.5	155.0	0.44	22.26	4.80	1.17	65.73	1.41	0.00001	0.008	40.35	13.05	0.0004	0.1378	15.45	29.02	0.0000
SW20	2014-04-09	7.65	142.00	923.0	142.5	0.05	619.08	2.54	0.22	85.54	0.20	0.00001	0.009	90.82	50.07	0.0004	0.0134	10.50	136.90	0.0000
SW21	2014-04-09	7.74	56.00	364.0	140.0	2.47	84.04	0.43	0.13	60.49	0.09	0.00001	0.008	41.06	14.19	0.0003	0.5580	8.75	37.62	0.0000
SW22	2014-04-09	7.60	48.00	312.0	117.5	0.08	50.74	5.40	0.18	58.78	0.52	0.00001	0.008	41.16	12.55	0.0003	0.0125	4.94	21.13	0.0000
SW23	2014-04-09	7.70	66.00	429.0	157.5	-0.01	139.24	0.30	0.32	56.92	0.08	0.00001	0.008	45.96	21.26	0.0003	0.0021	13.71	35.81	0.0000
SW24	2014-04-09	7.58	88.00	572.0	172.5	0.00	196.32	0.56	0.14	113.70	0.19	0.00001	0.007	80.53	29.04	0.0004	0.0209	20.68	32.47	0.0000
SW25	2014-04-09	7.30	58.00	377.0	90.0	0.13	98.55	9.54	0.70	77.50	1.38	0.00001	0.007	54.11	10.79	0.0004	0.0693	9.18	21.05	0.0000
SW26	2014-04-09	7.54	49.00	318.5	87.5	0.00	111.71	2.00	0.13	46.20	0.24	0.00001	0.008	35.27	10.27	0.0003	0.0311	6.55	30.91	0.0000
SW27	2014-04-09	7.36	53.00	344.5	147.5	-0.01	57.90	9.25	0.65	49.39	0.58	0.00001	0.008	39.82	15.20	0.0004	0.0003	9.83	27.16	0.0000
SW28	2014-04-09	7.84	42.00	273.0	92.5	1.27	66.90	0.15	0.16	42.96	0.08	0.00001	0.009	29.10	11.37	0.0003	0.0002	9.40	21.17	0.0000
SW29	2014-04-09	6.77	52.00	338.0	60.0	-0.01	91.66	23.96	1.68	51.11	4.21	0.00001	0.009	40.04	13.41	0.0005	0.3719	4.72	20.67	0.0000
SW30	2014-04-09	6.23	479.00	3113.5	5.0	-0.01	2553.21	3.82	0.18	699.92	1.18	0.00001	0.006	408.90	122.80	0.0633	0.0003	60.27	361.00	0.0000
SW31	2014-04-09	7.68	51.00	331.5	87.5	0.01	133.61	0.33	0.18	44.14	0.09	0.00001	0.009	42.77	12.38	0.0677	0.0148	7.34	28.92	0.0000
SW32	2014-04-09	7.70	194.00	1261.0	207.5	1.97	109.13	2.49	0.25	548.36	1.21	0.00001	0.006	254.10	47.74	0.0003	0.0584	29.44	30.51	0.0000
SW33	2014-04-09	8.07	52.00	338.0	130.0	1.01	77.82	0.87	0.14	53.61	0.15	0.00001	0.009	36.72	13.39	0.0002	0.5461	7.72	33.72	0.0000
SW34	2014-04-09	7.83	43.00	279.5	95.0	9.86	50.64	18.89	0.14	42.96	0.15	0.00001	0.009	33.24	12.18	0.0001	0.2210	6.44	21.04	0.0008
SW35	2014-04-09	7.56	103.00	669.5	215.0	-0.01	80.69	12.72	0.04	138.49	0.43	0.00001	0.008	57.76	23.21	0.7069	3.2870	84.52	38.24	0.0376

Site Name	DateTimeMeas	pH	EC mS/m	TDS mg/l	MALK mg/l	PO4 mg/l	SO4 mg/l	NO3-N mg/L	NH4 mg/l	Cl mg/l	NO2-N mg/L	Be mg/L	B mg/L	Na mg/l	Mg mg/l	Al mg/l	P mg/L	K mg/l	Ca mg/l	Ti mg/L
SW1	2014-07-14	7.52	145.00	942.5	210.0	0.21	475.83	8.91	4.91	93.93	0.43	0.00018	0.006	80.05	62.69	0.0043	0.2617	10.47	129.80	0.0027
SW2	2014-07-14	7.86	77.00	500.5	172.5	0.76	137.86	0.13	1.23	97.01	0.20	0.00018	0.005	66.87	19.67	0.0154	0.4917	10.73	57.92	0.0026
SW3	2014-07-14	7.23	110.00	715.0	107.5	0.85	308.65	23.48	2.62	86.52	4.62	0.00020	0.006	77.44	28.84	0.1995	0.3002	14.55	95.97	0.0051
SW4	2014-07-14	7.30	72.00	468.0	105.0	0.50	174.45	21.33	1.44	83.93	2.23	0.00019	0.007	59.76	18.46	0.0160	0.1323	10.94	48.96	0.0035
SW5	2014-07-14	7.01	65.00	422.5	50.0	0.12	247.38	5.78	4.13	67.14	0.68	0.00019	0.007	28.07	20.79	0.0005	0.0012	7.57	50.55	0.0022
SW6	2014-07-14	7.55	68.00	442.0	142.5	0.90	115.71	5.98	1.43	82.59	1.71	0.00019	0.007	59.49	16.83	0.0299	0.4350	9.70	47.53	0.0032
SW7	2014-07-14	8.07	57.00	370.5	105.0	0.27	99.15	4.26	1.03	72.81	0.36	0.00019	0.008	57.55	13.75	0.0182	0.0074	9.63	32.76	0.0031
SW8	2014-07-14	6.96	58.00	377.0	110.0	7.32	47.31	1.86	9.06	106.17	1.11	0.00019	0.008	57.64	9.36	0.0000	1.6590	13.77	22.52	0.0040
SW9	2014-07-14	7.29	70.00	455.0	162.5	10.68	42.10	8.51	9.72	110.43	2.03	0.00018	0.008	85.38	11.78	0.0001	2.0640	15.38	27.77	0.0047
SW10	2014-07-14	7.43	81.00	526.5	82.5	0.75	68.89	0.99	1.10	54.47	0.11	0.00018	0.008	40.57	9.34	0.0000	0.0009	7.65	26.24	0.0024
SW11	2014-07-14	7.58	64.00	416.0	130.0	1.46	103.94	9.78	1.30	75.95	0.96	0.00018	0.008	55.90	16.33	0.0113	0.4880	9.48	45.05	0.0070
SW12	2014-07-14	7.68	35.00	227.5	77.5	0.15	60.05	0.67	1.41	31.28	0.15	0.00019	0.008	24.05	10.15	0.0108	0.0012	5.67	26.45	0.0028
SW13	2014-07-14	7.21	162.00	1053.0	72.5	0.15	989.42	2.44	10.66	33.41	0.52	0.00018	0.005	53.14	98.04	0.0001	0.0003	15.81	145.70	0.0025
SW14	2014-07-14	7.93	67.00	435.5	120.0	2.39	86.72	18.11	2.62	102.57	2.03	0.00019	0.009	75.95	14.32	0.0040	0.5773	13.85	31.53	0.0031
SW26	2014-07-14	7.22	92.00	598.0	175.0	0.10	209.63	1.31	1.68	120.89	0.26	0.00019	0.007	79.12	21.62	0.1260	0.2088	11.88	76.83	0.0049
SW15	2014-07-14	7.67	48.00	312.0	130.0	1.11	31.41	0.27	1.44	64.86	1.29	0.00018	0.009	47.50	12.63	0.0002	0.2344	12.02	27.01	0.0025
SW17	2014-07-14	7.76	85.00	552.5	147.5	0.08	246.56	0.13	1.82	89.47	0.57	0.00019	0.009	62.73	25.97	0.0121	0.1806	13.18	69.10	0.0026
SW18	2014-07-14	6.90	261.00	1696.5	97.5	0.72	1476.65	31.84	10.84	161.00	2.43	0.00017	0.010	129.20	135.30	0.0103	0.3703	19.52	289.00	0.0030
SW19	2014-07-14	8.07	46.00	299.0	115.0	0.13	36.57	14.01	1.24	53.82	0.37	0.00019	0.010	42.50	13.35	0.0852	0.0012	9.99	31.37	0.0047
SW20	2014-07-14	8.00	186.00	1209.0	155.0	0.32	831.84	0.22	1.28	131.67	2.32	0.00018	0.010	118.80	83.86	0.0027	0.1746	16.12	195.50	0.0027
SW21	2014-07-14	7.78	77.00	500.5	175.0	1.27	134.03	0.14	1.48	97.15	1.95	0.00018	0.009	69.71	20.03	0.0000	0.7662	11.57	61.04	0.0038
SW22	2014-07-14	7.61	68.00	442.0	162.5	0.10	66.99	0.07	0.27	98.52	0.47	0.00018	0.009	72.76	21.44	0.0319	0.0003	7.09	39.16	0.0027
SW23	2014-07-14	7.72	100.00	650.0	235.0	0.59	171.97	0.18	1.28	74.60	0.22	0.00018	0.008	82.64	40.70	0.0559	0.2192	22.59	63.05	0.0060
SW24	2014-07-14	7.99	94.00	611.0	190.0	0.04	207.55	0.15	0.25	119.09	1.15	0.00020	0.009	94.75	33.90	0.0080	0.0843	24.64	44.11	0.0025
SW25	2014-07-14	7.40	72.00	468.0	127.5	0.20	108.86	14.14	3.52	100.63	2.57	0.00018	0.008	84.66	13.91	0.0166	0.0081	13.08	32.37	0.0031
SW16	2014-07-14	7.29	29.00	188.5	75.0	0.29	36.84	3.12	0.61	20.04	0.14	0.00019	0.001	16.90	9.31	0.1412	0.0035	4.52	22.50	0.0081
SW27	2014-07-14	7.03	58.00	377.0	125.0	0.03	90.16	0.09	3.45	51.40	2.76	0.00020	0.010	43.53	17.65	0.0000	0.0003	11.34	35.84	0.0023
SW28	2014-07-14	8.15	48.00	312.0	100.0	0.02	80.33	0.18	0.40	49.60	0.33	0.00019	0.010	36.90	14.60	0.0854	0.0011	12.18	34.27	0.0055
SW29	2014-07-14	7.47	40.00	260.0	77.5	0.55	55.05	0.06	2.45	41.53	0.77	0.00018	0.001	35.64	10.57	0.0418	0.1364	5.63	20.56	0.0031
SW30	2014-07-14	6.31	512.00	3328.0	5.0	0.25	2439.05	2.02	0.34	678.50	3.69	0.00026	0.007	549.80	164.30	0.1091	0.0023	84.19	490.10	0.0028
SW31	2014-07-14	8.36	58.00	377.0	90.0	0.00	152.64	0.08	0.32	53.81	0.28	0.00018	0.001	55.04	14.40	0.0225	0.3168	9.48	40.81	0.0035
SW32	2014-07-14	8.50	203.00	1319.5	230.0	0.17	98.51	0.76	0.43	492.69	14.81	0.00019	0.007	288.00	54.40	0.0649	0.3191	33.83	42.44	0.0051
SW33	2014-07-14	8.22	69.00	448.5	152.5	0.58	118.90	0.11	0.20	84.55	0.50	0.00019	0.001	61.06	18.55	0.0352	0.7091	10.31	54.39	0.0052
SW34	2014-07-14	7.18	49.00	318.5	105.0	3.38	51.91	0.05	5.50	47.94	1.72	0.00019	0.001	43.59	12.29	0.1647	1.2110	9.86	25.31	0.0131
SW35	2014-07-14	8.31	95.00	617.5	212.5	7.18	125.04	0.75	0.45	143.40	0.38	0.00019	0.001	73.38	26.59	0.2063	0.0012	53.68	56.77	0.0021

Appendix G: Surface Water Chemistry Trends

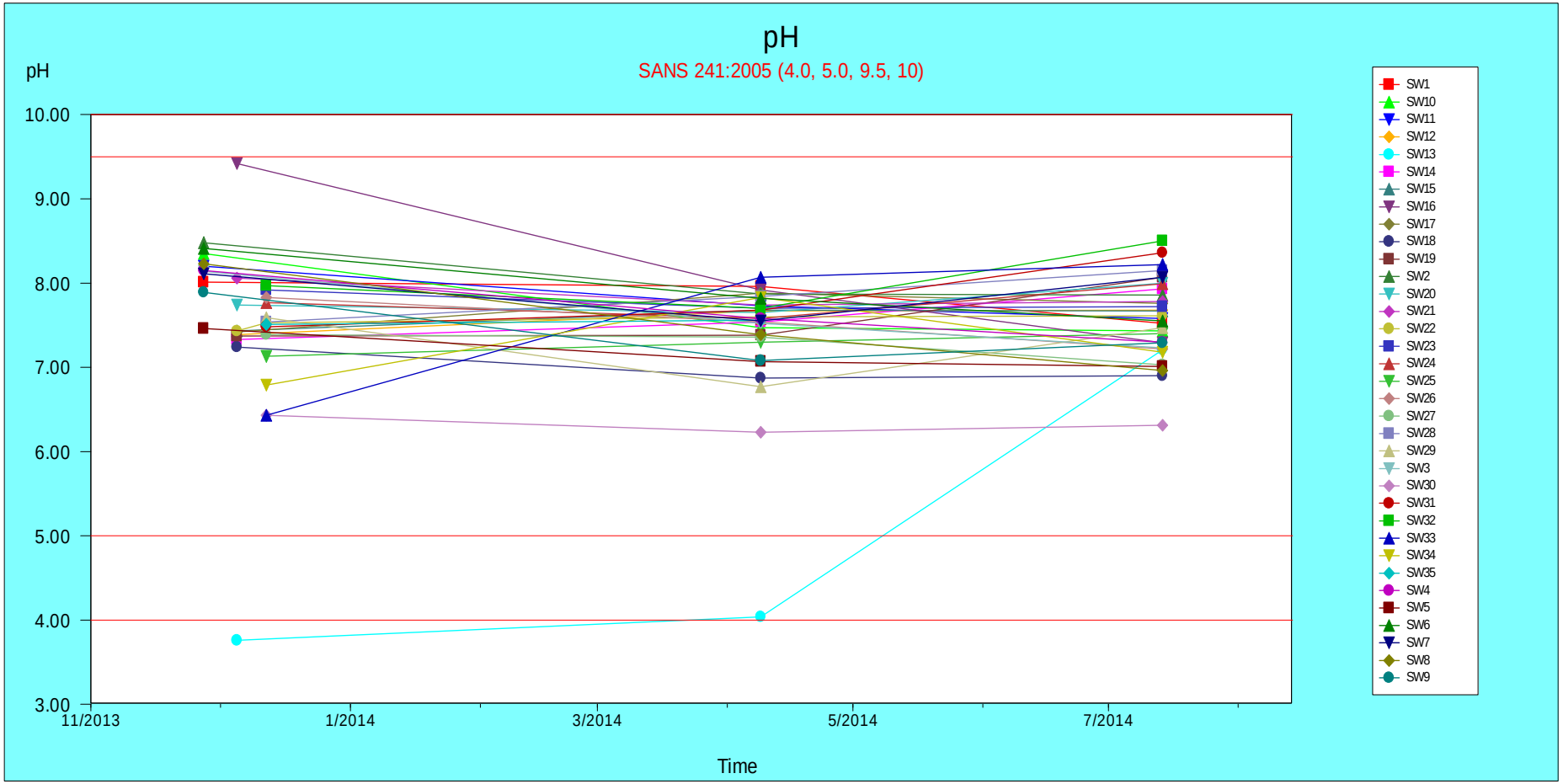
pH
SANS 241:2005 (4.0, 5.0, 9.5, 10)
pH
10.00
9.00
8.00
7.00
6.00
5.00
4.00
3.00
11/2013
1/2014
3/2014
5/2014
7/2014
Time
SW1
SW10
SW11
SW12
SW13
SW14
SW15
SW16
SW17
SW18
SW19
SW2
SW20
SW21
SW22
SW23
SW24
SW25
SW26
SW27
SW28
SW29
SW3
SW30
SW31
SW32
SW33
SW34
SW35
SW4
SW5
SW6
SW7
SW8
SW9

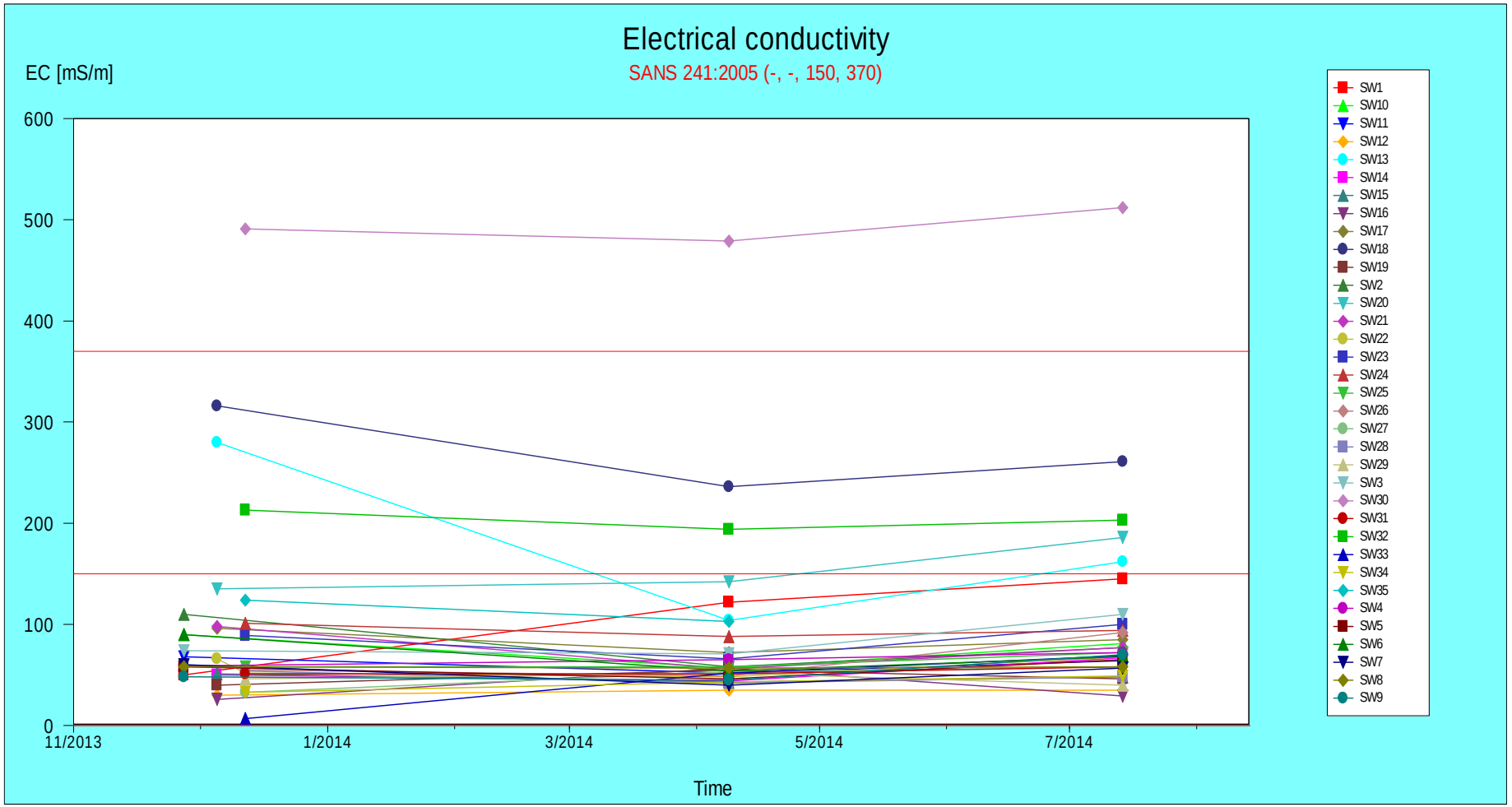
Electrical conductivity
SANS 241:2005 (-, -, 150, 370)
EC [mS/m]
600
500
400
300
200
100
0
11/2013
1/2014
3/2014
5/2014
7/2014
Time
SW1
SW10
SW11
SW12
SW13
SW14
SW15
SW16
SW17
SW18
SW19
SW2
SW20
SW21
SW22
SW23
SW24
SW25
SW26
SW27
SW28
SW29
SW3
SW30
SW31
SW32
SW33
SW34
SW35
SW4
SW5
SW6
SW7
SW8
SW9

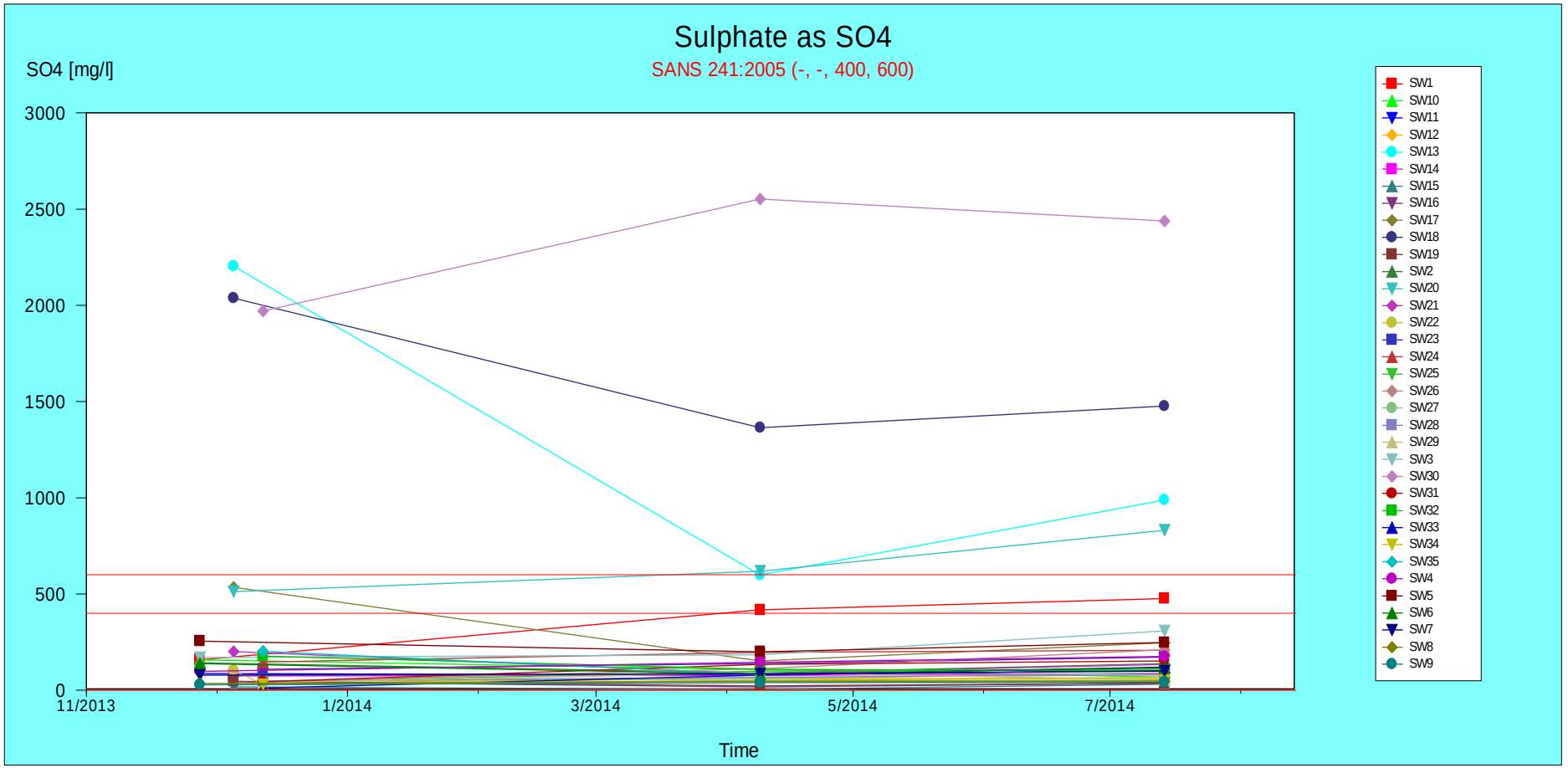
Sulphate as SO4
SANS 241:2005 (-, -, 400, 600)
SO4 [mg/l]
3000
2500
2000
1500
1000
500
0
11/2013
1/2014
3/2014
5/2014
7/2014
Time
SW1
SW10
SW11
SW12
SW13
SW14
SW15
SW16
SW17
SW18
SW19
SW2
SW20
SW21
SW22
SW23
SW24
SW25
SW26
SW27
SW28
SW29
SW3
SW30
SW31
SW32
SW33
SW34
SW35
SW4
SW5
SW6
SW7
SW8
SW9

Appendix H: Tailings and Waste Rock Dumps Sampled

Site Name	Latitude	Longitude
Tailing Storage Facilities		
TSF11	-26.166505	28.350185
TSF12	-26.174931	28.365832
TSF13	-26.180146	28.331328
TSF14	-26.201811	28.431630
TSF15	-26.217810	28.469440
TSF16	-26.221470	28.490607
TSF17	-26.233507	28.495823
TSF18	-26.298633	28.532194
TSF19	-26.297028	28.483290
TSF20	-26.317623	28.475760
TSF21	-26.324844	28.503041
TSF22	-26.395187	28.425209
TSF23	-26.412037	28.454363
TSF24	-26.407223	28.458642
TSF25	-26.273759	28.305921
TSF26	-26.286597	28.328120
TSF27	-26.304784	28.350359
TSF29	-26.362289	28.294955
Waste Rock Dumps		
WRD12	-26.171320	28.355401
WRD13	-26.186140	28.373030
WRD14	-26.179344	28.342161
WRD15	-26.211841	28.438450
WRD16	-26.242330	28.473355
WRD17	-26.292749	28.497959
WRD18	-26.297028	28.483294
WRD19	-26.317623	28.475760
WRD20	-26.335810	28.525775
WRD21	-26.363091	28.442594
WRD22	-26.409897	28.419860
WRD23	-26.414670	28.467810

Appendix I: ABA Methodology

The method is given by Usher *et al.* (2001: 10) and broadly entails the use of H_2O_2, described as follows.

1. Initial pH

- Use 1 g of crushed sample submitted for ABA
- Add 10 ml of deionised water
-

2. Final pH and preparation of sample

- Add 80 ml of H_2O_2, to 4 g of pulverised sample in a 500 ml wide mouth conical flask or equivalent. Cover with a watch glass and place in a fume-hood or well-ventilated area. The H_2O_2 should be at room temperature before commencing the test.
- Allow sample to react until 'boiling' or effervescing ceases.
- Allow solution to cool to room temperature, record the final pH as 'Oxidised pH' (NAG pH)
- Rinse the sample that has adhered to the sides of the flask down into the solution with deionised water.
- Analyse the supernatant for sulphate and back-calculate acid potential in kg/t
    - AP = S% x 31.25 kg $CaCO_3$ equivalent per ton

3. Neutralising Potential Method

- H_2SO_4 (0.06N) is added to the pulverised rock samples. The pH of the slurry must be below 2.5 after 24 hours, before back titrating to a pH of 7 is done with NaOH (0.06N). If the pH is >2.5, more H_2SO_4 is added and the sample is left another 24 hours for reactions to complete.

4. Calculations (retrieved from Usher *et al*. (2001: 12)

We will be analysing a closed system as this is happening in a TSF with regards to the following six (6) equations:

Equation 4.1

$$\mathbf{AP} = \frac{\mathbf{SO4}\left(\frac{\mathbf{mg}}{\mathbf{L}}\right)\mathbf{weight(g)}}{\mathbf{1000}}\mathbf{x\ ml\ H2O\ or\ H2O2} = \mathbf{kg}\frac{\mathbf{SO4}}{\mathbf{t}}\mathbf{of\ sample}$$

Equation 4.2

$$\mathbf{Acid\ Open}\left(\mathbf{AP\ CaCO3}\frac{\mathbf{kg}}{\mathbf{t}}\right) = \frac{\mathbf{SO4}\left(\frac{\mathbf{kg}}{\mathbf{t}}\right)}{\mathbf{48}}\mathbf{\ x\ 50}$$

Equation 4.3

$$\mathbf{Acid\ Closed} = \mathbf{Acid\ Open\ x\ 2}$$

Equation 4.4

$$\mathbf{Base\ Potential\ (NP)} = \mathbf{CaCO3}\frac{\mathbf{kg}}{\mathbf{t}} = \frac{(\mathbf{N\ H2SO4\ x\ ml\ acid}) - (\mathbf{N\ NaOH\ x\ ml\ Alkali})\ \mathbf{x\ 50}\ )}{\mathbf{weight\ (g)}}$$

Equation 4.5

$$\mathbf{NNP\ Open} = \mathbf{Base\ (NP)} - \mathbf{Acid\ Open\ (AP)}$$

Equation 4.6

$$\mathbf{NNP\ Closed} = \mathbf{Base\ (NP)} - \mathbf{Acid\ Open\ (AP\ x\ 2)}$$

5. Net Acid-Generating (NAG)

This test is based on the final pH and serves as a *rough* guideline to categorise the samples and is also used for correlating results.

Table A-1 : *Associated pH and Acid-generating Potential (Usher et al., 2001)*

Final pH in NAG Test	Acid-generating Potential
>5.5	Non-acid-generating
3.5 to 5.5	Low risk acid-generating
<3.5	High risk acid-generating

6. Net Neutralising Potential (NNP):

Often the use of NNP leads to uncertainties and according to Usher *et al.* (2001: vii) this is, because of a range between -20 to 20 kg/t $CaCO_3$, where the sample can become acidic or remain neutral. This uncertainty can be resolved by using the following reaction:

Neutralising Potential (kg/t $CaCO_3$) – Acid Generating Potential (kg/t $CaCO_3$)

Finally this method allows us to conclude if the sample is acid generating or acid neutralizing:

If NNP = NP-AP < 0 (Potential to generate acid)

If NNP = NP-AP > 0 (Potential to neutralise acid produced)

Usher *et al*. (2001, 209) specifies that any sample with a NNP < 20 is potentially acid-generating and a sample with NNP > -20, will not generate acid.

The use of NNP insures the following according to Usher *et al*. (2001, 209):

- Demonstration of the drop in pH (result of oxidation) of each sample.
- Accuracy of analyses can be done by studying the NNP value. These values must approximately coincide with zero to appear accurate.
- Compatibility of number of samples analysed to the representative spread in values on both axes.

Advantages of Acid Base Accounting according to Usher *et al.* (2001: 5) include:

- Short turn-around time for sample processing.

- Low cost.
- Relatively simple analytical procedures.
- Relatively simple interpretation results.
- Interpretation is based on decades of international research/experience.
- Correlation to field has been shown by case studies (local and abroad).

7. Neutralising Potential Ratio (NPR)

The NPR screening criteria is the ration of the NP to the AP and ranges between <1:1 to greater than 4:1. Thus in summary it concludes to the division of the NP value with the AP value, refer to the equation below.

NPR = (NP/AP)

Basically the acid generating potential is assessed with the NP:AP ratio, and is considered uncertain if the samples have a NPR of less than 4:1

Table A-2 : *NPR screening criteria to determine if the sample is acid generation (Usher et al., 2001)*

Potential Acid Rock Drainage	**Initial NPR screening criteria**	**Results and Comments**
Likely	<1:1	Like ARD generating
Possibly	1:1 to 2:1	Possibly ARD generating of NP is insufficiently reactive or is depleted at a faster rate than sulphides
Low	2:1 to 4:1	Not potentially ARD generating unless significant preferential exposure of sulphides along fracture planes, or very reactive sulphides in combination with insufficient reactive NP
None	>4:1	No further testing required unless materials are used as alkalinity source

Appendix J: Minerology

Trace Element	Trace Element Concentration	Trace Element	Trace Element Concentration	Trace Element	Trace Element Concentration
	A11		A12		A13 OZ
Al2O3	11,5	Al2O3	10,5	Al2O3	12,1
CaO	0,38	CaO	0,176	As2O3	0,00595
Cl	0,0127	Cl	0,015	BaO	0,00515
Cr2O3	0,0261	Cr2O3	0,0353	CaO	0,0117
Fe2O3	1,73	CuO	0,0064	Cl	0,00598
K2O	0,894	Fe2O3	1,77	Co3O4	0,00124
MgO	0,238	K2O	0,53	Cr2O3	0,0531
MnO	0,0188	MgO	0,285	CuO	0,00299
NiO	0,0122	MnO	0,00929	Fe2O3	0,866
P2O5	0,0474	Na2O	0,163	Ga2O3	0,000718
PbO	0,0107	NiO	0,00837	K2O	2,09
Rb2O	0,00222	P2O5	0,0385	MgO	0,134
SiO2	76,2	PbO	0,0143	Na2O	0,22
SO3	0,0691	Rb2O	0,00149	NiO	0,00388
SrO	0,00137	SiO2	77,3	P2O5	0,0353
TiO2	0,219	SO3	0,888	PbO	0,00212
WO3	0,0607	SrO	0,00183	Rb2O	0,00557
ZnO	0,56	TiO2	0,188	SiO2	76,5
ZrO2	0,0126	WO3	0,0785	SO3	0,638
		ZnO	0,006	SrO	0,000921
		ZrO2	0,0117	TiO2	0,266
				WO3	0,0561
				ZnO	0,00112
				ZrO2	0,014

Trace Element	Trace Element Concentration	Trace Element	Trace Element Concentration	Trace Element	Trace Element Concentration
	A13 SZ		A14		A15 OZ
Al2O3	12,7	Al2O3	5,66	Al2O3	11,4
BaO	0,00609	As2O3	0,00642	As2O3	0,0248
CaO	0,043	CaO	0,129	BaO	0,00644
Cl	0,0099	Co3O4	0,00913	CaO	0,263
Co3O4	0,00468	Cr2O3	0,0245	Cl	0,0144
Cr2O3	0,0459	CuO	0,00255	Cr2O3	0,0794
CuO	0,0326	Fe2O3	0,932	CuO	0,00802
Fe2O3	0,823	K2O	1,04	Fe2O3	2,51
K2O	1,91	MgO	0,142	K2O	2,15
MgO	0,3	Na2O	0,108	MgO	0,357
Na2O	0,23	P2O5	0,0294	Na2O	0,231
NiO	0,0227	PbO	0,00221	NiO	0,0144
P2O5	0,0286	Rb2O	0,00214	P2O5	0,0371
PbO	0,00195	SiO2	78,1	PbO	0,00192
Rb2O	0,00494	SO3	0,767	Rb2O	0,00582
SiO2	73,9	SrO	0,00143	SiO2	69,2
SO3	1,88	TiO2	0,272	SO3	2,64
SrO	0,000802	WO3	0,119	SrO	0,00148
TiO2	0,262	ZrO2	0,0187	TiO2	0,427
U	0,00193			V2O5	0,00176
WO3	0,0367			WO3	0,0552
ZnO	0,0106			ZnO	0,00361
ZrO2	0,0131			ZrO2	0,0199

Trace Element	Trace Element Concentration	Trace Element	Trace Element Concentration	Trace Element	Trace Element Concentration
	A15 SZ		A16 OZ		A16 SZ
Al2O3	9,17	Al2O3	9,16	Al2O3	10,2
As2O3	0,0284	As2O3	0,00695	BaO	0,00412
BaO	0,00685	BaO	0,00597	CaO	0,542
CaO	0,332	CaO	0,257	Cl	0,0296
Cl	0,0221	Cl	0,0215	Cr2O3	0,052
Cr2O3	0,055	Co3O4	0,0027	CuO	0,00388
CuO	0,00436	Cr2O3	0,0622	Fe2O3	1,56
Fe2O3	4,06	CuO	0,00358	K2O	1,29
K2O	2,01	Fe2O3	1,72	MgO	0,402
MgO	0,185	K2O	1,17	MnO	0,0109
Na2O	0,515	MgO	0,533	Na2O	0,251
Nb2O5	0,000917	MnO	0,0068	NiO	0,011
NiO	0,0108	Na2O	0,259	P2O5	0,0279
P2O5	0,0467	NiO	0,00799	PbO	0,0112
PbO	0,00225	P2O5	0,03	Rb2O	0,00315
Rb2O	0,00467	PbO	0,00357	SiO2	75
SiO2	65,8	Rb2O	0,00205	SO3	1,32
SO3	5,13	Sc2O3	0,00485	SrO	0,00167
SrO	0,00231	SiO2	76,4	TiO2	0,227
TiO2	0,381	SO3	1,16	U	0,00203
WO3	0,0712	SrO	0,00163	WO3	0,061
ZnO	0,00177	TiO2	0,224	ZnO	0,00291
ZrO2	0,0186	WO3	0,114	ZrO2	0,0138
		ZnO	0,00294		
		ZrO2	0,0151		

Trace Element	Trace Element Concentration	Trace Element	Trace Element Concentration	Trace Element	Trace Element Concentration
	A17 OZ		A17 SZ		A18
Al2O3	11	Al2O3	11,5	Al2O3	8,9
As2O3	0,0168	As2O3	0,0133	As2O3	0,00888
BaO	0,00348	BaO	0,00544	BaO	0,00628
CaO	0,351	CaO	0,208	CaO	0,432
Cl	0,02	Cl	0,0272	Cl	0,0147
Cr2O3	0,0658	Cr2O3	0,0719	Cr2O3	0,0567
CuO	0,00318	CuO	0,0083	Fe2O3	3,28
Fe2O3	2,42	Fe2O3	2,3	K2O	1,42
K2O	1,93	K2O	2,16	MgO	0,672
MgO	0,357	MgO	0,471	MnO	0,0184
Na2O	0,223	MnO	0,00364	Na2O	0,163
NiO	0,00765	Na2O	0,208	NiO	0,0142
P2O5	0,0404	NiO	0,0345	P2O5	0,0623
PbO	0,00247	P2O5	0,0452	PbO	0,00231
Rb2O	0,00563	PbO	0,00895	Rb2O	0,00362
SiO2	71,4	Rb2O	0,00566	SiO2	69,8
SO3	2,1	SiO2	72,5	SO3	1,88
SrO	0,00177	SO3	1,63	SrO	0,00126
TiO2	0,422	SrO	0,00161	TiO2	0,353
WO3	0,0758	TiO2	0,393	WO3	0,0706
ZnO	0,00168	U	0,00319	Y2O3	0,000856
ZrO2	0,0225	WO3	0,0717	ZnO	0,00118
		ZnO	0,00786	ZrO2	0,0272
		ZrO2	0,0201		

Trace Element	Trace Element Concentration	Trace Element	Trace Element Concentration	Trace Element	Trace Element Concentration
	A19		A20		A21
Al2O3	5,63	Al2O3	9,66	Al2O3	11,9
As2O3	0,0163	As2O3	0,0121	As2O3	0,00597
BaO	0,00359	BaO	0,00515	BaO	0,00624
CaO	0,233	CaO	0,171	CaO	0,2
Cl	0,0141	CeO2	0,0292	CeO2	0,0221
Co3O4	0,0325	Cl	0,0627	Cl	0,0367
Cr2O3	0,0452	Cr2O3	0,0501	Cr2O3	0,071
Fe2O3	3,23	CuO	0,00887	Fe2O3	4,76
K2O	0,57	Fe2O3	4,89	K2O	1,88
MgO	0,403	K2O	1,73	MgO	0,822
MnO	0,0121	MgO	0,522	MnO	0,0171
Na2O	0,198	MnO	0,015	Na2O	0,322
NiO	0,00604	Na2O	0,323	Nb2O5	0,000939
P2O5	0,0387	NiO	0,0146	NiO	0,0135
PbO	0,0177	P2O5	0,0639	P2O5	0,0654
Rb2O	0,00161	PbO	0,0097	PbO	0,0059
SiO2	77,3	Rb2O	0,00487	Rb2O	0,0062
SO3	1,29	SiO2	67,6	SiO2	69
SrO	0,00184	SO3	2,62	SO3	1,29
TiO2	0,165	SrO	0,001	SrO	0,00154
WO3	0,0686	TiO2	0,352	TiO2	0,356
ZnO	0,00324	WO3	0,0756	WO3	0,056
ZrO2	0,0156	ZnO	0,0068	ZnO	0,00653
		ZrO2	0,0198	ZrO2	0,0163

Trace Element	Trace Element Concentration	Trace Element	Trace Element Concentration	Trace Element	Trace Element Concentration
	A22		A23		A24
Al2O3	8,37	Al2O3	11,6	Al2O3	8,07
As2O3	0,00697	As2O3	0,0136	As2O3	0,0127
BaO	0,00563	BaO	0,00484	BaO	0,0052
CaO	0,391	CaO	0,338	CaO	0,142
Cl	0,0218	Cl	0,0188	Cl	0,0099
Cr2O3	0,0347	Cr2O3	0,0638	Cr2O3	0,0521
Fe2O3	3,71	CuO	0,00819	CuO	0,00692
K2O	1,24	Fe2O3	5,68	Fe2O3	3,06
MgO	0,716	K2O	1,98	Ga2O3	0,000264
MnO	0,0107	MgO	0,598	K2O	1,22
Na2O	0,247	MnO	0,0148	MgO	0,301
NiO	0,0108	Na2O	0,172	Na2O	0,21
P2O5	0,0516	NiO	0,0145	P2O5	0,0232
PbO	0,0036	P2O5	0,0819	PbO	0,0095
Rb2O	0,00287	PbO	0,00364	Rb2O	0,00307
SiO2	71,1	Rb2O	0,00566	SiO2	70
SO3	1,78	SiO2	66,9	SO3	3,34
SrO	0,00157	SO3	1,36	SrO	0,00185
TiO2	0,312	SrO	0,00216	TiO2	0,246
WO3	0,0689	TiO2	0,437	U	0,0069
ZnO	0,003	WO3	0,0556	WO3	0,0548
ZrO2	0,0164	ZnO	0,00776	ZnO	0,0096
		ZrO2	0,0198	ZrO2	0,0152

Trace Element	Trace Element Concentration	Trace Element	Trace Element Concentration	Trace Element	Trace Element Concentration
	A25		A26		A27
Al2O3	9,62	Al2O3	4,9	Al2O3	3,98
As2O3	0,0276	As2O3	0,00495	As2O3	0,224
BaO	0,00581	CaO	0,481	CaO	0,333
CaO	0,185	Cl	0,0105	Cl	0,0122
CeO2	0,0207	Cr2O3	0,0204	Cr2O3	0,0244
Cl	0,0256	CuO	0,00262	CuO	0,17
Cr2O3	0,0505	Fe2O3	1,67	Fe2O3	71,3
CuO	0,00324	K2O	0,648	K2O	0,521
Fe2O3	3,36	MgO	0,167	Na2O	0,215
K2O	1,91	Na2O	0,119	NiO	0,613
MgO	0,357	Nb2O5	0,000803	P2O5	0,0188
Na2O	0,511	NiO	0,0108	PbO	0,0231
Nb2O5	0,00106	P2O5	0,0442	SiO2	16,5
NiO	0,00452	PbO	0,00203	SO3	2,24
P2O5	0,0421	Rb2O	0,00113	TiO2	0,326
PbO	0,00708	SiO2	77,6	ZnO	0,0317
PtO2	0,000946	SO3	1,98	ZrO2	0,0069
Rb2O	0,00494	SrO	0,000355		
SiO2	69,5	TiO2	0,214		
SO3	3,17	WO3	0,0794		
SrO	0,00196	ZnO	0,00274		
TiO2	0,428	ZrO2	0,011		
WO3	0,072				
ZnO	0,000307				
ZrO2	0,0227				

Trace Element	Trace Element Concentration	Trace Element	Trace Element Concentration	Trace Element	Trace Element Concentration
	A29		AR11		AR13
Al2O3	7,26	Al2O3	9,33	Al2O3	12,7
As2O3	0,00815	CaO	0,0676	BaO	0,00343
BaO	0,00515	Cl	0,0151	CaO	0,683
CaO	0,516	Cr2O3	0,0601	Cl	0,0119
Cl	0,0168	CuO	0,00269	Co3O4	0,00742
Co3O4	0,0291	Fe2O3	7,01	Cr2O3	0,033
Cr2O3	0,0274	K2O	0,254	CuO	0,00465
CuO	0,00588	MgO	3,68	Fe2O3	1,14
Fe2O3	1,97	MnO	0,102	Ga2O3	0,000437
K2O	0,924	Na2O	0,0364	K2O	1,78
MgO	0,498	NiO	0,0331	MgO	0,793
MnO	0,00733	P2O5	0,0624	MnO	0,0662
Na2O	0,229	Pa	0,00153	Na2O	0,109
NiO	0,0051	SiO2	63,9	NiO	0,00752
P2O5	0,0367	SO3	0,189	P2O5	0,0157
Rb2O	0,00245	SrO	0,00087	Rb2O	0,00424
SiO2	74,5	TiO2	0,261	SiO2	70,1
SO3	1,57	WO3	0,0698	SO3	0,0675
SrO	0,000226	Y2O3	0,00115	SrO	0,00416
TiO2	0,315	ZnO	0,0136	TiO2	0,336
WO3	0,097	ZrO2	0,00741	WO3	0,0853
ZnO	0,00425			ZnO	0,000861
ZrO2	0,0239			ZrO2	0,0122

Trace Element	Trace Element Concentration	Trace Elements	Trace Element Concentration	Trace Element	Trace Element Concentration
	AR14		AR15		AR16
Al2O3	9,52	Al2O3	5,57	F	0,102
CaO	0,0919	CaO	0,0341	Al2O3	12,4
Cl	0,00806	Cl	0,0131	As2O3	0,00844
Co3O4	0,028	Co3O4	0,0183	BaO	0,00693
Cr2O3	0,0165	Cr2O3	0,0249	CaO	0,172
Fe2O3	0,373	CuO	0,00228	Cl	0,00847
K2O	0,367	Fe2O3	0,576	Cr2O3	0,0651
MgO	0,0527	K2O	0,98	CuO	0,0114
MnO	0,0031	MgO	0,0947	Fe2O3	7,73
Na2O	0,0892	Na2O	0,104	K2O	1,35
NiO	0,00664	P2O5	0,0211	MgO	2,18
P2O5	0,0433	Rb2O	0,00227	MnO	0,0344
SiO2	76,9	SiO2	80	Na2O	0,154
SO3	0,0677	SO3	0,196	NiO	0,0308
SrO	0,00148	TiO2	0,103	P2O5	0,0439
TiO2	0,107	WO3	0,105	Rb2O	0,0036
WO3	0,126	ZrO2	0,00323	SiO2	62
Y2O3	0,000662			SO3	0,384
ZnO	0,0000496			SrO	0,00197
ZrO2	0,00659			TiO2	0,354
				WO3	0,0604
				ZnO	0,00296
				ZrO2	0,00789

Trace Element	Trace Element Concentration	Trace Elements	Trace Element Concentration	Trace Element	Trace Element Concentration
	AR17		AR18		AR19
F	0,0817	Al2O3	12,8	Al2O3	15,7
Al2O3	22	Ba	0,00526	BaO	0,011
BaO	0,0174	CaO	0,0502	CaO	0,0814
CaO	0,853	Cl	0,00799	Cl	0,00834
Cl	0,0148	Cr	0,0414	Cr2O3	0,0734
Cr2O3	0,214	Cu	0,00441	CuO	0,00337
CuO	0,00799	Fe2O3	3,46	Fe2O3	6,1
Fe2O3	5,61	K2O	2,34	Ga2O3	0,0019
Ga2O3	0,00196	MgO	0,574	K2O	2,18
K2O	3,8	Mn	0,00801	MgO	1,14
MgO	2,1	Na2O	0,146	MnO	0,0348
MnO	0,0423	Ni	0,0102	Na2O	0,309
Na2O	0,547	P2O5	0,0465	NiO	0,0144
Nb2O5	0,00103	Pb	0,00356	P2O5	0,0633
NiO	0,0423	Rb	0,00479	PbO	0,00206
P2O5	0,0368	SiO2	68,5	Rb2O	0,00748
Rb2O	0,0116	SO3	0,843	SiO2	61,9
SiO2	52,9	Sr	0,000893	SO3	0,14
SO3	0,15	Ti	0,209	SrO	0,00214
SrO	0,00307	W	0,0649	TiO2	0,44
TiO2	0,63	Zn	0,00111	WO3	0,0486
WO3	0,0252	Zr	0,0107	ZnO	0,00794
ZnO	0,00561			ZrO2	0,0141
ZrO2	0,0186				

Trace Element	Trace Element Concentration	Trace Elements	Trace Element Concentration	Trace Element	Trace Element Concentration
	AR20		AR21		AR22
Al2O3	16,6	Al2O3	15,9	Al2O3	15,3
BaO	0,0094	BaO	0,0131	As2O3	0,0105
CaO	0,0321	CaO	0,137	BaO	0,00663
Cl	0,0126	Cl	0,00877	CaO	0,0694
Cr2O3	0,0618	Cr2O3	0,143	Cl	0,0157
Fe2O3	2,32	CuO	0,00459	Cr2O3	0,0901
Ga2O3	0,000585	Fe2O3	6,99	CuO	0,0108
K2O	2,03	Ga2O3	0,00022	Fe2O3	3,89
MgO	0,458	K2O	2,47	K2O	2,93
MnO	0,0146	MgO	3,99	MgO	0,9
Na2O	0,232	MnO	0,08	MnO	0,0175
Nb2O5	0,000752	Na2O	0,102	Na2O	0,159
NiO	0,015	NiO	0,0334	NiO	0,0335
P2O5	0,029	P2O5	0,0594	P2O5	0,0565
PbO	0,00739	Rb2O	0,0078	Rb2O	0,00805
Rb2O	0,00488	SiO2	53,9	SiO2	64
SiO2	67	SO3	0,107	SO3	0,742
SO3	0,161	SrO	0,000856	SrO	0,00104
SrO	0,00206	TiO2	0,498	TiO2	0,549
TiO2	0,358	WO3	0,0297	WO3	0,0683
WO3	0,0745	ZnO	0,0062	ZnO	0,00141
ZrO2	0,0151	ZrO2	0,0133	ZrO2	0,02

Trace Elements	Trace Element Concentration
	AR23
Al2O3	13,9
BaO	0,00627
CaO	0,0518
Cl	0,0102
Cr2O3	0,0463
CuO	0,00352
Fe2O3	3,02
K2O	1,7
MgO	0,889
MnO	0,0135
Na2O	0,167
NiO	0,0153
P2O5	0,0385
Rb2O	0,00474
SiO2	67,7
SO3	0,255
SrO	0,00176
TiO2	0,262
WO3	0,0768
ZnO	0,0083
ZrO2	0,0112

Appendix K: Leach Test Data

Sample Name:	A13OZ								
Units	Weeks								
mg/l	1	2	3	4	5	6	7	8	9
Ca	3.805	15.150	4.553	4.561	3.403	2.351	6.271	1.227	1.227
Mg	6.576	23.160	6.740	6.190	6.050	4.094	5.285	2.437	2.437
K	0.257	0.801	0.053	0.502	0.633	0.632	0.619	0.101	0.101
Na	0.751	1.194	0.507	0.535	0.632	0.529	0.699	0.007	0.007
SO_4	119.350	510.160	77.780	82.290	70.200	43.410	70.280	133.120	38.690
NO_3	0.110	0.120	0.430	0.090	0.180	0.240	0.050	0.090	0.080
Cl	0.600	1.740	0.660	0.800	0.630	0.440	0.490	0.470	0.350
Fe	0.335	1.772	0.031	0.583	0.616	0.612	0.609	0.660	0.660
Mn	0.149	0.524	0.268	0.151	0.149	0.097	0.132	0.062	0.062
Cu	0.486	1.893	0.533	0.482	0.504	0.317	0.491	0.207	0.207
Zn	0.342	1.236	0.347	0.375	0.370	0.236	0.428	0.142	0.142
B	0.000	0.000	0.000	0.038	0.000	0.000	0.000	0.000	0.000
pH		3.360	3.660	3.680	3.720	3.840	3.730	2.560	3.710
EC (mS/cm)	0.270	0.680	0.260	0.250	0.250	0.180	0.240	0.270	0.160
TAL $CaCO_3$/l	0.000	0.000	0.000	0.000	0.000	0.000	0.000	0.000	0.000

Sample Name:	A13SZ								
Units	Weeks								
mg/l	1	2	3	4	5	6	7	8	9
Ca	5.979	35.630	7.248	5.517	7.137	4.504	5.638	4.042	4.042
Mg	23.480	207.700	42.500	29.360	41.440	25.150	31.610	25.320	25.320
K	0.103	2.603	0.075	0.279	0.718	0.418	1.117	0.328	0.328
Na	0.456	0.937	0.325	0.264	0.482	0.238	0.959	0.007	0.007
SO_4	763.270	10076.900	1121.140	905.190	565.320	757.270	985.550	1971.200	1848.740
NO_3	3.870	18.580	11.050	3.610	3.290	4.970	2.790	4.960	8.180
Cl	0.530	1.450	0.890	1.240	0.730	0.960	0.930	0.760	1.360
Fe	8.572	402.500	83.220	64.460	153.700	81.220	153.300	153.000	153.000
Mn	0.533	4.882	1.125	0.722	1.004	0.610	0.776	0.613	0.613
Cu	10.820	96.550	21.680	15.620	21.700	13.270	16.830	13.610	13.610
Zn	4.376	39.750	8.950	6.984	10.290	6.143	7.834	6.314	6.314
B	0.099	0.034	0.000	0.032	0.000	0.000	0.009	0.000	0.000
pH		2.580		2.710	2.740	2.790	2.760	2.770	2.790
EC (mS/cm)	1.300	5.260	11.050	1.900	2.010	1.710	1.840	1.800	1.890
TAL $CaCO_3$/l	0.000	0.000	0.000	0.000	0.000	0.000	0.000	0.000	0.000

Sample Name:	AR14								
Units	Weeks								
mg/l	1	2	3	4	5	6	7	8	9
Ca	11.880	7.160	4.919	4.906	3.480	3.288	3.418	1.779	1.779
Mg	0.934	0.397	0.308	0.207	0.097	0.121	0.145	0.002	0.002
K	1.559	1.021	0.491	0.398	0.245	0.184	0.526	0.001	0.001
Na	1.429	0.731	0.349	0.363	0.150	0.148	0.601	0.007	0.007
SO_4	45.240	19.590	7.740	7.550	4.590	4.570	4.700	2.970	2.510
NO_3	0.430	0.460	0.590	0.150	0.480	0.330	0.530	0.450	0.430
Cl	1.480	1.090	0.640	0.810	0.650	0.630	0.620	0.420	0.440
Fe	0.000	0.131	0.002	0.038	0.033	0.008	0.083	0.123	0.123
Mn	1.459	0.612	0.459	0.328	0.224	0.219	0.181	0.110	0.110
Cu	0.000	0.019	0.014	0.003	0.000	0.001	0.008	0.000	0.000
Zn	0.006	0.012	0.008	0.004	0.000	0.010	0.028	0.000	0.000
B	0.000	0.000	0.000	0.029	0.000	0.000	0.008	0.000	0.000
pH		6.910	6.760	6.880	6.970	6.710	6.570	5.500	5.610
EC (mS/cm)	0.130	0.070	0.040	0.030	0.020	0.020	0.020	0.020	0.020
TAL CaCO3/l	5.000	10.000	12.500	10.000	7.500	7.500	10.000	7.500	7.500

Sample Name:	AR15								
Units	Weeks								
mg/l	1	2	3	4	5	6	7	8	9
Ca	23.840	38.480	17.100	15.780	8.351	6.092	6.325	3.363	3.363
Mg	4.239	4.322	1.567	4.014	1.200	0.637	0.732	0.080	0.080
K	1.712	1.921	0.861	0.736	0.503	0.460	0.583	0.066	0.066
Na	1.764	1.629	0.919	2.780	0.860	0.596	0.857	0.007	0.007
SO_4	122.260	180.790	42.760	61.430	25.840	16.820	18.710	36.660	11.740
NO_3	1.860	0.960	0.350	2.440	0.400	0.160	0.180	0.190	0.160
Cl	1.680	1.200	2.590	2.750	0.640	0.360	0.540	0.880	0.380
Fe	0.157	0.071	0.002	0.000	0.000	0.000	0.000	0.104	0.104
Mn	7.115	7.594	2.832	2.189	1.127	0.798	0.768	0.431	0.431
Cu	0.000	0.017	0.017	0.577	0.318	0.157	0.147	0.028	0.028
Zn	0.098	0.157	0.201	0.706	0.173	0.101	0.082	0.073	0.073
B	0.000	0.000	0.000	0.004	0.001	0.000	0.019	0.001	0.001
pH		5.780	6.480	6.460	6.510	6.380	5.610	4.530	5.000
EC (mS/cm)	0.270	0.360	0.130	0.160	0.080	0.050	0.060	0.100	0.040
TAL CaCO3/l	2.500	5.000	5.000	5.000	5.000	5.000	5.000	7.500	6.000

Sample Name:	A15OZ								
Units	Weeks								
mg/l	1	2	3	4	5	6	7	8	9
Ca	15.240	111.500	70.950	46.710	59.770	47.560	45.420	48.860	48.860
Mg	28.750	154.100	94.890	41.930	45.550	30.920	33.610	20.700	20.700
K	0.100	2.018	0.098	0.536	4.213	0.420	1.060	0.557	0.557
Na	0.856	0.732	0.457	2.123	4.908	1.055	1.678	0.007	0.007
SO_4	797.170	4239.650	1733.970	709.970	754.520	776.020	841.840	870.070	838.940
NO_3	0.840	11.400	8.510	13.490	4.410	1.300	1.240	1.260	0.980
Cl	6.020	24.790	13.780	7.550	6.530	4.130	4.140	3.470	2.700
Fe	0.047	4.061	0.025	1.294	1.080	1.169	1.369	2.147	2.147
Mn	0.853	4.982	3.340	1.333	1.457	0.992	1.079	0.651	0.651
Cu	1.192	6.254	4.005	1.659	1.972	1.340	1.482	0.951	0.951
Zn	0.908	4.949	3.055	2.149	2.169	1.384	1.591	0.888	0.888
B	0.000	0.014	0.000	0.007	0.000	0.000	0.007	0.000	0.000
pH		3.470	3.560	3.830	3.770	3.830	3.780	3.790	3.770
EC (mS/cm)	0.750	3.020	1.850	1.020	1.110	0.840	0.870	0.810	0.750
TAL $CaCO_3$/l	0.000	0.000	0.000	0.000	0.000	0.000	0.000	0.000	0.000

Sample Name:	A15SZ								
Units	Weeks								
mg/l	1	2	3	4	5	6	7	8	9
Ca	67.070	111.000	81.070	59.450	55.250	37.550	46.040	37.570	37.570
Mg	103.000	183.400	110.900	66.040	55.040	37.000	43.060	24.960	24.960
K	0.168	1.048	0.061	0.269	0.453	0.270	0.377	0.001	0.001
Na	1.464	2.083	1.286	1.656	1.139	0.599	0.666	0.007	0.007
SO_4	1935.000	4195.390	1291.580	777.920	703.840	435.810	516.560	503.750	412.950
NO_3	9.750	12.700	17.030	18.840	6.220	7.890	11.230	5.590	7.220
Cl	112.960	196.380	113.450	55.830	46.640	27.860	29.250	18.370	18.350
Fe	70.150	155.200	89.130	17.420	13.760	7.152	12.980	2.795	2.795
Mn	4.002	7.258	4.691	2.820	2.346	1.490	1.839	1.000	1.000
Cu	3.469	6.265	3.886	2.333	1.927	1.295	1.528	0.822	0.822
Zn	2.504	4.483	2.720	1.914	1.565	1.048	1.243	0.706	0.706
B	0.000	0.004	0.000	0.015	0.000	0.000	0.000	0.001	0.001
pH		2.590	2.610	2.760	2.830	2.950	2.920	3.040	3.030
EC (mS/cm)	2.770	4.130	2.810	2.010	1.760	1.290	1.380	1.130	1.130
TAL $CaCO_3$/l	0.000	0.000	0.000	0.000	0.000	0.000	0.000	0.000	0.000

Sample Name:	A17OZ								
Units	Weeks								
mg/l	1	2	3	4	5	6	7	8	9
Ca	43.920	447.600	143.400	44.570	45.910	20.980	24.140	20.500	20.500
Mg	12.980	529.300	16.600	4.861	21.730	2.261	3.054	2.086	2.086
K	0.043	-0.025	0.019	0.453	0.438	0.658	0.501	0.448	0.448
Na	0.488	0.556	0.517	1.080	0.603	0.469	0.532	0.007	0.007
SO_4	378.940	13954.820	489.490	173.620	475.520	76.310	90.530	108.770	107.550
NO_3	0.150	10.420	6.740	0.820	1.070	0.200	0.200	0.160	0.170
Cl	16.300	594.150	15.020	5.980	17.640	2.400	2.910	2.560	2.250
Fe	0.796	211.700	1.406	1.815	2.875	1.509	1.460	2.241	2.241
Mn	0.476	20.830	0.739	0.157	0.865	0.084	0.112	0.085	0.085
Cu	0.568	22.920	0.712	0.324	0.855	0.104	0.159	0.055	0.055
Zn	0.460	19.830	0.592	0.528	0.761	0.117	0.157	0.090	0.090
B	0.000	0.000	0.001	0.002	0.000	0.001	0.000	0.000	0.000
pH		2.560	2.980	3.750	3.230	3.580	3.550	3.540	3.590
EC (mS/cm)	0.710	8.900	1.190	0.370	0.860	0.260	0.280	0.300	0.300
TAL $CaCO_3$/l	0.000	0.000	0.000	0.000	0.000	0.000	0.000	0.000	0.000

Sample Name:	A17SZ								
Units	Weeks								
mg/l	1	2	3	4	5	6	7	8	9
Ca	13.910	200.000	56.420	71.770	64.170	50.150	94.170	28.490	28.490
Mg	6.257	113.100	13.340	15.540	17.560	15.390	27.270	9.395	9.395
K	0.537	0.267	0.082	0.000	0.081	0.185	0.550	0.004	0.004
Na	8.249	112.500	13.250	10.140	7.692	4.312	2.980	0.008	0.008
SO_4	169.580	4350.440	521.990	752.490	1086.660	925.490	1803.650	1145.780	1172.300
NO_3	0.370	7.320	4.720	11.680	7.830	14.900	14.670	9.160	9.980
Cl	11.840	163.030	18.800	17.140	17.320	12.580	14.610	7.380	6.780
Fe	0.561	186.300	50.500	140.100	263.200	261.600	609.600	179.100	179.100
Mn	1.129	22.340	2.677	2.886	2.954	2.414	3.527	1.023	1.023
Cu	0.132	4.754	1.000	1.323	1.567	1.339	2.117	0.668	0.668
Zn	1.256	27.430	3.559	4.818	5.324	4.374	6.308	1.974	1.974
B	0.000	0.000	0.000	0.000	0.001	0.000	0.000	0.001	0.001
pH		2.530	2.630	2.560	2.580	2.570	2.490	2.610	2.600
EC (mS/cm)	0.520	4.160	1.780	2.370	2.650	2.540	3.140	2.270	2.420
TAL $CaCO_3$/l	0.000	0.000	0.000	0.000	0.000	0.000	0.000	0.000	0.000

Sample Name:	AR21								
Units	Weeks								
mg/l	1	2	3	4	5	6	7	8	9
Ca	5.688	5.724	3.013	3.387	2.316	2.450	2.936	0.895	0.895
Mg	5.071	3.657	1.969	2.153	1.487	1.558	1.898	0.854	0.854
K	8.736	8.752	3.929	3.588	2.477	1.839	9.557	0.718	0.718
Na	2.111	1.399	0.462	0.413	0.298	0.242	1.466	0.008	0.008
SO_4	52.250	38.720	11.800	12.140	8.200	7.930	10.130	6.940	6.190
NO_3	0.650	0.260	0.100	0.300	0.150	0.170	0.320	0.280	0.380
Cl	1.960	1.240	0.330	0.630	0.370	0.320	0.900	0.370	0.380
Fe	0.001	0.016	0.002	0.231	0.144	0.106	0.351	0.125	0.125
Mn	0.616	0.410	0.315	0.279	0.206	0.223	0.270	0.178	0.178
Cu	0.000	0.000	0.004	0.000	0.004	0.010	0.017	0.000	0.000
Zn	0.000	0.000	0.007	0.000	0.000	0.012	0.063	0.000	0.000
B	0.005	0.000	0.001	0.000	0.000	0.000	0.009	0.000	0.000
pH		5.850	7.060	7.100	7.140	7.100	6.970	6.940	5.890
EC (mS/cm)	0.150	0.140	0.050	0.050	0.040	0.030	0.040	0.280	0.020
TAL $CaCO_3$/l	10.000	17.500	12.500	12.500	10.000	7.500	10.000	7.500	7.500

Appendix L: Sulphate/Sulphur Analysis Results

Marievale 1			
Depth (m)	Tot %S	% SO_4 of S	%S as S
0.143	0.217	3.048	96.952
0.286	0.520	42.348	57.652
0.430	0.300	5.293	94.707
0.573	0.519	63.102	36.898
0.716	0.546	67.723	32.277
0.859	0.264	38.872	61.128
1.002	0.440	45.101	54.899
1.145	0.205	63.596	36.404
1.289	0.335	54.763	45.237
1.432	0.808	50.099	49.901
1.575	0.493	32.426	67.574
1.718	0.437	53.251	46.749
1.861	0.323	65.014	34.986
2.005	0.398	49.045	50.955
2.148	0.495	81.645	18.355
2.291	0.589	54.320	45.680
2.434	0.251	56.665	43.335
2.577	0.657	55.256	44.744
2.720	1.098	50.989	49.011
2.864	0.856	57.937	42.063
3.007	0.605	64.993	35.007
3.150	0.365	64.237	35.763
3.293	0.392	68.633	31.367
3.436	0.608	60.737	39.263
3.580	0.290	59.248	40.752
3.723	0.772	58.657	41.343
3.866	0.996	62.604	37.396
4.009	0.781	52.107	47.893
4.152	0.362	70.088	29.912
4.295	0.356	56.440	43.560

4.439	0.444	64.289	35.711
4.582	0.788	44.628	55.372
4.725	0.668	43.443	56.557
4.868	0.693	57.098	42.902
5.011	0.919	73.643	26.357
5.155	0.553	67.625	32.375
5.298	0.779	74.775	25.225
5.441	0.403	58.701	41.299
5.584	0.540	65.044	34.956
5.727	0.798	53.797	46.203
5.870	0.415	63.926	36.074
6.014	0.782	68.479	31.521
6.157	0.322	59.608	40.392
6.300	0.798	49.887	50.113

Marievale 2			
Depth (m)	Tot %S	$\%SO_4$of S	%S as S
0.143	0.113	51.675	48.325
0.286	0.078	50.727	49.273
0.430	0.042	58.631	41.369
0.573	0.090	60.692	39.308
0.716	0.136	72.210	27.790
0.859	0.070	76.137	23.863
1.002	0.037	88.683	11.317
1.145	0.091	75.164	24.836
1.289	0.078	69.684	30.316
1.432	0.088	76.266	23.734
1.575	0.131	61.354	38.646
1.718	0.063	88.082	11.918
1.861	0.085	72.999	27.001
2.005	0.062	65.279	34.721
2.148	0.051	76.246	23.754
2.291	0.088	57.420	42.580
2.434	0.092	65.602	34.398
2.577	0.124	57.034	42.966
2.720	0.104	67.557	32.443
2.864	0.121	62.163	37.837
3.007	0.101	73.002	26.998
3.150	0.065	65.060	34.940
3.293	0.094	55.666	44.334
3.436	0.167	25.514	74.486
3.580	0.087	63.640	36.360
3.723	0.051	77.593	22.407
3.866	0.077	63.752	36.248
4.009	0.115	47.804	52.196
4.152	0.146	35.289	64.711
4.295	0.114	53.749	46.251
4.439	0.098	58.719	41.281
4.582	0.173	34.068	65.932
4.725	0.173	52.266	47.734

4.868	0.198	21.854	78.146
5.011	0.223	35.010	64.990
5.155	0.183	49.083	50.917
5.298	0.195	34.660	65.340
5.441	0.210	36.071	63.929
5.584	0.240	26.358	73.642
5.727	0.294	12.122	87.878
5.870	0.334	15.844	84.156
6.014	0.257	17.251	82.749
6.157	0.394	8.658	91.342
6.300	0.328	19.126	80.874

Marievale 3			
Depth (m)	Tot %S	$\%SO_4$of S	%S as S
0.137	0.388	15.232	84.768
0.274	0.315	42.495	57.505
0.411	0.138	47.561	52.439
0.548	0.127	70.073	29.927
0.685	0.167	42.557	57.443
0.822	0.175	52.610	47.390
0.959	0.097	72.396	27.604
1.096	0.115	56.381	43.619
1.233	0.086	81.283	18.717
1.370	0.066	79.576	20.424
1.507	0.074	31.579	68.421
1.643	0.062	74.713	25.287
1.780	0.079	77.600	22.400
1.917	0.098	68.704	31.296
2.054	0.078	82.793	17.207
2.191	0.101	71.078	28.922
2.328	0.049	83.225	16.775
2.465	0.035	86.259	13.741
2.602	0.077	68.742	31.258
2.739	0.021	90.696	9.304
2.876	0.176	37.712	62.288
3.013	0.028	79.451	20.549
3.150	0.116	42.409	57.591
3.287	0.176	25.032	74.968
3.424	0.136	36.483	63.517
3.561	0.130	36.350	63.650
3.698	0.177	7.221	92.779
3.835	0.206	20.248	79.752
3.972	0.183	22.047	77.953
4.109	0.138	23.799	76.201
4.246	0.179	14.038	85.962
4.383	0.175	24.331	75.669
4.520	0.169	22.792	77.208

4.657	0.135	28.639	71.361
4.793	0.164	27.797	72.203
4.930	0.208	15.644	84.356
5.067	0.176	20.612	79.388
5.204	0.197	19.071	80.929
5.341	0.159	23.987	76.013
5.478	0.162	20.315	79.685
5.615	0.199	18.824	81.176
5.752	0.172	29.014	70.986
5.889	0.284	19.325	80.675
6.026	0.273	14.559	85.441
6.163	0.299	13.132	86.868
6.300	0.208	18.510	81.490

Vlakfontein			
Depth (m)	Tot %S	$\%SO_4$of S	%S as S
0.143	0.039	39.280	60.720
0.286	0.019	59.751	40.249
0.430	0.067	21.622	78.378
0.573	0.045	37.983	62.017
0.716	0.035	47.321	52.679
0.859	0.045	64.572	35.428
1.002	0.059	70.980	29.020
1.145	0.104	50.048	49.952
1.289	0.090	74.748	25.252
1.432	0.082	65.193	34.807
1.575	0.151	85.014	14.986
1.718	0.110	60.196	39.804
1.861	0.044	83.277	16.723
2.005	0.220	57.439	42.561
2.148	0.149	56.283	43.717
2.291	0.162	56.221	43.779
2.434	0.046	91.056	8.944
2.577	0.090	61.852	38.148
2.720	0.087	74.376	25.624
2.864	0.077	81.227	18.773
3.007	0.075	83.495	16.505
3.150	0.060	80.046	19.954
3.293	0.069	82.744	17.256
3.436	0.215	50.081	49.919
3.580	0.051	89.108	10.892
3.723	0.213	36.883	63.117
3.866	0.232	35.969	64.031
4.009	0.181	39.801	60.199
4.152	0.147	39.762	60.238
4.295	0.242	47.871	52.129
4.439	0.237	37.361	62.639
4.582	0.238	39.813	60.187
4.725	0.265	40.045	59.955

4.868	0.115	50.000	50.000
5.011	0.226	39.246	60.754
5.155	0.158	30.985	69.015
5.298	0.150	46.512	53.488
5.441	0.240	25.466	74.534
5.584	0.229	54.098	45.902
5.727	0.104	80.946	19.054
5.870	0.128	52.390	47.610
6.014	0.097	75.987	24.013
6.157	0.261	36.540	63.460
6.300	0.798	6.238	93.762

Carnival City			
Depth (m)	Tot %S	$\%SO_4$of S	%S as S
0.143	0.103	17.297	82.703
0.286	0.102	46.997	53.003
0.430	0.066	55.078	44.922
0.573	0.048	45.885	54.115
0.716	0.059	75.326	24.674
0.859	0.062	72.463	27.537
1.002	0.045	78.558	21.442
1.145	0.066	74.189	25.811
1.289	0.022	84.626	15.374
1.432	0.089	65.041	34.959
1.575	0.079	69.733	30.267
1.718	0.070	72.900	27.100
1.861	0.121	51.252	48.748
2.005	0.771	12.322	87.678
2.148	0.832	13.440	86.560
2.291	0.866	27.361	72.639
2.434	0.859	31.141	68.859
2.577	0.719	18.448	81.552
2.720	0.839	16.297	83.703
2.864	0.856	21.048	78.952
3.007	0.936	17.588	82.412
3.150	1.039	39.940	60.060
3.293	1.676	15.055	84.945
3.436	0.726	24.551	75.449
3.580	0.715	21.519	78.481
3.723	0.456	33.846	66.154
3.866	0.592	19.862	80.138
4.009	0.791	19.636	80.364
4.152	0.729	16.807	83.193
4.295	0.701	25.067	74.933
4.439	0.835	18.148	81.852
4.582	0.904	16.018	83.982
4.725	0.844	21.487	78.513

4.868	1.066	17.700	82.300
5.011	1.022	16.397	83.603
5.155	0.949	21.144	78.856
5.298	0.967	19.889	80.111
5.441	1.031	15.884	84.116
5.584	1.025	15.366	84.634

Appendix M: Hydrus Modelled Water Content Results

Hydrus Modelled Moisture Content						
Depth (m)	Initial Profile	Time Step (Years)				
		1	2	3	4	5
0.1	0.199	0.1726	0.1681	0.1659	0.1644	0.1634
0.2	0.199	0.1973	0.195	0.193	0.1913	0.1898
0.3	0.1991	0.199	0.1987	0.1983	0.1979	0.1974
0.4	0.1991	0.1991	0.199	0.199	0.199	0.1992
0.5	0.1991	0.1991	0.1991	0.1995	0.2006	0.203
0.6	0.1991	0.1991	0.2003	0.2048	0.2119	0.2187
0.7	0.1991	0.2012	0.2145	0.2276	0.2359	0.241
0.8	0.1991	0.2264	0.2466	0.2541	0.2579	0.26
0.9	0.1991	0.266	0.2735	0.2749	0.2749	0.2746
1	0.1991	0.2959	0.2927	0.29	0.2879	0.2859
1.1	0.3974	0.315	0.3066	0.3016	0.2979	0.2948
1.2	0.3974	0.3281	0.317	0.3105	0.3056	0.3023
1.3	0.3974	0.3375	0.325	0.3175	0.3125	0.3083
1.4	0.3975	0.3455	0.3312	0.3235	0.3178	0.3137
1.5	0.3975	0.3501	0.3365	0.3284	0.3225	0.318
1.6	0.3975	0.3543	0.3408	0.3323	0.3266	0.3219
1.7	0.3976	0.3578	0.3441	0.336	0.33	0.3254
1.8	0.3976	0.3604	0.3471	0.339	0.3328	0.3284
1.9	0.3976	0.3624	0.3496	0.3415	0.3356	0.3309
2	0.3976	0.3636	0.3515	0.3436	0.3379	0.3332
2.1	0.3977	0.3642	0.353	0.3453	0.3399	0.3354
2.2	0.3082	0.3639	0.3539	0.3468	0.3416	0.3372
2.3	0.3082	0.3627	0.3544	0.348	0.343	0.3389
2.4	0.3082	0.3602	0.3543	0.3488	0.3441	0.3403
2.5	0.3082	0.559	0.3536	0.3492	0.345	0.3415
2.6	0.3083	0.3496	0.3523	0.3494	0.3457	0.3425
2.7	0.3083	0.3413	0.3504	0.3492	0.3463	0.3434
2.8	0.3083	0.3317	0.3477	0.3486	0.3466	0.344

2.9	0.3083	0.3235	0.3443	0.3477	0.3467	0.3445
3	0.3084	0.3196	0.3409	0.3465	0.3466	0.3449
3.1	0.3084	0.3203	0.3378	0.345	0.3463	0.3451
3.2	0.3084	0.3243	0.3356	0.3436	0.3459	0.3453
3.3	0.3084	0.3294	0.3348	0.3425	0.3453	0.3453
3.4	0.3681	0.3347	0.3354	0.3417	0.448	0.3453
3.5	0.3681	0.3398	0.337	0.3413	0.3444	0.3452
3.6	0.3682	0.3441	0.3393	0.3414	0.3441	0.3451
3.7	0.3682	0.3482	0.3417	0.342	0.344	0.3451
3.8	0.3682	0.3517	0.3441	0.3429	0.3442	0.3451
3.9	0.3683	0.3547	0.3466	0.344	0.3444	0.3451
4	0.3683	0.3574	0.349	0.3453	0.3449	0.3453
4.1	0.3683	0.3599	0.3512	0.3468	0.3456	0.3456
4.2	0.3683	0.362	0.3533	0.3484	0.3464	0.346
4.3	0.3684	0.3639	0.3551	0.35	0.3474	0.3466
4.4	0.3684	0.3656	0.3569	0.3515	0.3485	0.3472
4.5	0.3684	0.3673	0.3586	0.353	0.3496	0.348
4.6	0.3684	0.3688	0.3602	0.3544	0.3508	0.3488
4.7	0.3684	0.3703	0.3617	0.3557	0.352	0.3497
4.8	0.3985	0.3716	0.3631	0.357	0.3531	0.3506
4.9	0.3985	0.3727	0.3643	0.3583	0.3542	0.3515
5	0.3985	0.3739	0.3654	0.3595	0.3552	0.3524
5.1	0.3985	0.375	0.3666	0.3607	0.3561	0.3533
5.2	0.3986	0.3761	0.3677	0.3618	0.3572	0.3542
5.3	0.3986	0.3771	0.3687	0.3628	0.3582	0.355
5.4	0.3986	0.378	0.3697	0.3638	0.3592	0.3558
5.5	0.3987	0.3788	0.3706	0.3647	0.3601	0.3566
5.6	0.3987	0.3796	0.3715	0.3655	0.3611	0.3574
5.7	0.3987	0.3804	0.3723	0.3664	0.3619	0.3582
5.8	0.3988	0.3812	0.3731	0.3672	0.3628	0.3591
5.9	0.3988	0.3819	0.3738	0.368	0.3636	0.599
6	0.3988	0.3826	0.3745	0.3688	0.3643	0.3607
6.1	0.3889	0.3832	0.3752	0.3696	0.365	0.3614
6.2	0.3889	0.3838	0.3759	0.3703	0.3657	0.3622
6.3	0.3889	0.3844	0.3765	0.371	0.3663	0.3629

6.4	0.3889	0.3849	0.3772	0.3716	0.367	0.3635
6.5	0.389	0.3854	0.3778	0.3722	0.3677	0.3642
6.6	0.389	0.3858	0.3783	0.3728	0.3683	0.3648
6.7	0.389	0.3863	0.3789	0.3733	0.3689	0.33653
6.8	0.3891	0.3868	0.3793	0.3739	0.3696	0.3659
6.9	0.3891	0.3872	0.3798	0.3744	0.3702	0.3664
7	0.3891	0.3876	0.3803	0.3749	0.3707	0.367
7.1	0.3891	0.3879	0.3807	0.3754	0.3713	0.3675
7.2	0.3892	0.3883	0.3812	0.3759	0.3718	0.3681
7.3	0.3892	0.3886	0.3816	0.3764	0.3723	0.3686
7.4	0.3892	0.3889	0.382	0.3769	0.3728	0.3691
7.5	0.3893	0.3892	0.3825	0.3774	0.3732	0.3697
7.6	0.3893	0.3894	0.3829	0.3778	0.3736	0.3702
7.7	0.3893	0.3897	0.3833	0.3783	0.374	0.3707
7.8	0.3894	0.3899	0.3836	0.3787	0.3744	0.3711
7.9	0.3894	0.3902	0.384	0.3791	0.3749	0.3716
8	0.3894	0.3904	0.3843	0.3794	0.3753	0.372
8.1	0.3894	0.3906	0.3846	0.3798	0.3757	0.3724
8.2	0.3895	0.3908	0.3849	0.3801	0.3761	0.3728
8.3	0.3895	0.3909	0.3852	0.3804	0.3765	0.3732
8.4	0.3895	0.3911	0.3855	0.3807	0.3769	0.3736
8.5	0.3896	0.3912	0.3558	0.3811	0.3773	0.3739
8.6	0.3896	0.3913	0.386	0.3814	0.3776	0.3742
8.7	0.3896	0.3913	0.3863	0.3817	0.378	0.3746
8.8	0.3896	0.3914	0.3866	0.382	0.3783	0.3749
8.9	0.3897	0.3914	0.3868	0.3824	0.3787	0.3753
9	0.3897	0.3915	0.3871	0.3827	0.379	0.3756
9.1	0.3897	0.3915	0.3874	0.383	0.3793	0.3759
9.2	0.3898	0.3915	0.3876	0.3833	0.3796	0.3763
9.3	0.3898	0.3914	0.3878	0.3835	0.3799	0.3766
9.4	0.3898	0.3914	0.388	0.3838	0.3801	0.3769
9.5	0.3898	0.3914	0.3882	0.3841	0.3804	0.3772
9.6	0.3899	0.3913	0.3884	0.3843	0.3806	0.3775
9.7	0.3899	0.3913	0.3886	0.3845	0.3808	0.3777
9.8	0.3899	0.3912	0.3888	0.3847	0.381	0.3779

9.9	0.39	0.3912	0.3889	0.3848	0.3811	0.3781
10	0.39	0.3912	0.3889	0.3849	0.3812	0.3782